Development of methods for studying the subcellular trafficking of insulin-regulated glucose transporters

Dhesi, Jaswant Kaur

Award date:
2001

Awarding institution:
University of Bath

Development of Methods for Studying the Subcelluar Trafficking of Insulin-Regulated Glucose Transporters

Submitted by Miss Jaswant Kaur Dhesi
for the degree of PhD
of the University of Bath
2001

ProQuest LLC
789 East Eisenhower Parkway
P.O. Box 1346
Ann Arbor, MI 48106-1346

Table of Contents

Abstract

The facilitative glucose transporter, GLUT4 undergoes insulin-dependent movement to the cell surface in adipocytes. It appears to be sequestered out of an endosome system and into a reservoir or storage compartment from which it can be rapidly recruited in response to insulin. Due to the lack of sensitive markers and effective methods to study the movement of GLUT4 between compartments, novel markers were developed and described in this thesis. In particular a probe was needed that would tag cell surface GLUT4 and allow translocation kinetics to be followed without the need to fractionate the cells. The experiments described here test the efficiency of three new membrane-impermeant biotinylated photoaffinity labels, Bio-LC-ATB-BGPA, Bio-LC-G15 and Bio-SS-ATB-BGPA to detect GLUT4 in rat adipose cells. The Bio-LC-ATB-BGPA, Bio-LC-G15 labels GLUT4 efficiently. The Bio-LC-G15 compound has a very long spacer arm and this has allowed interaction with avidin in intact cells. The compound has therefore been successfully used to directly measure GLUT4 exocytosis. However, the Bio-SS-ATB-BGPA compound was ineffective in labelling GLUT4, probably due to its cleavable disulphide group. A polyclonal amino-terminal GLUT4 antibody has also been developed and characterised. This antibody showed similar characteristics to carboxyl-terminal GLUT4 antibodies when used in detecting GLUT4 by Western blotting. However, confocal microscopy revealed differences. The GLUT4 signal intensity was lower in basal than insulin-stimulated cells when using the carboxyl-terminal but not the amino-terminal antibody. It is suggested that this effect may be related to epitope masking of the GLUT4 carboxyl-terminus in the storage compartment of basal cells. Density gradient centrifugation was employed in an attempt to separate different populations of intracellular GLUT4 vesicles. From analysis of the sedimentation of GLUT4 on glycerol and self-forming iodixanol gradients it appeared that the levels of GLUT4 in the endosome compartment of rat adipocytes was very low. This situation contrasts with that reported for 3T3-L1 cells and it is postulated that the rat adipocytes have a more efficient mechanism for removing GLUT4 from the endosome system. Computer simulations of trafficking between intracellular compartments revealed that in order to establish high GLUT4 levels within the endosome system, it was necessary to have some retrograde movement from the GLUT4 storage compartment back into the endosome system.

Acknowledgements

I would like to thank Professor Geoff Holman for his guidance and support throughout my studies at Bath University. I am grateful to him for allowing me the opportunity to carry out my research in his laboratory.

I would like to express my heartfelt gratitude for the love and support from my parents, throughout my academic studies. My deepest thanks also goes to my husband Louis Constandinos, who has been patient with me in all those stressful moments in and out of the lab.

To all those members of Geoff Holman's laboratory, past and present I would like to say a big thank you: Jing Yang, Alison Gillingham, Françoise Koumanov, Alison Gibbard, Darren Harper, Paul Whitley and Makoto Hashimoto. I would like to thank Jing for her help in the labelling studies and her patience in teaching me all the valuable techniques needed for this research. Thank you to Makoto for the synthesis of the photoaffinity labels and to Darren for raising the amino-terminal GLUT4 antibody. I would also like to thank all the members of the lab for making it a fun and interesting place to work.

Abbreviations

ACRP30	Adipocyte complement related protein of 30 kDa
AEBSF	4-(2-Aminoethyl)benzenesulfonylflouride, HCl
ARF	ADP Ribosylation Factor
AP	Adaptor Protein
ATB-BMPA	2-*N*-4-(1-azi-2,2,2-trifluroethyl)benzoyl-1,3-bis(D-mannose-4-yloxy-2-propylamine
ATB-BGPA	2-*N*-4-(1-azi-2,2,2-trifluroethyl)benzoyl-1,3-bis(D-glucose-4-yloxy-2-propylamine
ATP	Adenosine Trisphosphate
Bio-	Biotinylated
BSA	Bovine Serum Albumin
CHO	Chinese Hamster Ovary Cells
Ci	Curies
CYT	Cytosol
Da	Daltons
°C	degrees Centigrade
DTT	DL-dithiothreitol
ECL	Enhanced chemiluminescence
EDTA	Diaminoethanetetra-acetic acid disodium salt
EEA1	Early endosomal autoantigen 1
EGTA	Ethylene glycol-bis(β-aminoethyl ether)N,N,N',N'-tetraacetic acid
GDP	Guanosine diphosphate
GLUT	Glucose Transporter
GLUT4	Insulin-regulated Glucose Transporter
g_{max}	maximum gravity
GSV	GLUT4 Storage Vesicles
GTP	Guanosine 5'-triphosphate
GTPγS	Guanosine-5'-O-(3-thiotriphosphate)
HDM	High Density Microsomes
HEPES	(N-[2-Hydroxyethyl]piperazine-N'-[2-ethenesulfonic acid])
HES	HEPES-EGTA-Sucrose
HRP	Horse radish peroxidase
IDDM	Insulin Dependent Diabetes Mellitus
IR	Insulin receptor
IRS	Insulin receptor substrate
KRH	Krebs-Ringer-HEPES
LDM	Low density microsomes
LC	Long chain linker (amino-caproate)
M6PR	Mannose 6-phosphate Protein Receptor
MES	2-[N-Morpholino]ethanesulfonic acid
NIDDM	Non-insulin Dependent Diabetes Mellitus
NSF	N-ethylmaleimide Sensitive Fusion
PBS	Phosphate-buffered Saline
PI	Phosphatidylinositol
PI 3-k	Phosphoinositide 3-kinase

PKB	Protein kinase B
PKC	Protein kinase C
PM	Plasma membrane
rpm	revolutions per minute
SDS-PAGE	Sodium Dodecyl Sulphate- Polyacrylamide Gel Electrophoresis
SNAP	Soluble NSF Attachment Protein
SNARE	Soluble NSF Attachment Protein Receptor
SS	Disuphide Unit
SSVs	Small Synaptic Vesicles
TES	Tris-EDTA Sucrose
TBS	Tris-Buffered Saline
TBS-T	Tris-Buffered Saline with Tween 20
TEMED	N, N, N', N'-tetramethyletyenediamine
TGN	*trans*-Golgi Network
TGN38	*trans*-Golgi Network Marker 38
Tf	Transferrin
TfR	Transferrin Receptor
TV	Tubulo-vesicular
t-SNARE	target SNAP receptor
UV	ultraviolet
v-SNARE	vesicle SNAP receptor
VAMP	Vesicle Attachment Membrane Protein

1.0 Introduction

1.1 The Facilitative Glucose Transporter Family

1.1.1 The Function and Tissue Expression of Glucose Transporters

In mammals, the major fuel of the tissues is the carbohydrate, glucose. In order to utilise this sugar, a family of integral membrane proteins termed glucose transporters, or GLUTs, mediate the transfer of sugars over the plasma membrane. The transporters are not coupled to any energy requiring components, such as ATP hydrolysis or a H^+ gradient, but act as facilitative transporters (Baldwin and Lienhard, 1981). The transport of the sugar is bi-directional, although the net transport always occurs in the direction of high to low sugar concentration. The glucose transporters display a strong specificity for D-stereoisomers of hexose sugars. Typical natural substrates for these transport proteins include D-glucose, D-galactose, D-mannose and D-xylose.

To date, eight glucose transporters have been identified using purification and recombinant DNA techniques, (Table 1.1). These glucose transporters have been denoted GLUT1 through GLUT5 and GLUT8/XI and GLUT9, according to their chronological identification. GLUT6 is a pseudogene with no protein product (Kayano *et al.*, 1990). GLUT 1, also known as the erythrocyte-type glucose transporter, has been extensively studied in relation other glucose transporters. GLUT1 is abundant in red blood cells (3-5% of the membrane protein) and brain microvessels but is also present in almost all tissues. Its function has been suggested to be to help meet the energy requirements of cells in basic non-stimulated conditions. GLUT1 was purified by Baldwin and colleagues (Baldwin *et al.*, 1982) which enabled researchers to generate antibody probes for the protein (Baldwin and Lienhard, 1981; Davies *et al.*, 1987a; Lowe and Walmsley, 1986; Walmsley, 1988). The antibodies were utilised to isolate the cDNA clone and the gene sequence for GLUT1 (Birnbaum *et al.*, 1986; Fukumoto *et al.*, 1988; Mueckler *et al.*, 1985; Williams, 1988). The GLUT1 cDNA was then used to probe libraries from various tissues. This approach led to the discovery of other mammalian glucose transporters, (Table 1.1).

Table 1.1: Major sites of expression of the different glucose transporters in human and rodent tissues.

Isoform	Tissue	Reference
GLUT1	Placenta; brain; blood-tissue-barrier; adipose and muscle tissue (low levels); tissue culture cells; transformed cells.	See review Seatter and Gould, 1999
GLUT2	Liver; pancreatic β-cell; kidney proximal tubule and small intestine (basolateral membranes)	Seatter and Gould, 1999
GLUT3	Brain and nerve cells in rodents. Brain, nerve; low levels in placenta, liver and heart (humans).	Seatter and Gould, 1999
GLUT4	Muscle, adipose and heart tissue.	Seatter and Gould, 1999
GLUT5	Small intestine (apical membranes), kidney, testis, brain, muscle adipose tissue, muscle and brain at low levels (human) Small intestine (apical membranes), kidney (rat).	Seatter and Gould, 1999
GLUT8/XI	Blastocyst/ neuronal cell bodies and the most proximal dendrites	Ibberson *et al.*, 2000
GLUT9	Brain and leucocytes	Doege *et al.*, 2000

1.1.2 Glucose Transporter Structure

When GLUT1 was molecularly cloned and sequenced (Baldwin *et al.*, 1982) a 12 membrane-spanning-domain model for GLUT1 was proposed. This was based on its hydropathy analysis (Mueckler *et al.*, 1985). The analysis of the predicted amino acids of all the mammalian glucose transporters show that they are highly homologous with one another. A schematic representation of the proposed structure of the glucose transporter is given overleaf (Figure 1.1).

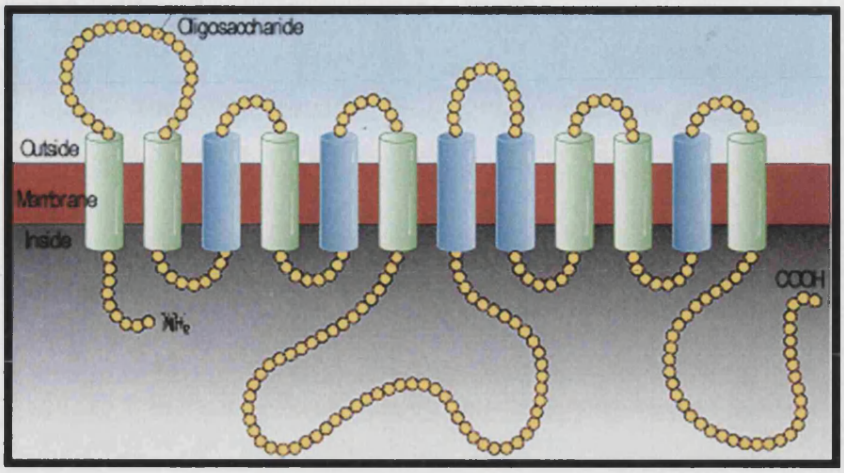

Figure 1.1: Schematic Representation of the structure of the glucose transporter

The common features which were revealed by sequence alignment of the glucose transporters are:

- 12 amphipathic helices arranged with the amino- (NH2) and carboxyl- (COOH) termini at the cytoplasmic surface.
- A large loop between helices 6 and 7 divides the structure into two halves, the amino-terminal domain and carboxyl-terminal domain.
- There is a large loop between helices 1 and 2.
- Loops between the remainder of helices at the cytoplasmic face are conserved and approximately 8 residues long. Loops at the extracellular surface of these proteins are relatively longer and have variable amino acid sequences.

With the advent of molecular biology, issues of structure-function relationships within the glucose transporters were addressed. It has been postulated that within GLUT1, the substrate passes through an aqueous channel, structurally made of five 12 membrane-spanning helices, (helices 3, 5, 7, 8 and 11) (Hresko *et al.*, 1994; Mueckler *et al.*, 1985). The residue Val165 in helix 5 of GLUT1 has been identified to be crucial in transport activity of sugar (Mueckler *et al.*, 1997). The substitution of the residue for groups with more bulky aliphatic side chains reduced transport activity. It was proposed that the residue Val165 lies within the aqueous pore through which the substrate sugars traverses, and thus hindering sugar transport by sterically occluding the pore. The transporters are said to exist in either of two conformations, with the sugar substrate binding site exposed to either the extracellular surface of the membrane, or the cytoplasmic face. Mutagenesis studies have

suggested that the putative transmembrane helices 7, 8 and 9 are involved in the exofacial binding site region (Hashiramoto *et al.*, 1992). The transmembrane helices 10 and 11 are thought to constitute at least part of the endofacial site (Inukai *et al.*, 1994).

It is thought that transmembrane 7 plays a major role in sugar transport by determining which sugar substrate is transported in each GLUT (Arbuckle *et al.*, 1996). Current investigations by Seatter and colleagues indicate that a QLS motif, (Gln -Leu-Ser) in helix 7 acts as a molecular filter that dictates the ability of GLUTs 1, 3 and 4 to transport D-glucose with high affinity but not D-fructose (Seatter *et al.*, 1998). The QLS motif is absent in helix 7 of GLUT2 and GLUT5, the GLUTs that are able to transport D-fructose. Using a range of chimeric glucose transporters comprised of GLUT2 (*HVA motif*) and GLUT3 (*QLS motif*) in Xenopus Oocytes, the abilities to transport D-fructose in these mutants were measured. There was an increase in D-fructose transport in the chimeric GLUT3 and a decrease in affinity for D-fructose in the chimeric GLUT2. The QLS region is thought to be intimately involved in substrate recognition at the exofacial binding site of the glucose transporter by interaction with the C-1 position of the incoming sugar. Other important residues which have been identified have been GRR (Gly-Arg-Arg) sequence in the intracellular loop between helices 8 and 9 (Saravolac *et al.*, 1997). Mutation of the GRR sequence between helices 8 and 9 of GLUT4 destroyed transport activity, but ligand binding to the exofacial and endofacial binding sites still occurred. Experiments indicate that the conserved GRR sequence in all glucose transporters may be involved in the conformational change that accompanies sugar transport (Schurmann *et al.*, 1997). Further work is necessary and is still being carried out to obtain a coherent picture of the structure-function of these glucose transporters, (for review see Barrett *et al.*, 1999).

1.2 GLUT4: The Insulin-Regulatable Glucose Transporter

1.2.1 GLUT4 in Insulin-Sensitive Cells

The effect of insulin on glucose transport has been studied extensively in rat white adipocytes. Isolated rat adipocytes exposed to insulin show a large increase (20-fold) in the rate of glucose transport (Simpson *et al.*, 1986). This increase in glucose transport activity is associated with an increase of Vmax, but with little or no change in the Km. For many years, researchers postulated that the increase in glucose transport activity in insulin-stimulated tissues was due to an alteration of the intrinsic activity of glucose transporters at the plasma membrane (Czech *et al.*, 1992). However, in the early 1980s, two independent groups discovered that the increase in glucose transport was due to a net 'translocation' of transporters from inside the cell membrane to the cell surface (Cushman and Wadzala, 1980; Suzuki and Kono, 1980). Since this landmark discovery, investigations to identify the glucose transporters that translocate to the plasma membrane in insulin-sensitive tissues have been pursued. With the application of molecular biology, cloning techniques by five independent groups identified the insulin-regulatable GLUT4 isoform (Birnbaum, 1989; Charron *et al.*, 1989; Fukumoto *et al.*, 1989; James *et al.*, 1989a; Kaestner *et al.*, 1989). The GLUT4 isoform is found only in insulin target cells i.e. white and brown adipose cells, cardiac myocytes and skeletal muscle. That GLUT4 translocation is responsible for the increase in glucose transport in muscle, fat and heart tissues, which is generally accepted. However, the mechanism by which its translocation is triggered with insulin and how it moves from intracellular site(s) of the cell are issues being addressed.

1.2.2 The Rationale for Studying GLUT4 Trafficking

Insulin from the β cells of the pancreatic islets of Langerhans (Deforonzo *et al.*, 1992) triggers an increase in GLUT4 at the plasma membrane of insulin target tissues. This enables the removal of high levels of glucose from the bloodstream by virtue of the increase in glucose transporter activity across the plasma membrane. The presence of insulin also acts to catalyse key enzymes for hepatic glycogen production from glucose, synthesis of proteins in muscle, and triglyceride formation in adipose tissue to allow the

storage of fuels. These actions enable glucose homeostasis to occur. Defects in the regulation of glucose transport underlie certain pathophysiological conditions such as non-insulin-dependent diabetes mellitus, (NIDDM). Diabetes Mellitus is a complex disease formed by the 'overproduction' of glucose by the liver and 'underutilization' by other organs such as muscle and adipose and other insulin-dependent tissues. There are two forms of this disease, Type 1 Diabetes, also known as juvenile onset (insulin-dependent diabetes mellitus: IDDM) and Type 2, maturity onset (non-insulin dependent diabetes mellitus: NIDDM). It is the Type 2 Diabetes that accounts for 90-95% of all cases of diabetes (American Diabetes Association, 1997). Type 1 (insulin-dependent) Diabetes appears mainly in childhood and is the result of the autoimmune destruction of the pancreases β cell population. In contrast, Type 2 Diabetes develops gradually over many years. In the early stage of Type 2 Diabetes, patients suffer from an inadequate response to insulin. This is termed 'insulin resistance'. At first, the pancreas may compensate for this by increasing insulin secretion causing high levels of plasma insulin. This is hyperinsulinemia. The β cells may however eventually become 'exhausted' which results in impaired function and the development of Diabetes. It has been postulated that defects in insulin-stimulation of the glucose transporter causes this insulin resistance (Garvey *et al.*, 1993; Garvey *et al.*, 1998). The worldwide prevalence of Diabetes is increasing at such a rapid pace that the World Health Organisation (WHO) has identified diabetes as an epidemic condition (King and Rewers, 1991). According to the World Health Report 1998, Diabetes in adults will more than double globally from 143 million in 1997, to 300 million by 2025 (World Health Organisation, 1998). Thus, the mechanisms of the components of glucose transport and the trafficking and targeting action of GLUT4 must be unearthed.

1.2.3 The Insulin Signalling Pathway

Many different insulin signalling pathways have been implicated in insulin-stimulated GLUT4 translocation. Although the work in this thesis does not touch upon insulin signalling, it is important to mention the main components of the system, as defects within this signal-transduction process may lead to insulin resistance (Section 1.2.2).

Insulin binds to the heterotrimeric ($\alpha_2\beta_2$) insulin receptor (IR), which results in autophosphorylation of tyrosine residues in the β-subunits. This in turn leads to the association and phosphorylation of downstream proteins. Target proteins for the insulin receptor include a family of multi-functional docking proteins known as insulin-receptor substrates (IRS). Four members of the IRS family have been described so far: IRS-1, (Sun *et al.*, 1991), -2, (Sun *et al.*, 1995), -3 (Lavan *et al.*, 1997a) and -4 (Lavan *et al.*, 1997b). IRS1 and IRS2 (White, 1998) are most notably the target proteins for the IR. Phosphorylation of these IRS proteins, triggers the activation of a number of signalling cascades, one of which includes activation of phosphatidylinositol 3-kinase (PI 3-kinase). This signal transduction pathway ultimately results in the exocytic translocation of GLUT4 vesicles from an intracellular pool to the plasma membrane.

Substantial data has supported a necessary role for the class 1a p85/p110-type, PI 3-kinase in insulin-stimulated GLUT4 transloaction. Wortmannin (Ui *et al.*, 1995) and LY294002 (Vlahos *et al.*, 1994) are specific inhibititors of PI 3-kinase. Inhibition of PI 3-kinase activity either with wortmannin (Clark *et al.*, 1994; Kotani *et al.*, 1995) or LY294002 (Kotani *et al.*, 1995) and by the expression of dominant interfering mutants of p85 (Hara *et al.*, 1994) in adipocytes, causes a complete block in insulin-stimulated GLUT4 trafficking. Conversely, expression of constitutively active PI 3-kinase stimulates glucose transport (reviewed in Shepherd *et al.*, 1998). PI 3-kinase forms 3' phosphoinositides, of which its product phosphoinositide-3,4-5-trisphosphate, (PIP3) is also required for GLUT4 translocation (Vollenweider *et al.*, 1999).

The insulin-stimulated generation of PIP3 at the plasma membrane functions to activate the phosphoinositide-dependent protein kinase 1 (PDK1), (Alessi *et al.*, 1997; Stokoe *et al.*, 1997), which phosphorlyates and activates two classes of downstream serine-threonine kinases: Protein kinase B (PKB/Akt) and Protein kinase Cζ (PKCζ/λ) (Currie *et al.*, 1999). Several recent studies have indicated that Akt2 is a key player in mediating insulin's full effects on GLUT4 translocation. Dominant negative Akt mutants and microinjection of Akt peptides into insulin-responsive cells inhibit insulin-stimulated GLUT4 translocation by 60% (Hill *et al.*, 1999; Wang *et al.*, 1999). Expression of a constitutively active Akt in adipocytes and L6 myotubes has been shown to stimulate GLUT4 translocation (Cong *et*

al., 1997; Wang *et al.*, 1999). Dominant negative PKCζ/λ mutants or microinjection of an anti-PKCλ antibody or pseudosubstrate peptides inhibit GLUT4 translocation (Bandyopadhyay *et al.*, 1999; Kotani *et al.*, 1998; Saad *et al.*, 1993; Yang *et al.*, 2000). Similar to Akt, the overexpression of wild-type or constitutively active PKCζ/λ stimulates GLUT4 translocation (Bandyopadhyay *et al.*, 1999; Etgen *et al.*, 1999; Kotani *et al.*, 1998). Investigators are now looking into downstream targets of either Akt or PKCζ/λ and their significance in GLUT4 trafficking. It has been reported that PKCζ interacts with Akt (Barthel *et al.*, 1998; Doornbos *et al.*, 1999). The significance of this interaction is unclear, although it has been suggested that the PKCζ masks the PIP3 binding sites for Akt, thus acting as a negative regulator (Doornbos *et al.*, 1999). The Akt is released in the presence of PDK1, allowing simultaneous activation of PKCζ and Akt.

In addition to the PI 3-kinase signalling, it has been recently demonstrated that a pathway, which includes the proto-oncoprotein Cbl, is involved in GLUT4 translocation. Insulin-stimulation results in Cbl tyrosine phosphorlyation via its adaptor protein, CAP, (Ahmed *et al.*, 2000; Krook *et al.*, 1997; Ribon *et al.*, 1998). The Cbl/CAP complex is proposed to initiate a signalling pathway that is independent of PI 3-kinase to generate GLUT4 translocation (Baumann *et al.*, 2000). The specific downstream signals of the Cbl/CAP complex and their interaction between PKCζ and Akt are yet to be determined, (reviewed in Watson and Pessin, 2001).

1.3 The Study of Trafficking of GLUT4 Vesicles

1.3.1 GLUT4 Vesicles

GLUT4 protein is found in small vesicles, which can be fractionated from fat cells. Simpson *et al.*, have established a standard experimental protocol of differential centrifugation of fractions from mature rat adipocytes (Simpson *et al.*, 1983). Subfractionation yields the plasma membrane (PM), high density microsomes, (HDM) which are enriched in endoplasmic reticulum and low density microsomes, (LDM), enriched in the Golgi apparatus. In the basal state, GLUT4 is found in the LDM and to a lesser extent in the HDM (Zorzano *et al.*, 1989). GLUT4 found in these fractions are uniform vesicles of around 50 nm, (Kandror *et al.*, 1995) with a sedimentation distribution close to that of ribosomes and with a buoyant density of about 1.12 g/cm^3 (Kandror and Pilch, 1996). GLUT4 vesicles in adipocytes show that they comprise 2-3% of the LDM fraction, and about 0.2% of cellular protein (James *et. al.,* 1987; Zoranzo *et. al.,* 1989).

1.3.2 GLUT4 Recycling Kinetics

In both the basal and insulin-stimulated states of fat and muscle cells, GLUT4 vesicles are continuously internalised and recycled back to the cell surface, (Yang and Holman, 1993). In basal adipocytes, GLUT4 has an exocytotic rate (kex) which varies between 0.01^{-1} min and 0.024 min^{-1} (Jhun *et al.*, 1992; Satoh *et al.*, 1993; Yang and Holman, 1993). In comparison to other recycling proteins such as GLUT1 (kex = 0.035 min^{-1}) and transferrin receptor (kex = 0.111 min^{-1}), the exocytotic rate of GLUT4 is very slow (Tanner and Lienhard, 1987; Yang and Holman, 1993). With insulin-stimulation the rate of GLUT4 exocytosis increased to between 0.32 min^{-1} and 0.86 min^{-1} (Jhun *et al.*, 1992; Satoh *et al.*, 1993). GLUT4 moves from an intracellular location to the cell surface with a half time of approximately 1.5 min. This is subsequently followed by the stimulation of glucose transport with a half time of this 2.5 min at 37 °C (Holman *et al.*, 1994).

As well as the 10-to 20-fold increase in the rate of GLUT4 exocyotsis studies have shown a decrease (1.3 - 3-fold) in the rate of GLUT4 endocytosis (Czech *et al.*, 1993; Czech, 1995; Holman and Cushman, 1996; Jhun *et al.*, 1992; Kandror and Pilch, 1996; Satoh *et al.*,

1993; Yang and Holman, 1993). These observations are consistent with the hypothesis that in the absence of insulin, GLUT4 is sequestered and stored into intracellular compartments or a specialised storage compartment. In the presence of insulin GLUT4 is mobilised and recycles back to the cell surface.

1.3.3 Methods used to Study GLUT4 Trafficking

Important information on the kinetics of GLUT4 (and GLUT1) movement from intracellular site(s) to the plasma membrane in the absence and presence of insulin has been generated using photoaffinity probes for GLUT4 (Yang and Holman, 1993). Photoaffinity labelling has also enabled the study of aspects of the structure and catalytic function of glucose transporters. Photoaffinity labelling requires the modification of the natural ligand by the incorporation of a chemically inert but photochemically labile group (Bayley and Knowles, 1977). The fungal metabolite cytochalasin B (Cushman and Wardzala, 1980), and the diterpene forskolin (Joost and Steinfelder, 1987) are lipophilic compounds which bind with high affinity to glucose transporters. These ligands inhibit glucose transport activity, and their binding to the transporters is in turn inhibitable by glucose. The photolabels have been used extensively to identify and characterise the glucose transporter isoforms. For example, the photolabelling with [^{3}H]cytochalasin B of different mutant glucose transporters has led to the identification of the amino acid residues that play an important role in glucose transport activity (Inukai *et al.*, 1994; Muraoka *et al.*, 1995). The derivative of forskolin, 3-[125I]iodo-4-azidophenethylamido-7-O-succinyldeacetyl-forskolin (IAPS-forskolin) has high specificity of photoincorporation into glucose transporters (Wadzinski *et al.*, 1987). With IAPS-forskolin an additional binding site to the transmembrane 10 has been described near the transmembrane 9 domain (Hellwig *et al.*, 1992; Schurmann *et al.*, 1993).

A series of photoaffinity compounds, that have generated a large amount of data used in quantifying glucose transporter levels and understanding the trafficking kinetics of the different glucose transport isoforms, are the bis-hexoses developed by Holman and colleagues (Clark *et al.*, 1990; Holman *et al.*, 1985; Midgley *et al.*, 1985a,b). Unlike cytochalasin B and forskolin the compounds developed by Holman and colleagues do not permeate the cell. This characteristic has enabled glucose transporters at the cell surface of

intact cells to be tagged. The determination of levels of glucose transporters at the cell surface, and subsequently their recycling kinetics between the plasma membrane and intracellular compartments, has been achieved (Calderhead *et al.*, 1990; Clark *et al.*, 1991; Holman *et al.*, 1990; Holman and Cushman, 1994; Yang *et al.*, 1992a; Yang and Holman, 1993).

The development of the membrane-impermeant hexose analogues first began in 1985 and is still on going in order to produce more sensitive probes to study glucose transporters. It was found that a compound synthesised with an amino group (propyl-2-amine bridge) between two D-mannose moieties had a high affinity for glucose transporters. This 1,3-bis-(D-mannos-4-yloxy)-2-propylamine (BMPA) compound was attached to a range of photoactivateable groups in order to use the compound as a photoaffinity label. The resulting compounds were hydrophilic and membrane-impermeant (Midgley *et al.*, 1985a). The photoreactive derivatives of BMPA were found to have a higher affinity for the glucose transporter than the parent compound D-mannose, but the affinity was much lower than that of cytochalasin B (Carter-Su *et al.*, 1982; Shanahan, 1982) and IAPS-forskolin compounds (Wadzinski *et al.*, 1987). The first effective photoactive label was from the azidosalicoyl derivative of BMPA, (ASA-BMPA). This compound produced selective labelling for the erythrocyte glucose transporter (Holman *et al.*, 1986), but this proved not to be as selective as the carbene precursor benzophenone derivative of BMPA, (BB-BMPA) (Holman *et al.*, 1988). The BB-BMPA required a relatively longer irradiation time to incorporate into the transporters than the ASA-BMPA compound. Eventually, an alternative diazirine substituent was utilised to produce the compound ATB-BMPA (Clark *et al.*, 1990). The structure of the ATB-BMPA compound is shown in Figure 1.2i, page 13 On irradiation, the diazrine of ATB group looses nitrogen and generates a short-lived carbene (Figure 1.2ii). This carbene interacts with the active-site protein side-chains. The ATB-BMPA compound has been shown to be highly selective for the glucose transporter. It has a high affinity for the erythrocyte glucose transporter GLUT1 (the Ki is 300 μM) and for the GLUT4 insulin-sensitive isoform in adipocytes (Ki for basal and insulin-stimulated glucose transport is 247 μM) (Holman *et al.*, 1990). The binding site of ATB-BMPA in the glucose transporter is proposed to be at the extracellular binding site. Proteolysis cleavage studies have revealed that the ATB-BMPA compound binds between the residues Ala 301

and Arg 330 on the transmembrane domain of GLUT1 (Baldwin, 1993; Gould and Holman, 1993).

The tritiated derivative of the ATB-BMPA compound combined with specific glucose transporter antibody immunoprecipitation, enabled estimation of the levels of glucose transporter isoforms in a range of cell types. The levels of GLUT4 and GLUT1 at the cell surface in insulin-treated rat adipocytes compared to basal cells increased by 15-20 fold and 3-5 fold, respectively (Calderhead *et al.*, 1990; Holman *et al.*, 1990). The levels of the glucose transporters at the cell surface have been directly compared to 3-O-methyl-D-glucose transport under different conditions. The ATB-BMPA photolabelling technique revealed that there were high levels of GLUT1 and low levels of GLUT4 present in 3T3-L1 cells when chronically treated with insulin compared with control cells (Palfreyman *et al.*, 1992). It was concluded that GLUT1 did not contribute as significantly as GLUT4 to 3-O methyl-D-glucose transport.

Further development of the ATB-BMPA compound has been pursued and have led to the development of labels which are not dependent on tritium for their detection (Koumanov *et al.*, 1998). These relatively new compounds rely on the attachment of a biotin molecule to the central core of the ATB-BMPA unit by a polyethylene glycol linker, (Figure 1.2iii). The detection of the tagged glucose transporter occurs by the interaction of biotin with avidin or streptavidin. The biotin-linked ATB-BMPA compounds have advantages over the tritiated compounds. Firstly, they provide a means for sensitive non-radioactive detection of cell surface transporters. Secondly, there is potential for studying glucose transporter translocation without fractionation. This is one of the issues studied in this thesis. The biotin attached to the label enables the tagged glucose transporter to be detected with fluorescent biotin antibodies in confocal microscopy.

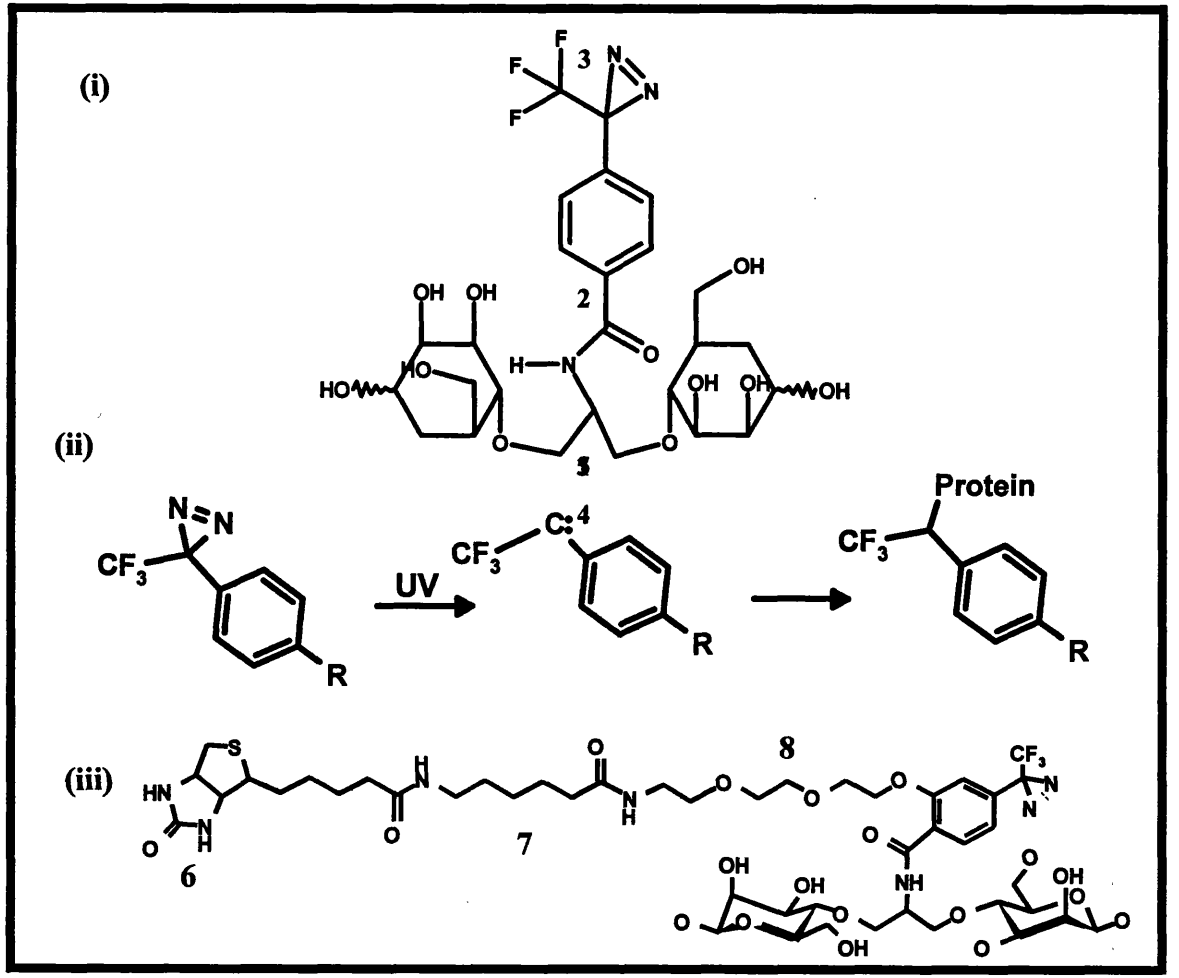

Figure 1.2: The Structure and Activation of the ATB-BMPA Compound with UV Irradiation. The ATB-BMPA, (2-N-(1-azi-2,2,2-trifluoroethyl)benzoyl-1,3-bis(D-mannos-4-yloxy)-2-propylamine) is represented in Figure 1.2i. The compound consists of a propylamine bridge (1) between two mannose units (2) and a photoreactive diazirine (3). Upon UV irradiation, a carbene (4) is generated which cross-links with the protein (5), (see Figure 1.2ii). A biotin group (6) attached to the ATB-BMPA compound with an amino-caproate (7) polyethylene glycol linker (8) is shown in Figure 1.2iii to give Bio-LC-ATB-BMPA.

1.3.4 Marker Proteins for Tracking GLUT4 Vesicles

To elucidate the mechanism in which GLUT4 is stored and shuttled within the cell, a comparison of trafficking of GLUT4 with other proteins found in the endosomal system and trans-Golgi network can be made. Examples of marker proteins to the different trafficking pathways are in Table 1.2 below.

Table 1.2: Established Marker Proteins

TGN	Recycling Endosome	Sorting Endosome	Late Endosome	Lysosomes
TGN38	TfR	TfR	CI-M6PR	lgp120
Furin	Rab11	EEA1	Rab7	LAMP-1
ß-COP	Rab4	Rab5	Rab9	Lysobisphosphatidic acid

Abbreviations used: TGN, *trans*-Golgi network; Rabs, small GTP-ases; CI-M6PR, cation-independent mannose-6- phosphate receptor; EEA1, early endosomal autoantigen 1; TfR, transferrin receptor; ß-COP, ß –cytosolic coat protein; LAMP, lysosome associated membrane protein. Table adapted from Clague (Clague, 1998)

The early endosome system is the major sorting station in the endocytic pathway. Material from this organelle is directed to either recycling endosomal systems (transferrin receptors); later endocytic compartments (EGF receptors) or regulated secretory vesicles (GLUT4). The TGN is the site of storing of newly synthesised membrane proteins. These can recycle between intracellular compartments and residence here are proteins such as the mannose-6-phosphate receptors (M6PRs), lysosomal proteins, and secretory proteins. The TGN (located in proximity to the *trans*-Golgi cisternae) is distinguished from endosomal elements by the use of the TGN38 marker protein (Luzio *et al.*, 1990; Reaves *et al.*, 1992) or furin (Bosshart *et al.*, 1994; Molloy *et al.*, 1994; Shapiro *et al.*, 1997). ß-COP (cytosolic coat protein), a protein found on the cis side of the Golgi complex in pancreatic acinar cells and on the lateral rims and trans face of the Golgi complex in spermatids (Oprins *et al.*, 1993; Martinez-Menarguez *et al.*, 1996) has also been used to track GLUT4, (see Section 1.5.2).

The trafficking of the transferrin receptor (TfR) is one of the best-characterised systems of protein trafficking. It moves between the cell surface and intracellular compartments of the cell. Studies on TfR (Tanner and Lienhard, 1987) recycling have defined a tubular 'recycling endosome' (see Section 1.5.1). Rabs (small GTPases) also mark

regions of the endosome system. The recycling endosome system is rich in the small GTPase Rab11, whereas Rabs 4 and 5 are found in early endosomes (Sheff *et al.*, 1999; Triscler *et al.*, 1999). It is proposed that Rab4 and Rab11 are involved in the regulation of recycling back to the plasma membrane, whilst Rab5 controls transport to early endosomes. The late endosomes represent the point in the endocytic pathway where the cation-independent (CI) mannose 6-phosphate receptor (M6PR) is most concentrated and from which it is recycled back to the TGN (Griffiths *et al.*, 1988). Degradative enzymes are active in the late endosome compartment, but are more concentrated in the lysosomes (Griffiths *et al.*, 1988; Tjelle *et al.*, 1996). All these compartments are established structures but ongoing research continually reveals the possibility of futher subdivisions within them. For example, the GTPases Rab4, Rab5 and Rab11 have been shown to have partial overlap with the TfR, thereby revealing many subdivisions of the transferrin compartment (Mohrmann and van der Sluijs, 1999).

In addition to the marker proteins, there are a number of proteins that are associated with GLUT4 vesicles. Some of these may be used to track GLUT4 vesicle movement. The insulin-responsive aminopeptidase (IRAP) shares many of the characteristics of GLUT4 and is used as a specific marker for GLUT4 trafficking (Garza and Birnbaum, 2000; Kandror and Pilch, 1994; Malide *et al.*, 1997b; Ross *et al.*, 1996). Its function is not yet defined. Sortilin is another GLUT4-vesicle associated protein (Lin *et al.*, 1997; Petersen *et al.*, 1997). This 110kDa protein has been found to be located primarily in the low density microsomes with GLUT4 in rat and 3T3-L1 adipose cells. Insulin caused a 1.7-fold increase in the amount of sortilin at the plasma membranes of 3T3-L1 adipocytes, as assessed by cell surface biotinylation (Morris *et al.*, 1998). The role of this protein is not known, but previous characterisation of sortilin has led to the suggestion that it functions to sort lumenal proteins from the *trans* Golgi network (Petersen *et al.*, 1997).

A 62 kDa carboxyl esterase (p62/CE) from rat adipose tissue has been recently identified to be associated with GLUT4 in rat adipose tissue (Lee *et al.*, 2000). Again, the function of the protein is unclear, but antibodies against p62/CE have been shown to abolish the insulin-induced recruitment of GLUT4 to the plasma membrane. GLUT4-enriched vesicles have also been found to be associated with acyl-CoA synthetase 1 (Sleeman *et al.*, 1998).

Other proteins that are being studied in comparison with GLUT4 vesicle trafficking include: leptin, an adipocyte complement related protein of 30 kDa (ACRP30), and a serine protease adipsin (Barr *et al.*, 1997; Hu *et al.*, 1996; Kitagawa *et al.*, 1989). The secretion of all three proteins is enhanced with insulin-stimulation and this process is dysregulated in obesity. However, studies so far have shown no evidence of leptin associating with GLUT4 vesicles (Barr *et al.*, 1997). Only 50% of GLUT4 vesicles are associated with adipsin (Millar *et al.*, 2000). Bogan and colleagues used endogenous ACRP30 and GLUT4 to define two different compartments for insulin-stimulated exocytosis in 3T3-L1 adipocytes (Bogan and Lodish, 1999). Pharmacologic PI-3 kinase inhibitors blocked ACRP30 secretion, similar to the inhibition of GLUT4 translocation. However, immunofluorescence showed no overlap in the subcellular distributions of GLUT4 and ACRP30 in unstimulated and in insulin-stimulated 3T3-L1 adipocytes. This was in contrast to the partial overlap of GLUT4 and the TfR. These studies showed that two different secretory pathways co-existed: one for ACRP30 and the other for GLUT4.

1.4 Regulated Vesicle Secretion and Membrane Trafficking

Many cells possess machinery that serves to regulate membrane traffic to the cell surface. Investigations have highlighted the fact that proteins trafficking from yeast to mammalian cells have similar basic mechanisms by which proteins move between intracellular compartments and the plasma membrane (Jackson, 1998; Le Borgne and Hoflack, 1998; Gu and Gruenberg, 1999; Marsh and McMahon, 1999). To gain an insight into the roles of proteins associated with GLUT4 vesicles, investigators have looked towards other membrane trafficking proteins and their involvement in regulated secretion, (for example neurotransmitter secretion), or constitutive intracellular vesicle trafficking pathways (such as the TfR). The movement of vesicles can be categorised into four general stages:

- Endocytosis or the formation of vesicles from specific cellular membranes
- Movement of the vesicle towards its target membrane
- Tethering/docking with the acceptor membrane
- Fusion of the lipid bilayers

Secretory granules are specialised vesicles containing bioactive molecules such as hormones and peptides. These vesicles are secreted in a regulated fashion when an external stimulus is received, resulting in their contents to be released. The secretory granules are found in all exocrine, endocrine, neuroendocrine and neuronal cells (reviewed by Tooze, 1998). A prime example is the regulated secretion of granules containing neurotransmitters that are stored near presynaptic terminals. Action potential entry into the presynaptic terminal results in calcium increases that trigger the exocytosis of the neurotransmitter granules and a release of their contents (reviewed by Martin, 1997). It has been suggested that GLUT4 may be analogous to neurotransmitters in that they are packaged into secretory granules and stored until insulin triggers their exocytosis (Martin *et al.*, 2000).

De novo biogenesis of secretory granules is required to replace the pool of secretory granules depleted by exocytosis. The biogenesis of secretory granules occurs at the TGN (reviewed by Tooze, 1998) whereas small synaptic vesicles are formed from the endosomal system (de Wit *et al.*, 1999) or directly from the plasma membrane (Schmidt *et al.* 1997). The biogenesis of secretory vesicles requires several regulated steps: (1) aggregation of regulated secretory proteins and their sorting to the membrane in the TGN; (2) budding from the TGN; (3) homotypic fusion of immature secretory granules; and (4) remodelling of the immature secretory granules by clathrin-mediated vesicle budding. This process generates larger, mature secretory granules. Maturation is highly regulated and results in the production of secretory granules with a precisely defined composition (reviewed by Tooze *et al.*, 2001).

1.4.1 Formation of Coated Vesicles

The first step in vesicle trafficking is the formation of coated vesicles with their selected material. Coats are derived from soluble, cytosolic precursors and bind to specific organelle membranes. Two basic types of coat complexes have been extensively characterised: COPI and COPII.

The clathrin-coated pit acts as the major port of entry for many receptors and proteins and is the paradigm for membrane-based sorting events in higher cells. Coated pits result from polymerisation of clathrin, adaptor complexes and a range of other molecules from the cytosol onto the membrane. Coat formation was first discovered by

Roth and Porter during their studies of yolk protein uptake in mosquito oocytes (Roth and Porter, 1964). They observed that when the yolk proteins bind to the oocyte surface, the membrane invaginates to form bristle-coated pits. These pits pinch off to form coated vesicles, which carry the adsorbed protein into the cell, the coat is then lost and the vesicles fuse to a storage granule. Their observations led to the proposal that the formation of coated pits and vesicles would be transient and that the coats would play a role in the formation of what is adsorbed and on the selectivity of the adsorbed material. Eventually, isolated coated vesicles from guinea pig brain were visualised by negative staining microscopy. The coats were shown to consist of a lattice-like polyhedral network (Kaneseki and Kadota, 1969). The major protein component of the vesicles was isolated and named clathrin (Pearse, 1975). Clathrin consists of both a heavy chain protein (HC) and two smaller polypeptide light chains (LC_a and LC_b), which assemble together (three heavy chains and three light chains) to form the basic clathrin assembly unit, the triskelion. Clathrin triskelions are heterogeneous in nature, as the distribution of the two different light chains is random (Hirst and Robinson, 1998). A number of proteins have been shown to internalise via clathrin coated pits, including low density lipoproteins (LDL), GLUT4 (Section 1.5.2), the TfR and the epidermal growth factor receptor (EGFR) (reviewed in Hirst and Robinson, 1998).

Many molecular interactions occur as the coated pit assembles, invaginates and pinches off (Gagescu *et al.*, 2000). Adaptor proteins, (Section 1.4.2) are targeted to the plasma membrane and trigger the subsequent assembly of clathrin into a curved polygonal lattice that pulls the membrane inward, forming a deep pocket. Adaptor proteins also interact directly with proteins to affect the concentration of proteins in coated pits. The GTPase dynamin, (Section 1.4.3) is targeted to the assembling clathrin lattice. On GTP binding, dynamin migrates to the necks of the emerging membrane bud and self-assembles into a small spiral structure, forming a "collar" at the neck of an invaginated coated pit (reviewed in Warnock and Schmid, 1996).

The COP (coatomer) coated vesicles were first identified and purified by Rothman from mammalian cells (Rothman, 1994) and by Schekman and colleagues from yeast (Pryer *et al.*, 1992). The COP proteins COPI and COPII, mediate vesicle formation in the endoplasmic reticulum (ER) and the Golgi (Springer *et al.*, 1999). Their assembly is regulated by the small GTP binding proteins, ADP-ribosylation factor (ARF1; Section 1.4.3) and Sar1 (Kuge *et al.*, 1994), respectively. COPI coats generally function in the

secretory pathway (Oprins *et al.*, 1983), although they may also act at the level of endosomes (Whitney *et al.*, 1995). COPII coats also act early in the secretory pathway but do so at a single site: they are responsible for forming ER transport vesicles, which then proceed toward cis-Golgi elements (Bednarek *et al.*, 1995).

1.4.2 Vesicular Targeting: Role of Adaptor Proteins

Vesicular traffic requires a set of recognition processes that differentitate the proteins to be moved from those that should remain in place. For example, COPI coats bind to ER-derived and Golgi membranes that form vesicles containing membrane proteins bearing the di-lysine motif, KKXX (Cosson and Letourner, 1994). Adaptor proteins are involved in regulating clathrin-coated vesicle formation.

Four adaptor complexes have been characterised to date. AP-1 localised to the TGN, AP-2 localised to the plasma membrane, AP-3 localised to the endosomal compartment and the newly described AP-4, targeted to or near the TGN, (the latter two protein coats do not seem to involve clathrin) (reviewed in Kirchhausen *et al.*, 1997; Dell'Angelica *et al.*, 1999). Adaptor complexes consist of two 100 kDa adaptins (γ-and β1- (AP-1), α- and β2 (AP-2), δ- and β3- (AP-3), ε- and β4 (AP-4)), and in addition, a medium $\approx$ 45 kDa μ chain (μ1, μ2, μ3, μ4) and a small $\approx$ 20 kDa σ chain (σ1, σ2, σ3, σ4) (reviewed Robinson and Bonifacino, 2001). All adaptor subunits are derived from protein superfamilies, the most distantly related are the α-, γ-, δ- and ε-subunits, which are thought to direct the complexes from the cytosol onto the host membranes (Schmid, 1997).

Adaptor proteins assist in uniform coat assembly under physiological conditions, (Zaremba and Keen, 1983). Evidence indicates that it is the β subunits of the adaptor complex which are responsible for the clathrin-adaptor interaction. Ahle and Ungewickell carried out binding assays of purified β2-adaptin interactions with clathrin. It was shown that the adaptin and clathrin bound with a stoichiometry of one to one, and could compete with the entire AP-2 complex for clathrin binding (Ahle and Ungewickell, 1989). However, not all adaptor complexes are thought to be involved in clathrin-coat assembly. The AP-3 complex is not enriched in purified clathrin-coated vesicles (Newman *et al.*, 1995; Simpson *et al.*, 1996). Furthermore, an *in vitro* system that reconstitutes the budding of synaptic-like microvesicles from PC12 endosomes is

dependent on AP-3 but apparently does not require clathrin (Shi *et al.*, 1998). Further work is necessary to characterise the function of AP-3 and AP-4 complexes.

In addition to their association with clathrin, adaptors also bind to the cytoplasmic tails of transmembrane receptors and transporters. The M6PR was shown to form aggregates with the plasma membrane adaptor complex AP-2 when incubated under non-denaturing conditions (Pearse, 1985). Later, *in vitro* binding assays revealed that adaptors at both the plasma membrane and the TGN bind to receptor tails (reviewed in Schmid, 1997). It is thought that the clathrin adaptor complexes bind to proteins via their sorting signals in their receptor tails including GLUT4 (see Section 1.6.2). Sorting signals, such as the tyrosine-based YXXϕ, (where X is any amino acid and Y is a bulky hydrophobic residue) or the dileucine motif are recognised by the subunits of the adaptor complexes. There is substantial evidence that these interact with all of the adaptor complexes via their μ- or β-subunits, presumably at differential binding sites within these subunits (for review see Kirchhausen., 1999).

1.4.3 GTP Binding Proteins in Vesicle-Coat Formation

There is a number of GTP binding proteins (GTPases), which control the formation of vesicle coats at distinct steps in intracellular membrane transport. These GTPases ae active when bound to GTP and inactive when bound to GDP. The presence of GTP has been shown to be important in GLUT4 translocation. Guanosine 5'-*O*-(3-thiotriphosphate (GTPγS) has been reported to stimulate glucose transport both by increasing the rate of exocytosis and by appreciably decreasing the rate of endocytosis (Shibata *et al.*, 1995).

Dynamin is a large, 100-kDa GTPase originally isolated from calf brain (Shpetner and Vallee, 1989). Three dynamin isoforms have been identified to date, sharing 80% homology at the amino acid level; a brain-specific isoform, Dynamin I, a ubiquitous isoform, Dynamin II and a testis-specific isoform, Dynamin III (Urrutia *et al.*, 1997). Dynamins consist of a tripartite GTP binding site in the N-terminus, a pleckstrin homology (PH) domain and a C-terminal proline rich region (reviewed in Urrutia *et al.*, 1997). Several studies have demonstrated a role for dynamin I in GLUT4 endocytosis. For example, Omata and colleagues compared the effect of wildtype dynamin to negative mutants of dynamin on GLUT4 endocytosis in CHO cells (Omata *et al.*, 1997).

The study showed an accumulation of GLUT4 at the cell surface under basal conditions in cells expressing the mutant dynamin. Similar results were produced in rat adipocytes (Al Hasani *et al.*, 1998), and in 3T3-L1 adipocytes (Kao *et al.*, 1998). Furthermore insulin was only able to recruit GLUT4 from the intracellular pool to the plasma membrane in cells expressing the wild-type dynamin, and not in cells expressing the mutant.

Dynamin II is also thought to have an effect on GLUT4 endocytosis. Volchuk and colleagues have studied the effect of dynamin II on GLUT4 endocytosis. In 3T3-L1 adipocytes insulin decreased the association of dynamin II with the plasma membrane by ~50% but there was no effect on the dynamin II associated with the low density microsome fraction (Volchuk *et al.*, 1998). In addition, these authors have also assessed the role of amphiphysin in GLUT4 trafficking. Amphiphysin is an SH3 domain containing protein, which binds to the proline-rich region of dynamin, and is thought to be important in recruiting dynamin to sites of endocytosis. Microinjection of a fusion protein containing the SH3 domain of amphiphysin into 3T3-L1 adipocytes inhibits TfR endocytosis and increased cell surface GLUT4. Furthermore, a peptide containing the proline-rich domain of dynamin (which binds to amphiphysin) inhibited GLUT4 re-internalisation following insulin stimulation. These data suggest that both dynamin II and amphiphysin play a role in GLUT4 endocytosis in 3T3-L1 adipocytes.

Other GTPases from the *Ras* superfamily, (Rad and ADP-ribosylation factors) have also been shown to be involved in GLUT4 translocation. The expression of Rad is increased in some type II diabetics and it has been hypothesised that it acts as a negative modulator of GLUT4 activity. Moyers and colleagues overexpressed Rad in the insulin-responsive cell lines, L6 rat myotubes and C_2C_{12} murine myotubes (Moyers *et al.*, 1996). This resulted in a 50-90% decrease in insulin-stimulated 2-dexoxy-D-glucose transport, with no detectable change in GLUT4 transloaction.

The ADP-ribosylation factors (ARFs) are 20-kDa nucleotide binding proteins which act as molecular switches for many trafficking pathways and are involved in the recruitment of coat proteins onto budding vesicles (reviewed in Roth, 1999). There are six ARF proteins identified in mammalian cells and two in *S. cerevisiae.* The mammalian ARFs fall into three classes based on sequence comparisons: class I contains ARFs -1,-2,-3; class II contains AFRs -4 and–5; class III contains AFR6.

ARF1 was discovered to be a component and requirement for the formation of COPI vesicles isolated from Golgi membranes (Rothman and Wieland, 1996). It also has a role in the formation of clathrin-coated vesicles, containing the adaptor proteins AP-1 at the TGN and AP-3 on the endosomes (Stamnes and Rothman, 1993; Ooi *et al.*, 1998). The function of the class II ARFs is unknown. AFR6 is found at the plasma membrane and is suggested to play a role in vesicle trafficking and in cytoskeletal organisation (Chavrier and Goud, 1999). The effect of insulin and AFR5 and ARF6 in GLUT4 trafficking has been analysed using ARF peptides (Millar *et al.*, 1999a). Insulin-stimulated glucose transport and GLUT4 translocation were inhibited by ~50% with a myristoylated AFR6 peptide. In contrast, the AFR5 peptide had no effect on GLUT4 translocation, but inhibited the appearance of TfR and GLUT1 at the cell surface. These authors suggest that ARF5 is involved in the regulation of endosomal traffic to the plasma membrane, while ARF6 controls the movement of GLUT4 in response to insulin, (Millar *et al.*, 1999a).

1.4.4 The SNARE Complex in Vesicle-Membrane Fusion

Before fusion can occur the vesicle has to be transported to its specific target membrane and docked there (Pfeffer, 1999). Several priming events prepare the vesicle for its fusion (Kleinchin and Martin, 2000). The fusion trigger, such as calcium then allows the release of its contents (Colombo *et al.*, 1997; Peters and Mayer, 1988).

In the 1980s Rothman and colleagues identified a pair of soluble proteins that were required for fusion of Golgi vesicles with acceptor Golgi stackes (Weidman *et al.*, 1989). These two proteins were NSF (*N*-ethyl-maleimide sensitive fusion protein) and SNAP (soluble NSF attachment protein). These proteins are thought to mediate the majority of intracellular trafficking events (review Bennett and Scheller, 1993).

Several proteins have been discovered to act as receptors for NSF and SNAP. These proteins are named SNAREs (for SNAP receptors) (Sollner *et al.*, 1993). The SNARE proteins were first categorised into either v-SNAREs or t-SNAREs, according to their vesicle or target membrane localisation. The first SNAREs to be discovered were syntaxin1 (t-SNARE), VAMP1 (vesicle-associated membrane protein, also called synaptobrevin) and SNAP-25 (25 kDa synaptosome associated protein) (Bennett *et al.*, 1992; Oyler *et al.*, 1989; Trimble *et al.*, 1998). Syntaxin and VAMP are anchored to the

membrane by a carboxyl terminal transmembrane domain. In contrast, SNAP-25 does not have a transmembrane domain. It presents two domains peripherally attached to the membrane by palmitoylation of four cysteine residues in the central region of the protein. The crystal structure of the neuronal SNARE complex has shown that one coil each of syntaxin and VAMP and two coils of SNAP-25 are involved to form a four-stranded coiled-coil structure, (Poirer *et al.*, 1998). The SNAREs are now classified according to conserved arginine (R-SNAREs) or glutamine residues (Q-SNAREs) in the center of the SNARE complex structure (Fasshauer *et al.*, 1998). This is in order to avoid ambiquity in the case of homotypic fusion (Fasshauer *et al*, 1998).

It was originally proposed that the SNAREs provided unique pairing and specificity of the vesicle for its target membrane and the ATPase activity of NSF drove the membrane fusion (Sollner *et al.*, 1993). However, other factors that interact with SNAREs have been characterised and are thought to act at the vesicle targeting and tethering stages (Pfeffer, 1999). In addition recent liposome fusion experiments showed some promiscuity between pairing of R-SNAREs and Q-SNAREs (McNew *et al.*, 2000). Small GTPases of the Rab family have been proposed to act at the vesicle targeting and tethering stage (reviewed by Zerial and McBride, 2001). Rab3A predominantly localises to synaptic vesicles and plays an important role in the regulation of neurotransmitter release (Fischer von Mollard *et al.*, 1990). In addition to Rab proteins, the synaptogamin family (Brose *et al.*, 1992) and nSec1 (neuronal homolog of the yeast Sec1 protein, also known as Munc18) family have been shown to interact with SNARE proteins (Pevsner *et al.*, 1994). Complexin (McMahon *et al.*, 1995) VAP33 (Skehel *et al.*, 1995) and synaptophysin (Wiedenmann and Franke, 1985) are also factors which interact with SNAREs. The precise nature of these interactions is yet to be determined.

The current hypothesis in vesicle docking and fusion is the 'zipper model' reviewed by Chen and Scheller (Chen and Scheller, 2001). It is thought that initially, syntaxin is bound to nSec1 and VAMP is bound to synaptophysin before the SNARE complex forms. Rab proteins have been hypothesised to dissociate nSec1 from syntaxin to allow coiling with VAMP and SNAP-25 (the four stranded coil-coiled SNARE complex). At this priming stage, calcium triggers the full 'zipping' of the coiled-coil complex (Scheggenburger and Neher, 2000). It is possible that a calcium binding protein such as synaptotagmin is involved at this stage. Once the vesicle contents are released, alpha SNAP and NSF are recruited to the SNARE complex. The hydrolysis of ATP by NSF

causes the SNARE complex to dissociate. This allows synaptobrevin, syntaxin and SNAP-25 to be free for another round of exocytosis (Banerjee *et al.*, 1996).

1.4.5 GLUT4 and SNARE Proteins

Proteins associated with GLUT4 and those involved in fusion have been identified. There are two forms of VAMPs, (VAMP2 and VAMP3) which are localised in insulin-stimulated tissues. The two VAMP members, VAMP2 and VAMP3 (cellubrevin) were shown in association with immunopurified GLUT4 vesicles from the LDM fraction of rat adipose cells. Both VAMPs translocated from the LDM to the plasma membrane with GLUT4 following stimulation by insulin (Cain *et al.*, 1992; Timmers *et al.*, 1996). VAMP2 is present on GLUT4 vesicles, which are insulin-stimulated, whilst cellubrevin is located on GLUT4 vesicles within the endosomal system (Malide *et al.*, 1997a; Martin *et al.*, 1996a; Martin *et al.*, 1998).

A protein related to the neuroendocrine specific synaptophysin has been identified in immunopurified GLUT4 (Brooks *et al.*, 2000). This protein, called pantophysin binds to VAMP2. Although its functional role is unclear, pantophysin may provide another marker for the analysis of GLUT4 vesicles in adipocytes.

Syntaxin 4 is predominantly found in insulin-regulated tissues. It is highly expressed in fat and muscle cells and is mainly targeted to the plasma membrane (Timmers *et al.*, 1996). It plays an important role in GLUT4 exocytosis. In permeabilised insulin-treated 3T3-L1 adipocytes, antibodies directed against syntaxin 4 or recombinant fusion proteins encoding the cytoplasmic tail of syntaxin 4 have been shown to block GLUT4 translocation (Volchuk *et al.*, 1996). SNAP-23 (syndet) is also present in the plasma membrane of these tissues (Rea *et al.*, 1998). It has been proposed that the two helical domains from SNAP23 associate with syntaxin 4 and VAMP2 to form a four-helix bundle structure. This structure is similar to that of the brain SNAREs (Sutton *et al.*, 1998).

Other proteins, which have been implicated in regulation of SNARE interactions on GLUT4 vesicles, are Munc-18c, synip and small molecular weight GTPases called Rabs. Munc 18c is a homologue of neuronal Munc18a, Munc 18b and the yeast protein nSec1 (Tellam *et al.*, 1995; Novick *et al.*, 1981). Munc 18c interacts with syntaxin 4 at

the plasma membrane. Using peptide constructs from Munc 18c, fusion between GLUT4 vesicles and the plasma membrane has been blocked (Tellam *et al.*, 1997). Synip also binds to syntaxin 4. This binding is restricted to basal cells and is reduced in insulin-stimulated cells (Min *et al.*, 1999). These observations suggest that insulin signalling might release synip from syntaxin 4, which in turn may lead to the increase in interaction with other proteins in the fusion process.

Small GTPases, called Rabs, interact with the docking step of v- and t-SNAREs and may catalyse the interactions of these, (Mayer and Whickner, 1997). In GLUT4 enriched vesicles, Rab4 and Rab11 have been isolated (Cormont *et al.*, 1996a; Kessler *et al.*, 2000). To study the role of Rab4 in rat adipocytes a transient co-expression of Rab4 with an epitope-tagged GLUT4 was used (Cormont *et al.*, 1996a). An enhanced retention of GLUT4 in the basal state was observed and the insulin-dependent release of GLUT4 was inhibited. The authors suggested that Rab4 might act in the storage and targeting of GLUT4. This notion is supported by work of Mora and colleagues (Mora*et al.*, 1997). The heterologous co-expression of Rab4 and GLUT4 in Xenopus oocytes lead to an increase in intracellular retention of GLUT4. A synthetic peptide corresponding to the C-terminal hypervariable domain of Rab4, inhibited insulin-stimulated glucose transport in rat adipocytes by about 50% without affecting the basal transport activity, (Shibata *et al.*, 1996). Insulin treatment resulted in the recruitment of Rab11 from the microsomal fraction to the plasma membrane. This is similar to that reported for GLUT4. At present, it is unclear how Rab11 or Rab4 affects targeting and translocation of GLUT4.

1.5 GLUT4 Storage and Trafficking

The observations from recycling kinetics of GLUT4 (Section 1.3.2) point towards a mechanism in which GLUT4 is sequestered and stored into intracellular compartments in the absence of insulin. It is suggested that in the presence of insulin, GLUT4 vesicles are allowed to mobilise from the specialised GLUT4 compartments. These vesicles subsequently recycle between intracellular compartments and the plasma membrane entering the bulk of endocytic traffic. Most studies have suggested that the intracellular compartments populated by GLUT4 include the early/sorting endosome, the recycling endosome and a specialised vesicular compartment, (Hashiramoto *et al.*, 2000; Kandror and Pilch, 1998). It is known that GLUT4 does not reside within late endosomes/lysosomes. This was revealed by the lack of co-localisation between GLUT4 and Lysotracker-Red marker for acidic regions in 3T3-L1 and CHO cells, (Powell *et al.*, 1999). It is not known how GLUT4 is sequestered in a specialised compartment, or how many GLUT4 vesicles reside within other compartments, such as the endosome recycling compartment.

1.5.1 The Endosomal Recycling Compartment

In mammalian cells, many internalised membrane proteins and lipids take an endosome-to-surface traffic pathway constitutively. Following endocytosis, plasma membrane proteins are endocytosed to the early endosome, which is characterised by the early endosomal autoantigen 1 (EEA1) and an early-endosome specific small G-protein, Rab5 (Christoforidis *et al.*, 1999; McBride *et al.*, 1999; Mills *et al.*, 1998; Mu *et al.*, 1995). The endosomes act as central sorting stations controlling the traffic of ligands, receptors and fluid, due in part to the fact that they maintain a slightly acidic internal pH (Mellman *et al.*, 1986). It is the low pH in the early endosomes, where receptor-ligand complexes are rapidly dissociated. The vacated recepetors then accumulate in the endosomes' tubular extensions otherwise known as the endosomal recycling pathway. Here the receptors may bud from the tubules and initiate recycling back to the plasma membrane, or in some cases to the TGN. Proteins destined for degradation are targeted to the late endosome or lysosomes from the early endosome, (Mellman, 1996).

The endosomal recycling compartment is concentrated in the pericentriolar region of the cell (Apodaca *et al.*, 1994; Tooze and Huttner, 1990). Although the recycling

compartment is in the same general region of the cell as the TGN and the Golgi complex, the recycling complex is distinct from these organelles, (McGraw *et al.*, 1993; Yamashiro *et al.*, 1984). Transfer from the recycling compartment to the plasma membrane is the rate-limiting step in recycling of lipids and receptors back to the cell surface, occurring with a half-time of ~12 min (Mayor *et al.*, 1993; Presley *et al.*, 1993).

The TfR is a well-characterised endosomal protein. The TfR binds to iron-loaded transferrin at the plasma membrane and is then internalised by clathrin-coats to the early (sorting) endosome compartment, where the low pH induces dissociation of iron from transferrin. The TfR (usually with transferrin still bound) recycles back to the cell surface directly from the early endosome. In addition, a proportion of the TfR traffics back to the cell surface through the endosomal recycling compartment (Hopkins *et al.*, 1994; Ullrich *et al.*, 1996). The TfR exits the early endosome rapidly (~4 min) but leaves the recycling compartment more slowly (~12 min), so at a steady state the majority of the TfR is concentrated in the endosomal recycling compartment (Mellman *et al.*, 1996).

Despite the relative simplicity of the TfR recycling system, evidence points to a greater complexity within the endosomal systems themselves. As mentioned in Section 1.3.4, further subdivision within the endosomal recycling system have been implicated with small GTPases Rab4, Rab5 and Rab11, (Mohrmann and van der Sluijs, 1999). The endosomal system has evolved to include different types of sorting endosomes (Schmidt *et al.*, 1997; Wilson *et al.*, 1997) and the presence of separate recycling systems (Ghosh and Maxfield, 1995; Gruenberg and Maxfield, 1995; Hopkins *et al.*, 1994; Ullrich *et al.*, 1996). It is possible that GLUT4 vesicles could be retained within the recycling endosomal compartment in the absence of insulin, although the translocation of TfR and GLUT1 to the plasma membrane with insulin-stimulation is far less than that observed for GLUT4 (reviewed in Kandror and Pilch, 1996).

1.5.2 The GLUT4 Storage Compartment

A reservoir compartment containing GLUT4 vesicles (termed GLUT4 storage vesicles, GSVs) is evident from several different studies. Double-label immunofluorescence microscopy in 3T3-L1 adipocytes has revealed differential intracellular targeting of GLUT1 and GLUT4 (Piper *et al.*, 1991). Using velocity sedimentation analysis on

neuroendocrine PC12 cells expressing GLUT4, a population of small GSVs were shown to segregate from endosomes (Herman *et al.*, 1994). A specific method which enables the endosomal system to be ablated has been used to identify a GLUT4 vesicle pool (Livingstone *et al.*, 1996). The assay relies on the TfR to deliver the transferrin (Tf) (conjugated to horseradish peroxidase (HRP)) into the recycling endosomal system. The cells are then exposed to diaminobenzidine (DAB) and hydrogen peroxide to generate a cross-linking species within the lumen of the endosomal compartments that have taken up the Tf-HRP, resulting in their ablation. The method selectively ablates the markers of the endosomal system (TfR, Rab5 and cellubrevin) leaving 60% of total GLUT4 unablated (Martin *et al.*, 1996a). Vesicle immunoadsorption studies reveal subpopulations of vesicles in adipocytes. Some of these vesicles are enriched with GLUT4 and not endosomal markers, whilst others are enriched in both GLUT4 and endosomal markers (Livingstone *et al.*, 1996; Robinson *et al.*, 1992; Zorzano *et al.*, 1989).

Additional observations which support the notion that the GSV is a separate entity from the endosomal system have been presented from studies of differentiated 3T3-L1 adipose cells (El Jack *et al.*, 1999; Ross *et al.*, 1998; Yang *et al.*, 1992a). El-Jack and colleagues have postulated that a distinct insulin-sensitive cargo compartment forms early during fat cell differentiation in 3T3-L1 adipocytes, (El Jack *et al.*, 1999). At the point of differentiation, the 3T3-L1 cells analysed on sucrose gradients showed a submaximal expression of IRAP. This coincided with a narrowing of intracellular GLUT1 and TfR distributions in sucrose gradients and an increased expression of IRAP and GLUT4. A recent study (using iodixanol density gradient sedimentation on 3T3-L1 adipose cells), has shown that a GLUT4 compartment can be isolated that is distinct from both endosomes and TGN and that is highly insulin responsive (Hashiramoto and James, 2000). This is discussed further in Chapter 5.

GLUT4 has also been localised by electron microscopy (EM) in white and brown adipocytes and in cardiac and skeletal muscle (Slot *et al.*, 1991a,b; Smith *et al.*, 1991; Ralston and Ploug, 1996; Slot *et al.*, 1997; Ploug *et al.*, 1998; Malide *et al.*, 2000). In all cases, under basal conditions, the majority of GLUT4 resides in tubulo-vesicular (TV) elements. These studies point to the presence of a GSV in adipocytes that is distinct from endosomes and the TGN. Immunoelectron microscopic studies found GLUT4 to be clustered TV elements adjacent to sorting endosomes (Slot *et al.*, 1991a). 80% of the

labelled cells were found to be associated with TV elements with the remainder being elsewhere in the cell. The study showed that 1.1% of GLUT4 in basal brown adipose tissue was present on clathrin-coated vesicles, in agreement with the amount of GLUT4 labelling on the entire plasma membrane in basal insulin-sensitive cells, (Robinson *et al.*, 1992). In the basal brown adipose tissue, approximately 3.8% of the GLUT4 was found to be associated with early endosomal vacuoles. Following insulin-stimulation, the amount of GLUT4 labelled in the TV elements decreased by 50% with a corresponding increase of 35% in the labelling of the plasma membrane and of both early endosomes and clathrin-coated pits and vesicles.

Three-dimensional electron microscopy has presented further morphological evidence for GLUT4 residing in a separate population of vesicles distinct from that of the TGN or endosome (Ramm *et al.*, 2000). A comparison of the distribution of GLUT4 with CD-M6PR, showed a population of GSVs that contained both proteins and a separate population that contained GLUT4 only. The existence of GSVs, which represent distinct functional pools is supported by the observation that insulin has a much more potent effect on the GLUT4-positive/CD-M6PR-negative population.

The amount of GLUT4 associated with the TGN in 3T3-L1 cells was examined with the marker protein, ß-COP (Bogan and Lodish, 1999). Bogan showed no overlap of immunostaining with GLUT4 and ß-COP. GLUT4 immunostaining was mostly separate from that of γ-adaptin, another TGN marker. Overall, the data showed that the perinuclear GLUT4 compartment did not correspond to the TGN. The data presented by Bogan and colleagues is similar to data from microscopy studies in insulinoma cells, transfected with GLUT4. GLUT4 in these transfected cells did not significantly overlap with the TGN marker protein, TGN38 (Thorens and Roth 1996). Other reports have described minimal overlap of GLUT4 and TGN38 in rat adipose cells, and of GLUT4 and giantin in cultured myotubes (Ralston and Ploug, 1996 and Malide *et al.*, 1997a). Biochemical studies of 3T3-L1 adipocytes found that only 5–10% of low density microsomal GLUT4 was copurified by immunoadsorption of vesicles using an antiserum to TGN38; the copurified GLUT4 did not correspond to the insulin-regulated GLUT4 compartment within the low density microsomal fraction (Martin *et al.*, 1994).

On Nycodenz gradients, GLUT4 was shown to sediment in the same fractions as AP-1 adaptor complex (Gillingham *et al.*, 1999). This is of particular interest, as this complex

is TGN localised, (for review see Hirst and Robinson 1998). The AP-1 adaptor complex is associated with clathrin-coated vesicles budding from the TGN, while the AP-2 adaptor complex is associated with clathrin-coated vesicles budding from the plasma membrane. AP-3 is recruited onto membranes of the TGN and a more peripheral compartment but does not appear to be associated with clathrin. Gillingham and colleagues found high levels of AP-1, some AP-3 but very little AP-2 adaptor complexes associated with isolated GLUT4 vesicles. The AP-1 complex with GLUT4 vesicles increased by approximately 4-fold by the addition of GTP-γ-S and an ATP regenerating system. The Nycodenz gradients separated the bulk of GLUT4 from TfR suggesting a specialised compartment distinct from recycling endosomes. The authors conclude that much of the GLUT4 may have budded from the TGN to form vesicles that are fusion competent, and may provide a TGN-derived pre-secretory compartment (see Figure 1.3; Section 1.5.2)

1.5.3 Intracellular Movement of GLUT4 Vesicles

We know that there are two main pathways for the movement of GSVs: internalisation from the plasma membrane and the insulin-responsive translocation to the cell surface. It is unclear if GLUT4 traffics to and from the TGN/endosomal system and if so, to what extent. Recent studies of GLUT4 trafficking with transfected CHO cells (Wei *et al.*, 1998), compartment ablation in 3T3-L1 fat cells (Martin *et al.*, 1996a) and confocal microscopy in rat adipocytes (Malide *et al.*, 1997a) suggest that GLUT4 segregates to a substantial degree from TfRs. Immunofluorescence microscopy has revealed some overlap between GLUT4 and endosomal/TGN markers as well as discrete labelling of an additional compartment (Malide *et al.*, 1997a). Thus, the trafficking of GLUT4 and TfRs may be quite different and involve different post-endosomal compartments. The precise biochemical and morphological relationship between these compartments remains uncertain. The current model from this laboratory (see Holman and Sandoval, 2001) is that there are two or more separate GLUT4 compartments in adipocytes, one of which is endosomal in origin and the other non-endosomal, (GSV) (Figure 1.3, page 31). It is thought that GLUT4 traffics from storage to the plasma membrane without re-mixing with endosomes.

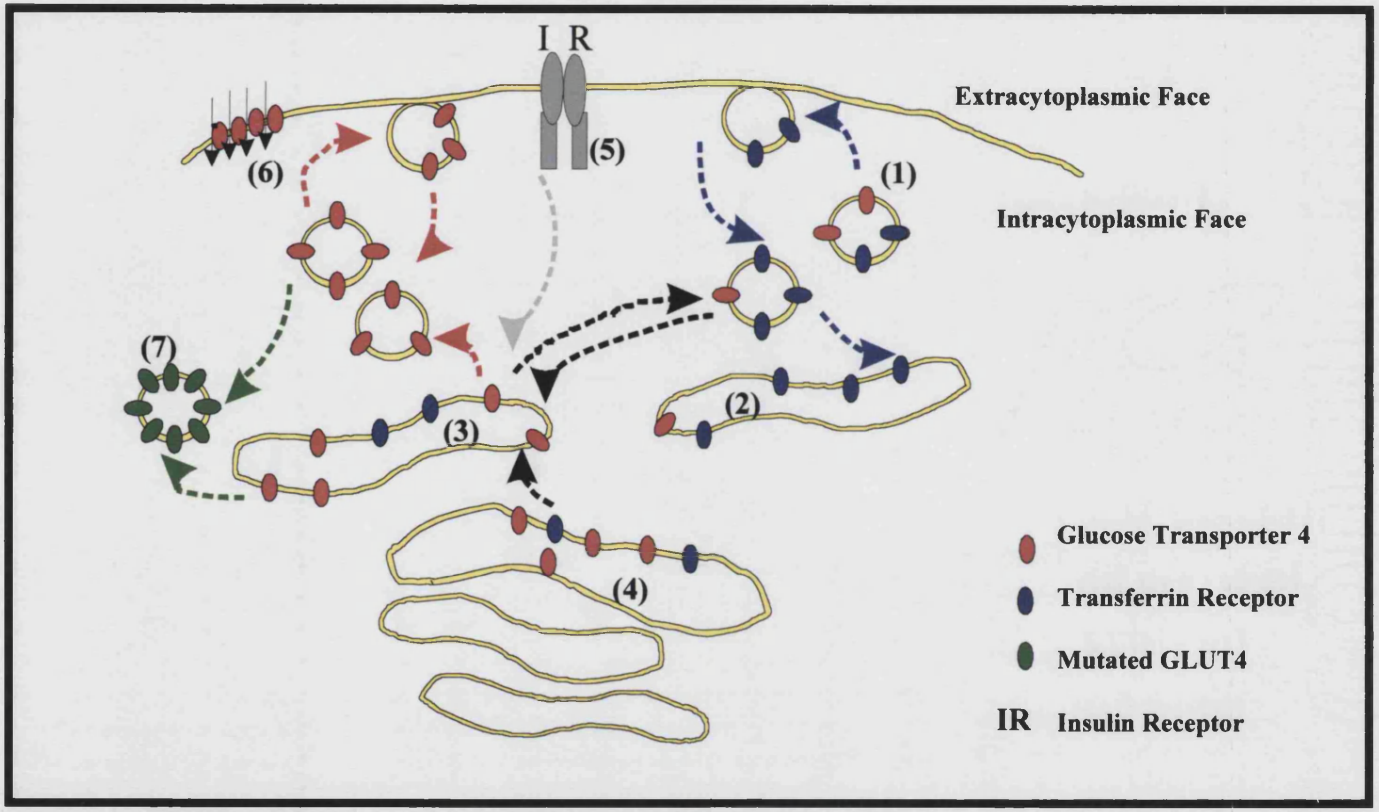

Figure 1.3: Proposed Model of GLUT4 Movement Between Different Intracellular Compartments. In the basal state, GLUT4 recycles with endosome receptors (1) from the endosome system (2) GLUT4 is sorted from transferrin receptors into a specialised GLUT4 storage compartment (GSV) (3). The GSV is similar in shape to that of the TGN and it is thought that some GLUT4 vesicles bud from the TGN (4). Upon insulin stimulation on the insulin receptor (5), GLUT4 is recruited to the plasma membrane to increase glucose transport into the cell (6). It is thought that mutated GLUT4 is re-directed elsewhere other than the plasma membrane in response to insulin (7).

Studies to support the notion that insulin may stimulate exit of GLUT4 from multiple intracellular pools have been recently published (Bogan and Lodish, 1999; Foran *et al.*, 1999; Hashiramoto *et al.*, 2000; Kandror, 1999; Kupriyanova and Kandror, 2000; Martin *et al.*, 2000; Millar *et al.*, 1999b; Millar *et al.*, 2000; Wei *et al.*, 1998). To test the hypothesis that there are two separate regulatable exit pathways for GLUT4 in adipocytes, Millar and colleagues studied the role of different v-SNARE proteins (Millar *et al.*, 1999b). It is thought that insulin and GTPγS both stimulate glucose transport and translocation of GLUT4 but for different compartments. A peptide encompassing the cytosolic tail of the v-SNARE cellubrevin inhibited GTPγS-stimulated GLUT4 translocation by ~40% but had no effect on the insulin response in 3T3-L1 adipocytes. Conversely, a fusion protein encompassing the cytosolic tail of VAMP2 had no significant effect on GTPγS-stimulated GLUT4 translocation but inhibited the insulin response by ~40%. Ablation of the recycling endosomal system caused almost quantitative inhibition of GTPγS-stimulated GLUT4 translocation but only partially reduced insulin-stimulated translocation. These data suggest that GTPγS selectively stimulated recycling of GLUT4 via the endosomal system in a process that is regulated by cellubrevin. In addition to regulating this pathway, insulin also stimulates the exocytosis of GLUT4 from a separate compartment (GSVs), which is distinguished by the unique role of VAMP2. Millar and colleagues also examined the localisation of Rab proteins in permeabilised 3T3-L1 adipocytes following stimulation with GTPγS. There was a marked accumulation of Rab4 and Rab5 at the cell surface, whereas other Rab proteins (Rab7 and Rab11) were unaffected.

Wei and colleagues (Wei *et al.*, 1998) compared GLUT4 trafficking with TfR trafficking in an attempt to resolve different GLUT4 pathways. It was observed that at 37 °C, cell surface-labeled GLUT4 (as well as TfR) was internalised into peripheral and perinuclear structures. At 15 °C, endocytosis of GLUT4 continued to occur at a slowed rate. GLUT4 tagged with a fluorescent label was seen to have accumulated within large peripheral endosomes. No perinuclear structures were labelled. A shift of temperature from 15°C to 37 °C resulted in the reappearance of GLUT4 in perinuclear structures and GSV reformation. In contrast, at 15 °C, TfR continued to traffic to perinuclear structures and the labelling of TfR was similar in distribution to that observed at 37°C. GLUT4 was suggested to be sorted differently from the TfR. The authors conclude that the sorting of GLUT4 from TfR may occur primarily at the level of the plasma membrane to form distinct endosomes.

From studies in which cell surface receptors were tagged with biotinylated cell impermeable reagents, Kandror concluded that adipose cells possess at least two distinct cell-surface recycling pathways for M6PR and TfR (Kandror, 1999). Under basal conditions, the first pathway was not considered to be active, and all cell surface recycling of both M6PR and TfR proceeded via a second pathway. The first pathway was thought to be mediated by GLUT4 vesicles, and the second bypassed this compartment. Incubation of basal adipocytes (up to 30 min) did not lead to biotinylation of any significant fraction of M6PR, TfR, or IRAP in GLUT4 vesicles. Stimulation of adipocytes with insulin changed the pattern of trafficking of these proteins. The amount of intracellular biotinylated GLUT4 and IRAP decreased with time, with an increase at the cell surface. Insulin-stimulation did not decrease intracellular biotinylated M6PR or TfR protein levels, nor did it substantially increase the concentration of these proteins at the plasma membrane. The authors suggest that two pathways are present: one where M6PR and TfR rapidly recycle between the intracellular compartments and the other that allows retention of IRAP and GLUT4 at the cell surface.

A comparison of the trafficking of the secreted serine protease adipsin and the integral membrane proteins GLUT4 and TfRs in 3T3-L1 adipocytes has provided evidence for more than one GLUT4 exit pathway (Millar *et al.*, 2000). Adipsin was secreted from the *trans* Golgi network to the endosomal system, and ablation of endosomes using Tf-HRP conjugates, strongly inhibited adipsin secretion. Phospholipase D has been implicated in export from the *trans* Golgi network, and insulin stimulates phospholipase D activity in these cells. Inhibition of phospholipase D action with butan-1-ol blocked adipsin secretion and resulted in accumulation of adipsin in *trans* Golgi network-derived vesicles. In contrast, butan-1-ol did not affect the insulin-stimulated movement of TfRs to the plasma membrane, although TfRs were ablated with Tf-HRP conjugates. Insulin-stimulated GLUT4 translocation was still observed after endosome ablation or inhibition of phospholipase D activity. Immunolabelling revealed that adipsin and GLUT4 were predominantly localised to distinct intracellular compartments.

A major constituent of synaptic vesicles, synaptogyrin is involved in regulation of exocytosis in PC12 cells, (Stenius *et al.*, 1995). A homologue of this protein, cellugyrin (Sugita *et al.*, 1999) is present in 50-60% of GSVs in rat adipocytes (Kupriyanova and Kandror, 2000). However, unlike GLUT4, cellugyrin is not re-distributed to the plasma membrane in response to insulin-stimulation. Kupriyanova and Kandror have been able to demonstrate that intracellular GLUT4 vesicles in rat adipocytes were a mixture of at

least two populations: cellugyrin-negative vesicles which were recruited to the cell surface with insulin and cellugyrin-positive vesicles which were not translocated by insulin.

The studies presented above provide evidence that GLUT4 resides in more than one population of vesicles, some of which are insulin-responsive. Kinetic data also supports the notion that there are multiple GSVs some of which are localised with the endosome (Holman *et al.*, 1994; Yeh *et al.*, 1995).

1.5.4 The Role of Actin in GLUT4 Movement

Actin was first identified as part of the protein complex acto-myosin responsible for producing the contractile force in skeletal muscle (Straub, 1942). It is one of the most abundant proteins in human tissues and is widely expressed in nearly all types of eukaryotic cells. This protein serves many cellular functions including transmitting internal stresses, providing mechanical strength to the cell cortex, regulation of enzymatic activities, and spatial organization of the cytoplasm and signal transduction pathways (reviewed in Elson, 1988; Evans, 1993; Janmey, 1998). Actin has been suggested to play a role in regulating vesicle trafficking and is thought to form scaffolds for transport vesicles to move along during vesicle sorting processes (Carlier, 1998; Rozelle *et al.*, 2000).

Many groups have studied the effect of insulin on actin and GLUT4 trafficking. Treatment of cells with the actin depolymerising agent, cytochalasin D, or the actin monomer binding latrunculins A or B resulted in a marked inhibition of insulin-induced GLUT4 translocation without effecting basal transport (Omata *et al.*, 2000; Tsakiridis *et al.*, 1994; Wang *et al.*, 1998). These studies show that actin is necessary for GLUT4 translocation. In addition, membrane ruffling was observed with insulin induced GLUT4 translocation (Tsakiridis *et al.*, 1994). The role of the membrane ruffling is unknown, but was shown to be inhibited by cytochalasin D. Oatey and colleagues were able to visualise the involvement of an intracellular scaffold in the maintenance of the internal population of GLUT4 using a green fluorescent protein chimera of GLUT4 (GFP-GLUT4) (Oatey *et al.*, 1997). The majority of the GFP-GLUT4 vesicles in the 3T3-L1 adipocytes were shown to be static as if tethered to an intracellular structure. The authors suggest that the role of insulin is to release the 'anchor' on the GFP-

GLUT4 vesicles allowing them to translocate to the plasma membrane. Together these data provide evidence for the role of actin filaments in glucose transport.

Investigations have shown that insulin stimulation results in cortical actin remodelling, followed by an increase in polymerised actin in the peri-nuclear region of L6 myotubes expressing GLUT4 (Khayat *et al.*, 2000; Tong *et al.*, 2001). Tong and colleagues studied the involvement of actin filaments in GLUT4 translocation and their possible defects in insulin resistance (Tong *et al.*, 2001). They used L6 myotubes expressing myc-tagged GLUT4. GLUT4myc was visualised by fluorescence microscopy and immunogold staining. There was a high density of GLUT4myc in membrane ruffles. Below the membrane, GLUT4 colocalised with the actin structures supporting the membrane ruffles. The presence of GLUT4myc in these areas was greatly reduced by jasplakinolide and by swinholide-A (drugs that affect actin filament stability and prevent actin branching, respectively). The effect of insulin resistance (Section 1.2.2) on actin remodelling was examined. Insulin resistance was generated by prolonged (24 hours) exposure of myotubes to high glucose and insulin. This diminished the acute insulin-dependent remodeling of cortical actin and GLUT4myc translocation, similar to the effect of swinholide-A. The authors propose that GLUT4 vesicle incorporation into the plasma membrane involves insulin-dependent cortical actin remodeling and that defective actin remodeling contributes to insulin resistance.

The exact role of insulin-induced actin remodelling and its subsequent effect on GLUT4 translocation is unknown. It has been hypothesised that insulin acts to facilitate the association of PI 3-Kinase (p85) with GLUT4 vesicles and, potentially, the arrival of GLUT4 at the cell surface (Khayat *et al.*, 2000). Microinjection of a constitutively active mutant of PI 3-kinase p110 causes the translocation of GLUT4 to the plasma membrane in 3T3-L1 adipocytes and induces the formation of actin filament ruffles (Martin *et al.*, 1996b). This effect is inhibited by wortmannin and by the use of a PI 3-kinase mutant with a point mutation in the kinase domain (Martin *et al.*, 1996b). Several studies have shown that PI 3-kinase is a key participant in the control of membrane ruffling, (Kotani *et al.*, 1994; Wennstrom *et al.*, 1994a,b). Inhibition of PI 3-kinase activity by wortmanin abolishes insulin-induced actin reorganisation (Kotani *et al.*, 1994; Tsakiridis *et al.*, 1995; Wennstrom *et al.*, 1994a,b) and membrane ruffling (Kotani *et al.*, 1995). These data suggests that the localisation of PI 3-kinase activity is important for insulin-stimulated GLUT4 translocation via the actin cytoskeleton.

Further molecules have been implicated in the insulin-induced translocation of GLUT4 and/or actin rearrangement. These include the small GTPase Rab4 (Vollenweider *et al.*, 1997), and the general receptor for phosphoinositides 1 (GRP1) (Clodi *et al.*, 1998). Cormont and colleagues first demonstrated that Rab4 is associated with intracellular GLUT4-containing membranes and upon insulin stimulation Rab4 is activated and released into the cytosol (Cormont *et al.*, 1993). It is now thought that activation and dissociation of Rab4 from the GLUT4 vesicles are controlled by PI 3-kinase activity (Cormont *et al.*, 1996a,b; Shibata *et al.*, 1997). The exact events facilitating GLUT4 movement remains elusive, however studies utilising subcellular fractionation of 3T3-L1 adipocytes suggested that at least a fraction of IRS-1-PI 3 kinase complexes may be preformed and remain associated with the cytoskeleton-rich fractions after internalisation in 3T3-L1 adipocytes (Clark *et al.*, 1998). This has been interpreted by others to suggest that the association of these complexes with the cytoskeleton, rather than interaction with GLUT4 vesicles, is the event that determines their intracellular distribution (Clark *et al.*, 1998; Shepherd *et al.*, 1998).

1.6 GLUT4 Sorting Signals

1.6.1 Amino- and Carboxyl- Targeting Motifs

Targeting of many transmembrane proteins to intracellular compartments is dependent on cytoplasmic sorting signals. The most widely used signals are tyrosine or leucine-based motifs. In an attempt to define the relevant targeting domains that direct the intracellular sequestration of GLUT4, many groups have examined motifs within the amino- and carboxyl-terminal domains of GLUT4. Two motifs within these domains have been identified: the $F^{5}QQI^{8}$ found within the amino-terminal domain (Piper *et al.*, 1992; Piper *et al.*, 1993) and a dileucine motif $L^{489}L^{490}$ within the carboxyl domain (Corvera *et al.*, 1994; Verhey *et al.*, 1993; Verhey *et al.*, 1994). The FQQI motif resembles a tyrosine based internalization motifs which have been identified in proteins which undergo endocytosis, such as the M6PR (Johnson *et al.*, 1992).

It has been established that the FQQI domain is important in the sorting process that separates GLUT4 away from the endosome system (Melvin *et al.*, 1999; Palacios *et al.*, 2001). The LL domain appears to be involved in the sorting between the TGN and GSV (Marsh *et al.*, 1998). Melvin and colleagues studied Tf-HRP ablation of GLUT4

compartments following the introduction of Phe-5 (FAG) and $L^{489}L^{490}$, (LAG) mutations of GLUT4 (Melvin *et al.*, 1999). The FAG mutant was localised to the recycling endosomal system, and was ablated more than LAG. The majority of the LAG was localised within the non-ablated intracellular compartment. The FAG data indicate that the amino-terminal of GLUT4 is important in endosomal recycling. The LAG mutants indicate that the dileucine motif may be involved in the movement of GLUT4 from the TGN to the recycling endosomal compartment. Comparisons have been made of the cellular distributions of antibody/biotin tagged-GLUT4 and a Ser5 GLUT4 mutant. The latter has a FQQI motif where its Ser5 has been substituted for Phe. This mutation (Phe5GlnGlnIle8) inhibited the recycling of endocytosed GLUT4 to the GSV and resulted in its transport to late endosomes/lysosomes where rapid degradation occurred (Palacios *et al.*, 2001).

Dileucine and FQQI motifs have been shown to regulate the trafficking of several recycling proteins and there have been many studies that have examined the role of residues adjacent to these motifs. Garippa and colleagues found that serine-488 adjacent to the dileucine motif in GLUT4 (SLL) played a modulatory role in regulated GLUT4 exocytosis (Garippa *et al.*, 1996). This was identified using a chimera of GLUT4 with TfR and studied in non-insulin responsive CHO cells. In the chimera the carboxyl-terminal 30 amino acids of GLUT4 were substituted for the amino-terminal cytoplasmic domain of the TfR. The chimera had a more prominent intracellular distribution compared to the TfR. The chimera was internalised 50% more rapidly and recycled 20% more slowly than the TfR.

The amino acid serine-488 adjacent to the dileucine motif in the carboxyl domain of GLUT4 may be significant. It has been shown that the phosphorylation state of serine residues adjacent to dileucine motifs in the cytoplasmic tails of CD-M6PRs regulates the entry of M6PR into clathrin-coated vesicles. These coated vesicles then exit the Golgi apparatus at the TGN (Le Borgne *et al.*, 1997; Mauxion *et al.*, 1996). Changes in the phosphorylation state of serine residues juxtaposed to dileucine motifs and upstream to these motifs have been proposed to modulate their sorting (Johnson *et al.*, 1990; Johnson *et al.*, 1992). Hence, phosphorylation and/or dephosphorylation of GLUT4 may be involved in GLUT4 intracellular sequestration. GLUT4 is phosphorylated in the basal state. Phosphorylation also occurs when cells are stimulated by isoproterenol (James, *et al.*, 1989b). Other agents such as okadaic acid have been shown to stimulate

GLUT4 phosphorylation (Lawrence, Jr. *et al.*, 1990). Interestingly, Marsh and colleagues have postulated that the serine-488 may be involved in GLUT4 sorting at the TGN (Marsh *et al.*, 1998). They used a chimera in which serine-488 was mutated to an alanine (SAG). The distribution of SAG in 3T3-L1 adipocytes was similar to GLUT4 in that it was largely excluded from the cell surface and was enriched in small intracellular vesicles. SAG also exhibited insulin-dependent movement to the plasma membrane (4- to 5-fold) comparable to GLUT4 (4- to 5-fold). Okadaic acid was also used in these studies, which also stimulated GLUT4 movement to the cell-surface. This resulted in the stimulation of both GLUT4 translocation and its phosphorylation at Ser-488. Using immunoelectron microscopy, GLUT4 was found to be localised to intracellular vesicles containing the Golgi-derived -γ-adaptin subunit of AP-1. This localization was enhanced when Ser-488 was mutated to alanine. These authors concluded that the carboxyl-terminal phosphorylation site in GLUT4 (Ser-488) might play a role in intracellular sorting at the *trans*-Golgi network.

The role of adjacent amino acids immediately distal to the dileucine motif (Glu-491, Gln-492 and Glu-493) has been examined by sequential replacement with alanine (Cope *et al.*, 2000). Substitution of Glu-491 or Glu-493 resulted in increased levels of these proteins at the cell surface, reduced insulin-stimulated translocation and increased susceptibility to endosomal ablation. In addition to these amino acids, a functional analysis of the extreme carboxyl-terminus of GLUT4 in 3T3-L1 adipocytes has provided evidence that the residues TELEYLGP provide targeting signals (Shewan *et al.*, 2000). Mutations within this motif resulted in constitutive accumulation of GLUT4 at the PM. These disrupted mutants were shown to be associated with endosomes. Shewan *et al.*, suggest that this targeting motif may be responsible for sorting GLUT4 out or recycling endosomes into a post-endocytic GLUT4 pool which is highly insulin responsive. These studies show that acidic residues near the LL motif are important in GLUT4 targeting. Interestingly, removal of the carboxyl-terminal acidic Pro(505)AspGluAsnAsp(509) sequence prevented the storage of GLUT4 in the VAMP2 positive compartment adjacent to the Golgi complex (GSV), and resulted in its targeting to GLUT4 and Rab7 to late endosomes (Martinez-Arca *et al.*, 2000). Acidic clusters are present in many targeted proteins. Acidic residues upstream of the FQQI in the amino-terminus of GLUT4 resemble those found in the targeting domain of GAD65 (membrane-associated form of glutamic acid decarboxylase) (Dirkx *et al.*, 1995). Basic

residues upstream of the dileucine motif in the carboxyl-domain of GLUT4 also play a role in trafficking (Sandoval *et al.*, 2000).

1.6.2 GLUT4 Sorting Motifs and Vesicle Formation

In addition to vesicle movement, targeting motifs also act as sorting signals for vesicle formation (Section 1.4.1). Clathrin adaptor protein complexes appear to bind directly to cytoplasmic tails containing tyrosine and dileucine based motifs (Pearse, 1988 and Section 1.4.2). According to the evidence from electron microscopy, at any particular moment approximately 1% of GLUT4 at the plasma membrane is associated with clathrin coated pits (Slot *et al.*, 1991a). Dynamin is also associated with GLUT4 vesicles (Section 1.4.3). If GLUT4 vesicles are clathrin coated and involved with dynamin, then it is logical that GLUT4 vesicles must be associated with certain adaptor proteins through their sorting motifs.

In 1998 a study of peptides, derived from a number of different proteins, was used to analyse the interaction of adaptor proteins with di-leucine motifs (Rapoport *et al.*, 1998). Using an approach in which samples were first frozen before cross-linking by photo-irradiation, Rapoport and colleagues have revealed a specific interaction of di-leucine containing peptides (including a C-terminal peptide of GLUT4) with AP-1. The site of binding was found to be on the β1 subunit, similar to that observed for the asialoglycoprotein (Beltzer and Spiess, 1991). In addition, medium chains (μ-subunits) have also been shown to interact with LL motifs (Rodionov and Bakke, 1998). Thus APs contain at least two physically separate binding sites for sorting signals.

Adaptor proteins have been shown to be important in endocytosis (Buckley *et al.*, 2000). Plasma membrane proteins that lack specific signals that specifiy interaction with AP-2 undergo endocytosis at a lower rate than normal (1% min^{-1} versus ~10-12% min-1). It has been proposed that sorting motifs may enable GLUT4 to interact with coated pits via adaptor proteins causing efficient endocytosis (Pearse and Robinson, 1990). In addition, GLUT4 has a phosphorylation site adjacent to its di-leucine motif. This may inhibit or enhance adaptor binding, depending upon its phosphorylation status in a similar fashion to M6PR, (see Section 1.6.1).

1.6.3 Epitope Masking

It is clear that both domains of GLUT4, the amino- and carboxyl-terminus are needed for efficient trafficking of GLUT4. The GLUT4 chimera and mutation studies that have led to elucidation of these requirements are reviewed in Holman and Sandoval, 2001. In addition to the targeting motifs, it has been suggested that eptiope masking in the carboxyl-terminal of GLUT4 may be involved in its translocation. This hypothesis came about from immunomicroscopy studies where GLUT4 was shown to be detected to different extents in insulin-stimulated cells dependent on the type of antibody used (Smith *et al.*, 1991; Wang *et al.*, 1996). Antibodies raised to the carboxyl-terminus of GLUT4 detected greater total GLUT4 in insulin-stimulated than basal. The amount of GLUT4 detected by amino-terminal GLUT4 antibodies did not change (Smith *et al.*, 1991). It is thought that the eptiope (carboxyl domain) may be masked in basal cells and the epitope is umasked with insulin-stimulation. This is discussed further in Chapter 3.

1.7 Aims of the Present Study

The overall aim of the experiments described in this thesis was to develop methods for examining GLUT4 trafficking and distribution between different subcellular locations in rat adipocytes. Intracellular GLUT4 is now known to reside in at least two intracellular compartments. On leaving the plasma membrane, it enters the endosomal system and is then sequestered into its storage compartment. Some literature on GLUT4 localisation in rat adipocytes (Chapter 3) has led to the suggestion that the carboxyl-terminus of GLUT4 is masked when GLUT4 is sequestered in the storage compartment. In experiments described in this thesis, a GLUT4 amino-terminal antibody was characterised. Using the amino-terminal and carboxyl-terminal antibody in confocal microscopy the concept of epitope masking was re-examined in the rat adipocyte system where GLUT4 is highly sequestered.

Previous studies on kinetics of GLUT4 trafficking have been carried out using fractionation to separate the plasma membrane from the intracellular membranes. An improvement was sought since the fractionation procedure was difficult to carry out for multiple samples. Two new approaches were examined here:

The first involved utilisation of the interaction of biotin (on a probe that can tag GLUT4) with extracellular avidin. It was postulated that this interaction would provide a means of distinguishing between cell surface GLUT4 that would interact with avidin and internalised GLUT4 that would not. A compound would need a long spacer arm between the GLUT4 and avidin and a compound of this sort was developed and tested for its utility in experiments described in this thesis.

The second approach that was thought to have potential in analysis of the separate cell surface and intracellular GLUT4 pools involved use of a compound with a cleavable disulphide bridge. It was postulated that it might be possible to use an impermeant cleavable reagent that would only interact with cell surface and not internal GLUT4 and therefore trace the GLUT4 movement between these compartments. A compound of this sort was developed and was tested for its utility in experiments described in this thesis.

The proportion of GLUT4 in endosomes and its storage compartment may be different in different cell types. To examine the extent of distribution of rat adipocyte GLUT4 between endosomes and storage compartments, gradient centrifugation was utilised in experiments described in this thesis. Different methodologies were compared to establish a method that most efficiently accomplished this separation of compartments. It was established using these procedures that the levels of sequestration of GLUT4 out of endosomes was higher in rat adipocytes than in other cell systems that have been described in the literature (Chapter 5). Computer simulations were therefore carried out in order to examine the importance of retrograde trafficking between storage and endosomes in the maintenance of a high proportion of GLUT4 in the endosome system.

2.0 Materials and Methods

2.1 General Materials

2.1.1 Chemical reagents

Laboratory chemicals and reagents were of analytical grade and obtained from Fisons Scientific U.K. Ltd., (Loughborough, U.K.,), Sigma-Aldrich Chemical Company (Poole, Dorset, U.K.,), or BDH Laboratory Supplies (Merk Ltd., Poole, Dorset, U.K.,). The reagents listed below were purchased elsewhere:

- Enhanced chemiluminescence (ECL) reagent, autoradiography film, (Hyperfilm^{TM} ECL^{TM}), Optiphase Safe^{TM} scintillation fluid and radiolabelled sugars were obtained from Amersham Pharmacia (Little Chalfont, UK).
- Collagenase was obtained from Worthington, (Freehold, NJ).
- Monocompetent porcine insulin was a gift from Dr. G. Danielison, (Novo Nordisk).
- Bovine Serum Albumin (BSA) (Bovine Cohn Fraction V) was from Intergen Company, (Purchase, NY).
- Thesit (Nonaethylene glycol dodecyl ether) was purchased from Roche, (Lewes, East Sussex, UK).
- Protein molecular weight markers were from Sigma or New England BioLabs (Hertfordshire, UK).
- Ammonium persulphate was purchased from Bio-Rad, (Hertfordshire, UK).
- Acrylamide Stock, (30% Acrylamide, 0.8% Bis-acrylamide) was obtained from Flowgen, (Leicestershire, UK).

2.1.2 Buffers

Buffers used routinely were made up as shown below, and stored at 0-4 °C for up to one month.

- *Ammonium persulphate:* 100 mg/ml stock, made up fresh each day
- *Digestion buffer*: 3.5% (w/v) BSA/KRH buffer containing 5 mM glucose and 700 μg/ml collagenase.
- *Electrophoresis Running buffer:* 0.025 M Tris-HCl, pH 6.3, 0.1% (w/v) SDS and 0.2 M glycine.
- *Gradient buffer:* 10 mM HEPES, pH 7.2, 150 mM NaCl, 1 mM $MgCl_2$ and 1 mM EGTA.
- *Hepes-Nycodenz buffer:* 20 mM HEPES, pH 7.2, 3 mM KCl and 0.3 mM EDTA.
- *HES buffer (Hepes/EDTA):* 10 mM HEPES, pH 7.2, 1 mM EDTA and 250 mM Sucrose.
- *Krebs-Ringer-HEPES, (KRH):* 10 mM HEPES, pH 7.4, 140 mM NaCl, 4.7 mM KCl, 2.5 mM $CaCl_2$, 1.25 mM $MgSO_4$ and 2.5 mM NaH_2PO_4.
- *MES buffer:* 10 mM MES, pH 6.0, 140 mM NaCl, 4.7 mM KCl, 2.5 mM $CaCl_2$, 1.25 mM $MgSO_4$ and 1% (w/v) BSA.
- *Phosphate-buffered Saline, (PBS):* 154 mM NaCl, 12.5 mM $Na_2HPO_4.12H_2O$, pH 7.2.
- *Ponceau Dye*: 0.1% Ponceau S (w/v) in 3% trichloroacetic acid (v/v), stored at room temperature.
- *Resolving Gel buffer:* 1.5 M Tris-HCl, pH 8.8 and 0.4% (w/v) SDS.
- *Sample buffer:* 10% SDS (w/v), 0.5M Tris-HCl, pH 6.8, 0.05% (w/v) bromophenol blue and 10% (v/v) glycerol.
- *Stacking Gel buffer:* 0.5 M Tris-HCl, pH 6.8 and 0.4% (w/v) SDS.
- *Transfer buffer*: 39 mM glycine, 48 mM Tris, pH 8.8, 0.0375% (w/v) SDS and 20% (v/v) methanol.
- *Tris-buffered Saline, (TBS-Tween):* 10 mM Tris, pH 7.4, 154 mM NaCl and 0.1% (v/v) Tween-20

Antipain, aprotinin, pepstatin A and leupeptin protease inhibitors were used in the buffers as stated in the experimental, (Sections 2.31, 2.33, 2.5.3. and 2.60). All protease inhibitors were made up in a stock of 0.5 mg/ml, stored at -20°C. Final concentrations of protease inhibitors in solution were at 1 μg/ml. 4-(2-aminoethyl) benzenesulfony fluoride (AEBSF) was also stored at -20 °C at a stock concentration of 100 mM and used at a final concentration of 100 μM.

2.1.3 Antibodies

The primary and secondary antibodies used are listed below, (Table 2.1 pages 45-46 and Table 2.2, page 47 respectively). The antibody source and working dilution for Western blotting (Section 2.2.5) and immunofluorescence (Section 2.2.6) have been given. All primary antibodies were diluted in TBS-Tween 20 containing 1% BSA and 0.02% (w/v) azide, unless otherwise stated. Glucose transporter rabbit antiserum was raised against either the carboxyl- (COOH) or amino- (NH_2) terminal of the protein. Rabbit antisera against GLUT4 and GLUT1 COOH-terminal peptides, (Holman *et al.*, 1990) were produced in a collaboration between Dr. S. W. Cushman (National Health, Bethesda, USA) and this laboratory. Secondary antibodies for Western blotting were diluted in 5% (w/v) Marvel® in TBS-Tween.

2.1.4 Biotinylated Photolabels

Biotinylated photolabels were synthesised either by Professor G.D. Holman or Dr. M. Hashimoto. The photolabels were synthesised from a modification of the synthesis of the bis-mannose photolabel, ATB-BMPA (Holman *et al.*, 1990). Photolabel structures are shown in Table 2.3, page 47.

Table 2.1: Primary Antibodies: Source and their Working Dilutions.

Antibody	Polyclonal/ Monoclonal Purified/Serum	Source	Working Dilution Western Blotting WB Immunofluorescence IF
Goat anti-avidin D	Polyclonal Purified	Vector Laboratories, Peterborough, U.K.	1:2000 WB
Mouse anti -Biotin FITC conjugate	Monoclonal Purified	Sigma, Poole, U.K.	5 μg/ml IF
Rabbit anti-Biotin FITC conjugate	Polyclonal Purified	Vector Laboratories, Peterborough, U.K.	5 μg/ml IF
Extravidin	Polyclonal Serum	Sigma, Poole, U.K.	1:2000 WB
Rabbit anti-COOH GLUT1	Polyclonal Serum	G.D. Holman, University of Bath, U.K.	1:1000 WB
Rabbit anti-COOH GLUT4	Polyclonal Serum	G.D. Holman, University of Bath, U.K.	1:4000 WB
Rabbit anti-COOH GLUT4	Polyclonal Purified	G.D. Holman, University of Bath, U.K.	1:4000 WB 5 μg/ml IF
Rabbit anti-NH_2 GLUT4	Polyclonal Purified	Sten Lund, Arahus University Hospital, Denmark.	1:500-1:2000 WB
Rabbit anti-NH_2 GLUT4	Polyclonal Purified	D. Harper, University of Bath, U.K.	1:1000 WB 1 μg/ml IF
Mouse anti-COOH GLUT4	Monoclonal (1F8) Purified	Biogenesis Ltd. Poole, U.K.	1:1000 WB 5 μg/ml IF
Mouse anti-EEA1	Monoclonal Purified	Transduction Laboratories, Kentucky, U.S.A.	1:1000 WB
Rabbit anti-EEA1	Polyclonal Serum	M. Clague, University of Liverpool, U.K.	1:1000 (in 5% Marvel, TBS without Tween 20) WB

Cont. Table 2.1: Primary Antibodies: Source and their Working Dilutions.

Antibody	Polyclonal/ Monoclonal Purified/Serum	Source	Working Dilution Western Blotting WB Immunofluorescence IF
Rabbit anti-IRAP	Polyclonal Purified	S.R. Keller, Dartmouth Medical School, Hanover, U.S.A.	1:1000 WB
Rabbit anti-αSNAP	Polyclonal Purified	J. Mitchell, University of Bath, U.K.	1:1000 WB
Rabbit anti-sortilin	Polyclonal Serum	Jorgen Gliemann, Arahus University Hospital, Denmark.	1:1000 WB
Rabbit anti-syntaxin4	Polyclonal Purified	S. Oldfield, University of Bath U.K.	1:5000 WB
Mouse anti-TGN38	Monoclonal (2F 7.1) Purified	G. Banting, University of Bristol and P. Luzio, Addenbrooke's Hospital, University of Cambridge, U.K.	1:1000 WB
Mouse anti-Transferrin FITC	Monoclonal Purified	C. Hopkins, University of London, U.K.	1:1000 IF
Mouse anti-Transferrin Texas Red	Monoclonal Purified	C. Hopkins, University of London.	1:1000 IF
Mouse anti -Transferrin Receptor	Monoclonal (CD 71) Purified	Chemicon International Inc., U.S.A.	1:1000 WB
Mouse anti -Transferrin Receptor	Monoclonal Purified	Zymed Laboratories, Inc., U.S.A.	1:1000 WB
Rabbit anti-VAMP2	Polyclonal (L220) Purified	M.A. Krepper, Renal Mechanisms Section, NIH, Washington D.C., U.S.A.	1:500- 1:1000 (made in 1% BSA instead of Marvel) WB
Mouse anti-VAMP2	Monoclonal (CL69.1) Purified	R. Jahn, Max Planck Institute, Germany.	1:1000 WB

Table 2.2: Secondary Antibodies: Source and their Working Dilutions

Antibody	Source	Dilution
Goat anti-mouse IgG peroxidase conjugate	Sigma ImmunoChemicals, St. Louis, U.S.A.	1:1000 WB
Goat anti-rabbit IgG peroxidase conjugate	Sigma ImmunoChemicals, St. Louis, U.S.A.	1:4000 WB 1:1000 WB (for EEA1 antibody)
Human anti-goat IgG peroxidase conjugate	Sigma ImmunoChemicals, St. Louis, U.S.A.	1:4000 WB
FITC anti-rabbit IgG	Jackson Immunoresearch Laboratories Inc., West Grove, PA, U.S.A.	1:100 (15 μg/ml) IF
Rhodamine anti-mouse IgG	Jackson Immunoresearch Laboratories Inc., West Grove, PA, U.S.A.	1:100 IF

Table 2.3: Biotinylated Photolabels for Tagging Glucose Transporters

Biotinylated Photolabel	Abbreviated Tag Name	Reference
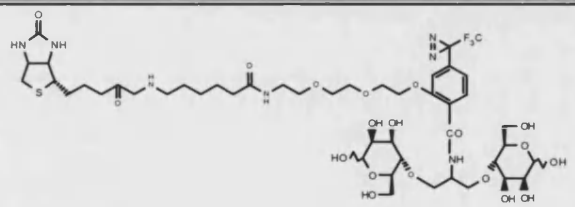	Bio-LC-ATB-BMPA	Koumanov *et al.*, 1998
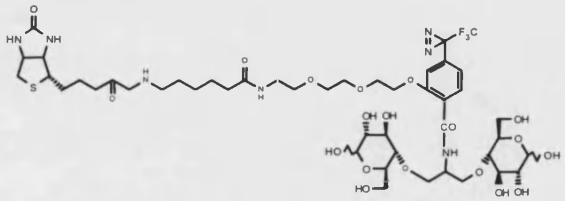	Bio-LC-ATB-BGPA	Hashimoto *et al.*, 2001b
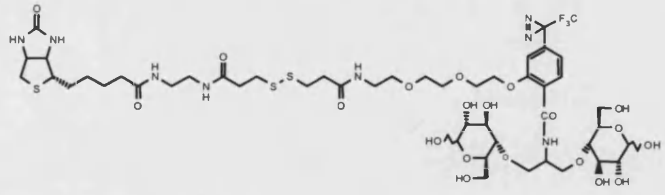	Bio-SS-ATB-BGPA	Hashimoto *et al.*, 2001b
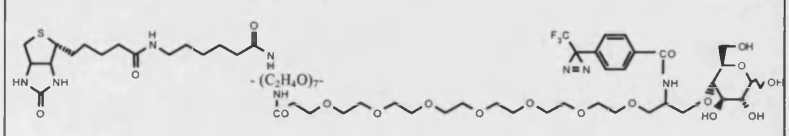	Bio-LC-G15	Hashimoto *et al.*, 2001a

2.2 Protein Biochemistry Techniques

The following section describes common protein biochemistry techniques used in experimental work.

2.2.1 Protein Assay

Protein concentrations were obtained by using the Pierce bicinchoninic acid (BCA) protein assay (Smith *et al.*, 1985). A standard curve of 0.2-1 mg/ml BSA in 0.1 M NaOH was constructed. Protein samples were diluted with 0.2 M NaOH to within the standard range. To all samples, 200 µl of working BCA reagent C was added. Working reagent C consisted of 50 parts reagent A; bicinchoninic acid solution, (Pierce & Warriner Ltd., Rockford, IL U.S.A.,) and 1 part reagent B: a 4% (w/v) copper sulphate solution. Samples were placed at 37 °C for 30 min and read by absorbance spectroscopy at 562 nm in a microplate spectrophotometer. All readings were carried out in triplicate.

2.2.2 SDS-Polyacrylamide Gel Electrophoresis (SDS-PAGE).

Electrophoresis was carried out using a modification of the method from Kato (Kato *et al.*, 1983) using the discontinuous buffer system of Laemmli (Laemmli, 1970). Protein samples were solubilised in Sample buffer for 5 min at 95 °C. Depending on the nature of the experiment either 10 mM DTT or 10% 2-β mercaptoethanol were also added to samples for disulphide bond reduction. Samples were loaded onto a polyacrylamide gels either by using the Protean II system or the Mini protein II system (both from BIO-RAD). All gels were 1.5 mm in thickness. Stock buffers (Section 2.1.2) were stored for up to one month at 0-4 °C. The amount used for gel reagents is shown below, (Table 2.4) for different percentage of gels.

Table 2.4: Quantities of stock solutions required to make up one 3 mm gel of 8, 10 or 12 percent acrylamide.

Stock Solutions	Resolving Gel			Stacking Gel
	8%	10%	12%	
Resolving gel buffer (ml)	25	25	25	-
Stacking gel buffer (ml)	-	-	-	3.4
Acrylamide stock (ml)	20	25	30	5
Double-distilled water (ml)	30	25	20	7.5
Ammonium persulphate (ml)	0.5	0.5	0.5	0.1
TEMED (µl)	40	40	40	20

Minigels were run at a constant 200 mA and Protean II gels were run at a maximum constant current of 25 mA through stacking gels and 35 mA through resolving gels. Gels were run until the dye front eluted from the bottom of the gel. Broad Range molecular weight markers (New England Biolabs) or High Molecular Weight markers (Sigma) were run on each gel. The molecular weight standards for the Broad Range markers were: myosin (212 kDa), maltose binding protein-β-galactosidase (158 kDa), β-galactosidase (116 kDa), phosphorylase *b* (97 kDa), serum albumin (66 kDa), Glutamic dehydrogenase (55 kDa), maltose binding protein (42 kDa), Lactate dehydrogenase (36 kDa), Triosephosphate isomerase (26 kDa), Trypsin inhibitor (20 kDa), Lysozyme (14 kDa), Aprotinin (6 kDa) and Insulin A, B chain (2-3 kDa). The molecular weight standards for the High Molecular Weight markers were: myosin (205 kDa), β-galactosidase (116 kDa), phosphorylase *b* (97 kDa), bovine albumin (66 kDa), egg albumin (45 kDa) and carbonic anhydrase (29 kDa).

2.2.3 Coomaise Blue Staining

Protein bands were visualised by staining with Coomaise brilliant blue reagent (0.2% (w/v) Coomaise blue R-250 in 30% (v/v) MeOH, 10% (v/v) glacial acetic acid, 60% (v/v) dH_2O) for half an h. Staining was followed by destaining (30% (v/v) MeOH, 10% glacial acetic acid, 60% (v/v) dH_2O). The gels were dried at room temperature between two layers of Biotrace membrane pre-soaked in destaining solution containing 8.7 (v/v) glycerol.

2.2.4 Electrophoretic Transfer of gels to Nitrocellulose

Gel proteins were transferred onto nitrocellulose (0.4 μM pore size from Biotrace, Pau Gelman Sciences) using the semi-dry transfer method as described by Towbin (Towbin *et al.*, 1979). Eighteen sheets of filter paper (3MM Whatmann paper) and a sheet of nitrocellulose were cut to the same size of the resolving gel. Filter paper, nitrocellulose and the gel were pre-soaked in transfer buffer, (Section 2.1.2). Both the anode and cathode electrodes were pre-soaked with distilled water. Nine sheets of filter paper were laid onto the anode electrode and then the nitrocellulose sheet was placed on top, followed by the gel and the remaining sheets of filter paper. All air bubbles were removed and the cathode electrode placed on top. Gel transfers were for 1 h and 50 min by applying a constant current (0.8 mA x gel area in cm). After transfer, the nitrocellulose was washed with distilled water and stained with ponceau dye, (Section 2.1.2) in order to visualise proteins.

2.2.5 Western Blotting

Nitrocellulose was rinsed briefly in TBS-Tween (Section 2.1.2). All of the Western blot procedures were carried out at room temperature with gentle shaking of the nitrocelluose. Blocking of non-specific proteins on nitrocellulose was carried out for 30 min using 5% (w/v) Marvel® dried skimmed milk in TBS-Tween. The nitrocellulose was washed briefly in TBS-Tween to remove all blocking solution and then incubated with the primary antibody. For a list of primary and secondary antibodies used for Western blotting, see Table 2.1 and Table 2.2, pages 45-47. The nitrocellulose was then washed 6 x 5 min with TBS-Tween, and then incubated with the secondary horseradish peroxidase (HRP) conjugated antibody for 30 min. After washes (6 times for 5 min) with TBS-Tween the nitrocellulose was incubated for 1 min or 5 min with ECL detection reagents. This allowed detection of proteins bound to the horseradish peroxidase chemiluminescent reagent. Exposure of the nitrocellulose to autoradiography film detected any chemiluminescent products.

2.2.6 Data Analysis

Densometric analyses of scanned Western blots were carried out using the program Molecular Analyst^{TM}/PC *version 1.5,* (Bio-Rad Laboratories). Graphical data were plotted using GraphPad PRISM *version 3*, (GraphPad Software Inc.,).

2.3 Preparation of Rat Adipocytes

Rat adipocytes were obtained from epididymal fat pads of male Wistar rats weighing 180 to 200 g. BSA stocks were prepared prior to the removal of fat pads. 100 g of BSA powder was dissolved in 500 ml of double-distilled water and dialysed for 24 h at 4 °C with two changes of ten times volume of double-distilled water. The BSA solution was made up to 10% (w/v) and filtered through a Millipore filter (type AA, pore size 0.8μm; Millipore V Corporation, Bedford, MA). The BSA solution was then adjusted to pH 7.4 with 10 M NaOH and stored in frozen aliquots at -20 °C.

The necks of male Wistar rats were broken and whole epididymal fat pads were removed quickly (Simpson *et al.*, 1983; Taylor *et al.*, 1981; Whitesell *et al.*, 1979). The fat pads were briefly washed in 1% (w/v) BSA/KRH buffer at 37 °C and chopped up finely with scissors in Digestion buffer. The tissue from four fat pads were digested in 5 ml of Digestion buffer by vigorous shaking for 40-50 min at 37 °C. Digestion was carried out in 25 ml Sterilin clear polystyrene tubes. Any undigested connective material was removed by filtration through a nylon gauze of 250 μm pore size, (Lockertex), into a 23 ml polystyrene flat-bottomed tube (Sarstedt). Cells were washed with 1% (w/v) BSA/KRH at 37°C. Once the fat cells were floating on top of the buffer, the infranatant buffer was removed using a needle 13 guage x 10 cm, (2 mm dia. x 100 mm) attached to a syringe. Cells were washed four times using this procedure or until the BSA/KRH buffer became clear. Cells were made up to 40% cytocrit.

2.3.1 Insulin-stimulation of Isolated Rat Adipocytes

1 mg of monocomponent porcine insulin was prepared by dissolving in 1 ml of 0.03 M HCl and made up to a volume of 3 ml with double-distilled water. 1 ml of this solution was then diluted to 50 ml with 1% (w/v) BSA/KRH buffer, pH 7.6. The insulin stock solution, (final concentration of 1 mM) was stored at –20 °C in 500 µl aliquots until required. The 1 mM insulin solution was not refrozen once thawed.

20 nM of insulin from the 1 mM stock was used to stimulate isolated rat adipocytes (40% cytocrit), for 20 min at 37°C. Basal cells were also maintained at 37 °C during this time. Cells were stimulated with 5 nM insulin for 20 min at 37 °C in studies involving GLUT4 internalisation, (Sections 2.5.2. and 2.6.3).

2.3.2 Subcellular Subfractionation of Rat Adipocytes

Cells were washed 3 times with HES buffer, (Section 2.1.2) containing protease inhibitors at 18 °C to remove albumin. A pulse spin to 1000 g in a bench centrifuge (IEC centr-3) was used to float the cells. The infranatant buffer was removed using a needle (2 mm dia. x 100 mm), and the cells were resuspended in 1.5 ml HES buffer for homogenisation. Cells were homogenised using 10 strokes in a 55 ml Potter-Elvehjem homogeniser (Thomas Scientific: clearance 0.15-0.25 mm) at a rotation speed of approximately 1600 rpm. The resultant homogenates were spun at 1000 g for 2 min producing a layer of fat and an infranatant layer. The infranatant layers were removed with a syringe and needle (21 gauge). The infranatants were subjected to sequential centrifugation with a TLA-100.3 rotor (Beckman TL-100) using a method described by Weber (Weber *et al.*, '88). Crude plasma membrane pellets (containing contaminating mitochondria and nuclei) were obtained by centrifugation at 17, 500 g_{max} (18, 000 rpm) for 20 min.

The supernatants were centrifuged at 49, 000 g_{max} (30, 000 rpm) for 9 min to produce the high density microsome pellets and post HDM supernatants. To obtain the low density microsomes the post HDM supernatants were spun at 541, 000 g_{max} (100 000 rpm) for 17 min. The crude plasma membrane pellets were resuspended in 300 µl HES buffer and loaded onto 0.6 ml sucrose cushions (1.2 M sucrose (38.3% (w/v), 20 mM HEPES pH 7.2, 1 mM EDTA) and centrifuged at 105, 000 g_{max} (35, 000 rpm) for 20

min in TLA-100 swingout rotor. The mitochondria and nuclei pellets were discarded and the plasma membranes were collected from the sucrose cushions, resuspended in HES buffer (containing protease inhibitors), to 3 ml and centrifuged at 74, 000 g_{max} (37, 000 rpm) for 9 min. The plasma membrane pellet was resuspended in 3 ml HES buffer and repelleted at 74, 000 g_{max} for 9 min. All membrane fractions were resuspended in HES and assayed for protein content, (Section 2.2.1).

2.4 Human Erythrocyte Preparation

2.4.1 Preparation of Erythrocyte Membranes

A method described by Baldwin and Lienhard was used to prepare protein depleted erythrocyte membranes (Baldwin *et al.*, 1989). A unit of human blood (450 ml) was distributed into six 250 ml tubes for the Sorvall GSA rotor and then diluted to 175 ml with 5 mM sodium phosphate, 150 mM NaCl, pH 8. The cells were pelleted for 10 min at 3, 300 g_{max} (4, 500 rpm). The supernatant was aspirated using a Pasteur pipette attached to a water pump. The cells were resuspended to 175 ml with 5 mM sodium phosphate, 150 mM NaCl, pH 8 buffer with gentle stirring with a glass rod. Cells were washed as before for another two times. Cells were then lysed by the addition of 5 mM sodium phosphate, pH 8 and adjusted to a volume of 175 ml. The membranes were pelleted by centrifugation at 21, 5000 g_{max} (11, 500 rpm) for 25 min. The supernatant was aspirated and the lysis step repeated 5 times until the membranes were faintly pink. Washed erythrocyte membranes were assayed for protein content and stored at -20°C.

2.4.2 Protein Depletion of Erythrocyte Membranes

To a 40 ml suspension of erythrocyte membranes (3-4 mg/ml), 210 ml of base solution (15 mM NaOH, 2 mM Na_2EDTA, 0.2 mM DTT) was added with constant stirring. The base solution was prepared by dissolving 180 mg EDTA in 250 ml 15 mM NaOH, bubbling through N_2 for 5 min to remove O_2 and adding 7.5 mg DTT just before use.

The mixture was then centrifuged at 43, 500 g_{max} (19, 000) rpm in SS34 tubes for 20 min, and the supernatant aspirated. Pellets were washed in 25 ml of ice-cold 50 mM Tris-HCl pH 7.4. The protein depleted membranes were pelleted again as described above. The pellets were resuspended in 3.8 ml of ice-cold 50 mM Tris-HCl pH 7.4 and

transferred to a 20 ml homogeniser vessel (Thomas Scientific). Homogenisation was carried out using 15-20 strokes and repeated with other 40 ml membrane suspensions after washing the vessel with 50 mM Tris-HCl pH 7.4. The homogenised samples were pooled together and stored at -20°C.

2.5 Glucose Transport Studies

2.5.1 Estimation of the Affinity of Photolabels for Glucose Transporters.

Affinities of labels were estimated from their level of competition with 2-deoxy-D-glucose for glucose transporter exofacial binding sites. This was carried out with modification of the method first described by Whitesell and Gliemann (Whitesell *et al.*, 1979). The transported substrate was used at a tracer concentration that was below the K_m. The tracer was made up to give a final concentration of 4 μCi of 2-Deoxy-[2,6-^{3}H]D-glucose (33 Ci/mmol) and 50 μM cold 2-deoxy-D-glucose in albumin free KRH. Uptake was measured with 20 μl of the tracer stock in round bottom 3 ml thin walled polyallomer tubes, (Nunc). The photolabels were serial diluted (final concentration in assays were 1.6 mM, 800 μM, 400 μM, 200 μM or 0 μM) to a volume of 20 μl in double-distilled water. The diluted photolabel was mixed with the tracer stock. Uptake of the 50 μM 2-deoxy-D-glucose was initiated by the addition of 50 μl of 40 % basal or insulin-stimulated rat adipocyte cells at 37 °C. Uptake was terminated after 1 min by the addition of 2.9 ml of a 300 μM phloretin solution in albumin-free KRH. The phloretin solution was made by dissolving 9 mg of phloretin in 500 μl of 95% (v/v) ethanol and subsequently adding this to 100 ml of KRH. Following the arrest of transport, 1 ml of silicon oil (Dow Corming 1000/200 cs, obtained from BDH) was layered on top of the aqueous phase (Gliemann *et al.*, 1972). The tubes were then centrifuged (MSE bench centrifuge, swingout rotor) at 1000 g for up to 2 min. The sample formed one or two 'islets' of cell layers on top of the oil, which were removed using small pieces of pipe cleaners (5 mm) and were placed in a scintillation vial. 7 ml of scintillant was added and radioactivity estimated in a Packard 1500 TRI-CARB or 1600TR liquid scintillation counter. All measurements were carried out in triplicate. Background values (zero-time uptake) were determined by adding phloretin to the isotope before the addition of the cells. This indicated the amount of extracellular trapped radioactivity.

The rate constant for uptake in the presence (V) and absence (Vo) of inhibitor (I) were then used to calculate the half-maximal inhibition constants for photolabels (Ki), (Baker *et al.*, 1973) according to the equation:

$$\mathbf{Vo/V = 1 + I/Ki}$$

This equation applies when the substrate concentration is low compared with its Km.

2.5.2 Photolabelling of Cell Surface Glucose Transporters.

Rat Adipocyte Photolabelling of Glucose Transporters

Rat adipocytes (40% cytocrit) in 1% BSA/KRH buffer were placed in 35 mm polystyrene dishes (Nunc/Gibco BRL). A range of concentrations of biotinylated photolabel was added to a volume of adipocytes, as indicated in the figure legends. The cells and label were mixed at 18 °C and irradiated for 1 min in a Rayonet RpR-100 photoreactor containing 'mixed lights', a 50:50 ratio of 300 and 350 nm lamps. Following irradiation, the cells were placed into either 20 ml Sterilin universal tubes or 50 ml Falcon tubes with the appropriate wash buffer. A pulse spin to 1000 g in a bench centrifuge (IEC centr-3) was used to wash excess label from the cells. The wash buffer used in experiments for detecting surface labelling of glucose transporters in whole cell rat adipocytes (lysates) was 0.1% (w/v) BSA/KRH at 18°C. For detection of labelled glucose transporters in rat adipocyte subfractions (Section 2.3.2), the wash buffer was HES buffer. The infranatant buffer was removed using a needle (2 mm dia. x 100 mm), and the cells were resuspended in buffer for re-washing. Samples were either solubilised for whole cell lysates by the addition of an equal volume of 2% (w/v) Thesit in PBS buffer or homogenised in HES buffer. Solubilisation or homogenisations were carried out at 18 °C with the presence of protease inhibitors in the buffers. The unsolubilised material was removed by centrifugation at 2000 g for 20 min. Samples were then processed as described in Section 2.5.3 and quantified for glucose transporter labelling (Section 2.2.6).

Human Erythrocyte Glucose Transporter Labelling

Protein depleted erythocyte membranes, (Section 2.4) were used in experiments in which glucose transporters were tagged using photolabels (Table 2.3, page 45). For

each condition, 50 μg of red blood cell ghosts were added to a total volume of 300 μl of ice-cold PBS containing protease inhibitors, (Section 2.1.2). The samples were placed in 35 mm polystyrene dishes (Nunc/Gibco BRL) with the photolabels as described in the figure legends. The cells were irradiated for 1 min in mixed lights and excess label was removed with washes (4 times 1.4 ml ice-cold PBS) and centrifugation at 20, 000 g for 15 min. After the final wash, the pellet was resuspended in 30 μl of 2% (w/v) Thesit in ice-cold PBS buffer containing protease inhibitors. The unsolubilised material was removed by centrifugation at 20, 000 g for 20 min. Samples were then processed as described in Section 2.5.3 and quantified for glucose transporter labelling, (Section 2.2.6).

Internalisation and exocytosis of biotin-tagged Glucose Transporters

Rat adipocytes (40% cytocrit) were stimulated with 5 nM insulin for 20 min. Cell surface glucose transporters were then tagged with biotinylated photolabels at 18 °C. Cells were then washed twice in MES buffer (Yang *et al.*, 1992b) at 37 °C and subsequently twice in 1% (w/v) BSA/KRH containing 2 mM D-glucose at 37 °C. Cells were left for 40 min to allow for glucose transporter internalisation (Clark *et al.*, 1991). For estimation of exocytosis rates, cells in which tagged GLUT4 had been internalised for 40 min were divided into 500 μl aliquots and re-stimulated with the addition of 20 nM insulin for 0-20 min. Neutravidin (Pierce & Warriner Ltd., Chester, U.K.,) at a final concentration of 40 μg was added to the cells simultaneously with the insulin (Clark *et al.*, 1991; Kono *et al.*, 1981). Exocytosis of the glucose transporters was inhibited at the appropriate time points with the addition of 2 mM KCN. Samples were left for 2 min prior to the addition of 500 μl of solubilisation buffer, (Section 2.5.2) and samples were then processed as described in Section 2.5.3. Cells were quantified for glucose transporter labelling (Section 2.2.6).

2.5.3 Detection of the covalent incorporation of photolabels into glucose transporters

Detection of tagged GLUT4 by Immunoprecipitation

The photolabelled transporters from solubilised supernatants or subfractions of adipocytes (Section 2.5.2) were immunoprecipitated overnight at 4 °C with rotation against 50 μl of streptavidin (50% slurry) beads (Pierce & Warriner Ltd.,) per condition.

Prior to immunoprecipitation, the beads were washed twice by spinning at 6000g for 1 min in 1 ml of ice-cold PBS buffer containing protease inhibitors. This removed the storage buffer from the bead. The streptavidin beads were then washed 4 times in 1% (w/v) Thesit in PBS buffer, 4 times in 0.1% (w/v) Thesit in PBS buffer and finally, once with 1 ml of PBS buffer. All buffers contained protease inhibitors. All buffer was removed and the bound biotinylated glucose transporters were eluted in 30 µl of SDS sample buffer (62.5 mM Tris-HCl, pH 6.7, 3% (w/v) SDS, 50% (v/v) glycerol, 0.02% bromophenol blue) by heating at 95 °C for 30 min. The eluate was collected and the procedure was repeated. The two eluates were pooled together with a final concentration of 4 mM of DTT. The samples were loaded onto 10% SDS-PAGE gels, transferred to nitrocellulose and blotted with rabbit COOH GLUT4 antibody.

Detection of Tagged GLUT1 in Human Erythocytes

Subsequent to the solubilisation of tagged GLUT1 on the red blood cell membranes, (Section 2.5.2) the samples were placed in Sample buffer containing 10 mM DTT and subjected to SDS-PAGE. The gels were transferred to nitrocellulose and detected for biotinylated GLUT1 with an extravidin-HRP conjugate (Section 2.1.3, Table 2.12, page 45).

2.6. Gradient Centrifugation

For each gradient experiment, 4 fat pads were isolated from male Wistar rats. Isolated rat adipocytes from the fat pads were treated as described in the figure legends, and then homogenised in HES buffer (Section 2.3.2). Post HDM supernatants or low density fractions from the homogenate were obtained and loaded onto gradients for centrifugation. The gradient centrifugation media (either iodixanol (Optiprep^{TM}), sucrose or glycerol), were prepared using gradient buffer (Section 2.3.2) containing protease inhibitors as first described by Clift-O'Grady and colleagues (Clift-O'Grady *et al.*, 1990). Iodixanol, glycerol and sucrose concentrations are expressed as a percentage (w/v).

2.6.1 Density Gradient Centrifugation

Glycerol or iodixanol media were used in Gradient buffer to prepare discontinuous step gradients. The gradients were constructed with an 8 ml 50% (w/v) sucrose cushion,

layered on top with 5.5 ml of step 5-25% (w/v) glycerol or iodixanol. Gradients were made on ice in polyallomer 25 x 89 mm (38 ml) centrifuge tubes, (Beckman Coulter, Bucks. U.K.,). 2 ml - 2.5 ml of Post HDM supernatants of LDM rat adipocyte subfractions were diluted 5 fold in Gradient buffer and layered carefully on top of the gradients. Gradients were centrifuged at 4 °C in a SW28 Titanium swing-out rotor (Beckman Instruments Inc.), at a speed of 80, 000 g_{av} (25, 500 rpm) for 90 min or 16 h. Gradient fractions (2 ml) were collected from the bottom to top of tube by the use of a capillary tube and peristaltic pump. Aliquots of each fraction (100 µl) were then subjected to SDS-PAGE, (Section 2.2.2) and Western blotting (Section 2.2.5) for the analysis of their component proteins.

2.6.2 Self-forming Gradients

Iodixanol, (Ford *et al.*, 1994; Graham *et al.*, 1994) self-generating gradients were prepared as described by Hashiramoto and James (Hashiramoto and James, 2000). LDM fractions were prepared from rat adipose cells as described above, (Section 2.3.1) and resuspended in HES buffer. The LDM was mixed with iodixanol to a 14% final concentration and the resultant sucrose in the mixture was 190 mM. Self-generating gradients were formed in 2 ml sealed tubes (Beckman Coulter) by centrifuging to equilibrium at 4 °C in a TLV-100 vertical rotor (Beckman Coulter) at 265, 000 g_{av} for 1, 2.5 or 4 hr. Fractions (approx. 200 µl) were collected from the top of the tube and analysed by Western blotting, (Section 2.2.5).

2.6.3 Analysis of Biotinylated GLUT4 Compartments on Gradients

Rat adipocytes (40% cytocrit) were stimulated with 5 nM insulin for 20 min after which cell surface glucose transporters were tagged with biotinylated photolabel at 18 °C, (Section 2.5.2). The photolabels used are indicated in the figure legends. Cells were then washed twice in MES buffer at 37 °C and subsequently twice in 1% (w/v) BSA/KRH containing 2 mM D-glucose at 37 °C. Cells were left for 4 or 40 min to allow glucose transporter internalisation. Trafficking was terminated by washing the cells in HES buffer at 18 °C, (Section 2.1.2) and the cells were homogenised and subfractionated to produce either LDM or post HDM supernatants (Section 2.3.2). The samples were loaded onto the appropriate gradients (see figure legends). Fractions from

the gradients were analysed for the presence of GLUT4, TfR and sortilin by Western blotting, (Section 2.1.3, Table 2.1). Fractions with GLUT4 and fractions with TfR present were pooled together and extensively dialysed overnight against PBS at 4°C. After concentrating the samples to 1 ml, the samples were analysed for the biotinylated GLUT4 content (Section 2.5.3).

2.6.4 Computer Modelling of Translocation Systems

The computer simulations were carried out using the interactive simulation software package ISIM, distributed by Simulation Science, Manchester, UK. The simulation methodology and strategy was followed from published methods (Holman *et al.*, 1994).

2.7. Confocal Microscopy

2.7.1 Preparation and Incubation of Adipose Cells

Rat adipocytes (40% cytocrit) were suspended in 1% (w/v) BSA/KRH, (Section 2.3.0) and were prepared for confocal microscopy as described by Malide and colleagues (Malide *et al.*, 1997a). Unless stated otherwise all procedures were performed at room temperature. For each condition, 1- 2 ml of rat adipocytes were used in Sarstedt tubes. After removal of the buffer, cells were gently rinsed three times with 7.5 ml PBS (pH 7.2) and fixed for 20 min by rocking in 7.5 ml of 2% (w/v) paraformaldehyde in PBS. Cells were washed 3 times in PBS, and quenched in 100 mM glycine in PBS for 10 min. Cells were rocked gently in 7.5 ml of Permeabilisation buffer, (0.1% saponin, 3% Goat Serum, 1% BSA in PBS) for 45 min. Floating cells (approximately 200 µl) were taken from the top of the buffer and placed in 1.5 ml microfuge tubes (Sartstedt). The buffer was removed and replaced with the appropriate primary antibodies, (Section 2.1.3, Table 2.1). The antibodies were made up in Permeabilisation buffer. The cells were rotated for 1 h at room temperature in the presence of the primary antibodies. After 1 h incubation, the cells were washed six times in wash buffer, containing 1% (w/v) BSA/PBS with 0.1% saponin. A 200 g, 30-second spin was used for washing and 21g needle and syringe was used to remove the infranatant wash buffer from the floating cells. Secondary antibodies (Section 2.1.3, Table 2.2) were incubated with the cells for 1 h in Permeabilsation buffer, after which the cells were washed three times and transferred to 2 ml Eppendorf tubes for rotation overnight. Cells were then washed

a further six times and 10 µl of the cells were mounted onto coverslips using Vectashield, (Vector Laboratories, Inc. Burlingame, CA).

2.7.2 Microscopy and Image Analysis

Fluorescent images were obtained using a Zeiss confocal laser scanning microscope, (LSM 510, Carl Zeiss Microscopy, Germany). The system utilised a 454/488 nm laser (for fluorescein labelled samples) or a 543 nm laser (for rhodamine labelled samples). Specimens were viewed at high magnification using planapochromat X 60/1.4 NA oil objectives. For each experimental condition, 3 images/cell were recorded from at least 3 cells. Images were collected sequentially for the two fluorochromes in the double-labelling experiments at an optical zoom setting of 2. Co-localisation was assessed by the examination of merged images.

3.0 Purification and Characterisation of an Amino-Terminal GLUT4 Antibody

3.1 Immunological Probes as Tools for Tracking GLUT4

With the use of cytochlasin B binding and subcellular fractionation, it was first shown in 1980 that the mechanism by which insulin increases glucose transport in cells is by the translocation of glucose transporters from the interior of the cell to the plasma membrane (Cushman and Wardzala, 1980). Since this discovery a number of technologies have been developed which have allowed researchers to define the glucose transporter responsible for this increased transport activity. One approach has extensively involved the use of immunological probes against glucose transporters. James and Pilch were the first to isolate a monoclonal antibody which recognised a protein subsequently shown to be GLUT4, (James *et al.*, 1988). GLUT4 antibodies have provided a means to investigate the association of GLUT4 with other proteins present in GLUT4 vesicles. Lienhard and colleagues were able to immunoadsorb GLUT4 vesicles from the low density microsomal membrane fraction using GLUT4 antibodies immobilised to a solid matrix, (Biber and Lienhard, 1986; Brown *et al.*, 1988)

Over ten years of research into GLUT4 trafficking have lead to the production of many different GLUT4 antibodies, (see Section 2.1.3 and Figure 3.1, page 63 for examples). These antibodies have been used to analyse GLUT4 distribution and translocation (Ploug *et al.*, 1998; Smith *et al.*, 1991; Wang *et al.*, 1996a). The current model that GLUT4 translocates from intracellular compartments to the plasma membrane in response to insulin has been firmly established using a combination of methods and these include quantitative ultrastructural examination using immunogold labelling (Slot *et al.*, 1991). However, there have been some studies that have suggested that the movement of GLUT4 in response to insulin may be more complicated than a simple translocation process. Two groups have proposed that the mechanism involves conformational changes which mask an antigenic epitope (Smith *et al.*, 1991; Wang *et al.*, 1996b). Wang and colleagues used a carboxyl-terminal GLUT4 antibody to detect for GLUT4 in frozen muscle cells. They observed an increase in the total native GLUT4 immunoreactivity in the insulin-stimulated compared to basal sections of muscle compared to basal muscle. This was assessed by both confocal microscopy and immunogold electron microscopy. The Smith *et al* study reported that in insulin-treated

rat adipocytes, the total number of labeled transporters detected by carboxyl-terminal GLUT4 antibodies increased by approximately 13-fold. However, this change was not observed when the group used an amino-terminal GLUT4 antibody. These results suggested that the carboxyl-terminal of GLUT4 was masked and that the unmasking of this epitope during translocation to the plasma membrane may be part of the mechanism for insulin-stimulation of glucose transport. This unmasking model seems feasible as the carboxyl-terminal cytoplasmic tail of GLUT4 lies in close proximity to a dileucine motif that confers insulin-sensitive targeting (Melvin *et al.*, 1999; Verhey *et al.*, 1994; Verhey *et al.*, 1995).

3.1.1 Antibodies against the Amino- and Carboxyl-Terminal Domains of GLUT4

The experimental aim of the work described in this chapter was to purify and characterise a novel polyclonal GLUT4 antibody raised against a peptide corresponding to the amino-terminus of GLUT4 in order to re-examine the possibility of epitope masking. A rabbit antiserum against GLUT4 was prepared using a synthetic peptide of the amino-terminus of GLUT4, IGSEDGEPPQQC. The carboxyl-terminal GLUT4 antibodies used were either the monoclonal 1F8 (James and Pilch, 1988) or the polyclonal raised against the peptide, CSTELEYLGPDEND (Holman *et al.*, 1990).

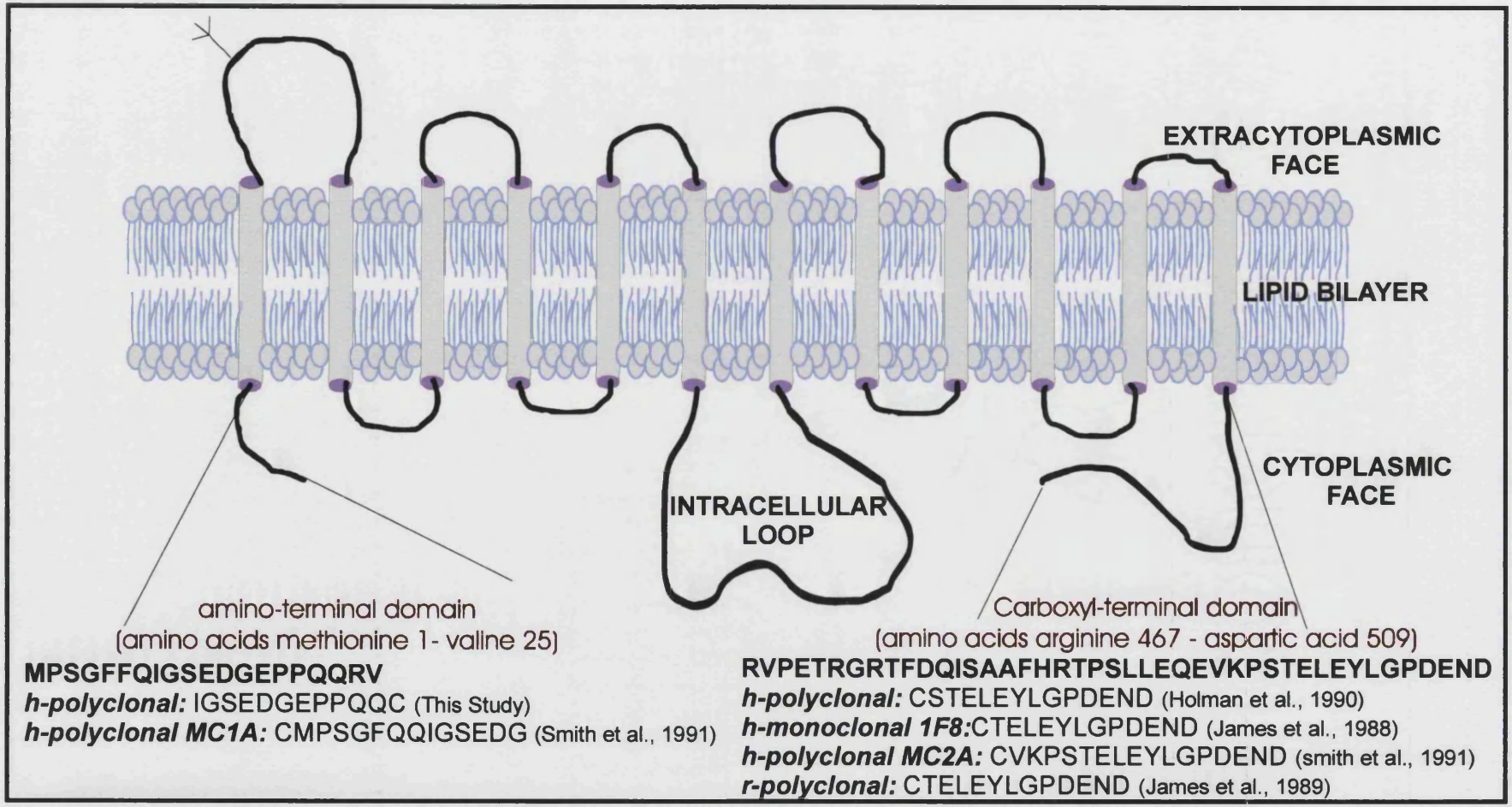

Figure3.1: Schematic representation of the amino- and carboxyl- terminal domains of GLUT4.
Examples of some synthetic GLUT4 amino- or carboxyl- peptides used to raise monoclonal or polyclonal antibodies against GLUT4 are shown.

3.2 Immunoaffinity Purification of an Amino-Terminal GLUT4 Antibody

3.2.1 Analysis of Rabbit Antisera raised against the synthetic GLUT4 peptides

Confirmation that the amino-terminal GLUT4 antibody (255 serum) bound specifically to the glucose transporter GLUT4 was sought using the technique of Western blotting, (Section 2.2.5). The serum detected a zone corresponding to the molecular weight range of 45-50 kDa on blots of rat adipocyte subfractions, (LDM: low density microsomal membrane fractions, PM: plasma membrane), (Figure 3.2, NH_2-GLUT4 Ab). The bands were compared with those detected using a polyclonal carboxyl-terminal GLUT4 antibody, (Figure 3.2, COOH-GLUT4 Ab). The amino-terminal GLUT4 antibody detected two bands, both around 45 kDa. In comparison, the carboxyl-terminal GLUT4 antibody only detected one band of molecular weight 45 kDa. The presence of two bands with the amino-terminal GLUT4 antibody may have been due to the recognition of two forms of glucose transporter in rat adipose cells (Horuk *et al.*, 1986) or due to an artifact of sample preparation for SDS-PAGE. Past studies have shown that the carboxyl-terminal GLUT4 antibody is specific for the glucose transporter isoform, GLUT4 (Holman *et al.*, 1990). This specificity of the carboxyl-terminal antibody has been shown in Figure 3.2. The reduction in binding of the antibody to GLUT4 from intracellular membranes in insulin-stimulated adipose cells, corresponds to the translocation of GLUT4 from the interior of the cell to the cell surface (Zorzano *et al.*, 1989).

There is no clear visual evidence of a reduction of the amino-terminal antibody binding to GLUT4 in LDM or a corresponding increase at the PM in the presence of insulin. The question was asked: Is the rabbit antisera (255 serum) specific for the GLUT4 isoform or is the sera detecting other proteins around 45kDa other than GLUT4. To address these questions, an attempt was made to remove any contaminants from the sera by immunoaffinity purification. It was hoped that the purification step would increase the specificity of the 255 serum for its antigen, GLUT4.

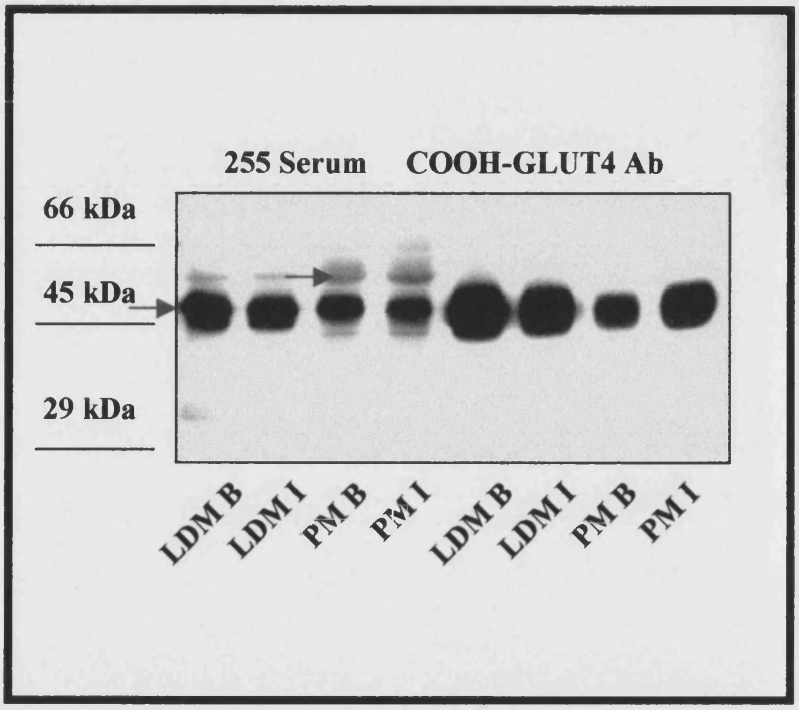

Fig 3.2: Western blot detection of GLUT4 in rat adipocyte subfractions with the use of amino- and carboxyl-terminal GLUT4 antibodies

Amino-terminal GLUT4 serum antibody (**255 serum**) and the carboxyl-terminal GLUT4 purified antibody (**COOH-GLUT4 Ab**) were used to detect for GLUT4 in rat adipocyte subfractions of 20 μg of plasma membrane, (**PM**) and 10 μg of low density micosomes, (**LDM**). Antibodies were used at a dilution of 1:1000 and 1:4000 in 1% (w/v) BSA TBS-Tween respectively. Rat adipocytes were stimulated with 20 nM Insulin for 20 min (**I**) or were maintained in the basal state (**B**) prior to subfractionation. High molecular weight markers were used. The size of these proteins is given in kDa. The blue arrows indicate the bands detected by the amino-terminal GLUT4 serum. The Western blot shown above is representative of three separate repetitions of this experiment.

3.2.2 Purification of amino-terminal GLUT4 rabbit antisera by a peptide column

Immunoaffinity purification of the amino-terminal GLUT4 serum (255 serum) was carried out by use of amino-terminal peptide as an antigen bound to a solid matrix. Several attempts were made to perfect the purification method before the correct column material was used, as described in this section.

Initial attempts to purify the 255 serum were carried out using a method similar to that of the purification of rabbit antisera against the synthetic peptide of the carboxyl-terminal of GLUT4, STELEYLGPDEND (Holman *et al.*, 1990). The carboxyl-terminal peptide was made with a cysteine linking moiety at the serine terminus (Davies *et al.*, 1987b). The amino-terminal GLUT4 peptide was also made with a cysteine moiety enabling affinity purification using a peptide column similar to that described by Oka and colleagues (Oka *et al.*, 1988). 5 mg of peptide was coupled to 2 ml of Reactigel-6X (Pierce and Warriner Chem. Co., Rockford, IL) in 0.1M sodium borate buffer, pH 8.5. The mechanism for the coupling reaction between peptide and Reactigel-6X is given in Figure 3.3A. After equilibrating the Reactigel in a small column with PBS, 4 ml of the rabbit antisera (255 second bleed) was circulated overnight. The reactigel was then washed in PBS and 2 M NaCl in 10 mM phosphate buffer, pH 7.2 to remove loosely bound non-specific impurities. The bound antibody was then eluted with 3.5 M sodium thiocyanate in 10 mM sodium phosphate buffer, pH 6.6 and dialysed overnight against PBS. Western blot analysis revealed that a large amount of the immunoreactive component of the serum was lost during the procedures of washing the column in PBS. This indicated that the coupling of the peptide to the matrix was not successful and purification procedures were terminated, (results not shown).

The 255 serum was affinity-purified against the peptide antigen covalently coupled to a SulphoLink® Coupling Gel column, (Pierce and Warriner Chem. Co., Rockford, IL). The SulphoLink® matrix contained a 12 atom spacer arm with iodoacetyl moieties for efficient conjugation to the small amino-terminal peptide via it's cysteine terminus, (Figure 3.3B). A 4 ml SulphoLink® Coupling Gel column which was conjugated to 4 mg of synthetic amino-terminal GLUT4 peptide (IGSEDGEPPQQC) was prepared by following the manufacturers instructions, (Pierce Chemical Company, 2000). The SulphoLink column

was washed with PBS and the column drained until the buffer was just 5 mm above the column. A volume of 8 ml of serum 255 (second bleed) was added to the column followed by recircluation overnight at 4 °C with a peristaltic pump. The flow-through was then collected and excess unbound serum was removed with washes of 40 ml of PBS. Bound antibody was eluted with 12 ml of 3.5 M sodium thiocyanate in 10 mM phosphate, pH 7.2 buffer. The elutant was extensively dialysed overnight against PBS at 4 °C and then concentrated by use of polyethylene glycol, (PEG 20, 000) to a volume of 6.5 ml.

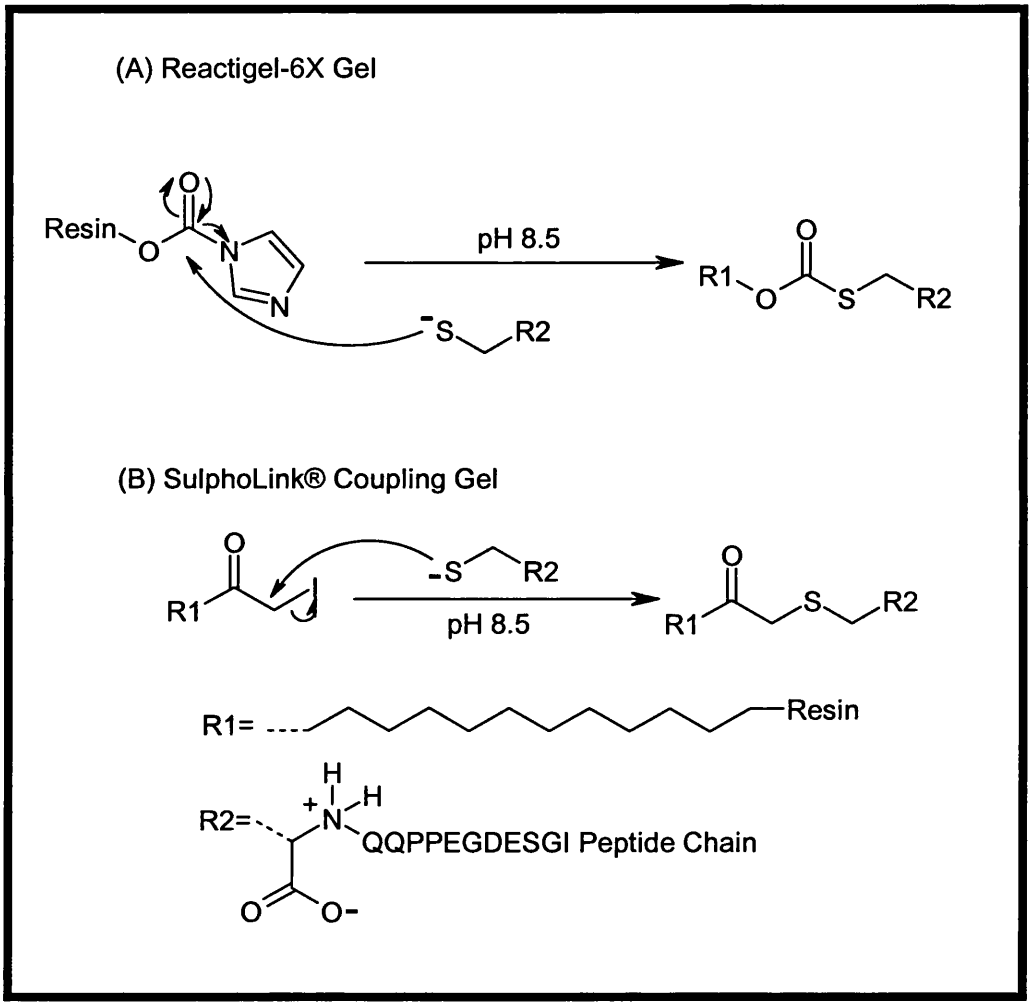

Figure 3.3. Schematic representation of the immobilsation of the amino-terminal GLUT4 peptide onto the Reactigel-6X or SulphoLink® Coupling Gel. (A) shows the amino-terminal GLUT4 peptide chain (R2) immobilsation mechanism with the Reactigel-6X. (B) denotes the 12-atom spacer arm linked to the resin and the iodoacetyl moitiy (R1). The immobilisation of the peptide to the resin occurs at pH 8.5, where there are free sulphydryl groups on the amino acid cysteine.

The concentration of the purified antibody was estimated at 238 μg of antibody/ml serum by the BCA protein assay, (Section 2.2.1). The antibody was stored in 30% (w/v) glycerol containing 0.02% sodium azide at –20 °C. The antigen binding activity of the purified amino-terminal GLUT4 antibody was compared to the original 255 serum, re-circulated serum and the PBS wash by Western blotting, (Figure 3.4). The purification led to a reduction in background on the Western blot produced by the amino-terminal GLUT4 antibody, (compare original serum to purified, Figure 3.4). The non-specific band which was present in the original serum was absent when using the purified antibody (compare original serum to purified, Figure 3.4). In addition, there was a clear increase in antibody binding to insulin treated PM indicating specificity of the purified antibody for the GLUT4 isoform, (compare PM B and PM I, Figures 3.2 and 3.4). There was negligible loss of activity of the antibody through purification. To directly compare antigen-antibody binding a Western blot analysis with the purified and non-purified amino-terminal antibody and carboxyl-terminal antibody were carried out on PM, LDM and cytosolic fractions of basal rat adipose cells, (Figure 3.5). GLUT4 is known to be absent in the cytosolic fraction of rat adipocytes (Simpson *et al.*, 1983). Both the purified amino-terminal and carboxyl-terminal GLUT4 antibodies did not detect GLUT4 in the cytosolic fraction. However, the unpurified amino-terminal GLUT4 antibody reacted non-specifically with proteins in the cytosol. Thus the serum had been successfully purified from contaminants.

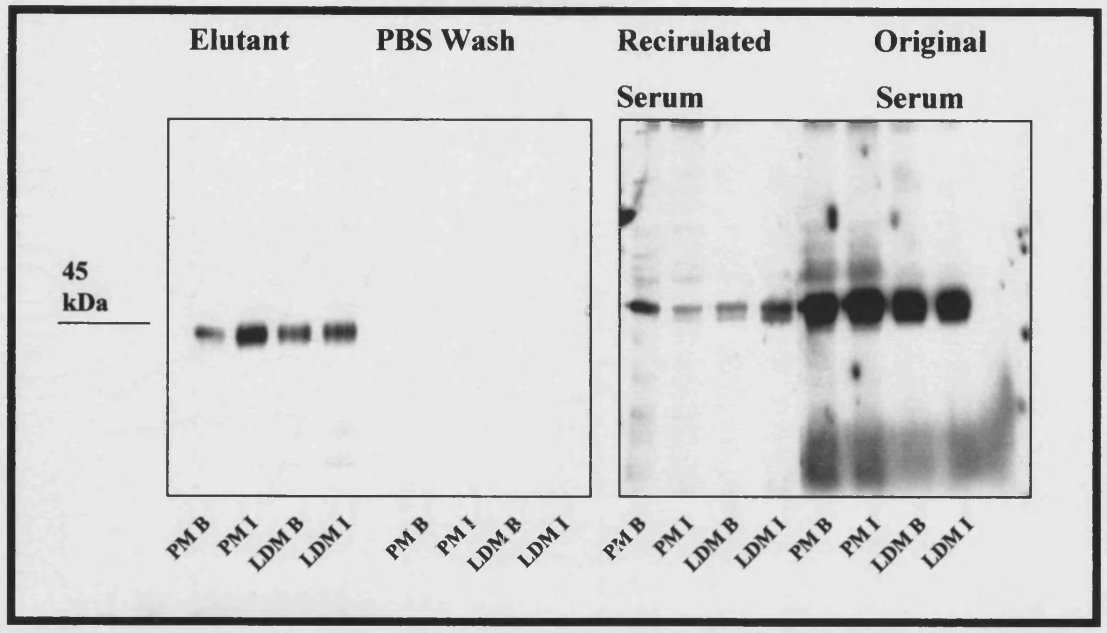

Figure 3.4: Immunoaffinity purification of the amino-terminal GLUT4 antibody.

The amino-terminal GLUT4 antibody was purified on a SulfoLink column. The purity was tested by analysis of the ability of elutant, original serum, recirculated serum and PBS washes to detect GLUT4 using Western blot techniques of rat adipocyte subfractions. 20 μg of PM or 10 μg of LDM from basal or insulin treated rat adipocytes were used. All probes were diluted to a concentration of 1:1000 in 1% (w/v) BSA TBS-Tween, Section 2.1.3)

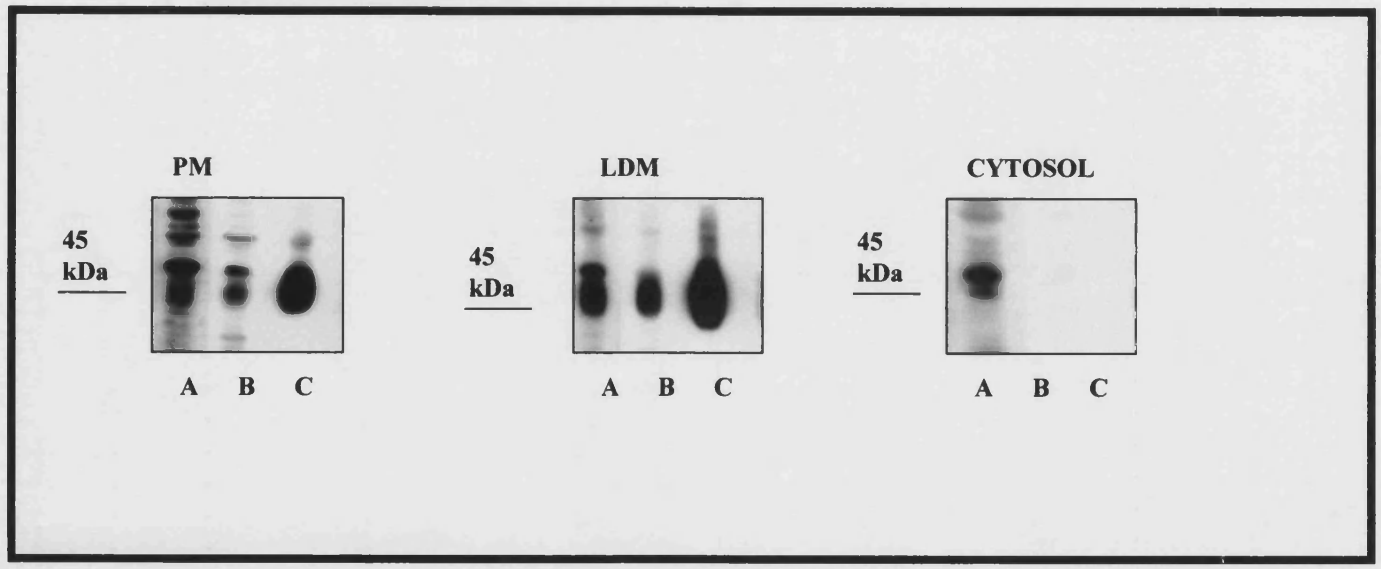

Figure 3.5: Detection of rat adipocyte GLUT4 using the purified amino-terminal GLUT4 antibody compared and the serum and carboxyl-terminal GLUT4 antibody.

50 μg PM, 20 μg LDM and 100 μg cytosolic fractions from rat adipocytes were run down a 10% SDS-PAGE gel, transferred to nitrocellulose and Western blotted for GLUT4. The antibodies used were (A) unpurified amino-terminal GLUT4, (B) purified amino-terminal GLUT4, and (C) carboxyl-terminal GLUT4. Amino-terminal antibodies were used at a working dilution of 1:1000 in 1% (w/v) BSA TBS-Tween and 1:4000 for the carboxyl-terminal antibody.

3.3 Antigen Binding Activity of GLUT4 Antibodies

The antigen binding activity of the purified amino-terminal GLUT4 antibody was compared to that of the polyclonal carboxyl-terminal GLUT4 antibody (Holman *et al.*, 1990) and monoclonal carboxyl-terminal (IF8) GLUT4 antibody (James and Pilch, 1988), (see Figure 3.6). The polyclonal carboxyl-terminal GLUT4 antibody demonstrated greater binding to GLUT4 than both the polyclonal amino-terminal GLUT4 and 1F8 antibodies, (Figure 3.6i). It must be noted that the carboxyl-terminal GLUT4 antibody was used at a 4-fold lower dilution than the 1F8 and amino-terminal GLUT4 antibodies. Both the carboxyl-terminal GLUT4 antibodies overall had higher binding affinity for GLUT4 (in both basal and insulin-stimulated cells) than the amino-terminal antibody. Interestingly, a comparison of the density counts from the binding of the antibodies to GLUT4 on western blots reveal that both the carboxyl-terminal GLUT4 antibodies detected 2-fold more GLUT4 in basal cells than in insulin-stimulated cells. The amino-terminal antibody revealed a 17-fold difference between GLUT4 in basal cells than in insulin-stimulated cells (Figure 3.6ii)

The Western blotting conditions were manipulated in order to enhance the binding affinity of the amino-terminal GLUT4 antibody to its antigen. Batleiger has shown that Tween-20 may be used as a blocking agent in the immunological detection of proteins transferred to nitrocellulose membranes (Batleiger *et al.*, 1982). However, some antibodies have weak binding capacities to their antigens, which can be further reduced by the presence of denaturants such as detergents (Tween-20). The detergent Tween-20 was omitted from the incubation and wash buffers of the immunoblotting, (Figure 3.7, lanes 1-3) and various concentrations of the primary and secondary antibody were used to optimise blotting conditions. The omission of Tween-20 produced greater background staining on the Western blots (Figure 3.7, lanes 1, and 2) and showed little improvement in the ability of the antibody to bind to its antigen. The conditions used in lane 6 were maintained for further Western blot analysis of GLUT4 using the amino-terminal antibody.

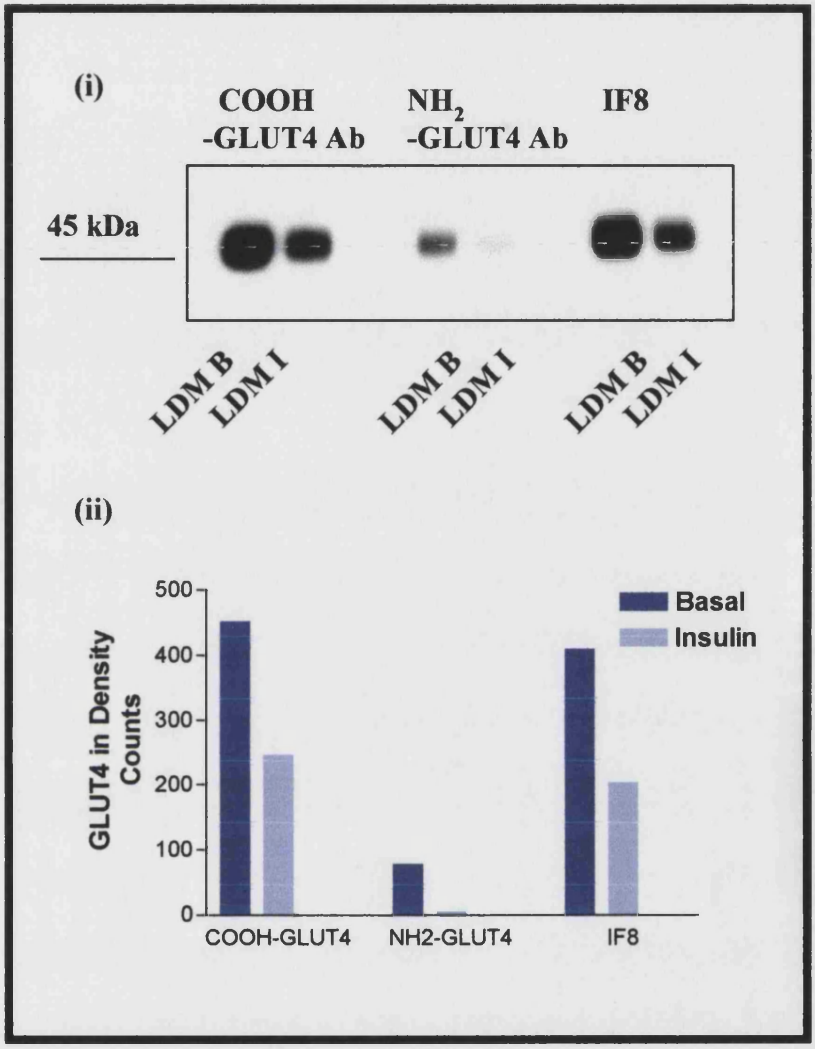

Figure 3.6: Comparison of GLUT4 detection using the amino-terminal and the carboxyl-terminal GLUT4 antibodies.

A 1:1000 dilution of the affinity purified amino terminal antibody in TBS-Tween was used to detect for GLUT4 in 10 μg of LDM basal (**LDM B**) or insulin-treated rat adipocytes (**LDM I**) by Western blotting (Fig 3.6i). Other antibodies used for GLUT4 detection were the monoclonal 1F8 antibody (1:1000) and the carboxyl terminal antibody (1:4000) in 1% (w/v) BSA TBS-Tween. Measurement of the amount of GLUT4 detected by each antibody was carried out by density measurements using Molecular Analyst and data was plotted graphically with Prism graphPad sotware, (Figure 3.6ii). The Western blot and its density analysis shown above are representative of two separate repetitions of this experiment.

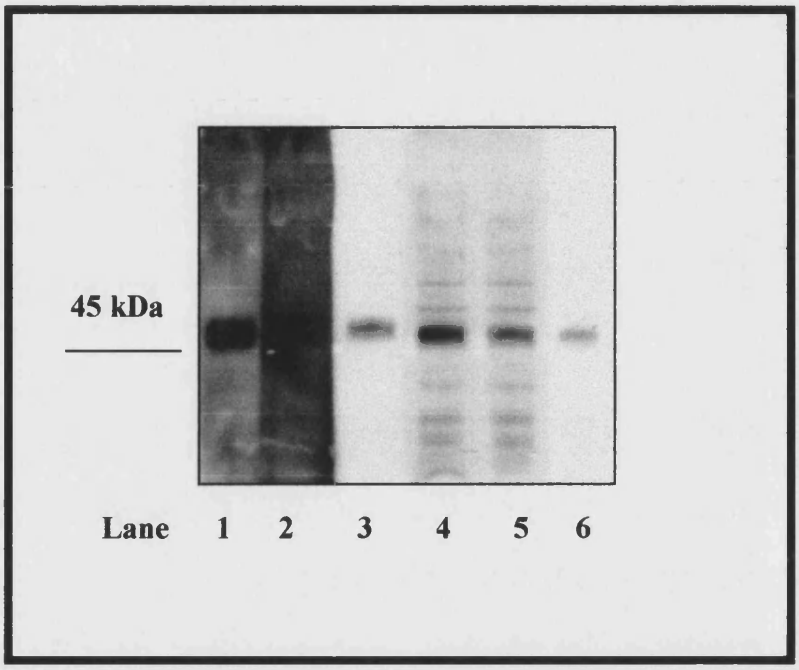

Figure 3.7: Optimisation of Western blotting conditions for the amino-terminal affinity purified GLUT4 antibody.

The detection of GLUT4 in 10 µg of Basal Rat Adipocyte LDM was caried outusing the affinity purified amino-terminal GLUT4 antibody under the conditions given below. Western Blotting was carried out in the absence (lanes 1, 2 and 3) or presence (lanes 4, 5 and 6) of 0.1% Tween. The Western blot shown above is representative of two separate repetitions of this experiment.

Lane	Dilution of Primary Ab	Dilution of Secondary Ab
1	1:500	1:1000
2	1:1000	1:1000
3	1:1000	1:4000
4	1:500	1:1000
5	1:1000	1:1000
6	1:1000	1:4000

3.4 Immunofluorescence Microscopy using GLUT4 Antibodies

Several groups have employed immunofluorescence microscopy to detect for GLUT4. The technique reveals high resolution three-dimensional distribution of whole-cell immunostaining.

Dual labelling of GLUT4 with the amino-terminal GLUT4 antibody and monoclonal 1F8 GLUT4 antibody were used in whole cell rat adipocytes, as described by Malide and colleagues (Malide *et al.*, 1997a). Representative pictures of the labelled cells are given in Figure 3.8. The fluorochrome secondary antibodies for the monoclonal 1F8 and polyclonal amino-terminal GLUT4 antibody were rhodamine (red) and fluoresceine (green), respectively. The images in Figure 3.8 show that the rat white adipose tissue is around 80 μm in diameter containing lipid. The thin cytoplasmic rim of approximately 1 μm surrounds the cells. In the absence of insulin, (Figure 3.8A) GLUT4 is found to be completely intracellular and juxtaposed to the nuclear region. In the presence of insulin, there is a large increase in staining at the cell surface (Figure 3.8B). The staining was also more prominent at the nucleus (Figure 3.8C). The yellow staining shows that both the amino-terminal GLUT4 antibody and the 1F8 are detecting the same GLUT4. As controls the primary antibodies were omitted from the staining. No visible staining was produced under these conditions. The staining of GLUT4 was more prominent with the 1F8 than the amino-terminal GLUT4 antibody. It must be noted that although the two antibodies (amino-terminal and 1F8) detect different antigens, the amino- and carboxyl- termini of GLUT4 may be in close proximity to each other and thus, the binding of one antibody would sterically hinder the binding of the subsequent antibody (Griffiths, 1993). To test the intensity of the staining in double-labelling experiments, the sequence of addition of the primary antibodies were reversed. This had no effect on the staining of GLUT4 with the amino-terminal GLUT4 antibody. It was noted that there was a large increase in total 1F8 staining in insulin-stimulated cells compared to basal cells whereas the amount of amino-terminal GLUT4 staining was consistent. The distribution of signal from the amino-terminal and IF8 GLUT4 antibodies moved from the perinuclear area to the cell surface after insulin-stimulation.

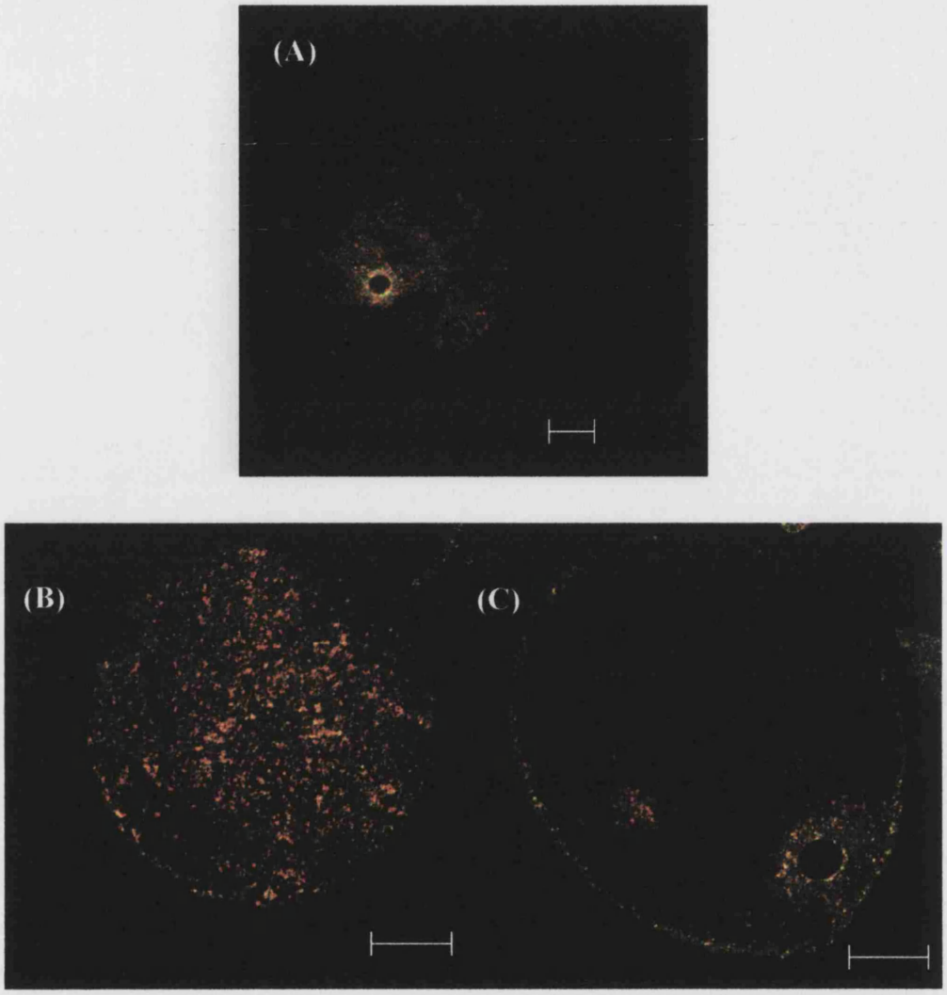

Figure 3.8: Detection of GLUT4 in intact rat adipocytes by dual labelling with amino- and carboxyl-terminal (1F8) GLUT4 antibodies.

Basal (A) and Insulin-stimulated (B-C) rat adipocytes were used to label GLUT4 with 5 μg/ml of 1F8, followed by an incubation of 5 μg/ml of anti-amino-terminal GLUT4 purified antibody. Rhodamine (red) and FITC (green) secondary antibodies were used to detect for the 1F8 and amino-terminal antibodies, respectively. Figure (**B**) represents the cell surface and figure (**C**) the nucleus. Bar Length: 20 μm. The pictures shown above are representative of two separate repetitions of this experiment.

3.5 Discussion

A novel polyclonal GLUT4 antibody raised against the amino-terminal GLUT4 peptide, IGSEDGEPPQQC has been purified and characterised. Purification of the antibody was carried out using a SulphoLink® Coupling Gel column and characterised by the means of Western blotting and Confocal Microscopy. The pattern of labelling of blots of GLUT4 found with the antisera raised against the amino-terminal of GLUT4 closely resembled patterns previously found using the polyclonal carboxyl-terminal GLUT4 antibody and the monoclonal IF8 antibody. Purification of the amino-terminal GLUT4 antibody abolished the cross-reactivity of the serum with other proteins found in the cytosolic fraction of rat adipocytes

In comparison to the polyclonal carboxyl-terminal GLUT4 antibody and the monoclonal 1F8 antibody, the amino-terminal antibody did not bind as strongly to GLUT4. The ability of the amino-terminal antibody to bind to GLUT4 may be related to the length of the peptide it was raised against and possible masking of epitopes within the GLUT4 protein. It was established that the presence of detergent (0.1% (w/v) Tween-20) was necessary to produce clean Western blots of GLUT4 using the amino-terminal GLUT4 antibody and that the detergent did not reduce the binding of antibody to antigen. The significantly low signal for GLUT4 detection by the amino-terminal antibody in comparison to the other GLUT4 antibodies may be due to length of intracellular loop and the length of peptide. It was hypothesised that the length of the GLUT4 terminus may play a part in the accessibility of antibodies to their antigens. The intracellular amino-terminal section of GLUT4 has 24 amino acids, whilst the carboxyl-terminal intracellular loop is approximately twice as long, (43 amino acids). It is therefore argued that the amino-terminal GLUT4 antibody cannot detect GLUT4 at a high intensity because of the shortness of the antigen. To date there has been no crystal structure of any member of the glucose transporter family, which could support this hypothesis.

Experiments were conducted in order to establish if insulin induced unmasking of the carboxyl-terminus of GLUT4 (Smith *et al.*, 1991). The purified polyclonal amino-terminal GLUT4 antibody and the monoclonal 1F8 were used to detect GLUT4 in insulin-stimulated

and basal rat adipocytes by confocal microscopy. The two antibodies were simultaneously used and the total labelling of GLUT4 by the antibodies were recorded. The antibody signals were highly co-localised in both basal and insulin-stimulated rat adipocytes. The strong labelling around the nuclear area decreased and cell surface labelling increased in the presence of insulin-stimulated cells. It was observed that the 1F8 antibody appeared to detect more total GLUT4 on the cell surface in the insulin state than the basal state in the rat adipocytes. Published results of immunoelectron microscopic studies using the 1F8 and a carboxyl-terminal antibody (raised against the peptide CVKPSTELEYLGPDEND) on rat adipocytes also revealed a similar increase in GLUT4 detection (Smith *et al.*, 1991). The results suggest that the intracellular carboxyl-terminal epitope may be masked under basal conditions. The masking may result from difference in the conformation of the carboxyl-terminus of the transporter protein or lipid surrounding the transporter. However, there is some controversy in the literature concerning the masking of carboxyl-terminal epitopes in insulin-regulated tissues (Malide *et al.*, 2000; Ploug *et al.*, 1998; Wang *et al.*, 1996).

Malide and colleagues used immunoelectron microscopic to study GLUT4 compartments in isolated rat white adipose cells. The total number of GLUT4 carboxyl-terminal epitopes detected by the immuno-gold method was shown not to be significantly different between basal and insulin-stimulated cells (Malide *et al.*, 2000). The measurement of binding of different GLUT4 antibodies to GLUT4 have also been analysed in other insulin-stimulated tissues (Ploug *et al.*, 1998). Ploug used a ^{125}I-labeled secondary antibody. Single fibers were labeled with either the carboxyl-terminal GLUT4 antibody or with an amino-terminal GLUT4 antibody or with caveolin-3. The latter antibody was used as an independent marker of the muscle cell surface to correct for differences in fiber and sarcomere length. The number of carboxyl-terminal and amino-terminal GLUT4 epitopes accessible to antibody binding was unaffected by stimulation with either insulin, muscle contractions or both stimuli combined. Their results do not support the concept of GLUT4 epitope masking.

Detecting of proteins by immunofluorescence carries its limitations. The rat adipose cells are comprised of a thin cytoplasmic rim surrounding a large lipid droplet. This limits the resolution. This combined with poor labelling efficiencies of antibodies compromises quantitative assignment of GLUT4 carrying membranes.

Conclusions

In conclusion the purification of the amino-terminal GLUT4 antibody has been successful. The amino-terminal GLUT4 antibody has been shown to be specific for GLUT4 in Western blot analysis. However, immunofluorescence studies using the amino-terminal GLUT4 show that this technique may be limiting in detecting the precise location and quantity of GLUT4 vesicles in rat adipose cells. Recently, a novel morphological approach for studying the distribution of GLUT4 in isolated rat adipocytes has been developed by Ramm and co-workers (Ramm *et al.*, 2000). The method preserves 3-D information of GLUT4 compartments and at the same time results in efficient immunogold labelling. It would be of interest to use this technique to further quantify GLUT4 labelling with different markers.

4.0 Novel Photoaffinity Labels for Tagging GLUT4

4.1 Labelling of GLUT4 with Membrane-Impermeant Glucose Analogues

The development of a series of bis-hexoses developed by Midgley was followed by the synthesis of ATB-BMPA which is a membrane–impermeant photoaffinity label (Holman *et al.*, 1985; Midgley *et al.*, 1985a). This has proved valuable in defining quantitative data for glucose transporter levels at cell surfaces (Clark *et al.*, 1990). Subsequently, a series of biotinylated compounds have been synthesised to replace the tritiated ATB-BMPA form. This has provided a safer means, and more effective way, of tracking glucose transporters (Koumanov *et al.*, 1998). This chapter describes a range of new compounds, Bio-LC-ATB-BGPA, Bio-SS-ATB-BGPA and Bio-LC-G15 that have been used to label glucose transporters and which have been developed in the Holman Laboratory. The biological properties of the three novel compounds were assessed in comparison to the characterised labels, Bio-ATB-BMPA and Bio-LC-ATB-BMPA. The chemical structures of the photolabels are shown in Figure 4.1. All labels contained a photolabile ATB group and a biotin group used in the macromolecule (the tagged glucose transporter) detection system. The chapter describes the experiments used to address the following questions:

- Does the replacement of the bis-mannose hexose derivative with the bis-glucose analog or with mono-glucose alter the affinity of the label for glucose transporters?
- Does the increase in linker length between the photoreactive diazirine group and the biotin groups alter the affinity of the label for glucose transporters?
- Is the biotin detectable in intact cells?
- Will the introduction of a cleavable disulphide (SS) in the spacer between the biotin and the diazirine moiety permit an easy release of the tagged protein from the macromolecule detection system?

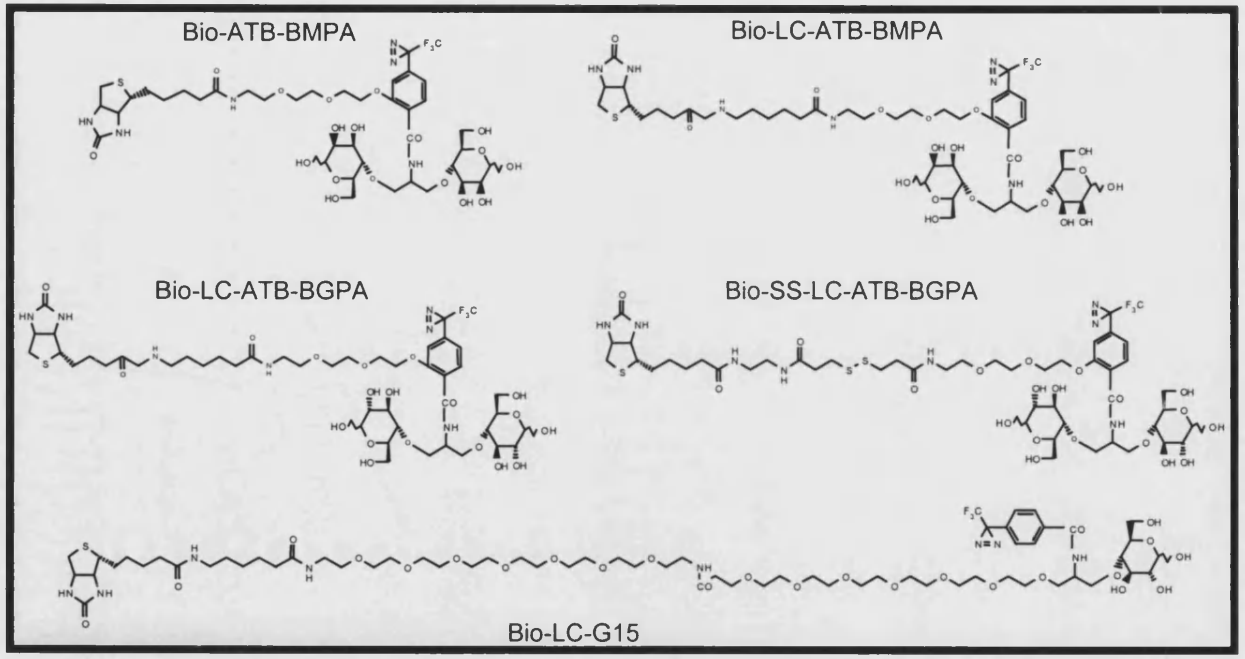

Figure 4.1: Chemical Structure of Photoaffinity Labels for Glucose Transporters.
The chemical structure of the three novel labels, Bio-LC-ATB-BGPA, Bio-LC-ATB-BGPA and Bio-LC-G15 are shown. The compounds Bio-ATB-BMPA and Bio-LC-ATB-BMPA are also shown. The bis-mannose in the BMPA compound was substituted by a bis-mannose unit to produce the Bio-LC-ATB-BGPA label. A disulphide bond was placed in the long-chain in the Bio-LC-ATB-BGPA to give the label Bio-SS-LC-ATB-BGPA.

4.2 Affinity of Photolabels for the Glucose Transporter

The affinities of the interaction between the labels and GLUT4 were determined by using the labels as competitive inhibitors of 2-deoxy-D-glucose uptake into insulin-stimulated rat adipocytes, (Section 2.5.1). The half-maximal inhibition constants of the compounds (Ki values) are given in μM, (Table 4.1 and Figure 4.2).

Table 4.1: Half-Maximal Inhibition of Photoaffinity Labels

The Ki values were tabulated from the indicated number of experiments (n) for each compound, each with transport rates from at least 5 concentrations of inhibitor determined in triplicate. The spacer atom length was taken as the number of atoms between the carbon of the diazirine group and the carboxylate of the biotin group.

Compound	Spacer atom length	Ki (μM)	n	Reference
Bio-ATB-BMPA	none	247	3	Holman *et al.*, 1990
Bio-LC-ATB-BMPA	21	273	3	Koumanov *et al.*, 1998
Bio-LC-ATB-BMPA	21	299*	1	This Study
Bio-LC-ATB-BGPA	21	204.5 and 163.6 Average: 193.4	2	This Study
Bio-SS-ATB-BGPA	26	141.0 and 168.8 Average:153.7	2	This Study
Bio-LC-G15	63	484*	1	This Study

* Similar Ki values were obtained in experiments performed by other members of the Holman laboratory.

The affinities of the labels were estimated from their competition with the 2-deoxy-D-glucose for glucose transporters exofacial binding sites (Section 2.5.1). The rate constants for uptake in the presence (**V**) and absence (**Vo**) of inhibitor (**I**) were then used to calculate the half-maximal inhibition constants for photolabels (**Ki**) (Baker *et al.*, 1973) according to the equation: $Vo/V = 1 + I/Ki$.

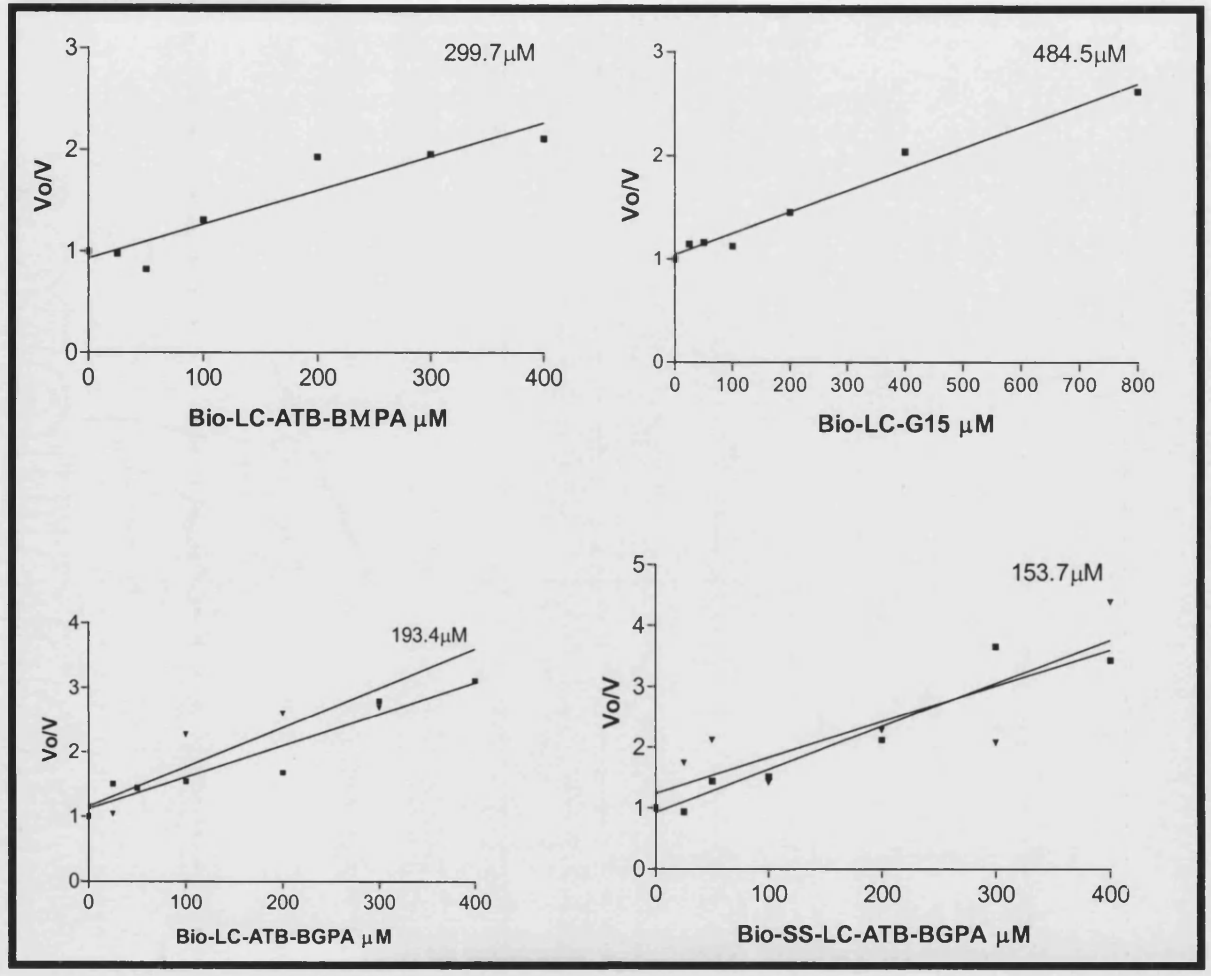

Figure 4.2: Estimation of the affinity of photolabels for glucose transport in rat adipocytes.
The half maximal inhibition 9Ki) of the photolbales are given in μM (Section 2.5.1). Each point on the graph are from triplicate samples.

4.2.1 Affinity of the Bis-Glucose Labels for GLUT4

The Ki of the Bio-LC-ATB-BGPA and the Bio-SS-ATB-BGPA for the GLUT4 in rat adipose cells was found to be lower (~1.5-fold and 2–fold respectively) than the original compounds, Bio-ATB-BMPA and its long-chain derivative, Bio-LC-ATB-BMPA. (see Table 4.1 and Figure 4.2, pages 81-82). The increase in affinity for the BGPA compounds was attributed to the substitution of glucose for the mannose units in the BMPA compounds. It is known that GLUT4, as well as the other glucose transporters have stereoselectivity for their substrates. The structure of D-glucose and D-mannose (the glucose transporter substrates) are given in Figure 4.3, below. The spatial requirements for glucose transporter substrate sugars have been analysed by substituting alkyl groups for the hydroxyl units. It has been shown by Holman and colleagues that the C-1 and C-3 positions of the substrate sugar form important hydrogen binding sites with the transporter (Holman *et al.*, 1981). The C-4 and C-6 positions have less crucial hydrogen binding sites than the C-1 and C-3 positions in the adipocyte system (Rees *et al.*, 1981). In addition, a bulky group at C-2 is not accepted, causing a decrease in affinity of the substrate for GLUT4 (Barnett *et al.*, 1973; Holman *et al.*, 1981). It has been established that the C-1 faces inside whilst the C-4 faces outside solution when the sugar approaches the transporter from the external face (Holman *et al.*, 1981). The C-1 is recognised first, following with the C-4/C-6 sites. The recognition is reversed when the sugar approaches the endofacial site of the transporter. In this study the C-2 epimer of D-glucose, (D-mannose) has a lower affinity for GLUT4. This may be due to steric hindrance of the OH group when positioned above the pyranose ring.

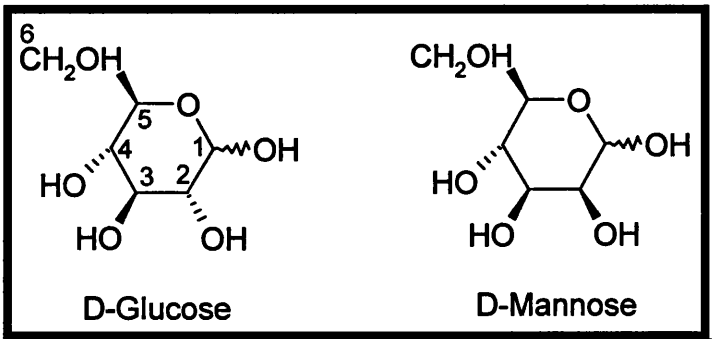

Figure 4.3: Structure of D-glucose and D-mannose. The structures show the hydroxyl units above and below the pyranose ring. Carbon-numbering is given in blue.

4.2.2 Demonstration that the Mono-Glucose Label has Affinity for GLUT4

The Ki of the mono-hexose label, Bio-LC-G15 was ~2-fold higher than that determined for the bis-hexose labels. The decrease in affinity of the label for GLUT4 could be due to the loss of hydrophilicity in its structure. Parkar and colleagues examined a series of bis (D-mannose) compounds for their affinity for GLUT4 in rat adipocytes. The group found that the introduction of a second mannose unit, increased the affinity of their compounds by 2-fold and increased the solubility of the compounds in aqueous buffers (Parkar *et al.*, 1985). The bis-hexose unit has been postulated to increase the hydrophilicity of the labels compared with the mono-hexose compounds. The single mannose is thought not to balance out the hydrophobicity of the aryl-trifluoroethylazi group in the label. Also, the presence of two sugars increases the statistical chance of binding by 2-fold. It should be noted that the spacer atom length of the Bio-LC-G15 is considerably longer than that of the Bio-LC-ATB-BMPA, (Table 4.1). In comparison to similar mono-hexose labels with different length spacer atom lengths (30-72), it was shown that the very long spacer arm of the Bio-LC-G15 did not markedly alter the affinity (Hashimoto *et al.*, 2001a). Similarly, the Ki value for the Bio-ATB-BMPA was not altered significantly when a long-chain (LC) linker was placed within the compound, to give the Bio-LC-ATB-BMPA label.

4.2.3 Western Blot Analysis of Tagged GLUT4 using Novel Photoaffinity Labels.

Initial experiments were carried out to test the three novel photoaffinity labels for their reactivity with GLUT4 in rat adipocytes, (Figure 4.4). Basal or insulin-stimulated rat adipose cells were photolabelled with 200 μM of label. Samples were processed for analysis of biotin-tagging by streptavidin precipitation. The levels of biotinylated GLUT4 that were precipitated were analysed by Western blotting, using the polyclonal carboxyl-terminal GLUT4 antibody (Figure 4.4i). Band density was quantified using density scanning software, (Section 2.2.6). An insulin-dependent increase of cell surface GLUT4 labelling (in comparison with the basal condition) was observed with all labels.

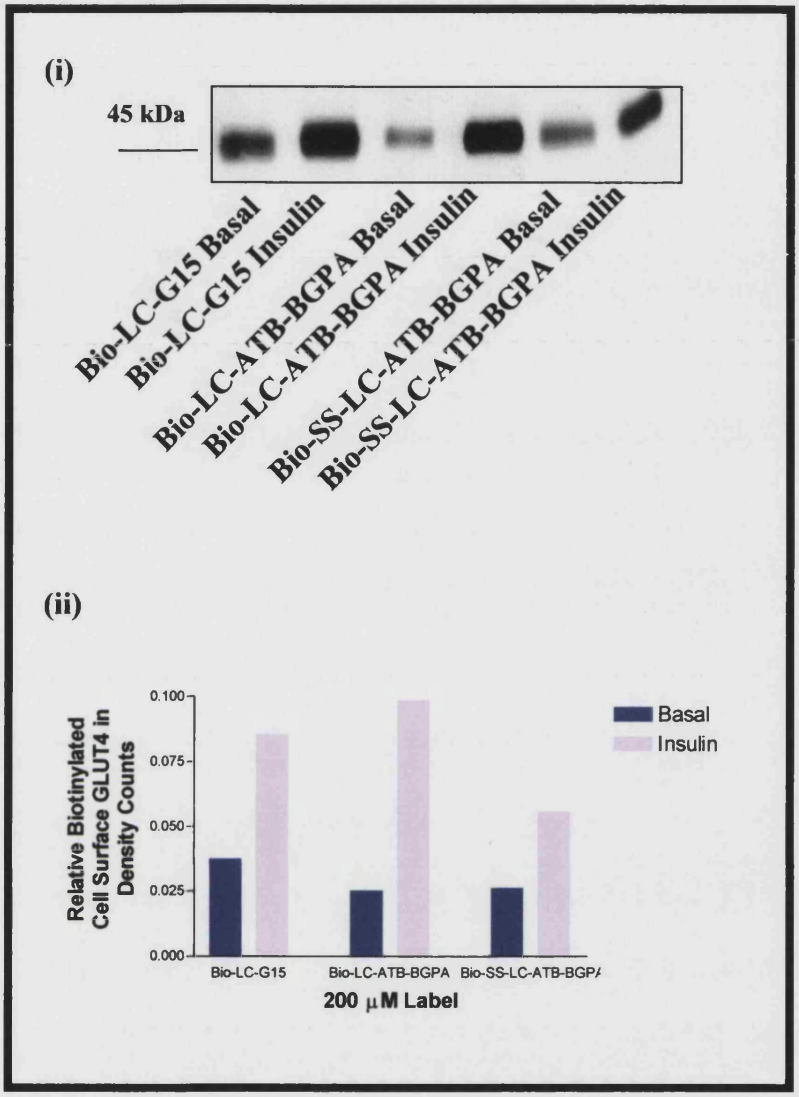

Figure 4.4: Comparison of GLUT4 cell surface labelling in rat adipocytes with three novel glucose transporter photoaffinity labels.

200 μM of label was used on either 500 μl basal or insulin stimulated rat adipocytes (40 % cytocrit), (*Section 2.5.2*). Irradiation was for 1 min under 350 nm lamps. Cells were washed and lysates were precipitated overnight with streptavidin beads. The precipitates were washed and processed for cell surface GLUT4 labelling, (*Section 2.5.3)* . The elutants were run on a 10% SDS-PAGE gel , transferred to nitrocelluose and Western blotted for GLUT4, (Figure 4.4i). Measurement of the biotinylated GLUT4 was carried out by density measurements using Molecular Analyst and data was plotted graphically with Prism graphPad sotware, (Figure 4.4ii). The Western blot and density analysis shown above is representative of two separate repetitions of this experiment.

The cell surface GLUT4 labelling produced by use of Bio-LC-ATB-BGPA, Bio-SS-ATB-BGPA and Bio-LC-G15 were found to increase by 4-fold, 2-fold and 2-fold, respectively in insulin-stimulated cells compared to basal cells, (Figure 4.4ii). These results indicated that all three labels had successfully tagged GLUT4, but the levels of basal labelling were higher than expected. However, the conditions for labelling may not have been optimal.

4.3 Cell Surface Labelling of Bio-LC-ATB-BGPA

4.3.1 Labelling of Bio-LC-ATB-BGPA compared to Bio-LC-ATB-BMPA

The cell surface labelling of GLUT4 in rat adipocytes with the novel Bio-LC-ATB-BGPA label was compared to Bio-LC-ATB-BMPA, (Figure 4.5, page 87). Identical concentrations of 200 μM of label were used tag GLUT4 in 500 μl of rat adipocytes (40% cytocrit). There was an increase in cell-surface GLUT4 labelling in insulin-stimulated rat adipocytes in comparison with basal cells, (~2-fold). In addition the density and pattern of the novel label was similar to the Bio-LC-ATB-BMPA.

Past experiments for labelling GLUT4 have used high concentrations (~500 μM) of the compound Bio-LC-ATB-BMPA. The high concentration of label limited the number of experiments that could be carried out. Investigations were carried out in order to decrease the concentration of the Bio-LC-ATB-BGPA and to optimise the labelling technique, (Figure 4.6, page 88). The cells were efficiently labelled for GLUT4 using 200 μM of the tag in 250 μl of cell volume.

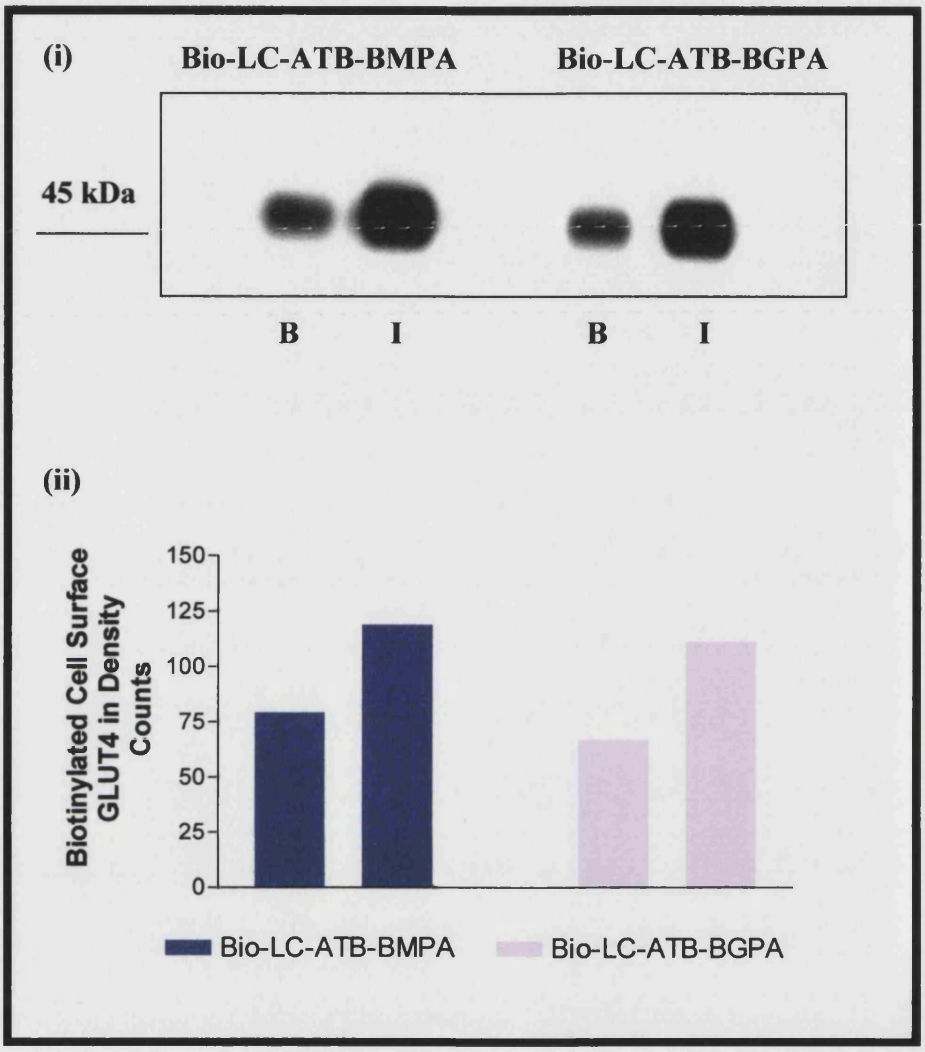

Figure 4.5: Detection of cell surface GLUT4 labelling on rat adipocytes with the photolabels, Bio-LC-ATB-BMPA and Bio-LC-ATB-BGPA.

200 μM of the labels were used to detect glucose transporters in insulin stimulated (**I**) and non-insulin stimulated (**B**) rat adipocytes (40% cytocrit). Irradiation was for 1 min under 350 nm lamps. Cells were washed and lysates were precipitated overnight with 50 μl of a 50% slurry of streptavidin agarose beads. The precipitates were washed as described in *Section 2.5.3* and photolabelled glucose transporters were eluted from the beads in sample buffer. The elutants were run on a 10% SDS-PAGE gel , transferred to nitrocelluose and Western blotted for GLUT4, (Figure 4.5i) Measurement of the biotinylated GLUT4 was carried out by density measurements using Molecular Analyst and data was plotted graphically with Prism graphPad sotware, (Figure 4.5ii). The Western blot and its density analysis shown above are representative of two separate repetitions of this experiment.

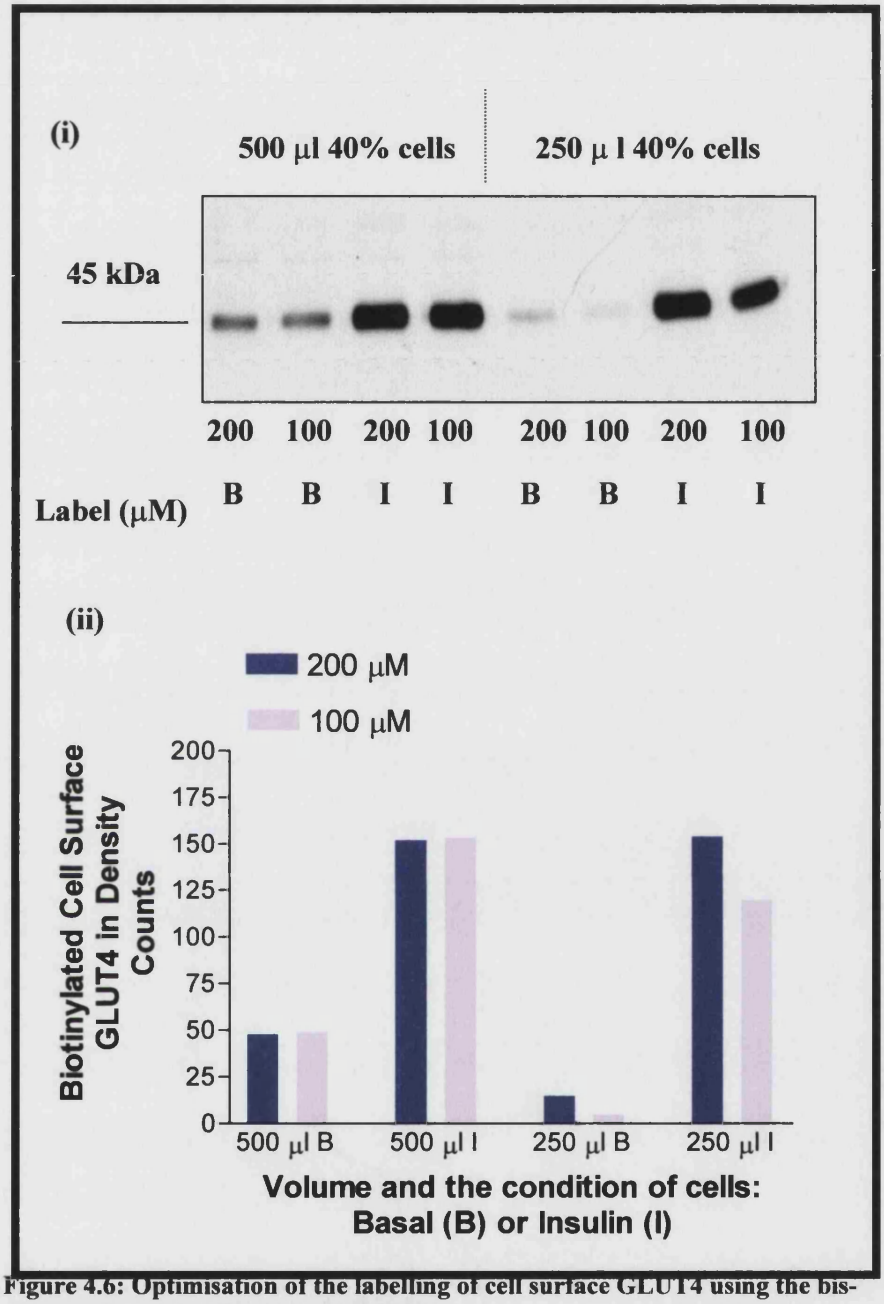

Figure 4.6: Optimisation of the labelling of cell surface GLUT4 using the bis-glucose photolabel Bio-LC-ATB-BGPA.

200 µM (■) or 100 µM (■) of label was used to biotinylate GLUT4 in insulin stimulated (**I**) and basal (**B**) rat adipocytes (40% cytocrit). The volume of the cells used were either 500 µl or 250 µl . Irradiation was for 1 min under 350 nm lamps. Cells were washed and lysates were precipitated overnight against 50 µl of a 50% slurry of streptavidin agarose beads. The precipitates were washed as described in *Section 2.5.3* and the photolabelled GLUT4 were eluted from the beads in sample buffer. The elutants were run on a 10% SDS-PAGE gel, transferred to nitrocellulose and Western blotted for GLUT4, (Figure 4.6i). Data was analysed and plotted graphically, (Figure 4.6ii). The Western blot and its density analysis shown above are representative of two separate repetitions of this experiment.

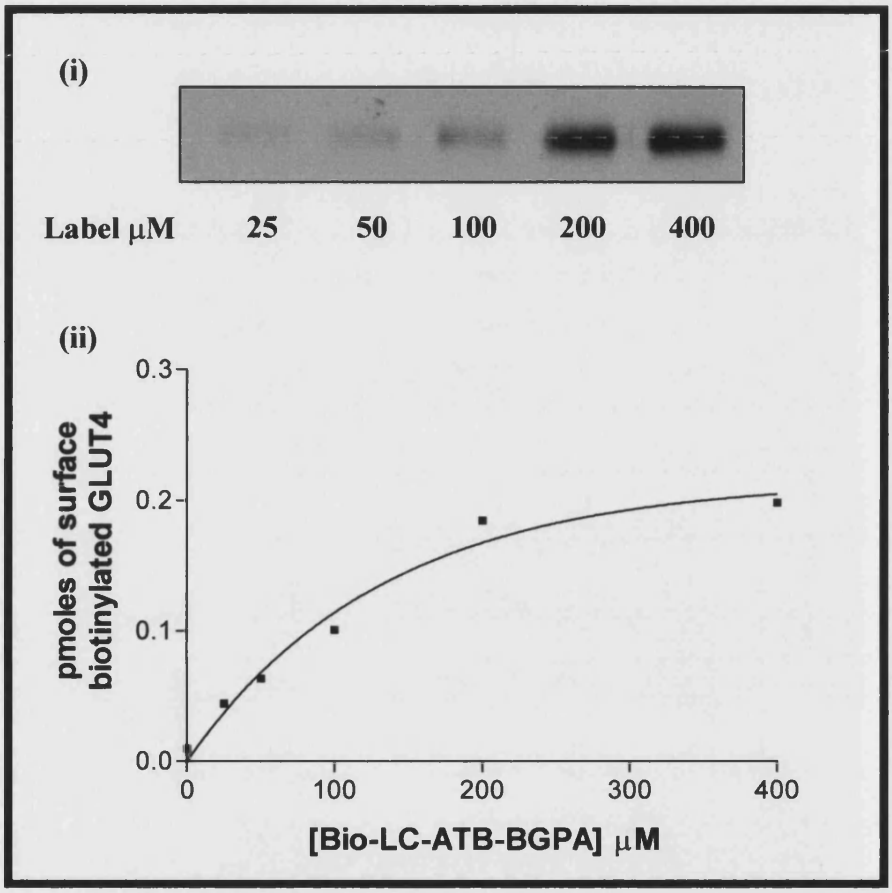

Figure 4.7: Estimation of biotinylated cell surface GLUT4 labelling with Bio-LC-ATB-BGPA.

A series of concentrations (0-400 μM) of the Bio-LC-ATB-BGPA label were used to biotinylate glucose tranporters in 250 μl of insulin stimulated rat adipocytes (40% cytocrit). Irradiation was for 1 min under 350 nm lamps. Cells were washed and lysates were precipitated overnight with streptavidin agarose beads. The precipitates were washed and processed for cell surface GLUT4 labelling, *Section 2.5.3*. Amounts of GLUT4 labelling were calculated by construction of a standard curve of pmoles GLUT4 in basal LDM.

The amount of Bio-LC-ATB-BGPA label required for maximal labelling of cell surface GLUT4 was analysed, (Figure 4.7, page 89). The Western blot signals of biotinylated GLUT4 obtained from rat adipocytes tagged with the label at various concentrations of 0-400 μM are shown in Figure 4.7i. The pmoles of biotinylated GLUT4 were estimated by comparison with a GLUT4 standard curve. The pmoles of GLUT4 in these LDM samples were converted to density counts. To reach maximal cell-surface GLUT4 binding, approximately 200 μM of Bio-LC-ATB-BGPA label was needed, (Figure 4.7ii).

4.3.2 Applications for the Bis-Glucose Labels

Previous studies have shown that the use of tagged proteins with cleavable-linkers can provide an effective means of measuring protein endocytosis (Garza and Birnbaum, 2000). Garza and Birnbaum were able to measure endocytosis of biotinylated IRAP in 3T3-L1 adipocytes. They used a disulphide cleavable linker, sulfo-NHS-SS-biotin to label the IRAP at 0-4 °C. Internalisation of biotinylated IRAP was followed at 37°C. Tagged IRAP at the cell surface was cleaved from the biotin group with the use of glutathione that reduced the disulphide bond. The biotin on internalised IRAP remained intact under these conditions and therefore time courses for internalisation could be followed. The Bio-LC-ATB-BGPA label was synthesised with a cleavable disulphide unit, SS. The Bio-SS-ATB-BGPA label was synthesised for its potential use in providing a means of measuring GLUT4 endocytosis, similar to the method employed for the biotinylated IRAP. Before the cleavable label could be used in trafficking studies, the compounds disulphide cleavable properties were first examined.

Two disulphide reducing agents, glutathione and 2-mercaptoethanesulfonic acid sodium salt, (MESNa) were tested against the cleavable label, Bio-SS-ATB-BGPA to establish whether the label could be used for GLUT4 trafficking studies, (Figure 4.8, page 92). Both the glutathione and MESNa are impermeant reagents with the ability to reduce the disulphide bond joining the biotin moiety to the protein binding diazirine group. GLUT4 in insulin-stimulated rat adipocytes was photolabelled with the Bio-SS-ATB-BGPA at 18 °C in 1% (w/v) BSA/KRH. The cells were then washed to remove excess label at 10 °C in 1% (w/v) BSA/KRH. The adipocytes were washed at a low temperature, (10°C) as this is

known to reduce internalisation (Ezaki *et al.*, 1982). As the translocation is slowed, the tagged glucose transporters remain at the cell surface during the cleavage of the disulphide bond. The disulphide reducing reagents were added to the cells at a concentration of 10 mM in 1% (w/v) BSA/KRH, whilst the control samples were either immediately solubilised or incubated with 10 mM glycine in 1% (w/v) BSA/KRH. The reducing reagents did not produce an effective reduction in the amount of cell-surface tagged GLUT4 when compared to the controls, (Figure 4.8). One explanation for the lack of reduction in disulphide bond cleavage was thought to be due to the harsh conditions in which the cells were incubated. The reduction of the disulphide bonds was carried out at 10 °C. It was thought that the low incubation temperature at which the rat adipocytes were incubated could have reduced the viability of the cells and consequently the final analysis of biotinylated GLUT4.

The exposure of adipocytes to a low temperature is known to mimic insulin in that it induces a large net translocation of glucose transporters (Ezaki *et al.*, 1982). However, it has been shown that at 18°C, there was no loss of cell surface glucose transporter activity even after 40-60 min (Holman *et al.*, 1990). The published data suggests that it is possible to use low incubation temperatures to keep GLUT4 at the cell surface so that reduction of the disulphide bonds can be carried out. However, it was postulated that the low temperature may decrease the viability of the cells and thus reduce any effects from the disulphide cleavage reagents on biotinylated GLUT4. Experiments were carried out to detect surface biotinylated GLUT4 before and after the cells were incubated at 10°C, (Figures 4.9i and 4.9ii, page 93). As a control the non-cleavable Bio-LC-ATB-BGPA label was also used. The 10 °C buffer reduced detection of biotinylated GLUT4 by 1.2 fold and 1.7 fold for the non-disulphide and cleavable disulphide photolabels, respectively.

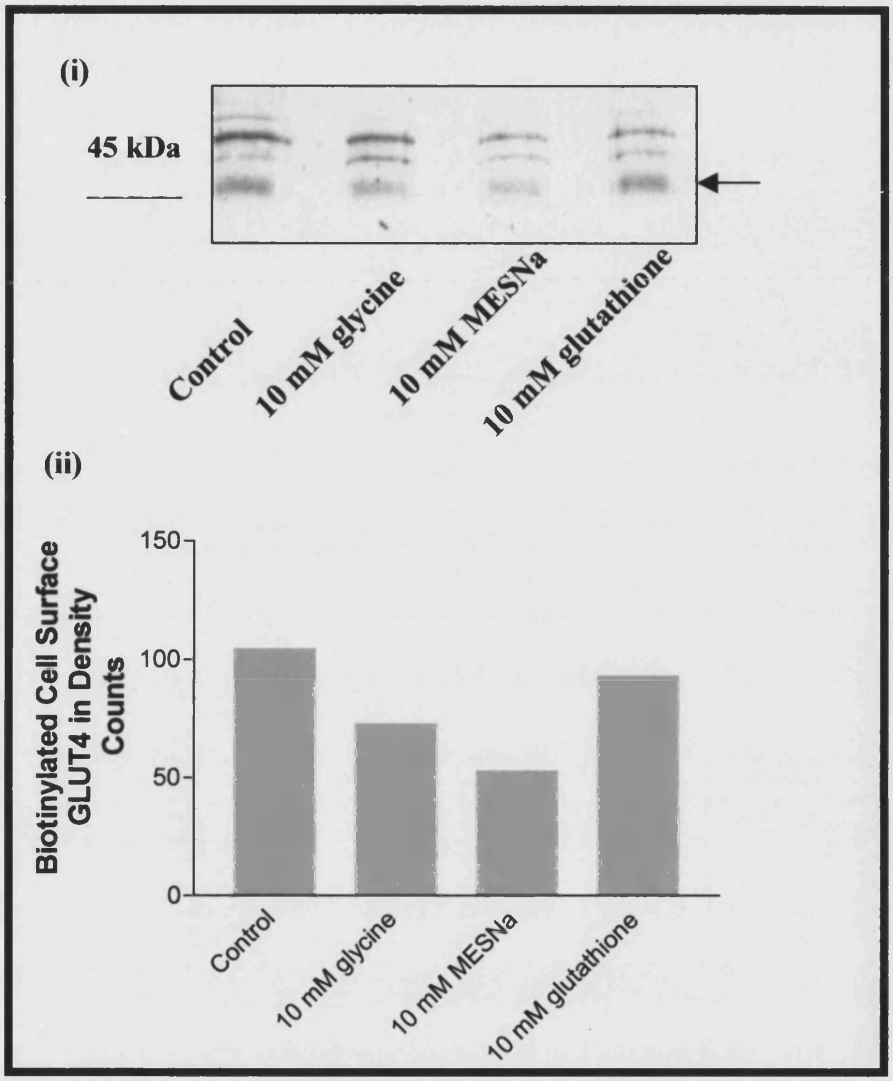

Figure 4.8: The effect of disulphide reducing agents on the cell surface GLUT4 labelling of rat adipocytes with the Bio-SS-LC-ATB-BGPA photolabel.

150 μM of the Bio-SS-ATB-BGPA label was used to tag glucose transporters on insulin stimulated rat adipocytes (40% cytocrit). Irradiation was for 1 min under 350 nm lamps at 18°C. Cells were then washed in 1% BSA/KRH and incubated at 10°C for 2 x 15 minutes in disulphide cleavage buffer shown above. Control samples contained 10 mM glycine or were immediately washed in 0.05 % BSA/KRH before solubilising in 2% Thesit PBS. All lysates were precipitated overnight with 50 μl of 50% slurry of streptavidin agarose beads and biotinylated GLUT4 was detected as described in *Section 2.5.3*. The Western blot of GLUT4 in samples is given in Figure 4.8i and the amount of GLUT4 in density counts for each sample in Figure 4.8ii. The bands quantified are shown with an arrow. 10 mM DTT was used in the sample buffer. The Western blot and its density analysis shown above are representative of two separate repetitions of this experiment.

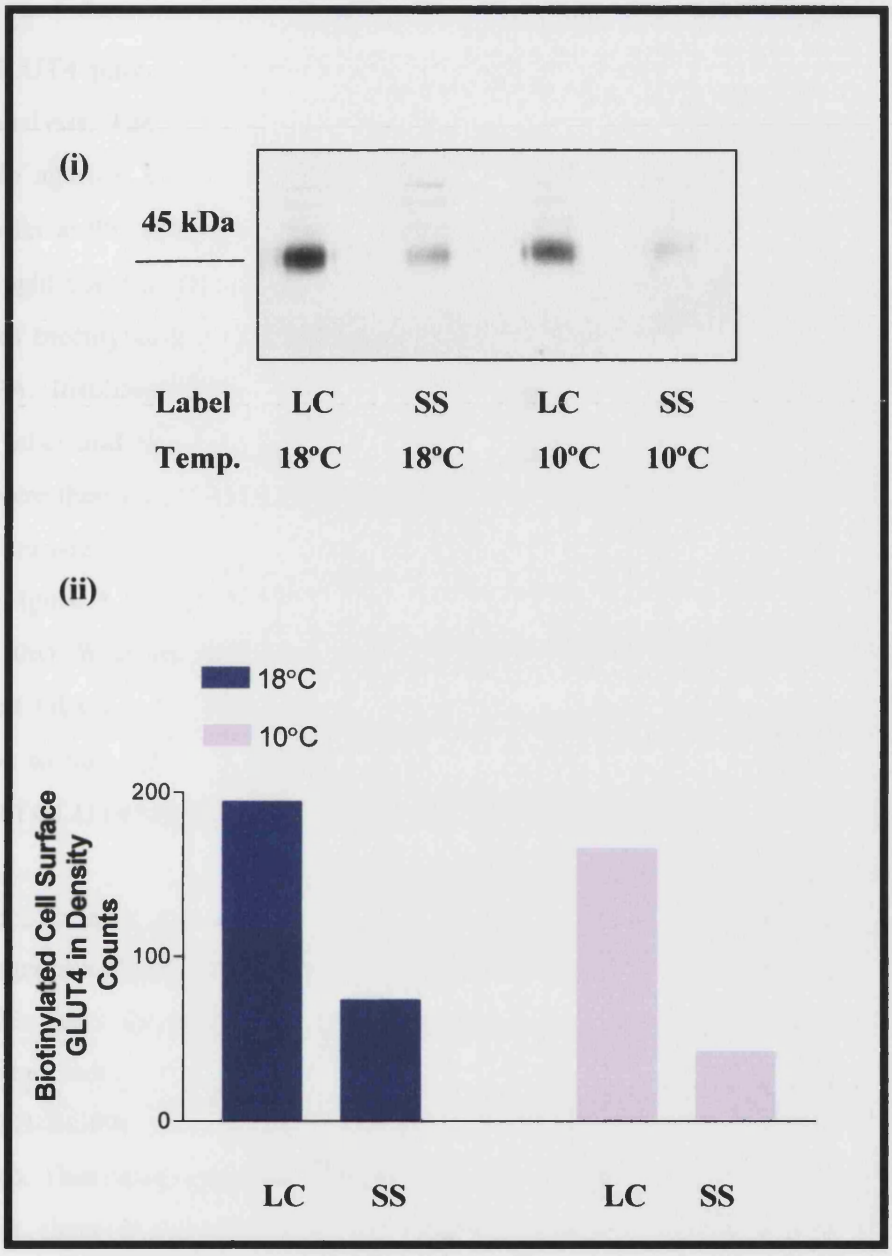

Figure 4.9: The effect of temperature on the labelling of GLUT4 on rat adipocytes with Bio-SS-ATB-BGPA and Bio-LC-ATB-BGPA.

150 μM of the Bio-SS-ATB-BGPA label , (denoted **SS**) or the Bio-LC-ATB-BGPA label, (denoted **LC**) was used to photolabel glucose transporters in insulin stimulated rat adipocytes (40% cytocrit). Irradiation was for 1 min under mixed light conditions at 18°C. Cells were then washed in 1% BSA/KRH and either incubated at 10°C for 30 min or washed in 0.05% BSA/KRH at 18°C and immediately solubilised. All samples were precipitated with streptavidin agarose beads, eluted and run down SDS gels in the presence of 10mM DTT. The levels of GLUT4 were tested by Western blotting, (Figure 4.9i). Densometric analysis was carried out to quantify levels of GLUT4 labelled at the cell surface, (Figure 4.9ii). The Western blot and its density analysis shown above are representative of two separate repetitions of this experiment.

Normal GLUT4 photolabelling techniques involve the use of DTT in the final stages of SDS-gel analysis. The GLUT4 in rat adipose cells is photolabelled and precipitated using streptavidin agarose beads. Samples are then eluted from the beads in the presence of sample buffer at 95 °C before they are run down SDS-PAGE gels in the presence of DTT. It was thought that the presence of the disulphide reducing reagent, DTT would effect the detection of biotinylated GLUT4 when using the disulphide cleavable compound, Bio-SS-ATB-BGPA. Insulin-stimulated cells were tagged with Bio-LC-ATB-BGPA or with the cleavable label and then solubilised and precipitated against streptavidin agarose beads. Samples were then eluted and run down SDS-PAGE gels either with or without DTT. The gels were transferred to nitrocellulose and analysed for biotinylated GLUT4 by Western blotting, (Figure 4.10i, page 95). The GLUT4 blots were quantified for density counts, (Figure 4.10ii). With the DTT in the sample buffer, there was a decrease in the amount of biotinylated GLUT4 detected using the Bio-SS-ATB-BGPA tagged rat adipose cells in comparison to non-DTT treated samples, (~3.5-fold). There was no effect of the DTT on the levels of GLUT4 tagged with Bio-LC-ATB-BGPA.

The ineffective reduction of GLUT4 tagged with Bio-SS-ATB-BGPA in the presence of reducing agents added to intact cells led to other considerations. It was hypothesised that the cleavable label did not tag glucose transporters in rat adipocytes sufficiently for there to be any further reduction in the signal. The levels of biotinylated GLUT4 detected with the Bio-SS-ATB-BGPA label were less than the non-cleavable Bio-LC-ATB-BGPA label, (Figure 4.4). This result can be contrasted with the 2-deoxy-D-glucose transport inhibition studies that showed that the affinity of the cleavable label was higher than the non-cleavable label, (Table 4.1). The cell surface labelling of GLUT4 and GLUT1 in rat adipocytes and in red blood cell ghosts with the Bio-SS-ATB-BMPA compound was therefore analysed as previous studies by Dr. Hashimoto of this laboratory indicated good labelling of GLUT1 by this compound. The non-cleavable label produced a greater level of biotinylated glucose transporters in both the rat adipose cells and red blood cells in comparison to the cleavable label, (Figure 4.11, page 96). The cleavable label tagged more glucose transporters in the red blood cells than the rat adipocytes.

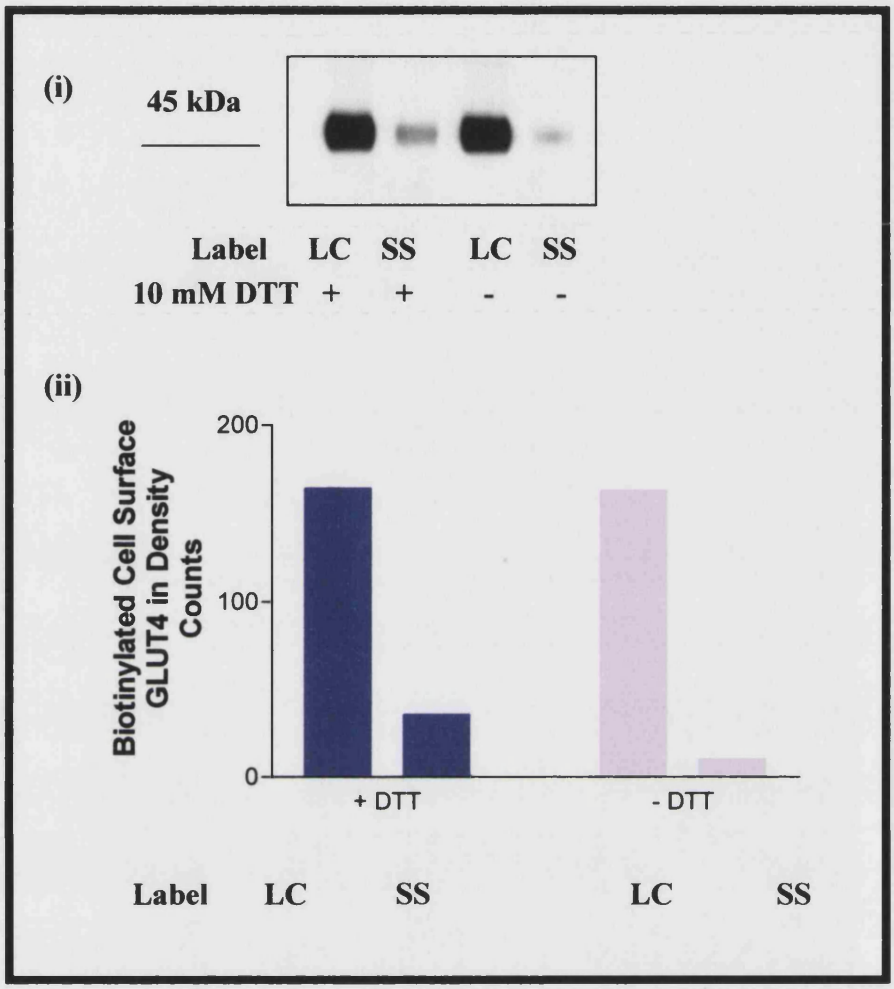

Figure 4.10: Comparing the effect of sample buffer with DTT on the detection of labelling cell surface GLUT4 using the Bio-LC-ATB-BGPA and Bio-SS-ATB-BGPA to sample buffer without DTT.

150 μM of the Bio-SS-ATB-BGPA label , (denoted **SS**) or the Bio-LC-ATB-BGPA label, (denoted **LC**) was used to photolabel glucose transporters in insulin stimulated rat adipocytes (40% cytocrit). Irradiation was for 1 min under 350 nm. Lysates were precipitated with streptavidin agarose beads, eluted and tested for GLUT4 levels by Western blotting, (Figure 4.10i). Densometric analysis was carried out to quantify levels of GLUT4 labelled at the cell surface, (Figure 4.10ii). The Western blot and its density analysis shown above are representative of two separate repetitions of this experiment.

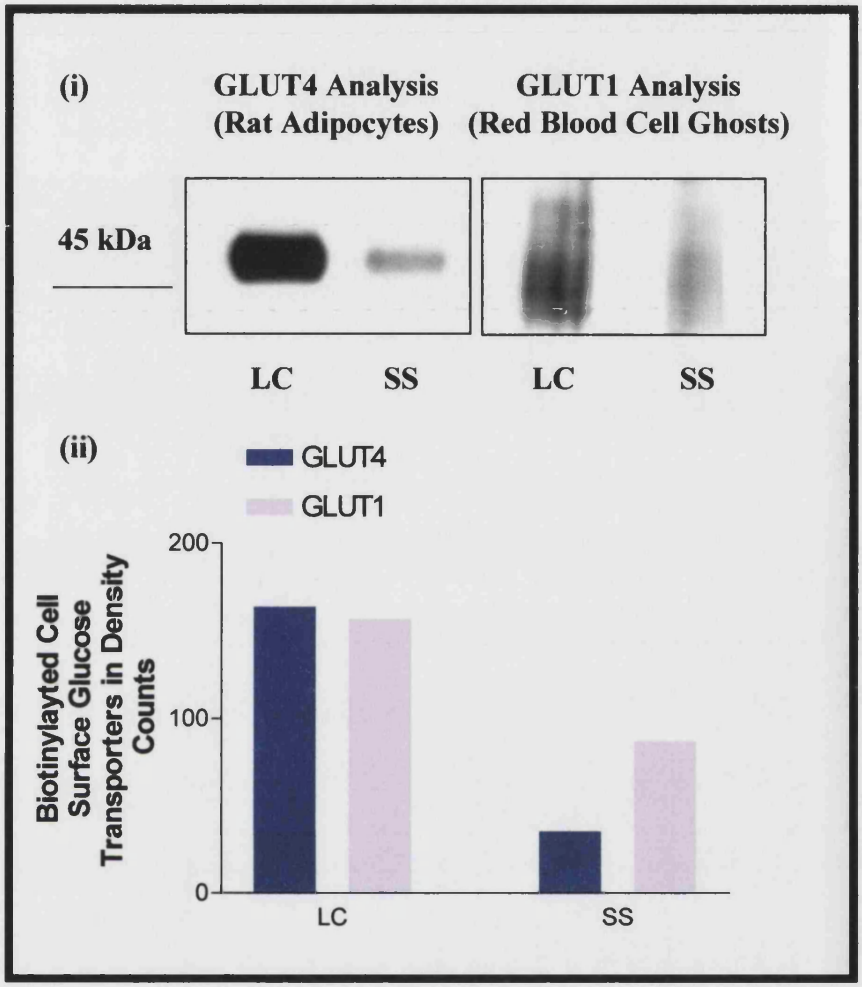

Figure 4.11: Comparison of GLUT4 and GLUT1 surface labelling produced by the reaction with bis-glucose photolabels, Bio-SS-ATB-BGPA and Bio-LC-ATB-BGPA.

150 μM of either Bio-SS-ATB-BGPA label (denoted **SS**) or Bio-LC-ATB-BGPAlabel (denoted **LC**) were used to tag glucose transporters in 500 μl of insulin stimulated rat adipocytes (40 % cytocrit) or 50 μg of red blood cell ghosts. Photolabelling was carried out by irradiation under 350 nm lamps for 1 min. Biotinylated glucose transporters were detected by precipitation of the lysates with streptavidin agarose beads. The eluates from the beads were analysed for GLUT4 and GLUT1 in the rat adipocyte and red blood cell ghost samples, respectively, (Figure 4.11i). Data was analysed and plotted graphically, (Figure 4.11ii). DTT was ommitted from all samples.

4.4 Studies on Mono-Glucose Photolabels

4.4.1 Cell Surface Labelling

As the affinity of Bio-LC-G15 was lower than the bis-hexose compounds, it was considered necessary to determine the levels of the reagent required to saturate the surface GLUT4 binding sites. The amount of Bio-LC-G15 label needed for maximal labelling of cell surface GLUT4 was analysed, (Figure 4.12, page 98). An example of the Western blot of biotinylated GLUT4 obtained from rat adipocytes tagged with the label at various concentrations of 0-500 μM is shown in Figure 4.12i. The pmoles of biotinylated GLUT4 that became tagged were estimated using a standard curve of pmoles GLUT4 in basal LDM samples versus density counts from the Western blots. To reach maximal cell-surface GLUT4 binding approximately 300 μM of Bio-LC-G15 was needed, (Figure 4.12ii).

It is known that avidin and biotin cross-link to form a strong bond. The binding between biotin and avidin is characterised by a dissociation constant of 10^{-15} M, (Green, 1975). It was thus postulated that avidin would be effective in masking cell-surface biotinylated GLUT4. In this laboratory it has been shown that the photolabels, Bio-LC-ATB-BMPA and Bio-LC-ATB-BGPA do not interact with avidin when added to intact cells (Hashimoto *et al.*, 2001b). The Bio-LC-G15 label was synthesised with a long atom spacer arm (63-atom spacer arm) in order to allow the biotin group to interact with avidin molecules in intact rat adipocytes. There was a clear decrease in labelling of cell-surface GLUT4 with the Bio-LC-G15 label in the presence of avidin, (Figure 4.13, page 99).

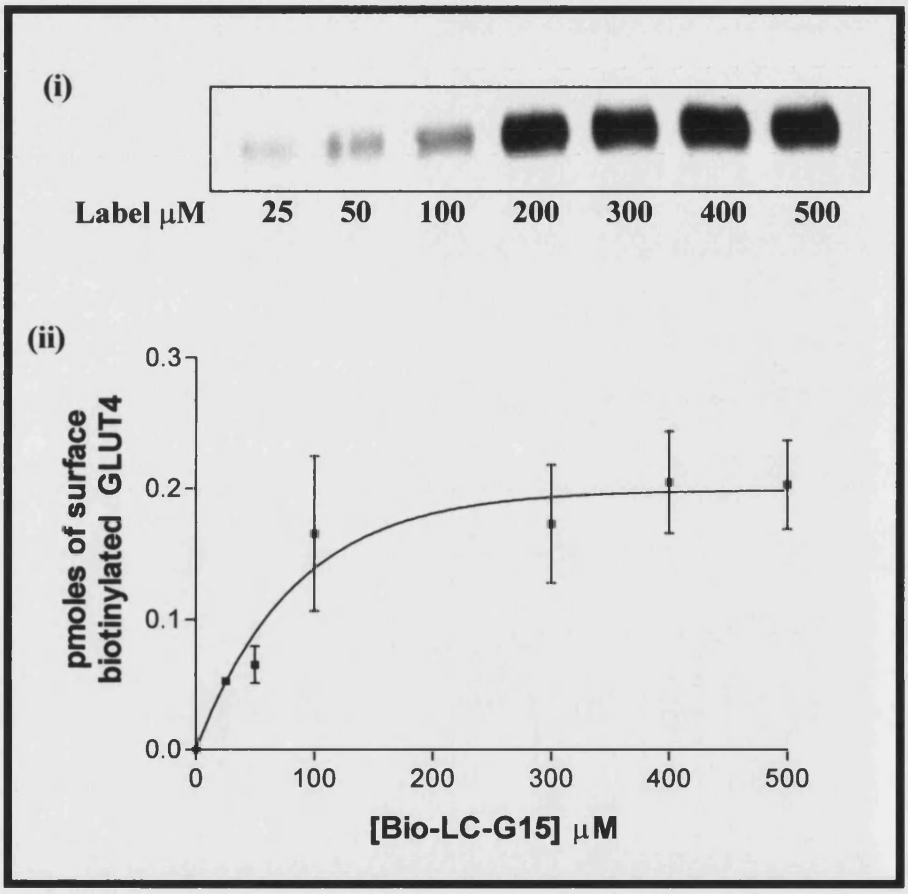

Figure 4.12: Estimation of biotinylated cell surface GLUT4 labelling with Bio-LC-G15.

A series of concentrations (0-500 μM) of Bio-LC-G15 label was used to biotinylate glucose tranporters in 250 μl of insulin stimulated rat adipocytes (40% cytocrit). Irradiation was for 1 min under 350 nm lamps. Cells were washed and lysates were precipitated overnight with streptavidin agarose beads. The precipitates were washed and processed for cell surface GLUT4 labelling by Western blot analysis, (*Figure 4.12i, Section 2.5.4.1)* . The amount of GLUT4 labelling (in pmoles) was calculated by construction of a standard curve of the amount of GLUT4 in basal LDM versus their density counts, (*Figure 4.12ii*). The Western blot and shown above is representative of two separate repetitions of this experiment. Each point on the graph was carried out in triplicate.

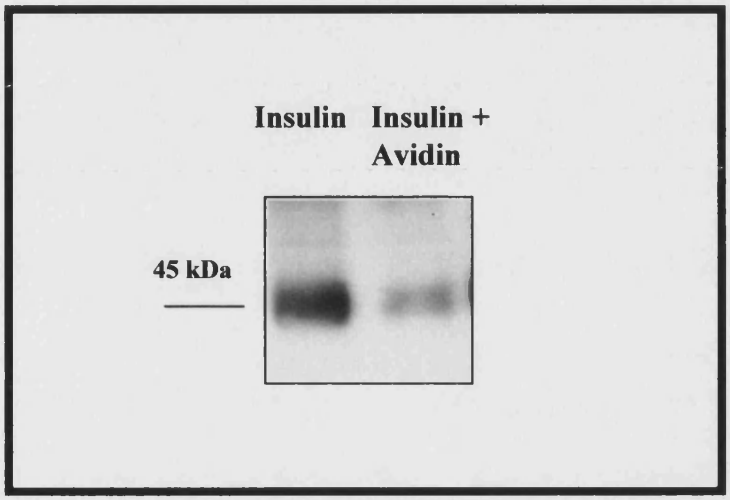

Figure 4.13: Effect of avidin on the detection of cell-surface labelling of GLUT4 using Bio-LC-G15.

500 μM of Bio-LC-G15 was used to label 500 μl of insulin stimulated rat adipocytes (40% cytocrit) to tag GLUT4. Irradiation was for 1 min using 350 nm lamps. 0.3 μM of avidin was then used to block the cell surface tagged transporters. Cells were washed and lysates were precipitated overnight against 50 μl of a 50% slurry of streptavidin agarose beads. The beads were washed and eluted for biotinylated GLUT4, (*Section 2.5.3).* Biotinylated *GLUT4* was detected by Western Blotting. The Western blot shown above is representative of two separate repetitions of this experiment.

4.4.2 Applications of the Bio-LC-G15 Label

The set of biotinylated bis-hexose probes that included Bio-LC-ATB-BMPA and Bio-LC-ATB-BGPA were used for detection of GLUT4 in detergent solubilised extracts of labelled cells. However, these labels were not suitable for applications in intact cells (Hatanaka *et al.*, 1994; Koumanov *et al.*, 1998). As interaction of the biotin group in the Bio-LC-G15 label with avidin was observed, (Section 4.4.1), the Bio-LC-G15 label was further employed to measure the rate of GLUT4 exocytosis and to detect glucose transporters in intact cells by confocal microscopy. The Bio-LC-G15 label was applied to experiments to measure GLUT4 exocytosis rates. The experimental is described in Section 2.5.2, page 55. The amount of biotinylated GLUT4 remaining in the cells was analysed as described in Section 2.5.3. The rate of tagged GLUT4 exocytosis was calculated from the following equation: $Y=\exp(-kx)$ where x represented the time after insulin-stimulation, Y the fraction of internal tagged GLUT4 and k the rate constant for exocytosis. The rate for exocytosis was calculated to be 0.24 min^{-1} (that is a fraction 0.24 of total labelled GLUT4 reached the plasma membrane per min). The Western blot and graphical data are shown in Figure 4.14 . A means to detect GLUT4 in intact cells with photolabels using confocal microscopy was tested. The method involved the tagging of GLUT4 with the photolabel followed by detecting the photolabel with fluorescent antibodies, FITC-labelled avidin or FITC-labelled biotin antibodies, (Section 2.7.0). The Bio-LC-ATB-BGPA and Bio-LC-ATB-BMPA labels produced non-specific GLUT4 labelling. This high background labelling was possibly due to the interaction of the fluorescent biotin antibodies with cellular biotin. Likewise, the GLUT4 that was tagged with Bio-LC-G15 could not be detected using confocal microscopy of rat adipocytes. However, glucose transporters that had been tagged with Bio-LC-G15 have been detected by confocal microscopy in red blood cell ghosts (Hashimoto et al., 2001a). Hashimoto was able to abolish the glucose transporter labelling in the presence of avidin or by competition of the label with glucose. Several questions need to be addressed before the labels are used in intact rat adipocytes: Is the amount of endogenous biotin in rat adipocytes greater than in red blood cell ghosts? This would explain the high background fluorescence found in rat adipocytes by confocal microscopy. Would an increase in the length of the linker chain (LC) in Bio-LC-ATB-BGPA enable the biotin on the label in intact cells to be easily detected with fluorescent antibodies?

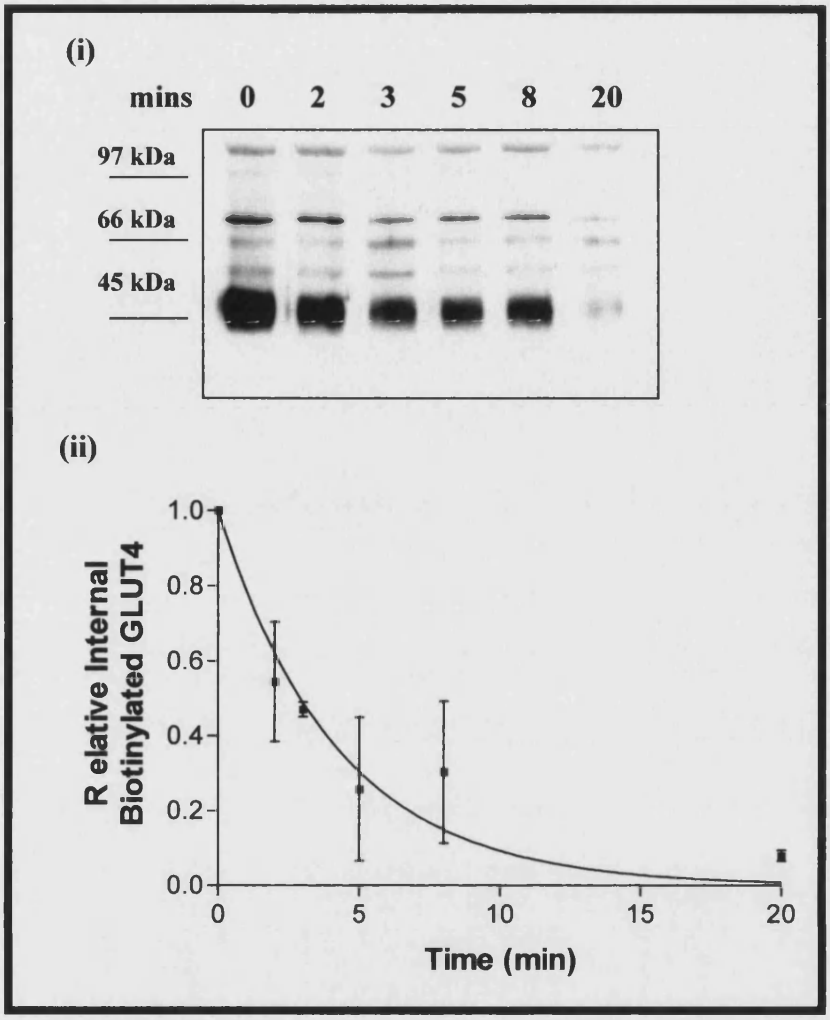

Figure 4.14 Rate of Exocytosis of Internalised GLUT4 tagged with Bio-LC-G15 label.

Rat adipocytes (40% cytocrit) were stimulated with 5 nM insulin for 20 mins after which cell surface glucose transporters were tagged with 500 μM Bio-LC-G15, (*Section 2.5.2*). Cells were then washed twice in MES buffer at 37°C and subsequently twice in 1% (w/v) BSA/KRH containing 2 mM D-glucose at 37°C. Cells were left for 40 min to allow glucose transporter internalisation. Cells were then divided into 500 μl aliquots and stimulated with the addition of 20 nM insulin for 0-20 min. Neutravidin at a final concentratiion of 40 μg was added simultaneously with the insulin. Exocytosis of the glucose transporters were inhibited at the appropriate time points with the addtion of 2 mM KCN. Samples were left for 2 min prior to the addition of 500 μl of solubilisation buffer, (*Section 2.5.3*). Cells were processed for the quantification of tagged internalised GLUT4 Measurement of the biotinylated GLUT4 was carried out by density measurements using Molecular Analyst and data were plotted graphically with Prism graphPad sotware. Figure 4.14i is an example of the Western blot obtained of biotinylated GLUT4 at the indicated time points. Figure 4.14ii is the relative amount of GLUT4 found after 0-20 min of 20 nM insulin stimulated exocytosis. The Western blot shown above is representative of two separate repetitions of this experiment. Each point on the graph was carried out in triplicate.

4.5 Discussion

Many photoaffinity labelling reagents have been used for studying glucose transporter subcellular trafficking (Clark *et al.*, 1990; Clark *et al.*, 1991; Holman *et al.*, 1990; Jhun *et al.*, 1992; Koumanov *et al.*, 1998; Satoh *et al.*, 1993; Yang *et al.*, 1992a; Yang and Holman, 1993). This chapter describes three novel glucose transporter photolabels, Bio-LC-G15, Bio-LC-ATB-BGPA, and Bio-SS-ATB-BGPA, that have been synthesised by G.D. Holman and M. Hashimoto (Hashimoto *et al.*, 2001a; Hashimoto *et al.*, 2001b). Initial experiments with the labels revealed that the amount of tagged GLUT4 at the cell surface of insulin-stimulated rat adipocytes, increased by approximately 2-4 fold in comparison to basal cells. In contrast, Clark and colleagues were able to produce a 15-fold increase of GLUT4 at the cell surface with a corresponding 30-fold increase in glucose uptake in adipocytes (Clark *et al.*, 1991). One explanation for the small apparent increase of GLUT4 at the cell surface in the study here may be that over-exposure of Western blots occurred. The polyclonal carboxyl-terminal GLUT4 antibody used to detect for the biotinylated GLUT4 has very high affinity for its antigen. Even a one second exposure of the antibody to the tagged antibody with ECL reagent to autoradiography film, produced over-exposure of the film, (Section 2.2.5).

The Bis-Glucose Affinity Labels

The biological properties of the labels, Bio-LC-ATB-BGPA and Bio-SS-ATB-BGPA and their ability to tag cell-surface GLUT4 on rat adipocytes were examined in detail. The two compounds were based on the design of the Bio-LC-ATB-BMPA label (Koumanov *et al.*, 1998). Experiments were carried out to test if the Bio-LC-ATB-BGPA had similar GLUT4 labelling properties to the Bio-LC-ATB-BMPA label. Both labels produced similar patterns in Western blotting for cell-surface tagged GLUT4. The affinity of the Bio-LC-ATB-BGPA label for GLUT4 was shown to be slightly higher than that of the BMPA derivative, (Ki: 193 μM and 299 μM respectively). This may be explained by the substitution of the bis-glucose for the bis-mannose unit in the label. GLUT4 binds with a strong affinity to the sugar, glucose rather than the mannose isoform. The high affinity of Bio-LC-ATB-BGPA for GLUT4 in rat adipocytes can be reflected by its ability to tag GLUT4 using low concentrations of label, (200 μM) and in a low volume of cell adipocytes, (250 μl). The

maximum amount of labelled GLUT4 was 0.2 pmoles of GLUT4.

The Bio-SS-ATB-BGPA was synthesised in order to study GLUT4 trafficking using the potential ability to cleave any label remaining at the cell surface. Although the label had strong affinity for the GLUT4 in rat adipocytes, (Ki of 154 μM) it did not sufficiently tag GLUT4. Western blots showed that there was little labelled GLUT4 present on the surface of rat adipocytes in comparison to the non-cleavable label. The cleavable label tagged GLUT1 with more efficiency in red blood cell ghosts than GLUT4 in the rat adipocytes. Possible explanations for the lack of labelling of GLUT4 with the Bio-SS-ATB-BGPA label in rat adipocytes have been put forward. Firstly, it was thought that the disulphide bond in the label could not withstand cleavage under harsh incubation conditions (low incubation temperatures and the presence of DTT). It was also proposed that the diazirine group of the label might be susceptible to intramolecular rearrangements with the disulphide bond under photolysis. However if this were the case, there would have been little labelling of GLUT1 in the red blood cells. It must be noted that the erythrocyte ghost labelling was carried out in PBS, whilst the rat adipocyte photolabelling buffer contained 1% (w/v) BSA. Perhaps there was the possibility that the disulphide bond in the Bio-SS-ATB-BGPA label crosslinked with the disulphide bonds in BSA under photolysis causing a dramatic reduction in tagged GLUT4 in rat adipocytes. This hypothesis was put forward based on studies on the effects of photolysis on human and bovine albumin sera which have shown that UV irradiation produces free disulphide bonds (-SH) (Stepuro *et al.*, 1981; Stepuro *et al.*, 1986). The disulphide bonds in the BSA may have interacted with the disulphide bond in the Bio-SS-ATB-BGPA label. This crosslink between the two compounds may have caused a dramatic reduction in tagged GLUT4 in rat adipocytes. Further experiments are necessary to eliminate these hypotheses. Mass spectroscopy could be used in future studies to analyse interactions between the albumin and photolabels. A recent experimental technique has been developed by Epps and colleagues, which measures the affinity of drugs binding to human serum albumin, (HSA) (Epps *et al.*, 1999). The method involves the use of fluorescence quenching of the single tryptophan (Trp) residue in HSA excited at 295 nm to measure drug-binding affinity. Modification of this technique could lead us to find out if the Bio-SS-ATB-BGPA label interacts with BSA, which would explain the ineffective labelling of glucose transporters with this label.

Mono-Glucose Photolabels

The Bio-LC-G15 had a lower affinity for GLUT4 in rat adipocytes than the bis-glucose labels, (Table 4.1). The maximal amount of cell surface GLUT4 labelled (0.2 pmoles of GLUT4) was similar to that of the Bio-LC-ATB-BGPA label. The long spacer arm enabled the tag to interact with avidin, (Figure 4.13). In this laboratory, it has been shown that other labels developed in the Holman laboratory cannot interact with avidin in intact cells, (Hashimoto *et al.*, 2001a). This property of Bio-LC-G15 label to interact with avidin was used to detect GLUT1 in intact red blood cells by confocal microscopy. In addition, the ability of the Bio-LC-G15 to bind to avidin enabled the label to act as a tool for measuring the exocytosis rate of GLUT4. The appearance of the tagged glucose transporter, GLUT4 at the cell surface of adipocytes after insulin-stimulation occurred with no lag period. The maximal GLUT4 at the cell surface was reached after approximately 20 min. The data was consistent with published data (Clark *et al.*, 1991). The rate constant of exocytosis for tagged GLUT4 (kex) was calculated to be 0.24 min^{-1}. This rate of exocytosis is large in comparison to values produced from experiments using tracer-tagged GLUT4 with the impermeant bisglucose photolabel B3GL and the impermeant bismannose photolabel, ATB-BMPA (Jhun *et al.*, 1992; Satoh *et al.*, 1993; Yang and Holman, 1993). Jhun used the B3GL to photolabel GLUT4 in rat adipocytes and found that the kex of GLUT4 increased from 0.024 min^{-1} to 0.078 min^{-1} with insulin-stimulation (Jhun *et al.*, 1992). In 3T3-L1 adipocytes the kex increased from 0.010 min^{-1} to 0.086 min^{-1} with insulin-stimulation (Yang and Holman, 1993). The labelling of GLUT4 with the tritiated ATB-BMPA photolabel in insulin-stimulated rat adipocytes produced a kex of 0.106 min^{-1} with a corresponding kex of 0.077 min^{-1} detectable by Western blotting (Satoh et al., 1993). Estimates of the endocytic and exocytic rate constants obtained by, Jhun, Yang, Satoh and colleagues assumed that there was the existence of only two pools of glucose transporters, one in the low density microsomes and one at the plasma membrane. The 2-pool model of GLUT4 translocation over-simplifies as it predicts that the $t_{1/2}$ values of recycling in the insulin-stimulated state and for the transition between the basal and insulin steady states should be the same. Experiments have provided evidence that the site of insulin action in stimulating glucose transporter translocation lies in the exocytosis part of the recycling process and that there is no significant decrease in the rate of endocytosis (Satoh *et al.*,

1993). Researchers investigating the effect of insulin on actin filaments in rat adipocytes, suggest that disruption of the actin filaments inhibit GLUT4 exocytosis but have no effect on the endocytosis of GLUT4 (Omata *et al.*, 2000). It is evident that there may be possibly four or maybe even five occluded pools in which GLUT4 traffics (Holman *et al.*, 1994). Thus, the exocytotic rate of GLUT4 at 0.24 min^{-1} may be feasible as it measures exocytosis more directly than previous methods. Previous methods have extracted exocytosis information from steady state kinetic data and this approach brings into play the movement of GLUT4 through multiple recycling compartments. The Bio-LC-G15 label has potential to be used to establish endocytosis rates of GLUT4 in the rat adipocyte and to study the kinetics of GLUT4 trafficking between different intracellular pools of GLUT4.

Conclusions

The Bio-LC-ATB-BGPA label and Bio-LC-G15 both effectively label cell surface GLUT4. The Bio-SS-ATB-BGPA did not bind sufficiently to GLUT4, which is thought to be due to interactions between the bovine serum and the disulphide unit in the label. The Bio-LC-G15 label has been found to be a useful tool for tracking GLUT4 exocytosis and should be used in further kinetic studies of GLUT4. It would be interesting to use the label to examine the kinetics of GLUT4 between different intracellular compartments (Holman *et al.*, 1994). However, at present the separation of two or more GLUT4 intracellular pools has been unfruitful. Studies directed towards identifying these compartments are discussed in Chapter 5.

5.0 Separation of GLUT4 Compartments

5.1 The GLUT4 Compartment

It is well established that integral membrane proteins recycle between the plasma membrane and specific intracellular loci through an endosomal recycling system, (for review see Clague, 1998). Immunoelectron microscopy techniques have revealed that GLUT4 is localised to several elements of the recycling pathway. The majority of GLUT4 was located in small vesicles and TV structures, clustered in the cytoplasm and often beneath the cell surface. Relatively small amounts of GLUT4 were shown to be associated with the clathrin-coated vesicles and endosomes. Use of subcellular fractionation and immunoabsorption studies, indicated that there was a co-distribution of GLUT4 with markers of several intracellular membrane compartments including GLUT1, transferrin receptor, (TfR) and mannose-6-phosphate receptor, (M6PR) (Kandror and Pilch, 1996; Rea and James, 1997). However, it has been observed by several independent groups that there is a separate subpopulation of GLUT4 vesicles (GSVs) that differ from vesicles of the constitutively recycling endosomal system, (see Section 1.5). Despite considerable progress in our understanding of insulin-regulated GLUT4 movement, several questions remain unanswered. For example, do GSVs represent a separate specific class of vesicles, how many separate GLUT4 populations exist and how are they associated with other intracellular recycling pathways? There has been little study on the rates of trafficking of GLUT4 between these compartments. This is probably due to the predicaments that face the researcher - a lack of biochemical methods to effectively separate different compartments. Gradient centrifugation was employed as a means to separate compartments in adipose cells has been employed in previous studies (Herman et al., 1994; Hashiramoto and James 2000 and Lee et al., 1999). However, due to the different starting materials the authors have come to different conclusions:

- Glycerol gradient centrifugation carried out in neuroendocrine cells (PC12) expressing GLUT4 identified a population of GLUT4 vesicles approximately 50-100 nm in diameter not associated with endosomes (Herman *et al.*, 1994).
- Hashiramoto and James prepared a crude intracellular membrane fraction from 3T3-L1 adipocytes and subjected it to iodixanol equilibrium sedimentation analysis to reveal two subpopulations of GLUT4: one being more insulin-sensitive than the other, (Hashiramoto and James, 2000).
- Lee (Lee *et al.*, 1999) used glycerol gradient centrifugation to separate three intracellular GLUT4 compartments in rat adipocytes: plasma-membrane containing fraction, endosome-associated fraction and an exocytotic vesicles fraction.

A combination of biochemical and immunological techniques were used in rat adipocytes to further define the nature of the insulin-responsive GLUT4 compartments and their relation to the constitutively recycling endosome compartments. The overall aim in the study described here were to physically separate the different GLUT4 compartments in rat white adipose tissue by their buoyant densities. Specifically the experiments described investigate the following:

- The factors affecting GLUT4 Sedimentation Characteristics:
  Media used for gradients
  Time for centrifugation
  Preformed gradients versus self-generating gradients
- The distribution of GLUT4 in relation to other recycling proteins on the gradients
- The effect of insulin-stimulation of rat adipose cells on the subsequent GLUT4 sedimentation on gradients.

5.2 Centrifugation Techniques and Choice of Gradient Material

The criteria for an ideal density gradient medium have been set out by (Hartman *et al.*, 1974). It should a) form a solution covering the density range needed for the particular application, b) form solutions of low viscosity, c) possess some property, such as refractive index, by which its concentration may be measured, d) be readily removable after the separation and e) not interfere with the analysis of the separated particles. The properties of the more common gradient materials are given in Table 5.1. Non-ionic media, such as sucrose, glycerol, Metrizamide, Ficoll and Percoll are generally considered to be more gentle than the ionic salts, such as caesium chloride and potassium bromide, and require relatively lower centrifugal fields to achieve an adequate separation of particles. Sucrose is the most popular compound for density gradient formation. It forms solutions, which cover the density range of all the larger constituents of cells. It has little effect on intermolecular bonding and is very cheap. The disadvantages of using this medium are that sucrose itself inhibits enzymes at high concentrations in the assay medium and it will damage complex structures like mitochondria and whole cells. Sucrose exerts very high osmotic effects even at very low concentrations, (i.e. approximately 10% (w/v) concentration). Glycerol gradients are sometimes preferred to sucrose gradients, as the glycerol appears to protect enzyme activity (Friefelder, 1973). The glycerol penetrates most biological membranes (Wallach, 1967) and is highly osmotic. The hyperosmotic effects of the media glycerol and sucrose lead to slow sedimentation rates for small particles and loss of water from subcellular organelles. The iodinated density gradient media were developed to overcome these problems. These include Metrizamide, Nycodenz and the collodial silica, Percoll (Pertoft *et al.*, 1978; Rickwood *et al.*, 1978). Percoll has no osmotic effects, whilst Metrizamide and Nycodenz form iso-osmotic solutions at around 37% (w/v) and 30 % (w/v), respectively, equivalent of densities 1.192 and 1.159 mg/ml. Recently, a new iodinated density gradient compound called iodixanol (Optiprep™) was developed by Ford and co-workers (Ford *et al.*, 1994). Iodixanol was prepared as a dimer of Nycodenz. Iodixanol's aqueous solutions are iso-osmotic up to a density of 1.32 mg/ml and it is capable of forming gradients in 1 to 3 h. Iodixanol has an advantage of other media due to its low toxicity towards biological materials.

Table 5.1: Commonly used Gradient Materials and their Applications

Medium	Mol.Wt.	Ionic Strength of Solution	Osmotic Effect	Max. Density of aqueous solution at 20 °C (g cm^{-3})	Ultraviolet Absorbance	Common Uses	References
Sodium bromide	102.91	+++	+++	1.53	+	Fractionation of lipoproteins	Wolf and Brown, 1967.
Caesium chloride	169.4	+++	+++	1.91	+	Banding of nucleic acids and nucleoprotein	Wolf and Brown, 1967.
Percoll (Pharmacia)		-	+	1.30	+++	Separation of whole cells and subcellular particles	Pertoft *et al.*, 1978
Metrizamide	789	-	++*	1.46	+++	Separation of whole cells, subcellular particles, nuclei, ribonucleoprotein particles, and membranes	Rickwood *et al.*, 1973
Sucrose	342.3	-	+++	1.32	+	Separation of subcellular particles, proteins viruses, and membranes	Wolf and Brown, 1967.
Glycerol	92.09	-	+++	1.26	+	Banding of membrane fragments, proteins, fractionation of nuclei	Wolf and Brown, 1967.

Cont. Table 5.1: Commonly used Gradient Materials and their Applications

Medium	Mol.Wt.	Ionic Strength of Solution	Osmotic Effect	Max. Density of aqueous solution at 20 °C (g cm^{-3})	Ultraviolet Absorbance	Common Uses	References
Ficoll (Pharmacia)	400,000	-	+	1.17	+	Separation of whole cells, subcellular particles, viruses	Harwood, 1974 Pretlow *et al.*, 1969
Dextran	72,000	-	+	1.13	+	Separation of whole cells, banding of microsomes	Graham, 1972 Wolf and Brown, 1967.
Bovine Serum Albumin	60,000	-	+		+++	Separation of whole cells	Wolf and Brown, 1967. Harwood, 1974
Nycodenz (Sigma)	821.1	-	++*	1.42	+++	Separation of whole cells, subcellular particles, nucleoproteins, membranes, viruses.	Rickwood, 1983.
Iodixanol (Sigma)	1550	-	++*	1.320 at 60%(w/v) solution	+++	Separation of whole cells, subcellular particles, nucleoproteins, membranes, viruses	Ford *et al.*, 1994

+++, High; ++, medium; +, low; -, non-ionic. (*) Osmotic effect increases almost linearly with concentration.

In this study, isopycynic (isodensity or equal density) gradients were chosen to attempt separation of GLUT4 compartments from the endosomal recycling system. This was performed on either pre-formed discontinuous step-density gradients or by self-forming gradients. The discontinuous step-density gradients were made from an overlayering method. Known volumes of decreasing density were allowed to run slowly down the centrifuge tube to form layers over each over. The diluted sample was overlayed on the least dense layer of the gradient. The gradient media had the density range covering the density of the particles in the sample solution that were to be fractionated. During the centrifugation, sedimentation of the particles occurred until the buoyant density of the particle and the gradient were equal. At this point of isodensity no further sedimentation occurred, (irrespective of the length of time for centrifugation), as the particles were floating on a cushion of material that had density greater than their own. The self-formed gradients (referred to as an equilibrium isodensity gradients) were prepared by initially mixing sample with the gradient media to give a solution of uniform density. The gradients self-formed by sedimentation equilibrium during centrifugation. Glycerol and iodixanol media were used in the pre-formed gradients. Glycerol was chosen due to low cost, whilst Iodixanol was used due to its low osmotic effects on particles. The iodixanol was used in the self-generating gradients. Glycerol media were not used in the self-generating gradients. It is known that glycerol and sucrose do not sediment significantly and tend to produce shallow gradients even at very high centrifugal fields (Ford *et al.*, 1974).

5.3 Use of Pre-Formed Discontinuous Step-Density Gradients

Methods to isolate intracellular storage vesicles of GLUT4 by density gradients were developed by Herman (Herman *et al.*, 1994) by modification of a method from Clift-O' Grady and colleagues (Clift-O'Grady *et al.*, 1990). Post nuclear samples from the neuroendocrine cell line PC12 transfected with GLUT4 were subjected to sedimentation analysis on a 5-25% (w/v) step glycerol gradient with a 50% (w/v) sucrose pad. Samples were centrifuged for 1 h and it was observed that there were two separate pools of GLUT4, one associated with the slow-sedimenting endosomes and the other in a fast-sedimenting region. In the study described in this chapter, the method by Herman was repeated but with the use of post HDM supernatant samples from basal or insulin treated rat adipocytes,

(Sections 2.3.1 and 2.3.2). Samples were centrifuged on the density glycerol gradients for 90 min and fractions were collected from the bottom of the gradient with a peristaltic pump. A fifth of each fraction was run down 8% SDS-PAGE gels. To detect for the TfR (190 kDa dimer), samples were run down the gel in the absence of DTT in the sample buffer. The gels were transferred onto nitrocellulose and Western blotted for GLUT4 and TfR using the polyclonal carboxyl-terminal GLUT4 antibody and the monoclonal TfR antibody respectively. The TfR was chosen as an endosome marker. The Western blot analysis of the subcellular distribution of GLUT4 in post HDM supernatants, showed that the majority of GLUT4 sedimented rapidly and was found at a higher density than the TfR, (see Figure 5.1 basal samples, page 113). GLUT4 was found to be in fractions 6-14 of the gradient, whilst the TfR was detected in fractions 14-19. The effect that 20 nM insulin-stimulation had on the sedimentation characteristics of GLUT4 on the velocity glycerol gradients was also analysed. The distribution of GLUT4 along the gradient differed slightly in the presence of insulin in comparison to the basal cells. There was a reduction in the amount of GLUT4, which was expected due to translocation of GLUT4 to the plasma membrane. There was a slight shift of GLUT4 on the gradient to the more dense area of the gradient (fast-sedimenting) in the presence of insulin.

To verify the sedimentation pattern of GLUT4 on the velocity glycerol gradient, the gradient was analysed for proteins known to be associated with GLUT4, (Figure 5.2, page 114). 1F8 and VAMP2 antibodies were used as markers for GLUT4, (Figure 5.2b,d). A Rab4 antibody was used as a marker for recycling endosomes on the gradient, (Figure 5.2e). Western blots were scanned and analysed for the densitometry of the bands. The distribution of protein content in the gradient was measured by the BCA protein detection system, (Figure 5.2f). Both VAMP2 and the 1F8 antibodies detected their respective proteins in the same fractions as the polyclonal GLUT4 antibody, (fractions 10-14). However the polyclonal GLUT4 antibody also detected GLUT4 in fractions 6-9 as well as fractions 10-14.

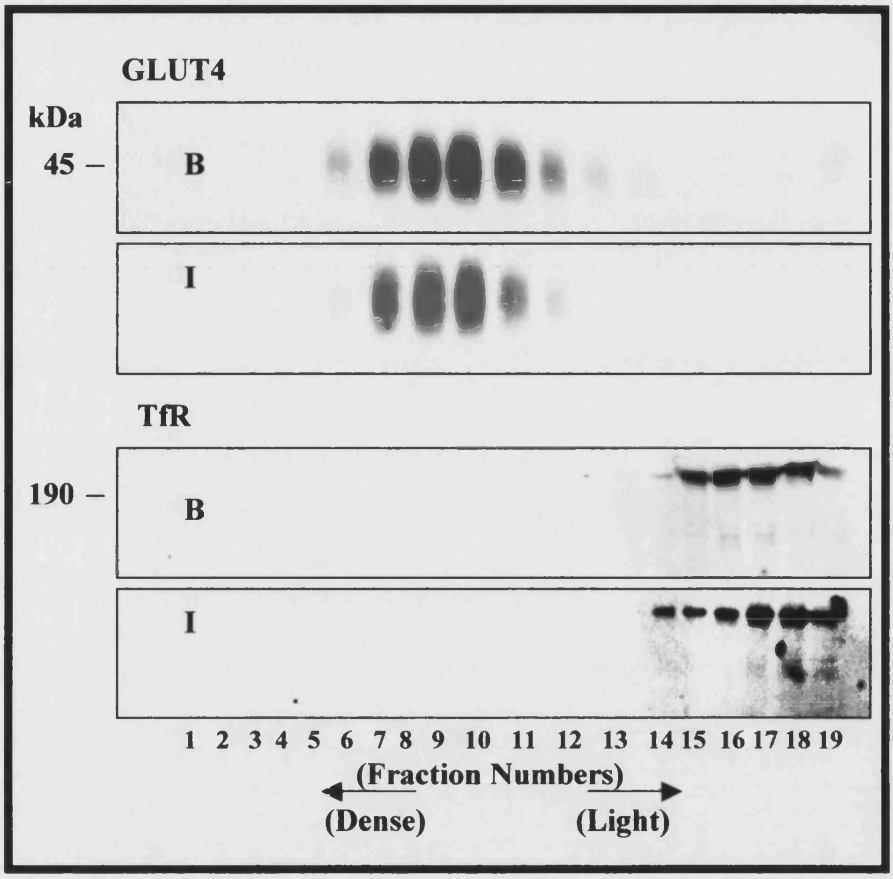

Figure 5.1: The Sedimentation Characteristics of GLUT4 in Comparison to the Transferrin Receptor in rat adipocytes along a 5%-25% (w/v) Glycerol Velocity Gradient.

Rat adipocytes were subjected to either basal (**B**) or 20 nM insulin treatment (**I**) prior to homogenisation, (Section 2.3.2). Post HDM supernatant was layered onto a 5%-25% (w/v) glycerol gradient. The velocity gradient was centrifuged for 90 min, (Section 2.6.1). 2 ml fractions were collected from the bottom of the gradient. 100 µl from each fraction were run down a SDS-PAGE gel, transferred to nitrocellulose and Western blot for transferrin Receptor (TfR) and GLUT4 (using polyclonal anti carboxyl-terminal GLUT4 antibody). Electrochemilumenesence was used to detect for the proteins by the ECL system from Amersham. The experiments were carried out three times and similar patterns of protein distribution were observed.

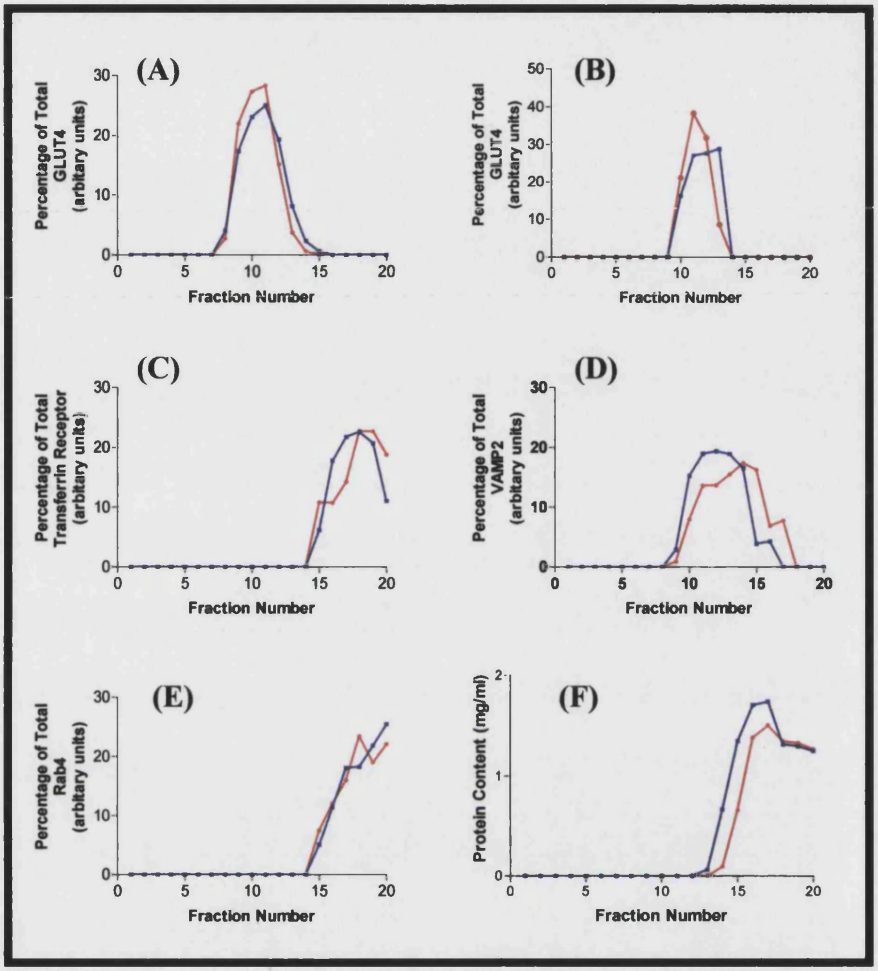

Figure 5.2: Comparison of Sedimentation of GLUT4 to Transferrin Receptor, VAMP2 and Rab4 from rat adipocyte post HDM supernatant on a 5%-25% Velocity Glycerol Gradient.

4 ml of 40% cytocrit rat adipocytes were treated with 20 nM insulin for 20 mins (●) or kept under basal conditions (■) prior to homogenisation and subfractionation. Post HDM supernatants from the adipocytes were layered onto 5-25% glycerol gradients. 2 ml fractions were collected. 100 µl from each fraction were run down a SDS-PAGE gel, transferred onto nitrocellulose and Western blot for the following proteins: GLUT4 (**A**), GLUT4 using the IF8 antibody (**B**), transferrin receptor (**C**), VAMP2 (**D**) and Rab4 (**E**). Antibodies were detected using ECL (Amersham). Densometric analysis of the bands were carried out using the programme Molecular Analyst ™ (from Bio-Rad Laboratories). The level of protein was expressed as a percentage of the total density in arbitary units (**F**). Protein content in each fraction was determined by the BCA method, (Section 2.2.1). The experiments were carried out three times and similar patterns of protein distribution were observed.

Differences in the apparent GLUT4 distribution along the gradient using the IF8 antibody and polyclonal GLUT4 antibody may be due to the different antigen-antibody binding affinities. The majority of GLUT4 detected by the different antibodies was found in the same fractions, none of which co-sedimented with TfR (fractions 14-20). Rab4 (recycling endosome) was detected in fractions 14-20. In gradients from insulin-stimulated cells the sedimentation characteristics of, TfR, Rab4 and surprisingly VAMP2 was unchanged compared to basal cells. In both basal and insulin-stimulated cells, GLUT4 on the gradients was found to be separated from the bulk of protein, (compare figure 5.2a to figure 5.2f) whilst the TfR was not, (compare figure 5.2b to figure 5.2f).

Iodixanol media, a non-ionic solute was used in a 5-25% (w/v) step velocity density gradient to establish whether ionic-effects of glycerol were having an effect on the sedimentation characteristics of GLUT4, (Figure 5.3, page 116). GLUT4 in the iodixanol gradient sedimented in fractions 5-14 compared with fractions 8-15 for the glycerol gradient. The TfR was in fractions 15-20 in both gradients. Iodixanol step gradients had no effect on the sedimentation characteristics of TfR but GLUT4 vesicles were found to be less resolved and more spread out over the gradient than the glycerol step gradients.

The distribution of GLUT4 and TfR on a 4 h 2-25% (w/v) iodixanol or glycerol step gradients were analysed. A 2% (w/v) layer of glycerol or iodixanol were included on the gradients to allow the TfR protein to move further into the gradient away from the surface layer. A 4 h spin was used to equilibrate the GLUT4 into a single peak. However it was found that the TfR did not move further into the gradient, and GLUT4 protein became more spread out on the gradient, Figure 5.4 (page 117).

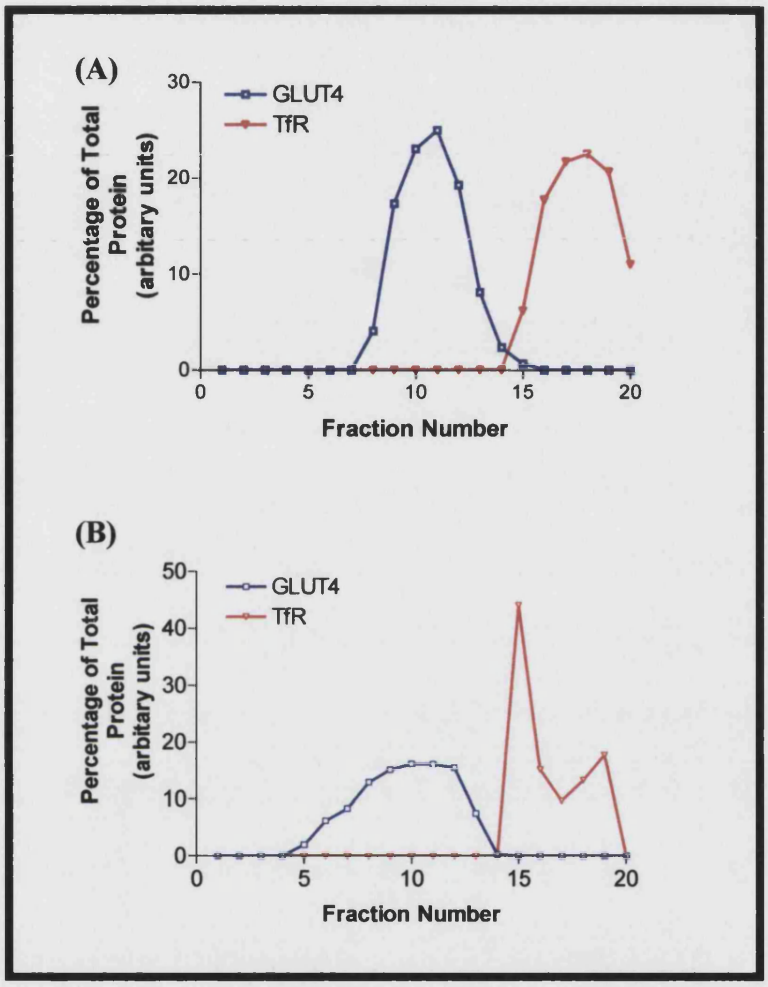

Figure 5.3: Comparison of GLUT4 Sedimentation to Rab4 and TfR on 5%-25%(w/v) Glycerol and Iodixanol Velocity gradients.

4 ml of 40% cytocrit rat adipose basal cells were homogenised and subfractionated for the post HDM supernatant. The supernatant was layered onto a 5%-25% (w/v) gradient consisting either of glycerol diluted in gradient buffer (**A**) or iodixanol diluted in gradient buffer (**B**), (Section 2.6.1). Gradients were centrifuged for 90 min and 2 ml fractions were collected from the bottom of the gradient. 100 µl from each fraction was run down a SDS-PAGE gel, transferred onto nitrocellulose and Western blot for the following proteins: GLUT4, TfR and Rab4. Antibodies were detected using ECL (Amersham). Densometric analysis of the bands were carried out using the programme Molecular Analyst ™ (from Bio-Rad Laboratories). The amount of protein was expressed as a percentage of the total density in arbitary units. The experiments were carried out twice and similar patterns of protein distribution were observed.

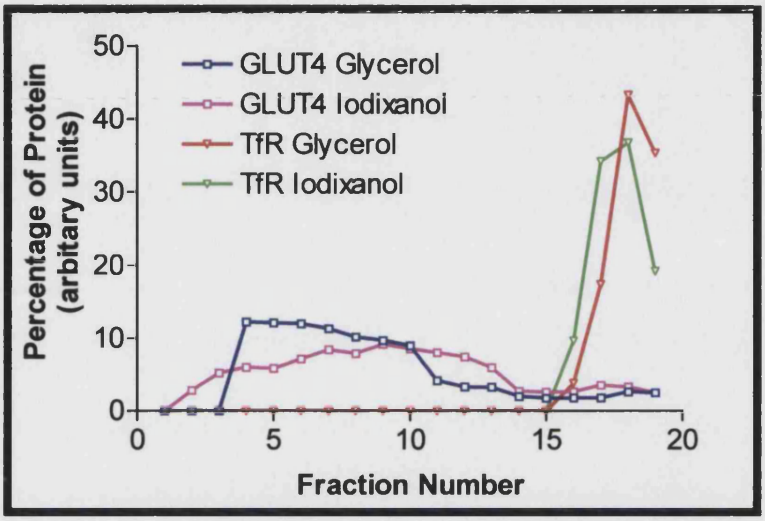

Figure 5.4: Comparison of GLUT4 Sedimentation to TfR on a 2%-25% (w/v) Glycerol and 2%-25% (w/v) Iodixanol 4 h step gradient.

4 ml of 40% cytocrit rat adipose basal cells were homogenised and subfractionated for the post HDM supernatnt. The supernatant was layered onto a 5%-25% (w/v) gradient consisting either of glycerol or iodixanol diluted in gradient buffer, (Section 2.6.1). Gradients were centrifuged at 80, 000 g_{av} for 4 h and 2 ml fractions were collected from the bottom of the gradient. 100 µl from each fraction were run down a SDS-PAGE gel, transferred onto nitrocellulose and Western blot for the following proteins: GLUT4, TfR and Rab4. Antibodies were detected using ECL (Amersham). Densometric analysis of the bands were carried out using the programme Molecular Analyst ™ (from Bio-Rad Laboratories). The level of protein was expressed as a percentage of the total density in arbitary units. The experiments were carried out twice and similar patterns of protein distribution were observed.

Once it had been established that the media glycerol could be effectively used to produce a distinct zone for GLUT4 on the step-gradients, subsequent studies were aimed at completely separating GLUT4 from the TfR on the gradient. The post HDM supernatants from rat adipose cells were layered onto step-glycerol gradients and centrifuged overnight for 16 h. 16 h was employed in order for equilibrium to be fully established between the particle sizes with the density of the gradient. GLUT4 was resolved in a single large peak in fractions 3-7 on the gradient, (see Figure 5.5A basal rat adipose post HDM supernatant, page 119). The TfR was found in fractions 11-14, clearly away from the GLUT4 on the gradient, (Figure 5.5A basal rat adipose post HDM supernatant). The increase in time for centrifugation (90 min to 16 h) shifted GLUT4 from fractions 7-15 in the 90 min gradient (Figure 5.2A) to fractions 4-7 in the 16 h gradient, (Figure 5.5A). A shift was not observed for the TfR. The shift in GLUT4 from the slow sedimenting material (low density) to that of the rapid sedimenting material (high density) indicated that the gradient had reached an equilibrium after 16 h. In gradients from insulin-stimulated cells, GLUT4 shifted from fractions 4-6 to 3-6 in the 16 h gradient, (Figure 5.5B, page 120). Similar banding was produced when LDM instead of post HDM supernatant was used as the starting material, (Figure 5.6, page 121). However all of the above mentioned gradients did not resolve GLUT4 into more than one band.

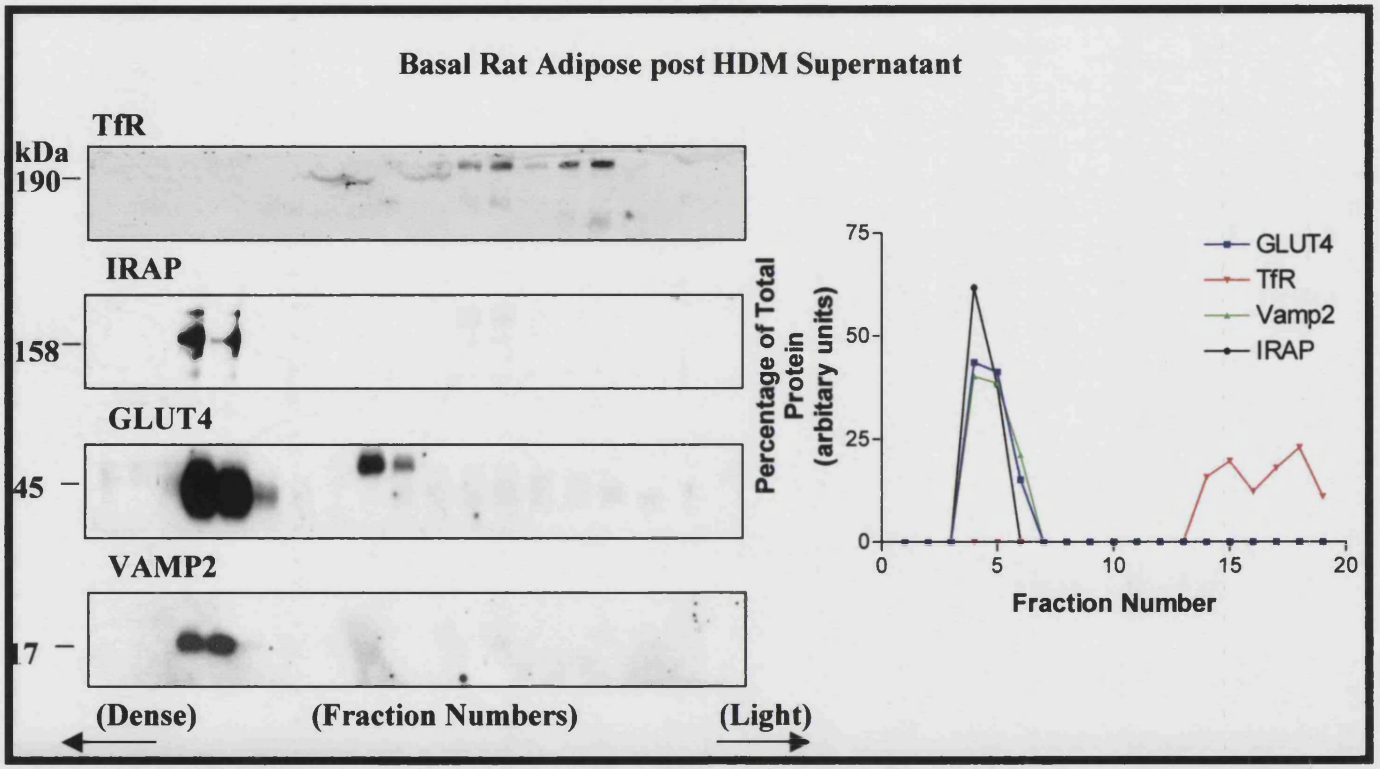

Figure 5.5A: Separation of Basal GLUT4 containing vesicles from TfR on an Equilbrium Density Glycerol Gradient.
4 ml of 40% cytocrit rat adipose basal cells were homogenised and subfractionated for the post HDM supernatant. The supernatant was layered onto a 5%-25% (w/v) glycerol gradient diluted in Gradient Buffer. The gradients was centrifuged for 16 h and 2 ml fractions were collected from the bottom of the gradient. 100 µl from all fractions were analysed for the following proteins using Western blotting: GLUT4, TfR, VAMP2 and IRAP. The Western blots and their density analyses are representative of two separate repetitions of this experiment.

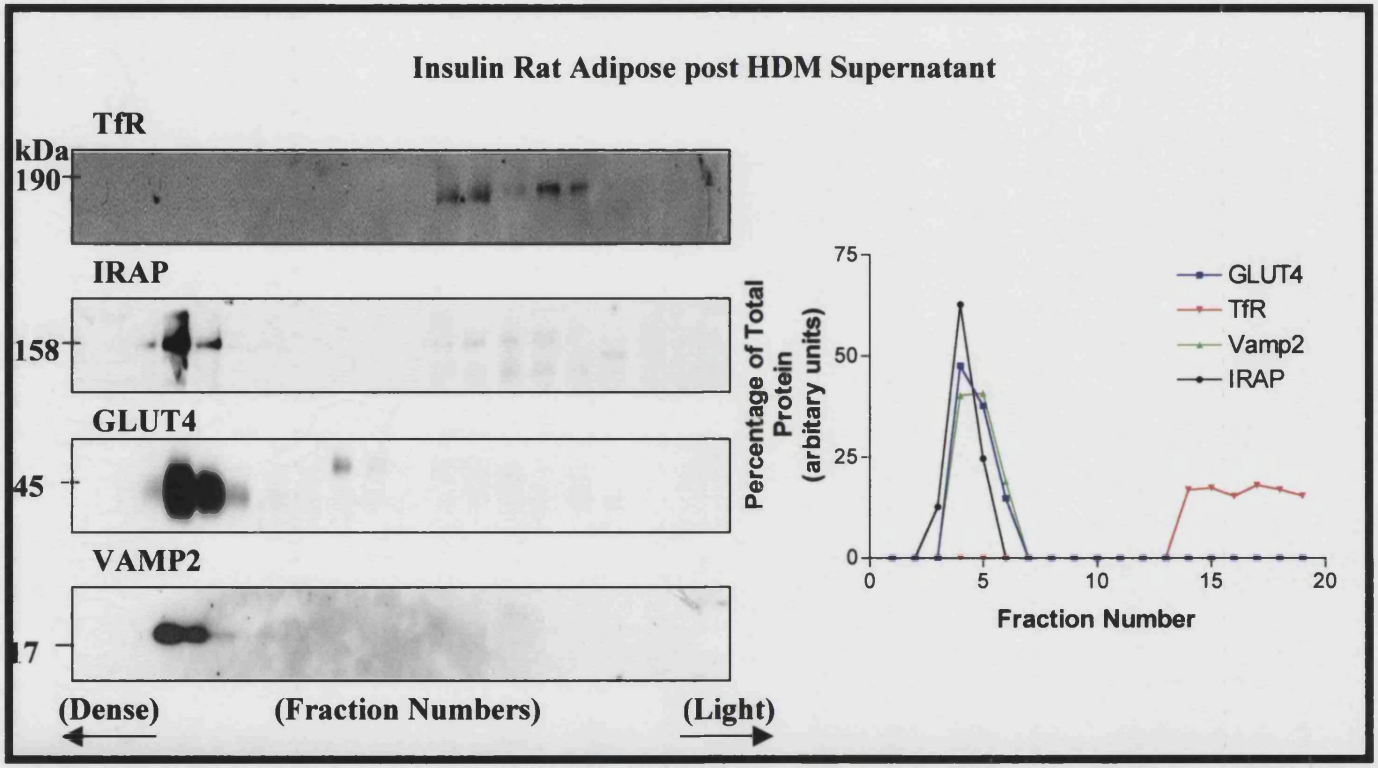

Figure 5.5B: Separation of Insulin-stimulated GLUT4 containing vesicles from TfR on an Equilbrium Density Glycerol Gradient. 4 ml of 40% cytocrit rat adipose insulin stimulated cells were homogenised and subfractionated for the post HDM supernatant. The supernatant was layered onto a 5%-25% (w/v) glycerol gradient diluted in Gradient Buffer. The gradients was centrifuged for 16 h and 2 ml fractions were collected from the bottom of the gradient. 100 µl from all fractions were analysed for following proteins using Western blotting: GLUT4, TfR, VAMP2 and IRAP. The Western blots and their density analyses are representative of two separate repetitions of this experiment.

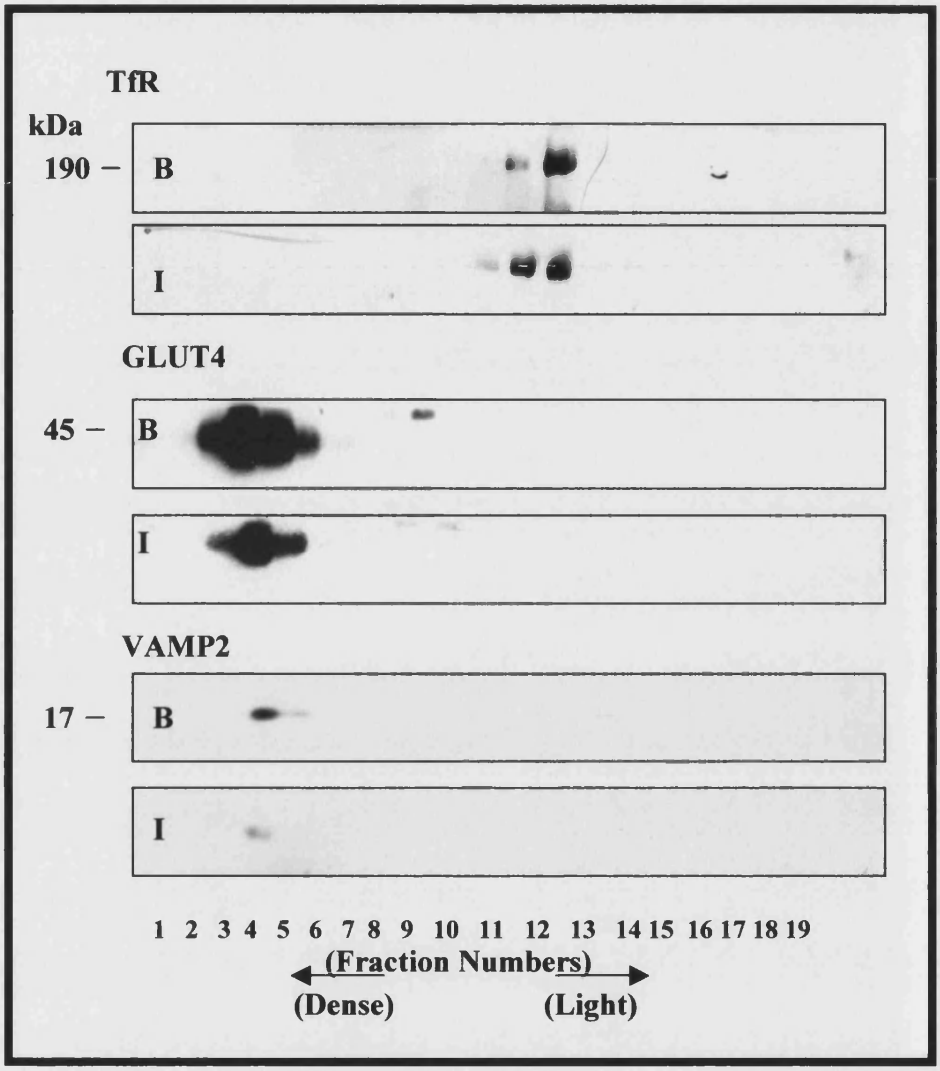

Figure 5.6: Separation of GLUT4 from TfR in LDM of rat adipose cells on a 16 h equilbrium density glycerol gradient.

4 ml of 40% cytocrit rat adipose basal or insulin stimulated cells were homogenised and subfractionated for the LDM. The LDM was resuspended in gradient buffer and layered onto a 5%-25% (w/v) glycerol gradient diluted in Gradient Buffer. The gradients was centrifuged for 16 h. 2 ml fractions were collected from the bottom of the gradient. 100 µl from each fraction were run down a SDS-PAGE gel, transferred onto nitrocellulose and Western blot for the following proteins: GLUT4, TfR and VAMP2. Antibodies were detected using ECL (Amersham). The Western blots shown above are representative of two separate repetitions of this experiment.

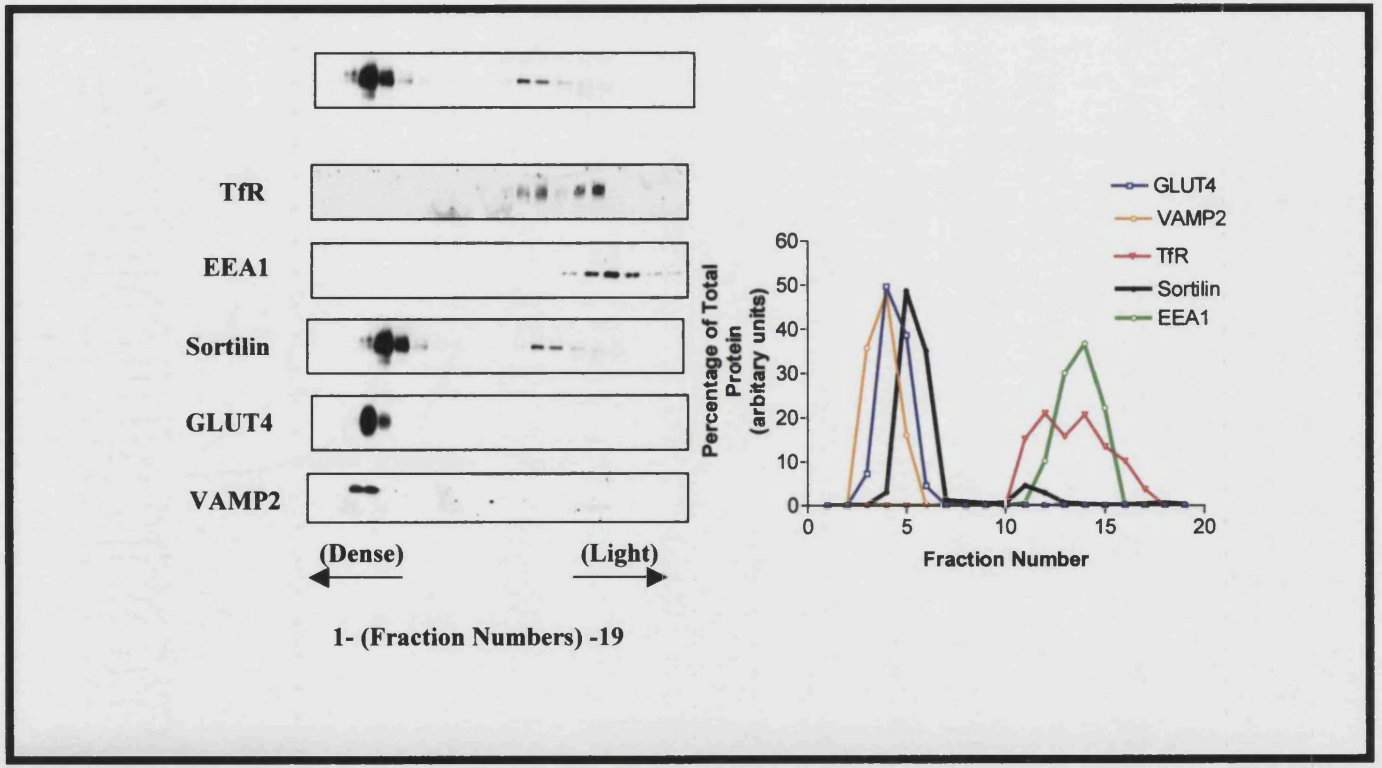

Figure 5.7: Sedimentation Characteristics of GLUT4 in Comparison to TfR, EEA1, Sortilin and VAMP2 on a post HDM Supernatant Equilbrium Density Glycerol Gradient. 4 ml of 40% cytocrit rat adipose insulin stimulated cells were homogenised and subfractionated for the post HDM supernatant. The supernatant was layered onto a 5%-25% (w/v) glycerol gradient diluted in Gradient Buffer. The gradients was centrifuged for 16 h and 2 ml fractions were collected from the bottom of the gradient. 100 µl from all fractions were analysed for following proteins using Western blotting: GLUT4, TfR, VAMP2 and sortilin and EEA1. The Western blots and their density analyses are representative of two separate repetitions of this experiment.

The buoyant density analysis of GLUT4 and TfR on the 16 h glycerol density gradients did not provide sufficient data as to whether there were several GLUT4 intracellular compartments. However, it was of interest to analyse the distribution of GLUT4 in comparison to that of other proteins from adipose cells that were known to be associated with certain organelles, i.e. the TGN and early endosome compartment. Basal rat adipose cells were subfractionated for the post HDM supernatant and analysed on 16 h glycerol gradient for GLUT4, TfR, EEA1, sortilin, and VAMP2, (Figure 5.7, page 122). Sortilin was used to mark the movement of proteins from TGN to late endosomes (Petersen *et al.*, 1997), and EEA1 as an early-endosome marker, (Patki *et al.*, 1997). The majority of sortilin sedimented in the fractions 3-6 where GLUT4 and VAMP2 also sedimented. Approximately 5% of the sortilin was found in fractions 13-15. The fractions containing sortilin at the top and bottom of the gradient may represent the endosomes and TGN compartments of the adipose cell, respectively. EEA1 protein was found in fractions 14-19; partially co-sedimented with TfR. VAMP2 was completely co-sedimenting with GLUT4 protein.

5.4 Use of Self-Forming Iodixanol Gradients

Hashiramoto and James were able to isolate two distinct GLUT4 pools from the LDM of 3T3-L1 adipocytes by the use of 14% iodixanol self-forming gradients (Hashiramoto and James, 2000). The method was repeated so that GLUT4 pools from the LDM of rat adipose tissue could be isolated. LDM (approximately 500 μg in HES buffer) from basal or insulin treated cells were mixed with 14% iodixanol in Gradient buffer. Tubes were sealed and spun in a vertical rotor for 1 h, 2.5 h or 4 h. 4 h were chosen as Hashimoto and James used this time to separate GLUT4 pools in 3T3-L1 adipocytes. Various times were used for centrifugation to find ideal conditions for resolving two GLUT4 pools. In the James and Hashiramoto study, 4 ml sealed-tubes were used, but in the following studies 2.2 ml sealed-tubes were used, which were expected to shorten the time needed to separate GLUT4 compartments. 200 μl fractions were collected from the top of the gradient and 10 μl from each fraction were analysed for their protein components. Bands on the Western blots were analysed for the immunoreactivity. Results were expressed as a percentage of total band density for each protein, (arbitrary units) and plotted graphically. The figures (5.8, 5.9 and

5.10) give examples of the Western blots produced for GLUT4, TfR, sortilin and EEA1 protein for centrifuge times 1 h, 2.5 and 4 h. For comparison purposes the distribution of the protein, GLUT4 and TfR are shown graphically for each of these times in Figure 5.11. All experiments were carried out at least twice. (Percentages are only an approximate value). IF8 antibody was used to confirm the distribution of GLUT4 along the gradients that was detected by the polyclonal carboxyl-terminal GLUT4 antibody.

The percentage of the total amount of intracellular GLUT4, sortilin, TfR and EEA1 in the 1 h 14% iodixanol gradient is summarised in Table 5.2. The results are percentages of protein distributions from one represenative experiment and no statistical analyses were carried out. The gradients were repeated twice, and distribution of proteins followed similar patterns.

Table 5.2: Percentage of Protein Distribution Along the 1 h 14% Iodixanol Gradient

Protein	**Light fractions 1-6 (Pool 1)**		**Dense fractions 7-11 (Pool 2)**	
	Basal	*Insulin*	*Basal*	*Insulin*
GLUT4	16%	25%	84%	75%
TfR	55%	51%	45%	49%
Sortilin	31%	35%	69%	65%
EEA1	97%	94%	3%	6%

Note: Percentages are from one represenative experiment and are not statistically significant.

The total amount of GLUT4 present along the 1 h iodixanol gradient was distributed into two pools: Pool 1, fractions 1-6 (top of gradient) and pool 2, fractions 7-11 (bottom of gradient), (see Figure 5.8 pages 127-128). 84% of GLUT4 was shown to be at the bottom of the gradient, (fractions 7-11). The remaining 16% of GLUT4 were shown to be in the top end of the gradient, (fractions 1-6). In the presence of insulin the amount of GLUT4 found at pool 2 dropped to 75%, which is reflected by the density decreasing in insulin-treated cells on the Western blots. However, the significance of this is unclear as experiments were not carried out more than twice. The highest percentage point of GLUT4 on the gradient shifted from fraction 10 to 9 with insulin-stimulated cells. There was an increase from 16% to 25% of GLUT4 in pool 1 from basal to insulin-stimulated cells.

Sortilin was used as a marker for TGN and EEA1 for the early endosome compartments. 69% of sortilin was in pool 2 and 31% in pool 1. In insulin-stimulated cells, the amount of sortilin in the two pools did not vary from basal cells significantly: 35% in pool 1 and 65% in pool 2. There was little effect of insulin on TfR distribution along the gradient. In basal cells TfR was roughly equally distributed between the two pools, 55% (w/v) and 45% of total TfR in pools 1 and 2, respectively. In the presence of insulin the amount of TfR was 51% and 49%, in pools 1 and 2, respectively. EEA1 was found at the top of the gradient only, in peak 1 fractions 1-6. In basal stimulated cells, 97% of EEA1 sedimented in pool 1 and 94% in insulin-stimulated cells.

The protein distribution of GLUT4, TfR, sortilin and EEA1 from LDM rat adipose cells along a 14% 2.5 h iodixanol gradient is shown in Figure 5.9 (pages 129-130). The increase in centrifuge time from 1 h to 2.5 h led only a slight shift in the pool of GLUT4 protein; fraction 10 to fraction 9. This pool of GLUT4 was slightly shifted again in insulin-stimulated cells (fraction 8). Similar protein distribution shifts were seen for sortilin and TfR but not EEA1. The percentage of GLUT4 in pools 1 and 2 were 34% and 66%, respectively. In the insulin-stimulated state there was a shift of GLUT4 to pool 1, 53% compared to 47% in pool 2. Insulin did not have such a large effect on the distribution of TfR, EEA1 or sortlin although the TfR and sortilin were found in two separate pools. In the basal state TfR was found approximately in equal amounts of 53 and 47% in pool 1 and pool 2, respectively. With insulin the values changed to 61% and 41%. In basal cells, the percentage of sortilin present was 47% and 53% in pools 1 and 2. In insulin-stimulated cells sortilin values were 52% and 46% in the two pools, 1 and 2 respectively.

The protein distribution of GLUT4, TfR, sortilin and EEA1 from LDM rat adipose cells along a 14% 4 h iodixanol gradient is shown in Figure 5.10 (pages 131-132). When the 14% iodixanol LDM gradients were spun for 4 h there was little evidence of a pattern of two pools of GLUT4. GLUT4 was found in fractions 3-8, as was the TfR and sortilin. EEA1 was found at the top of the gradient, fractions 1-7. The majority of the sortilin was found in the same fractions as GLUT4.

Table 5.3: Distribution of GLUT4 Along the 14% Iodixanol Gradients

14% Iodixanol Gradient	Light fractions 1-6 (Pool 1)		Dense fractions 7-11 (Pool 2)	
	Basal	*Insulin*	*Basal*	*Insulin*
1 h	16%	25%	84%	75%
2.5 h	34%	53%	66%	47%
4 h	72%	78%	28%	22%

Note: Percentages are from one represenative experiment and are not statistically significant.

The amount of protein in each of the 11 fractions obtained from the 14% iodixanol gradients were analysed by the BCA detection system. The data was graphically plotted and is shown in Figure 5.11 (page 133). For 1 h centrifugation time, the amount of protein falls into two major pools, fractions 1-6, (pool 1) and 7-11, (pool 2). GLUT4 and TfR follow this pattern. An increase in the time for centrifugation caused a shift of protein towards the top of the gradient, with the largest amount of protein being in fraction 1. The effect of the time of centrifugation was also to cause a shift in GLUT4 and TfR to the top end of the gradient. This resulted in the two pools merging and becoming less resolved. Table 5.3 represents the distribution of GLUT4 along 14% iodixanol gradients after 1 h, 2.5 h and 4 h centrifugation times. The percentages from the gradients are only from one experiment, although the protein distribution was seen to be similar when the gradients were repeated.

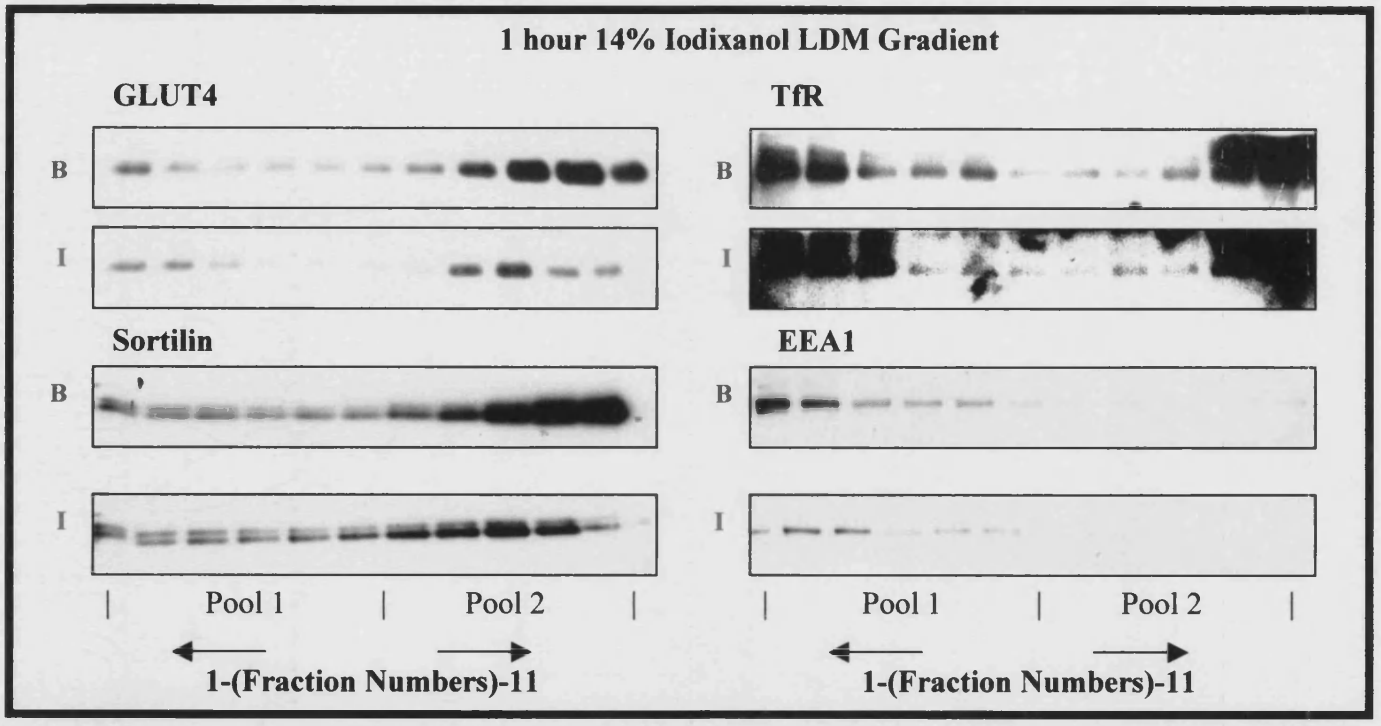

Figure 5.8A: Analysis of protein distribution from the LDM of rat adipose cells on a 1 h 14% Iodixanol Gradient. 500 μg of LDM taken from basal (B, ■) or insulin-treated (I, ▲) rat adipose cells were analysed on a 1 h 14% iodixanol self-generating gradient. (Section 2.6.2). 200 μl fractions were collected from the top of the gradient. 10 μl from all fractions were analysed and Western blot for the following proteins: GLUT4, TfR Sortilin and EEA1. Antibodies were detected using ECL (Amersham). Densometric analysis of the bands were carried out using the programme Molecular Analyst ™ (from Bio-Rad Laboratories), and results were plotted graphically with Prism software. The Western blots shown above are representative of two separate repetitions of this experiment.

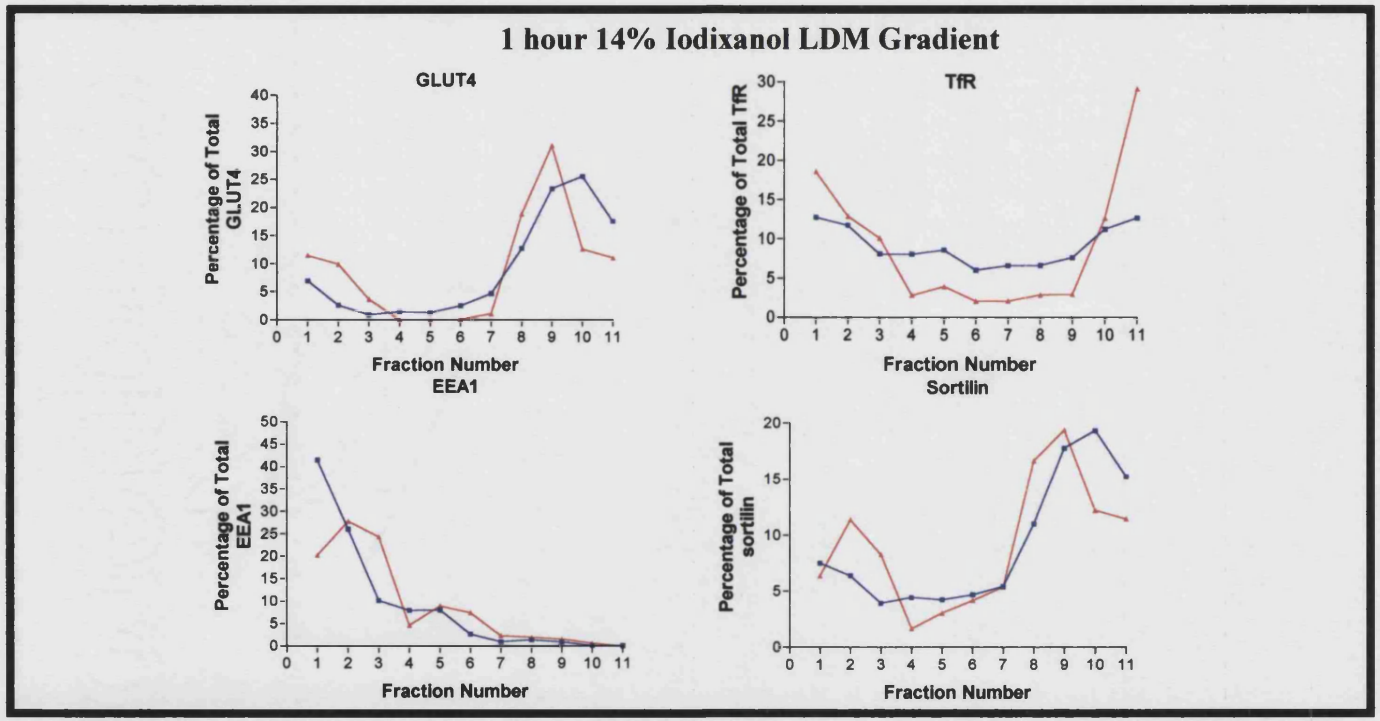

Figure 5.8B: Analysis of protein distribution from the LDM of rat adipose cells on a 1 h 14% Iodixanol Gradient. 500 μg of LDM taken from basal (B,■) or insulin-treated (I,▲) rat adipose cells were analysed on a 1 hour 14% iodixanol self-generating gradient, (Section 2.6.2). 200 μl fractions were collected from the top of the gradient. 10 μl from all fractions were analysed and Western blot for the following proteins: GLUT4, TfR Sortilin and EEA1. Antibodies were detected using ECL (Amersham). Densometric analysis of the bands were carried out using the programme Molecular Analyst ™ (from Bio-Rad Laboratories), and results were plotted graphically with Prism software. The protein distributions are representative of two separate repetitions of this experiment.

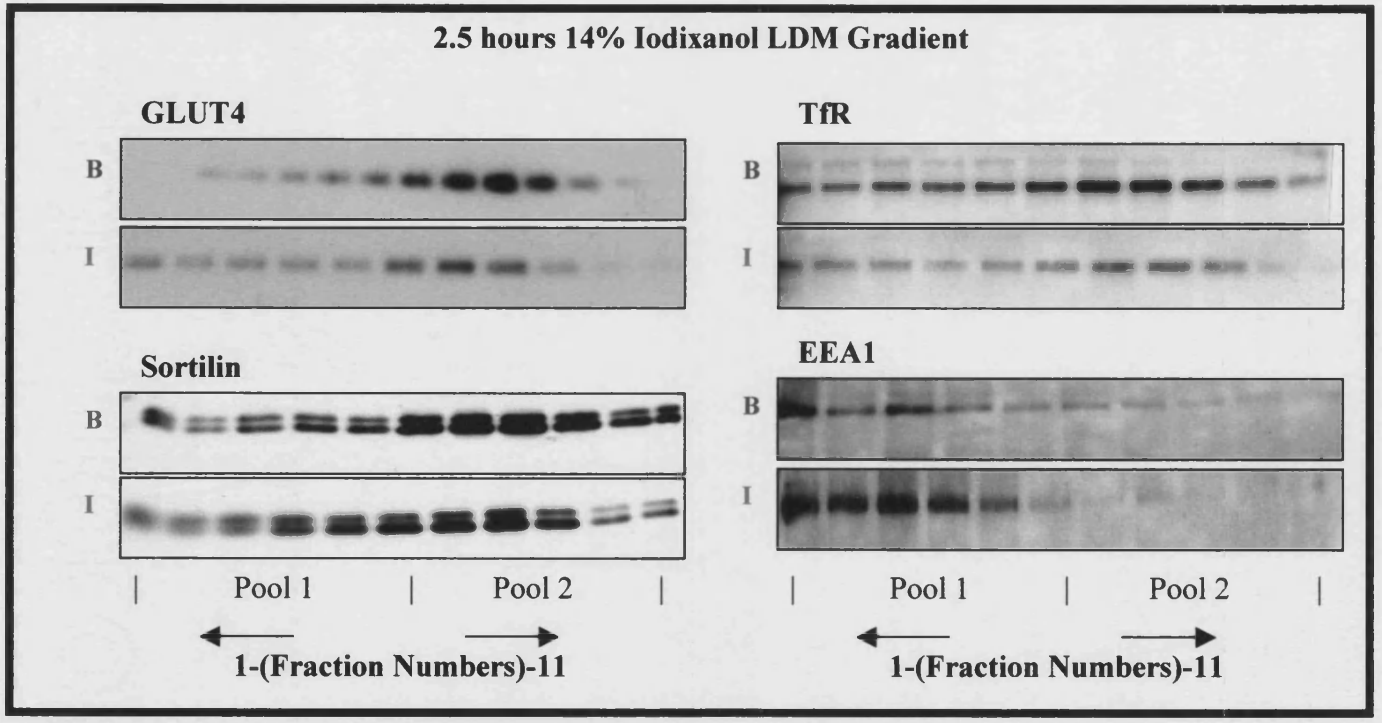

Figure 5.9A: Analysis of protein distribution from the LDM of rat adipose cells on a 2.5 h 14% Iodixanol Gradient. 500 µg of LDM taken from basal (B,■) or insulin-treated (I,▲) rat adipose cells were analysed on a 1 hour 14% iodixanol self-generating gradient, (Section 2.6.2). 200 µl fractions were collected from the top of the gradient. 10 µl from all fractions were analysed and Western blot for the following proteins: GLUT4, TfR Sortilin and EEA1. Antibodies were detected using ECL (Amersham). Densometric analysis of the bands were carried out using the programme Molecular Analyst ™ (from Bio-Rad Laboratories), and results were plotted graphically with Prism software. The Western blots shown above are representative of two separate repetitions of this experiment.

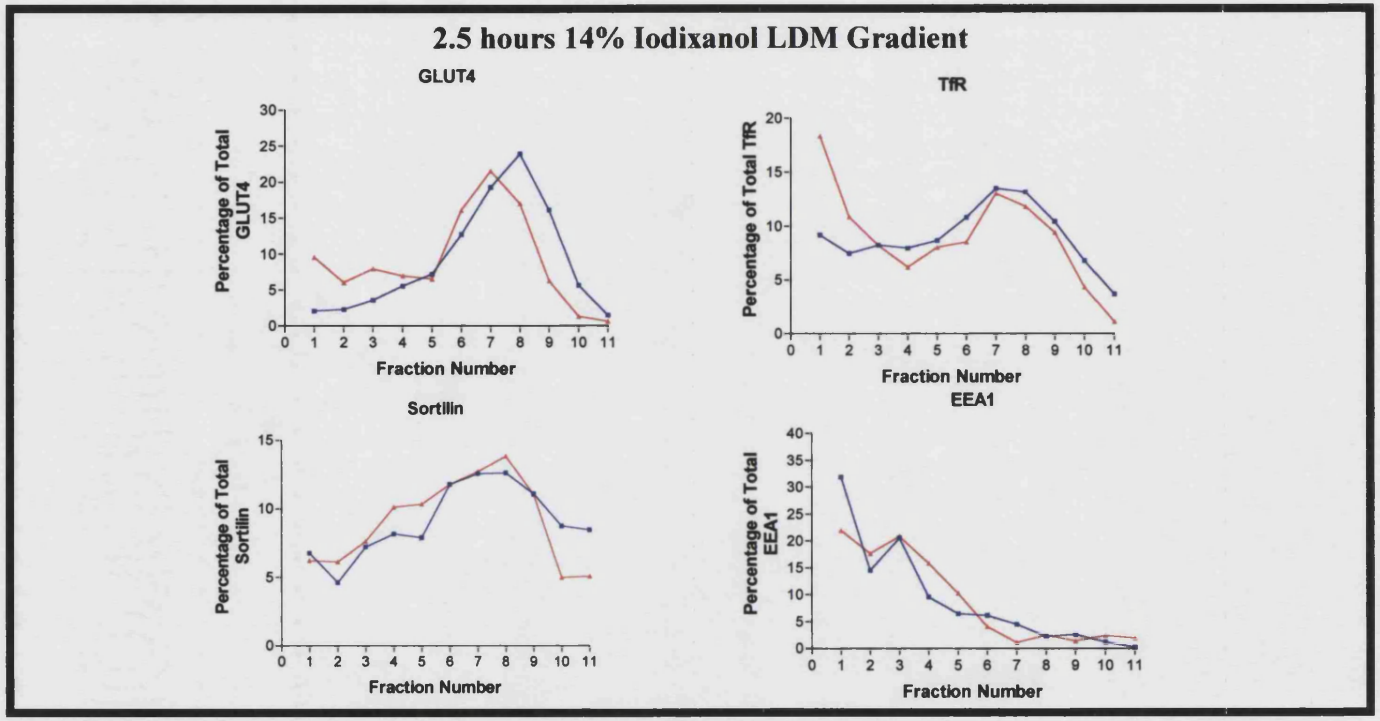

Figure 5.9B: Analysis of protein distribution from the LDM of rat adipose cells on a 2.5 h 14% Iodixanol Gradient. 500 µg of LDM taken from basal (B, ■) or insulin-treated (I, ▲) rat adipose cells were analysed on a 1 hour 14% iodixanol self-generating gradient, (Section 2.6.2). 200 µl fractions were collected from the top of the gradient. 10 µl from all fractions were analysed and Western blot for the following proteins: GLUT4, TfR Sortilin and EEA1. Antibodies were detected using ECL (Amersham). Densometric analysis of the bands were carried out using the programme Molecular Analyst ™ (from Bio-Rad Laboratories), and results were plotted graphically with Prism software. The protein distributions are representative of two separate repetitions of this experiment.

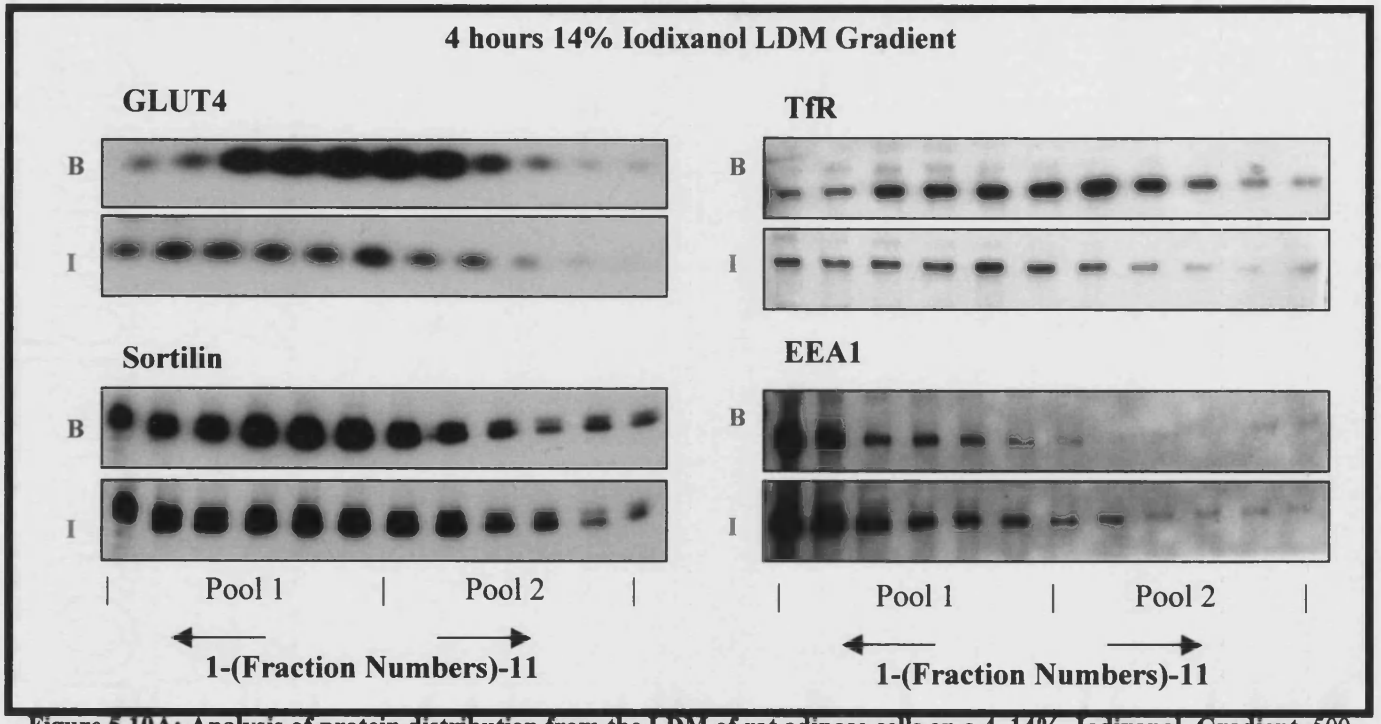

Figure 5.10A: Analysis of protein distribution from the LDM of rat adipose cells on a 4 14% Iodixanol Gradient. 500 µg of LDM taken from basal (B, ■) or insulin-treated (I, ▲) rat adipose cells were analysed on a 1 hour 14% iodixanol self-generating gradient, (Section 2.6.2). 200 µl fractions were collected from the top of the gradient. 10 µl from all fractions were analysed and Western blot for the following proteins: GLUT4, TfR Sortilin and EEA1. Antibodies were detected using ECL (Amersham). Densometric analysis of the bands were carried out using the programme Molecular Analyst ™ (from Bio-Rad Laboratories), and results were plotted graphically with Prism software. The Western blots shown above are representative of two separate repetitions of this experiment.

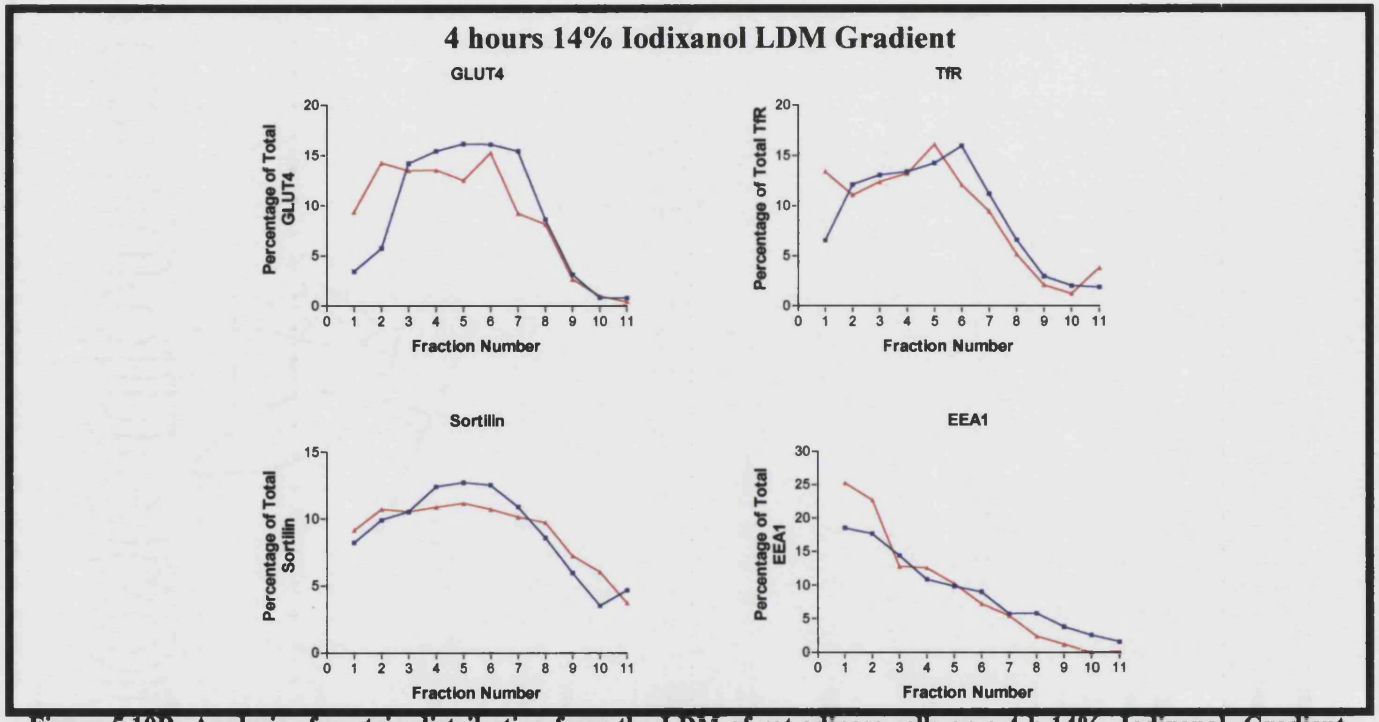

Figure 5.10B: Analysis of protein distribution from the LDM of rat adipose cells on a 4 h 14% Iodixanol Gradient. 500 µg of LDM taken from basal (B, ■) or insulin-treated (I, ▲) rat adipose cells were analysed on a 4 h 14% iodixanol self-generating gradient, (Section 2.6.2). 200 µl fractions were collected from the top of the gradient. 10 µl from all fractions were analysed and Western blot for the following proteins: GLUT4, TfR Sortilin and EEA1. Antibodies were detected using ECL (Amersham). Densometric analysis of the bands were carried out using the programme Molecular Analyst ™ (from Bio-Rad Laboratories), and results were plotted graphically with Prism software. The protein distributions are representative of two separate repetitions of this experiment.

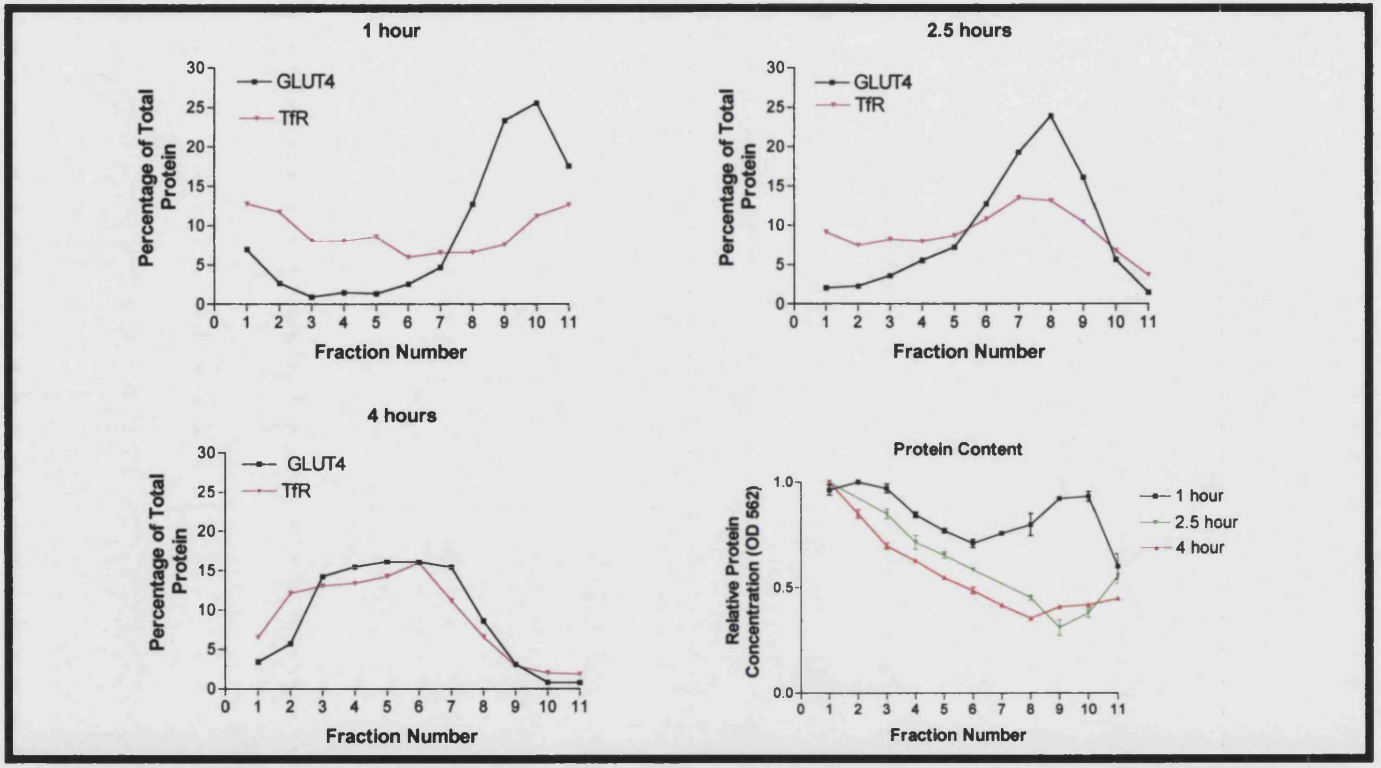

Figure 5.11: Comparison of TfR and GLUT4 distribution along 1, 2.5 and 4 h 14% (w/v) Iodixanol Gradients.
500 µg of LDM taken from basal rat adipose cells were analysed on 14% iodixanol self-generating gradients, (Section 2.6.2). 200 µl fractions were collected from the top of the gradient. 10 µl from all fractions were analysed and Western blot for the GLUT4 and TfR. The protein content of the gradients were also tested using the BCA detection method, (Section 2.2.1). The protein distributions shown above are representative of two separate repetitions of the gradients.

5.5 Tracking Internalised GLUT4 on Gradients

There is evidence that as much as 40% of total GLUT4 in 3T3-L1 adipocytes is associated with the endosomal pathway. This has been shown by the co-localisation between GLUT4 and TfR in endosomal ablation studies, (Livingstone *et al.*, 1996; Martin *et al.*, 1996a). This proportion appears to be smaller in white and brown adipose tissue (Malide *et al.*, 1997a; Slot *et al.*, 1991a). The findings on the glycerol gradients reported in this chapter support the idea that the amount of GLUT4 in the endosome compartment is smaller in rat adipocytes than it is in 3T3-L1 cells. There was hardly any co-sedimentation between GLUT4 and TfR on the glycerol gradients, (Section 5.3). One possible explanation for this apparent lack of co-sedimentation may have been the comparative excess of GLUT4 found at the dense region (termed the GLUT4 storage compartment) to the light region (endosomal compartment) of the glycerol gradient. It was thought that a more sensitive tool was needed to detect the presence of GLUT4 associated with the TfR on the glycerol gradients, than basic Western blotting of the two proteins. To do this, rat adipocytes were irradiated in the presence of biotinylated photolabels to label cell surface GLUT4 that was subsequently internalised into intracellular compartments. The quantification of biotinylated GLUT4 were carried out by immunoprecipitation of pooled glycerol gradient fractions (dense fractions versus light fractions) using streptavidin-agarose beads. To compare movement between the endosomal pathway and the intracellular sequestered GLUT4 compartment, the biotinylated glucose transporters were allowed to internalise for 4 or 40 min. The short time of 4 min was chosen to 'capture' GLUT4 at the endosomal compartment. It is known that GLUT4 is completely internalised after 20 min, (Clark *et al.*, 1991). 40 min internalisation time was chosen to ensure all tagged GLUT4 had been sequestered inside the cells.

The experimental methods described here are detailed in Section 2.6.3. Biotinylated GLUT4 in post HDM supernatants from 4 or 40 min internalised rat adipose cells were loaded onto 5-25% 16 h glycerol density gradients. The fractions were collected from the bottom of the gradients and analysed for GLUT4, sortilin and TfR by Western blotting, (Figure 5.12, page 136). GLUT4 sedimented to the same fractions (fractions 3-5) after 4 or 40 min of internalisation. There is a slightly higher amount of GLUT4 found in these

fractions after 40 min of internalisation compared with 4 min. Sortilin was found to be more prominent in the lighter fractions (9-15) after 4 min of internalisation compared to the 40 min internalised sample. GLUT4 was absent from fractions 9-15 in both samples. The separate fractions 3-5 (dense region/GLUT4 storage compartment) and 9-15 (light region/endosomal compartment) were pooled, dialysed against PBS, concentrated and analysed for biotinylated GLUT4, (Figure 5.13, page 137). There was a greater amount of GLUT4 in fractions 3-5 after 4 min of internalisation than 40 min, (Figure 5.13i). It was predicted that the amount of GLUT4 at fractions 3-5 after 40 min of internalisation would exceed the 4 min internalised sample. However, analysis of the densities of the bands for each sample show that approximately 35 % of the total labelled GLUT4 is internalised in fractions 3-5, (Figure 5.13ii). It should be noted that overall, the amount of total GLUT4 labelled with the 4 min sample is greater than the 40 min sample. A reasonable explanation could be that discrepancies in the measuring of label or amount of cells used for labelling, may have occurred. The experiment failed to detect biotinylated GLUT4 in fractions 9-15 on the glycerol gradients for either the 40 min or 4 min incubated samples.

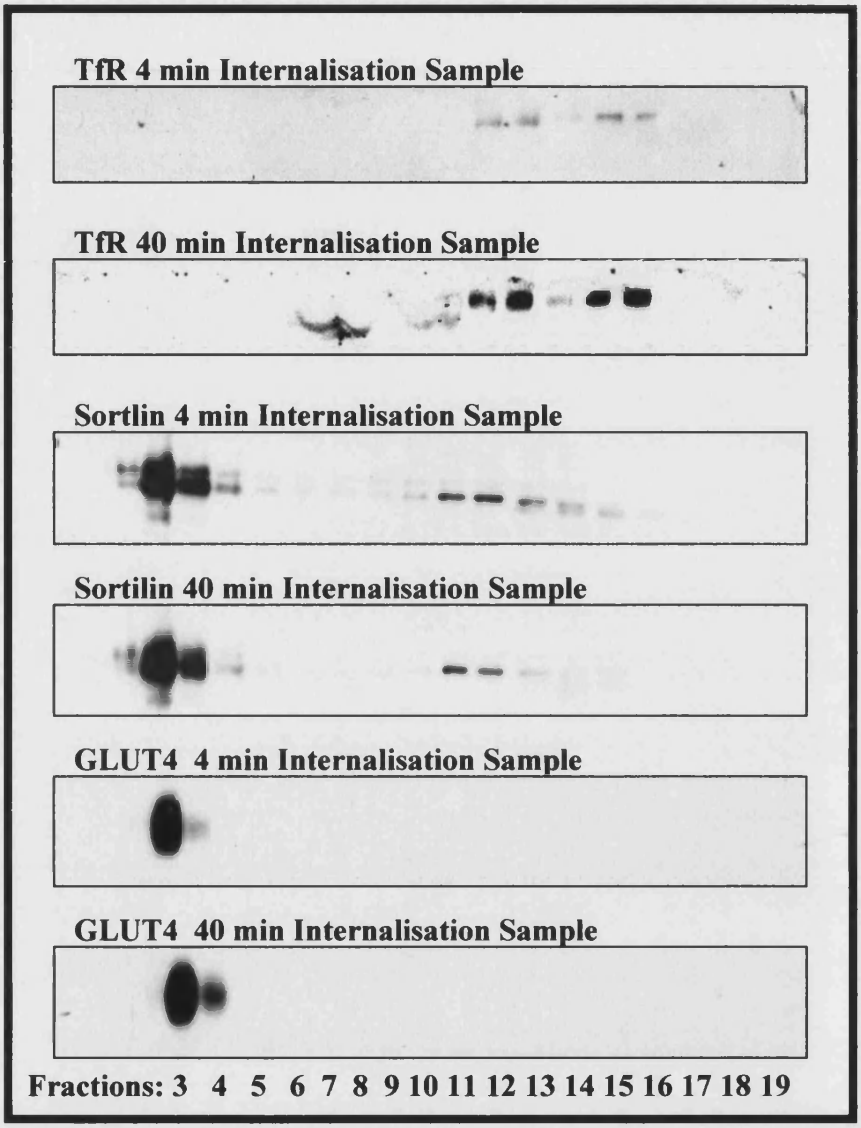

Figure 5.12: Preparation of Internalised Photolabeled GLUT4 in Rat Adipocytes for use on 16 hour Glycerol Gradients.

200 μM of Bio-LC-ATB-BGPA was used to tag cell surface GLUT4 on insulin-stimulated rat adipose cells, (Section 2.5.2). Cells were then washed twice in MES buffer at 18°C and subsequently twice in 1% (w/v) BSA/KRH containing 2 mM D-glucose at 37°C. Cells were left for 4 or 40 mins to allow for glucose transporter internalisation. The cells were washed in HES Buffer and homogenised for the post HDM supernatants, (Section 2.3.3). Post HDM supernatants were layered onto a 16 hour glycerol density gradient, (Section 2.6.1). Fractions were collected from the bottom and analysed for GLUT4 sortilin or TfR using Western blotting techniques. Fractions 3-5 and 9-15 fractions were pooled together to detect for biotinylated GLUT4, (Figure 5.12). The experiments were carried out twice and example Western blots are given above

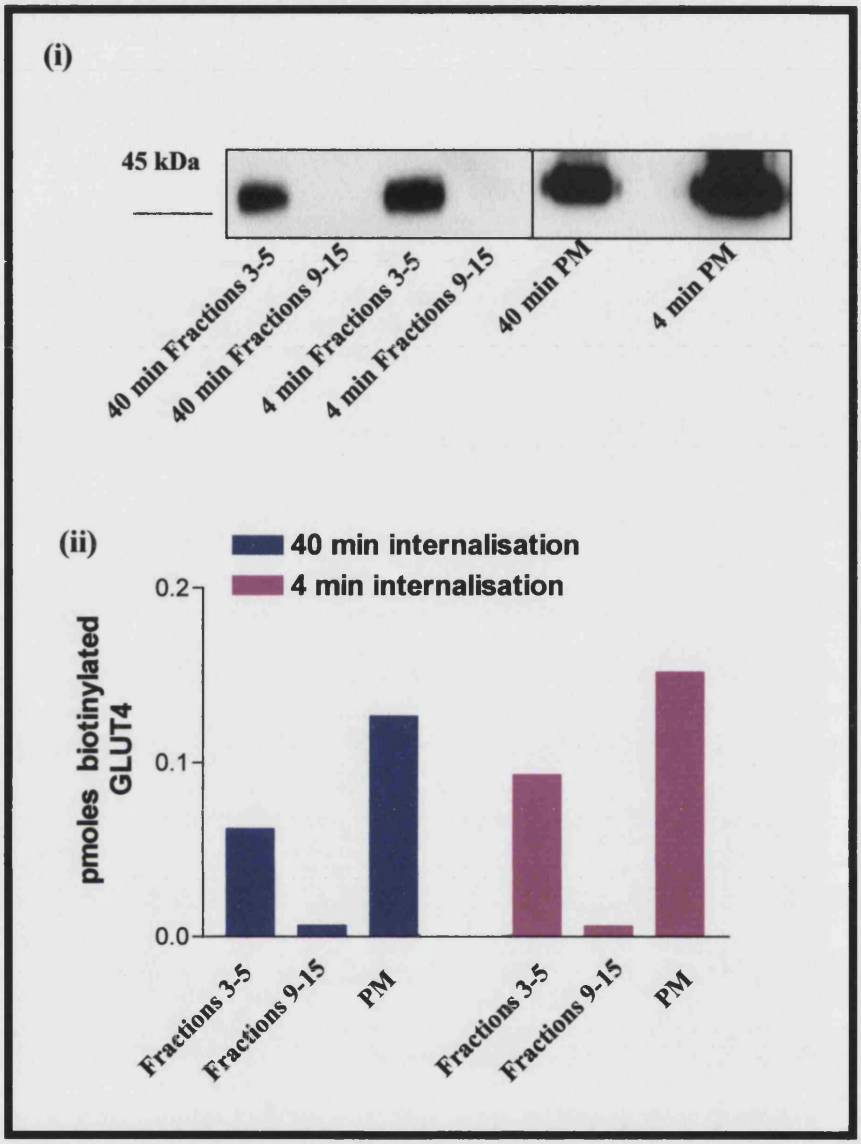

Figure 5.13: Biotinylated GLUT4 Labelling in Frations 3-5 and 9-15 of 16 hour glycerol gradients.

The GLUT4 fractions (3-5) and the TfR fractions (9-15) were pooled together from a 16 hour glycerol gradient (Figure 5.12) and dialysed overnight against PBS. The pooled fractions were concentrated to 2 ml using PEG 20000 and analysed for biotinylated GLUT4 using streptavidin immunoprecipitation, (Section 2.5.2). The immunoprecipitations were washed eluted and processed for GLUT4 labelling by Western blotting, (Figure 5.13i) . Amount of GLUT4 labelling in pmoles was calculated by construction of a standard curve of pmoles GLUT4 in basal LDM versus density counts, (figure 5.13ii). The experiments were carried out twice and similar patterns of protein distribution were observed. The Western blot and its density analysis shown are representative of two separate repetitions of this experiment.

5.6 Discussion

Resolving GLUT4 Compartments

To identify the GLUT4 associated compartments in rat adipocytes buoyant density analysis using glycerol and iodixanol gradients were used. The sedimentations of proteins from the rat adipose cells were subject to centrifugation using pre-formed discontinuous density gradients or self-generating density gradients.

Discontinuous step density gradients were used to separate intracellular rat adipocyte membrane fractions under two conditions, at equilibrium (16 h centrifugation time) and under non-equilibrium conditions after a shortened centrifugation time, (90 min). Direct Western blotting revealed that 5%-25% (w/v) glycerol densities in the gradient produced a GLUT4 peak in comparison to gradients with iodixanol media. On both non-equilibrium and equilibrium glycerol gradients, GLUT4 did not co-sediment with TfR. Previous studies have revealed that the insulin regulated intracellular membranes containing GLUT4 are specialised and appear to exclude some other recycling proteins, i.e. TfR and GLUT1, (Livingstone *et al.*, 1996; Millar *et al.*, 1997). Here it was found that GLUT4 sedimented to a higher density than the bulk of all microsomal proteins, including TfR and EEA1. This was verified by detection of VAMP2 and IRAP in the same fractions as GLUT4. 90% of the total sortilin protein was found to be associated with GLUT4. The remaining 10% was found to co-sediment with TfR. The EEA1, (early endosome compartment marker) and Rab4 sedimented very slowly and were found at the top of the gradient with partial co-localisation with TfR.

The results described above are inconsistent with the findings by Kandror and colleagues. A 10-30% (w/v) non-equilibrium velocity sucrose gradient of rat adipose cells suggested that 60% of GLUT4 co-sedimented with TfR, and both sedimented away from the bulk of microsomal proteins, (Kandror *et al.*, 1995; Kandror and Pilch, 1998). The results in this chapter show that GLUT4 is not associated with TfR and that the TfR sediments with the bulk of the microsomal proteins. However, other published results complement our findings, (Haney *et al.*, 1991; Herman *et al.*, 1994; Marshall *et al.*, 1993; Piper *et al.*, 1991). The analysis of GLUT4 and GLUT1 from 3T3-L1 preadipocytes on sucrose density gradients revealed that GLUT4 compartments were distinct from other intracellular vesicles including GLUT1, (Haney *et al.*, 1991). Marshall and colleagues employed a 12%-50% sucrose density gradient to show similar

results using Xenopus oocytes transfected with GLUT4, (Marshall *et al.*, 1993). Glycerol gradients of PC12 cells transfected with GLUT4 showed that the majority of TfRs migrated in fractions which are separate from the major GLUT4 pool, (Herman *et al.*, 1994). The buoyant density of GLUT4 in the sucrose gradients were found to be approximately 1.13 g/cm^3 (Haney *et al.*, 1991; Kandror *et al.*, 1995). In the glycerol gradients the fractions in which GLUT4 sedimented partially contained 50% (w/v) sucrose and 25% (w/v) glycerol. The glycerol corresponds to a density of 1.06 g/ cm^3

The separation of the bulk of GLUT4 from TfR on the glycerol gradients suggests a specialised compartment exists which is distinct from the recycling system. In the presence of insulin the GLUT4 pool was shifted by one fraction from the slow to high sedimenting area of the gradient. This shift in GLUT4 buoyancy has been shown in previous studies, (Kandror *et al.*, 1995). The increase in density of the GLUT4 vesicles could be accounted for the priming of the vesicles with adaptor proteins to dock with the PM, (Gillingham *et al.*, 1999). The shift may also represent the generation of a separate GLUT4 compartment that cannot be resolved using density glycerol gradients. James and Pilch also tried and failed to resolve distinct intracellular GLUT4 compartments with sucrose density gradients, (James and Pilch, 1988). The technique of density gradient analysis (using glycerol or sucrose) to separate GLUT4 compartments may be limiting. The presence of different GLUT4 compartments associated with the TGN, endosome or in a separate specialised compartment may not have been detected with gradient analysis, as all the vesicles will show similar characteristics of density and size.

Recently, a novel method involving hypotonic lysis and glycerol velocity sedimentation of rat adipocytes has provided evidence for three distinct pools of intracellular GLUT4: a major insulin sensitive storage pool, an insulin sensitive exocytotic compartment, and a insulin insensitive fraction, (Lee *et al.*, 1999). The paper argues that hypotonic lysis of rat adipocytes to produce ghosts, (Rodbell, 1967) instead of conventional mechanical homogenization provides better material for the analysis of different GLUT4 pools. The results presented in this chapter show little evidence for different GLUT4 pools. This could be due to a loss of information on compartment-specific protein functions caused by vesiculation from the mechanical shearing of homogenising the cells. Guilherme has recently carried out gradient studies and has identified microtubule filaments associated with GLUT4 enriched membranes purified by novel means, (Guilherme *et al.*, 2000).

The purification of GLUT4 enriched membranes involved a 10%-35% (w/v) sucrose velocity centrifugation, (Heller-Harrison *et al.*, 1996; Kandror *et al.*, 1995) followed by loading the GLUT4 containing fractions onto a 10-65% (w/v) equilibrium sucrose density gradient. This method produced two GLUT4 pools, an insulin-sensitive and an insulin-insensitive pool. The large amount of GLUT4 was found to be insulin-insensitive. Guilherme and colleagues also found that the TfR and VAMP2 were completely co-sedimenting to the insulin sensitive fractions of the GLUT4 pool on the gradients. However, TfRs are thought to be present mostly in recycling endosomes which show only a small sensitivity to insulin (Hashiramoto *et al.*, 2000; Millar *et al.*, 1999b). The results from Guilherme seem to suggest that recycling endosomes may have contaminated the insulin-sensitive fractions.

The 1 h 14% iodixanol self-forming gradient with white rat adipocytes resolved GLUT4 into two pools: one large pool at the bottom of the gradient and the other a smaller pool at the top of the gradient. An approximate 84% of total intracellular GLUT4 resided in the larger pool, which declined with insulin-stimulation. There was a slight shift (of one fraction) of GLUT4 towards the lighter end of the gradient. Whether this is significant, or not it is not certain. However, a similar shift in GLUT4 distribution has been seen in the glycerol gradients presented in this study and in others, (Gillingham *et al.*, 1999). When cells were insulin-stimulated the smaller GLUT4 pool did not show a reduction in the amount of GLUT4. Instead there was a slight increase in the amount of GLUT4 in pool 1. This increase may be from entry of GLUT4 from pool 2. This increase of GLUT4 associated with endosomes after insulin-stimulation has also been seen in brown adipocytes and white rat adipocytes (Slot *et al.*, 1991a; Ramm *et al.*, 2000). Only 16% of GLUT4 vesicles (in pool 1) co-sedimented with 97% of EEA1. Ramm and colleagues also reported a lack of co-localisation between EEA1 and GLUT4 (Ramm *et al.*, 2000). The results suggest that the GLUT4 vesicles from pool 1 are associated with endosome and the GLUT4 vesicles from pool 2 acts as an insulin-responsive storage compartment. The majority of sortilin resided in pool 2. With insulin-stimulation the highest peak of sortilin shifted towards the lighter end of the gradient as did GLUT4, but there was no decline in the levels of sortilin. To support these findings, sortilin has been found to be associated with GLUT4 (Lin et al., 1997; Petersen et al., 1997) but insulin has only elicited a 1.7-fold increase in the amount of sortilin at the plasma membrane in 3T3-L1 adipocytes, (Morris *et al.*, 1998). This explains the shift in sortilin distribution along the gradient and the lack of response of sortilin to insulin. The TfR

was not insulin-responsive in either pool 1 or 2. This was expected as insulin is known to increase TfR at the plasma membrane only by 3-fold (Davis *et al.*, 1986). Surprisingly, the endosomal TfR was distributed equally between both GLUT4 pools. It was expected that pool 1 would contain more TfRs than pool 2. How can we be sure that pool 2 represents a GLUT4 storage compartment, when the TfR has been shown to co-sediment here? The overlap in distribution of GLUT4 and TfR may suggest that GLUT4 vesicles in pool 2 are probably derived from recycling endosome and/or TGN. Perhaps the GLUT4 vesicles are continuously recycling between the GLUT4 storage pool and the endsosomes. To support this hypothesis, Wei and colleagues have identified a population of small vesicles where GLUT4 trafficking is blocked in a non-insulin responsive compartment at room temperature (Wei *et al.*, 1998).

Hashiramoto and James resolved GLUT4 from 3T3-L1 adipocytes into two peaks on 14% iodixanol gradients: dense pool, 44%: light pool, 39% (Hashiramoto and James, 2000). The dense pool was relatively devoid of endosomal markers and corresponds to the GSVs. Interestingly, this insulin-sensitive pool lost its ability to translocate GLUT4 when cells were exposed to chronic insulin, (Maier and Gould *et al.*, 2000). The work described in this chapter on the analysis of the 14% iodixanol LDM gradients of the rat adipocytes differed from the results on 3T3-L1 adipocytes in several aspects (Hashiramoto and James, 2000). Firstly, there was roughly an equal distribution of GLUT4 between the two GLUT4 pools (dense pool, 44%: light pool, 39%) when the LDM from 3T3-L1 adipocytes were used. This contrasts with the results from the rat adipose tissue. Only 16% of the total rat adipocyte GLUT4 was found in the lighter pool of the gradient compared to 84% in the dense fractions. An explanation for this observation may be due to cell type. The bulk of rat adipose GLUT4 was found in one major pool (compared to other GLUT4 containing cell types e.g. 3T3-L1 and CHO cell lines), which indicates that there is more effective sequestration of GLUT4 in rat adipocytes. Malide and colleagues have noticed that rat adipocytes cultured for 24 h produced an altered staining of GLUT4 to that seen in freshly isolated cells, (compare Malide *et al.*, 1996 to Malide *et al.*, 1997a). It was proposed that GLUT4 may be excluded from the early endosome system in freshly isolated rat adipose cells due to very efficient sorting of GLUT4 from recycling receptors which may be lost in cell lines. The rat adipose cell may express numerous storage compartments that accumulate on gradients in the insulin-responsive pool. Interestingly, CHO cells have less GLUT4 in the gradient peak exhibiting the higher insulin responsiveness in comparison to the

3T3-L1 adipocytes (Hashiramoto and James, 2000). The opposite was found with rat adipose cells. The results suggest that the storage compartment may exist in rat adipocytes, but is far abundant than that found in CHO cells or 3T3-L1 cells. 3T3-L1 cells are thought to be less phenotypically mature than rat adipocytes, in part because they express more GLUT1 than GLUT4, (Calderhead et al., 1990). The rat adipose iodixanol gradients clearly show that the majority of GLUT4 resides in a compartment away from the early endosomes and is insulin-responsive.

GLUT4 Association with Endosomal Compartments

Most studies agree that there is a major GLUT4 compartment that is distinct from endosomes and TGN, however the degree of overlap is variable dependent on the experimental method or cell type used, e.g., isolated rat adipocytes versus 3T3-L1 adipocytes. Can we be sure that GLUT4 in all cell types has the same association with TfR? Table 5.4 (page 143) compares studies where the amount of GLUT4 associated with the endosomal system varied.

A comparison of the 3T3-L1 and rat adipocyte iodixanol gradients has shown a difference in the amount of GLUT4 associated with endosomes. This needs to confirmed with further repetitions of the same experiments. To examine the amount of GLUT4 associated with endosomes in various tissue types, we have used mathematical constructs that were originally developed by Holman and colleagues (Holman et al., 1994). The constructs were designed to demonstrate the recycling of GLUT4 based on one or multiple intracellular GLUT4 compartment systems with the aid of kinetic and biochemical data of GLUT4 movement. The model of one intracellular GLUT4 pool has been shown not to support any of the biochemical data outlined above. The three state model, (Figure 5.14, page 144) was used to consider whether GLUT4 moved from the cell surface through the early endosome/TGN recycling system, (Hresko *et al.*, 1994; Slot *et al.*, 1991a; Slot *et al.*, 1991b) to form TV elements in an intracellular sequestered compartment, (Herman *et al.*, 1994; Livingstone *et al.*, 1996; Malide *et al.*, 1996; Martin *et al.*, 1996a). Direct evidence has not been produced for the movement of GLUT4 vesicles between early endosome and a GSV compartment, but several studies have suggested that this model may be feasible, (Wei *et al.*, 1998; Ramm *et al.*, 2000; for review see Rea *et al.*, 1997).

Table 5.4: Proportion of Cellular GLUT4 Associated with the Endosomal System

Reference	Technique	Cell Type	Basal GLUT4 associated with endosomal compartments/markers
Tanner and Lienhard, 1989	Immunoadsorption	3T3-L1 adipocytes	33% of GLUT4 predicted to associate with TfR
Kandror and Pilch, 1998	Immunoadsorption	White rat adipocytes	60% of total TfR associated with GLUT4
Aledo *et al.*, 1995	Immunoadsorption	Rat skeletal muscle	None
Livingstone *et al.*, 1996; Martin *et al.*, 1996a	Endosome Ablation	3T3-L1 adipocytes	40% of GLUT4 non-ablated
Millar *et al.*, 1999b	Endosome Ablation	3T3-L1 adipocytes	Inhibition of 30% of insulin-stimulated GLUT4
Herman *et al.*, 1994	Glycerol gradient velocity sedimentation	PC12 cells transfected with GLUT4 cDNA	none
Lee *et al.*, 1999	Glycerol gradient velocity sedimentation	White rat adipocytes	50% of GLUT4 in same fractions as TfR
Aledo *et al.*, 1997	Discontinous sucrose gradient	Rat skeletal muscle	Partial overlap with TfR
Hashiramoto and James, 2000	14% Iodixanol Gradients	3T3-L1 adipocytes	39% of GLUT4 in same fractions as TfR
This Study, Chapter 5	14% Iodixanol Gradients	White rat adipocytes	16% in same fractions as EEA1 and associated with 50% of TfR
Hudson *et al.*, 1993	Immunofluorescence microscopy	PC12 cells transfected with GLUT4 cDNA	Partial overlap
Malide *et al.*, 1997a	Immunofluorescence microscopy	White rat adipocytes	No co-localisation with TfR
Bogan and Lodish, 1999	Immunofluorescence microscopy	3T3-L1 adipocytes	50% associates with TfR
Powell *et al.*, 1999	Immunofluorescence microscopy	3T3-L1 adipocytes	Partial overlap with TfR
Slot *et al.*, 1991a	Immunogold electron microscopy	Brown rat adipocytes	3.8% of GLUT4 associated with early endosomes
Ralston and Ploug, 1996	Immunofluorescence microscopy and Immunogold electron microscopy	Cultured skeletal myotubes	Little overlap with TfR
Ploug *et al.*, 1998	Immunogold electron microscopy	Rat skeletal muscle	50% overlap with TfR
Ramm *et al.*, 2000	Immunogold electron microscopy	White rat adipocytes	No co-localisation with EEA1

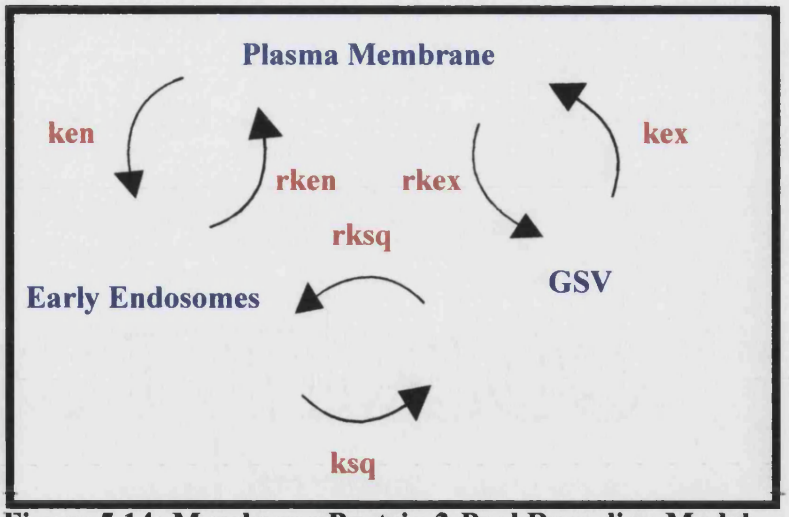

Figure 5.14: Membrane Protein 3-Pool Recycling Model.

GLUT4 is thought to recycle between the plasma membrane, early endosomes and GLUT4 Storage Vesicles (GSV). The model takes into account the possibility of forward and reverse rate constants for endocytosis, exocytosis and sequestered GLUT4.

The three-pool model was assigned forward and reverse rate constants for endocytosis, exocytosis and sequestered GLUT4, termed ken, kex and ksq, respectively. The equations used for the mathematical model are shown in Appendix I. Using the parameter values previously described, a very small pool size for the endosomal/TGN compartment is predicted. Although this may be appropriate in simulation of the rat adipocyte situation, other systems probably have a greater proportion of GLUT4 in this compartment. Therefore the parameters for the model are altered here to determine which most markedly alters the distribution of GLUT4 between the two intracellular pools. The mathematical model was used to generate a graph representing the movement of internalised labelled and total GLUT4, (for example see Figure A, page 145). The graphs generated were for the internalisation of GLUT4, internalisation of the label and the proportion in endosomes using the parameters published by Holman and colleagues, (Figure A). The values of the rate constants are also given in each simulation, (Figure A). At time 0 min the cells are insulin-stimulated and after 40 min of internalisation the cells are in the basal state. The total cellular pool of GLUT4 is distributed between a plasma membrane form (Tp) and the two intracellular pools, the early endosomes (Tee) and the intracellular sequestered compartment, otherwise known as the GSV (Tisc). The labelled GLUT4 is distributed between a plasma membrane form (Lp) and the two intracellular pools, the early endosomes (Lee) and the GSV (Lisc). Several different combinations of rate constants were examined so that the fraction of the total cellular GLUT4 associated with the early endosomes (FTee) would

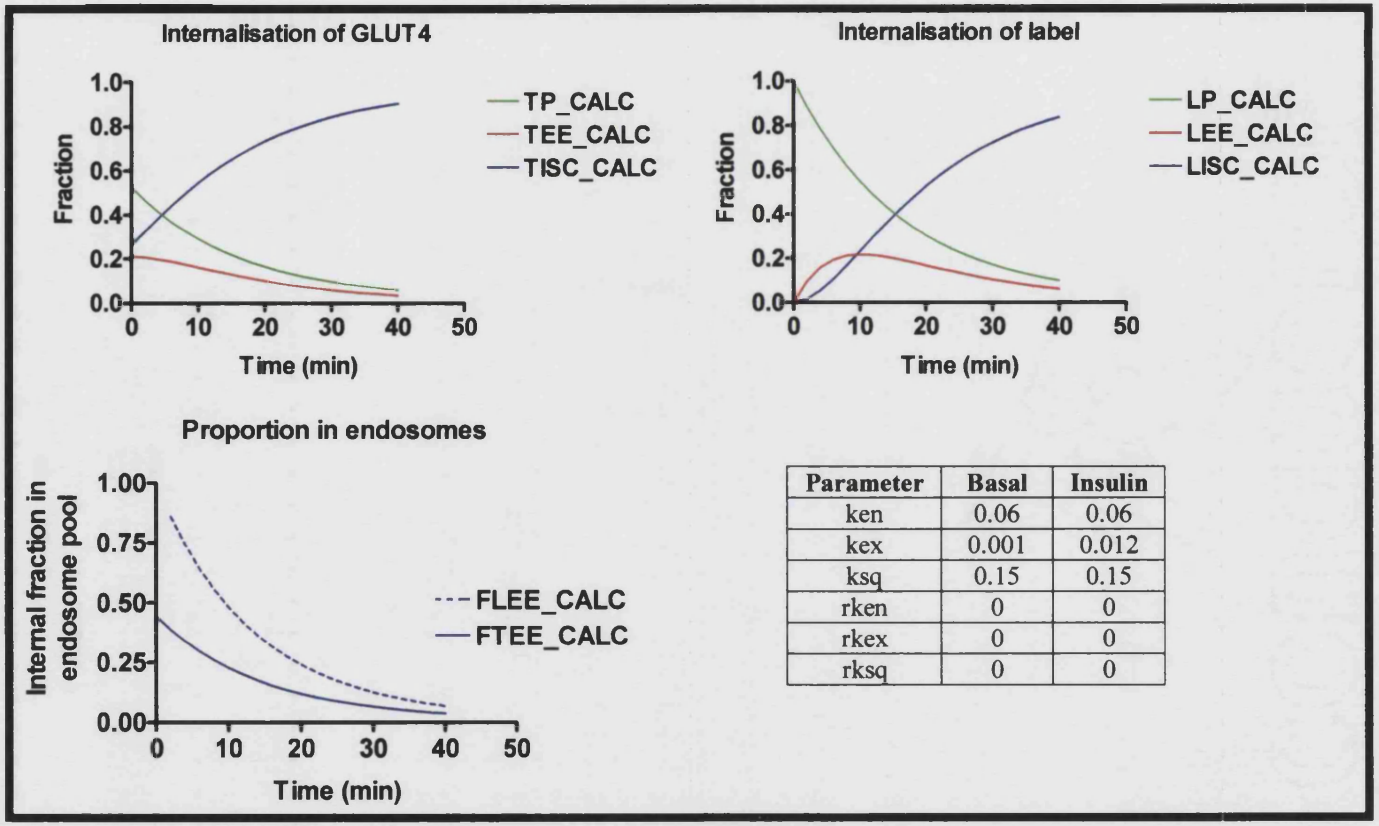

Parameter	Basal	Insulin
ken	0.06	0.06
kex	0.001	0.012
ksq	0.15	0.15
rken	0	0
rkex	0	0
rksq	0	0

Figure A: Simulation of the glucose transporter subcellular trafficking using the 3-pool membrane protein recycling model. The fractional steady state pool sizes of Tp, Tee, and Tisc in the basal (40 mins) and insulin-stimulated states (0 mins) are 0.059, 0.037, and 0.90, and 0.53, 0.21, and 0.26, respectively. The cell surface labelled GLUT4 at the plasma membrane, early endosomes and GSV are respectively, 1, 0 and 0 for the insulin-stimulated state and 0.1, 0.06 and 0.8 after internalisation. Only a fraction of 0.038 and 0.069 of the total cellular GLUT4 and labelled GLUT4, respectively, resides in the early endosome compartment at the basal state.

membrane. These values seem to fit the 14% iodixanol 3T3-L1 data. A reverse rate constant, rken was introduced into the simulations, (Figure G). This reduced the amount of basal GLUT4 at the endosomes, leaving more cellular GLUT4 at the plasma membrane.

From the simulations it has been shown that altering the rksq, alters the net sequestration of GLUT4 to produce the best fit to the biochemical data of this study and the James and Hashiramoto study. A large rksq gave a small net sequestration of GLUT4 with a large population of GLUT4 associated with endosomes (3T3-L1 adipocytes). In contrast, a small rksq gave a large net sequestration of GLUT4 with a small population of GLUT4 associated with endosomes (rat adipocytes).

Conclusions

Glycerol equilibrium density gradient centrifugation has been shown to be inadequate in resolving distinct intracellular pools of GLUT4. Self-forming gradients using 14% iodixanol were more successful in resolving different GLUT4 pools. Two pools of GLUT4 vesicles were successfully separated into an insulin sensitive and insulin-insensitive pool. The insulin-sensitve pool in the rat adipocytes was much larger than that found in 3T3-L1 adipocytes. This suggested that the 3T3-L1 cells may not generate net sequestration GLUT4 into its storage compartment as readily as in rat adipocytes. The computer simulations show that the inclusion of a reverse rate constant in the model improves the fit to data on 3T3-L1 cells and cells in which the endosome compartment is large. This is less necessary in rat adipocytes where the proportion of GLUT4 in the endosome compartment is quite small.

Table 5.5: Amount of GLUT4 associated with endosomes, plasma membrane and an intracellular sequestered compartment with altered rate constants

Figure (pages 144, 149-154)	Altered Parameter	Percentage of basal cellular GLUT4 associated with:		
		Tee	Tisc	Tp
A	-	3.8	90	5.9
B	ksq 0.06 min^{-1}	13	82	4.6
C	ksq 0.01 min^{-1}	63	35.	1.6
D	rksq 0.15 min^{-1}	48	47	4.4
E	rksq 0.06 min^{-1}	28	66	5.2
F	rksq 0.01 min^{-1}	8.9	85	5.8
G	rken 0.06 min^{-1}	4.7	81.5	13

Note: Parameters set at the beginning before alterations are: ken: 0.06 min^{-1}; ksq: 0.15 min^{-1}; kex basal/insulin: 0.001/0.012 min^{-1}.

The ksq was reduced from 0.15 min^{-1} to 0.06 min^{-1} (Figure B) or 0.01 min^{-1} (Figure C). When the ksq was altered to 0.06, the amount of total cellular GLUT4 in the plasma membrane, early endosomes and GSV of insulin-stimulated and basal cells were 40%, 40% and 20%, and 4.6%, 13% and 82%, respectively. The proportion of total cellular GLUT4 in the endosomes was 13%. A decrease in the ksq to 0.01 simulated total cellular GLUT4 to be 13%, 80.9% and 6.7%, in insulin-stimulated plasma membrane, early endosomes and GSV, respectively, (Figure C). The total basal cellular GLUT4 was 1.6%, 63% and 35%, in the plasma membrane, early endosomes and sequestered compartment. The proportion in the endosomes was too high to fit both the 3T3-L1 and rat adipocyte 14% iodixanol data.

To simulate GLUT4 dynamically moving from the GSV to the early endosomes, the rksq parameter was included in the 3-pool membrane recycling model. With the rksq of 0.15 min^{-1} the total cellular GLUT4 in the endosomes is roughly equal to that found in the sequestered compartment, (Figure D). The rksq was reduced to 0.06 min^{-1} and 0.01 min^{-1}, Figures E and F, respectively. The simulation with the parameter set at rksq 0.01 min^{-1} leaves 8.9% of cellular GLUT4 at the endosomes in the basal state which would approximately fit the data on 14% iodixanol gradients with rat adipocytes. The intermediate rksq gives a reasonable amount of total cellular GLUT4 (28%) in basal endosomes. This also reduces the amount of cellular GLUT4 found at the plasma

be 3-40% (depending on cell type, see Table 5.4) without substantially altering the amount of GLUT4 known to be associated in the TV elements and the plasma membrane.

To examine which parameters had the greatest effect on the endosome pool size only some parameters were altered as follows. The endocytosis value, ken was kept constant It has been shown by this lab and others that insulin does not significantly effect the rate of internalization of GLUT4 in comparison to GLUT4 exocytosis. The rate of GLUT4 endocytosis has been shown to decrease (1.3 - 3-fold) (Czech *et al.*, 1993; Czech, 1995; Holman and Cushman, 1996; Jhun *et al.*, 1992; Kandror and Pilch, 1996; Satoh *et al.*, 1993; Yang and Holman, 1993). The ken was kept at 0.06 min^{-1} and the kex at 0.001 min^{-1} (basal state) or 0.12 min^{-1} (insulin-stimulated state) (Holman *et al.*, 1994). To ascertain if a trafficking route between the early endosomes and GLUT4 storage compartment is feasible the parameters altered where the ksq, rksq, and rken.

The fractional steady state pool sizes of Tp, Tee, and Tisc in the basal (40 min) and insulin-stimulated states (0 min) are 0.059, 0.037, and 0.90, and 0.53, 0.21, and 0.26, respectively, (Figure A). The cell surface labelled GLUT4 at the plasma membrane, early endosomes and GSV are respectively, 1, 0 and 0 for the insulin-stimulated state and 0.1, 0.06 and 0.8 after internalisation. Clearly it can be seen that only a fraction of 0.038 and 0.069 of the total cellular GLUT4 and labelled GLUT4, respectively, resides in the early endosome compartment at the basal state. The fractions shown can be expressed as a percentage by multiplying the values by 100, giving only 3.8% of total cellular GLUT4 in the endosomes (FTee). A summary of the altered parameters and their outcomes is given in Table 5.5, page 147.

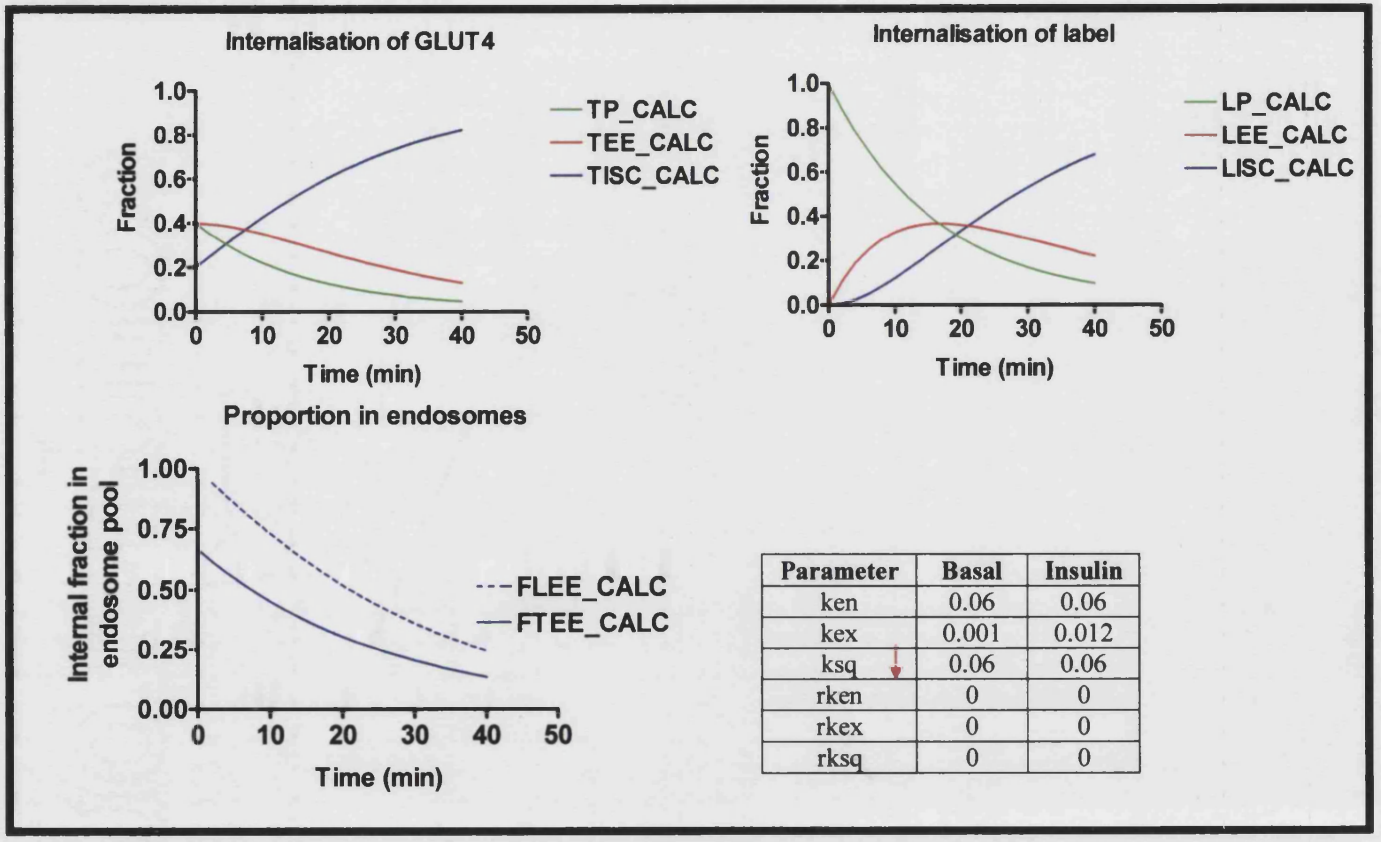

Parameter	Basal	Insulin
ken	0.06	0.06
kex	0.001	0.012
ksq ↓	0.06	0.06
rken	0	0
rkex	0	0
rksq	0	0

Figure B: Simulation of the glucose transporter subcellular trafficking with ksq decreased to 0.06 min^{-1}. The fractional steady state pool sizes of Tp, Tee, and Tisc in the basal (40 mins) and insulin-stimulated states (0 mins) are 0.046, 0.13, and 0.82, and 0.4, 0.4, and 0.2, respectively. The cell surface labelled GLUT4 at the plasma membrane, early endosomes and GSV are respectively, 1, 0 and 0 for the insulin-stimulated state and 0.097, 0.22 and 0.68 after internalisation. 13% of the total cellular GLUT4 resides in the early endosome compartment at the basal state.

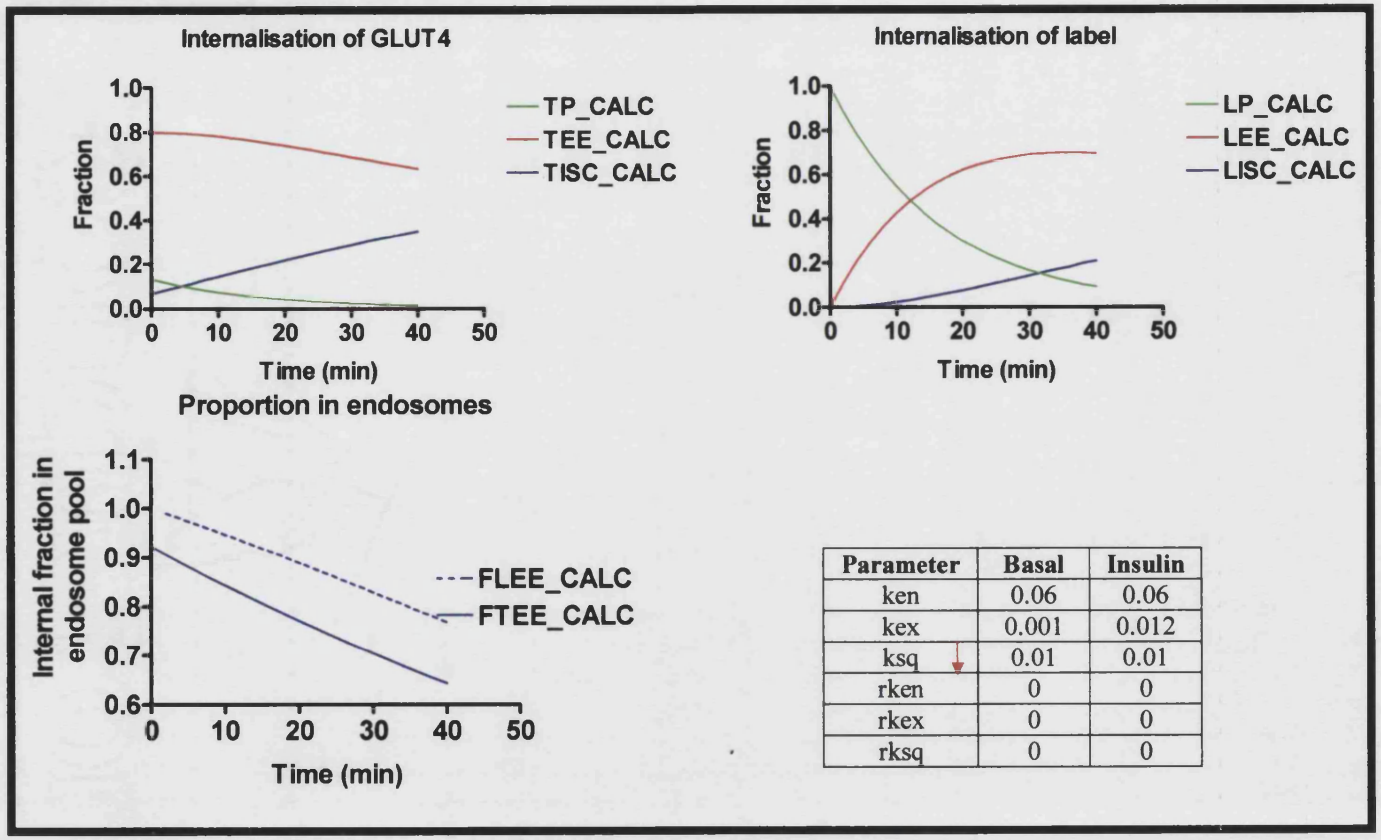

Parameter	Basal	Insulin
ken	0.06	0.06
kex	0.001	0.012
ksq ↓	0.01	0.01
rken	0	0
rkex	0	0
rksq	0	0

Figure C: Simulation of the glucose transporter subcellular trafficking with ksq decreased to 0.01 min^{-1}. The fractional steady state pool sizes of Tp, Tee, and Tisc in the basal (40 mins) and insulin-stimulated states (0 mins) are 0.016, 0.63, and 0.35, and 0.13, 0.80, and 0.066, respectively. The cell surface labelled GLUT4 at the plasma membrane, early endosomes and GSV are respectively, 1, 0 and 0 for the insulin-stimulated state and 0.09, 0.69 and 0.21 after internalisation. 63% of total cellular GLUT4 resides in the early endosome compartment at the basal state. There is very little total cellular GLUT4 in the GSV (time 40 mins) or the plasma membrane (time 0 mins).

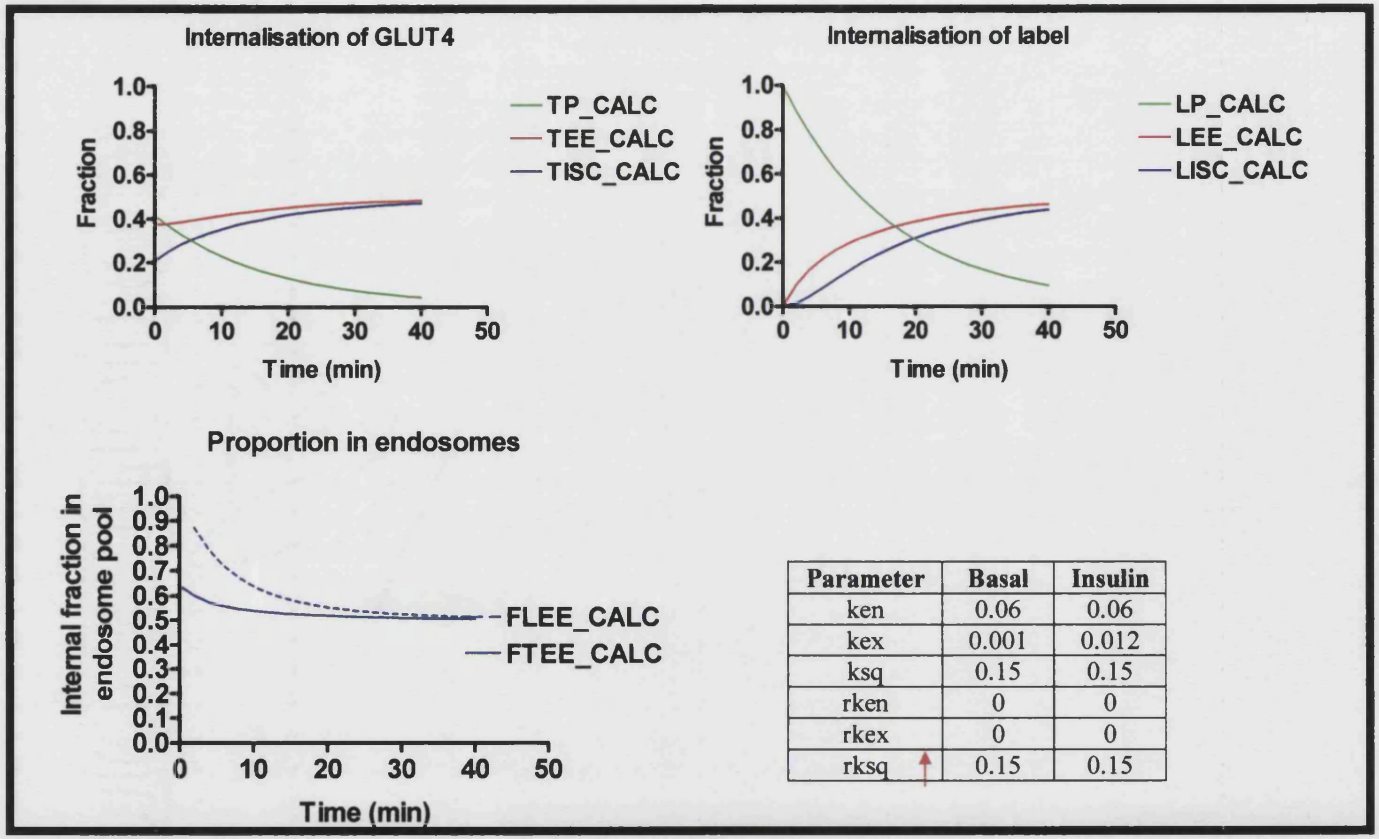

Parameter	Basal	Insulin
ken	0.06	0.06
kex	0.001	0.012
ksq	0.15	0.15
rken	0	0
rkex	0	0
rksq ↑	0.15	0.15

Figure D: Simulation of the glucose transporter subcellular trafficking with rksq at 0.15 min^{-1}. The fractional steady state pool sizes of Tp, Tee, and Tisc in the basal (40 mins) and insulin-stimulated states (0 mins) are 0.044, 0.48, and 0.47, and 0.41, 0.38, and 0.21, respectively. The cell surface labelled GLUT4 at the plasma membrane, early endosomes and GSV are respectively, 1, 0 and 0 for the insulin-stimulated state and 0.096, 0.46 and 0.44 after internalisation. 50% of total cellular GLUT4 resides in the early endosome compartment at the basal state.. The total cellular GLUT4 in the GSV is also 50%.

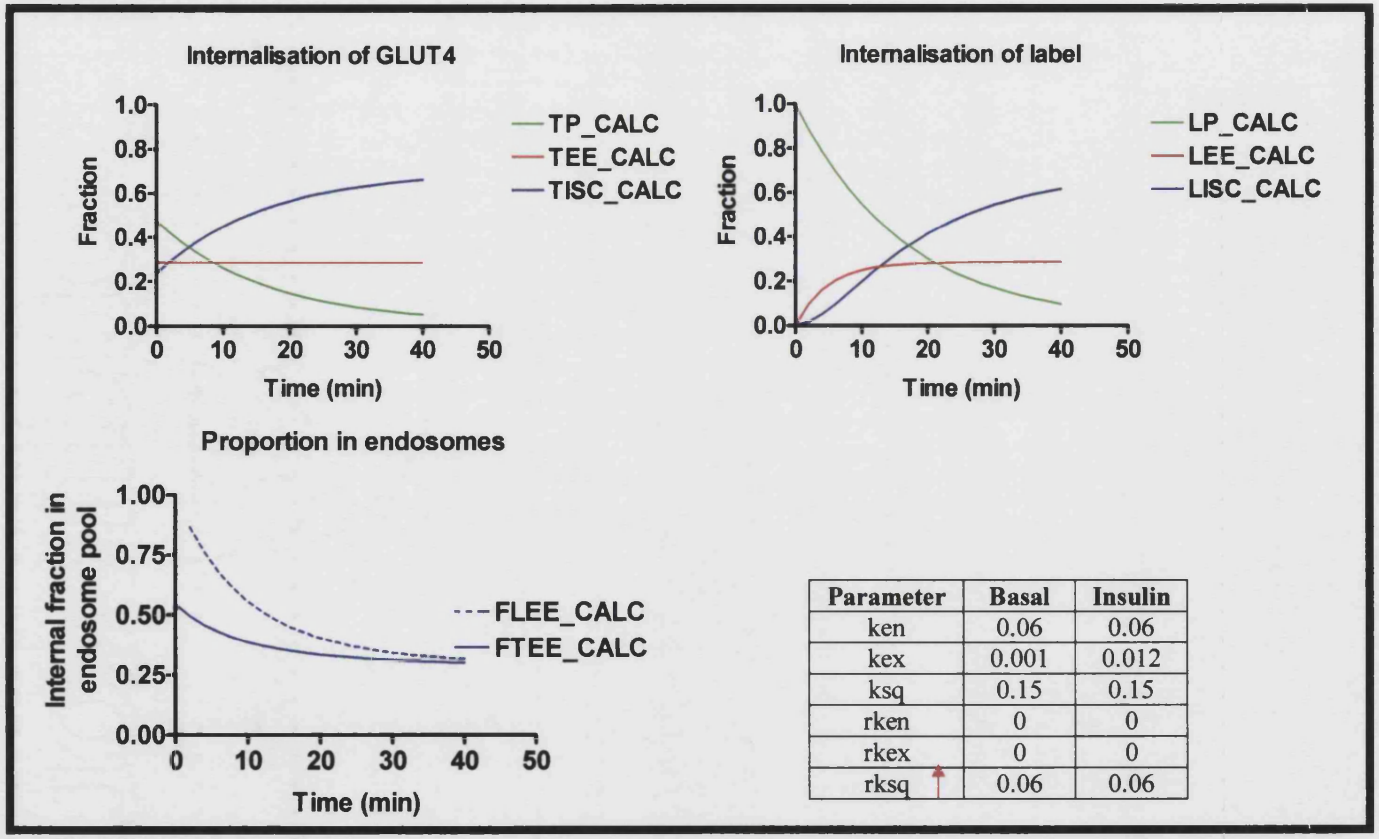

Parameter	Basal	Insulin
ken	0.06	0.06
kex	0.001	0.012
ksq	0.15	0.15
rken	0	0
rkex	0	0
rksq	0.06	0.06

Figure E: Simulation of the glucose transporter subcellular trafficking with rksq at 0.06 min^{-1}. The fractional steady state pool sizes of Tp, Tee, and Tisc in the basal (40 mins) and insulin-stimulated states (0 mins) are 0.052, 0.28, and 0.66, and 0.47, 0.28, and 0.23, respectively. The cell surface labelled GLUT4 at the plasma membrane, early endosomes and GSV are respectively, 1, 0 and 0 for the insulin-stimulated state and 0.09, 0.28 and 0.61 after internalisation. A fraction of 30% of cellular GLUT4 resides in the early endosomes.

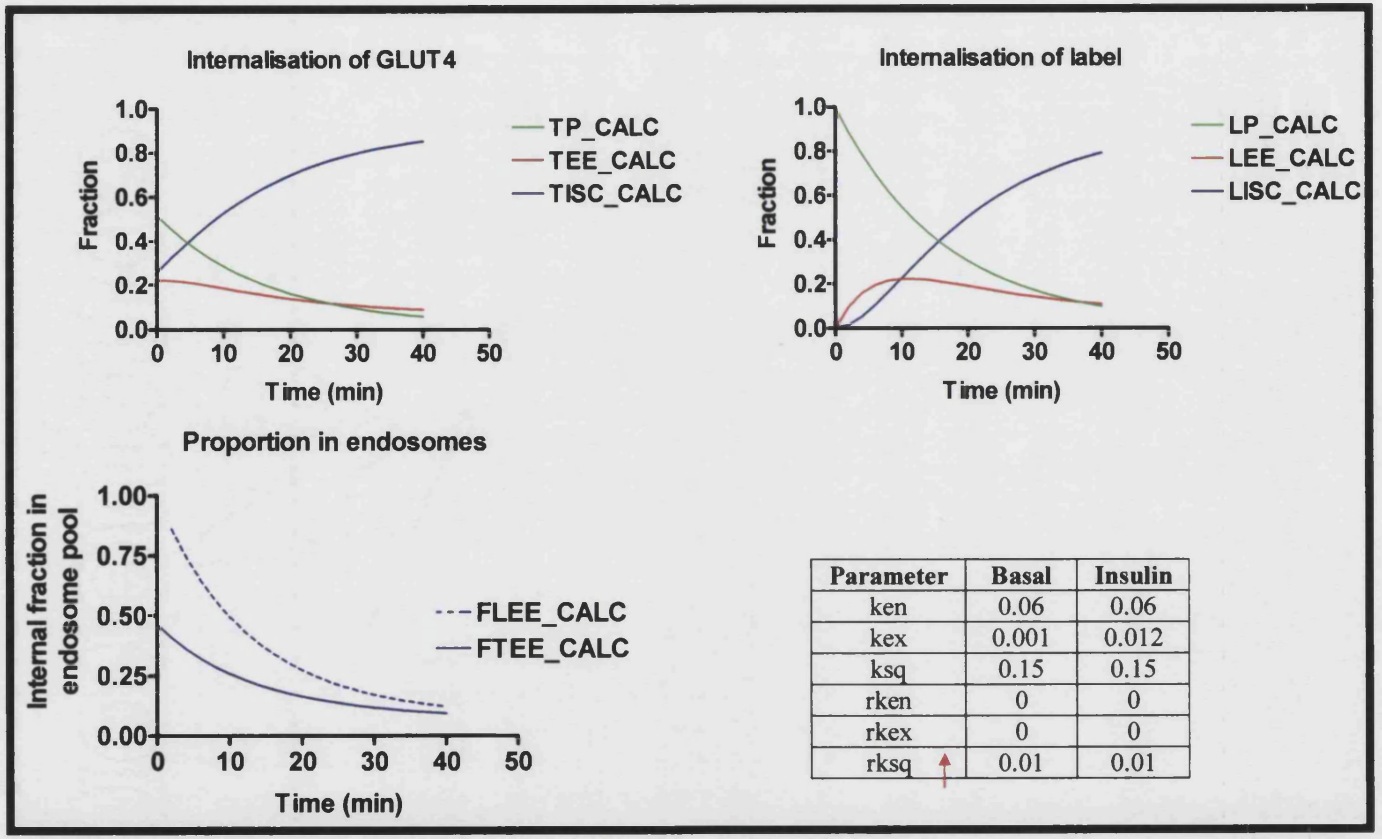

Parameter	Basal	Insulin
ken	0.06	0.06
kex	0.001	0.012
ksq	0.15	0.15
rken	0	0
rkex	0	0
rksq ↑	0.01	0.01

Figure F: Simulation of the glucose transporter subcellular trafficking with rksq at 0.01 min^{-1}. The fractional steady state pool sizes of Tp, Tee, and Tisc in the basal (40 mins) and insulin-stimulated states (0 mins) are 0.058, 0.088, and 0.85, and 0.51, 0.22, and 0.25, respectively. The cell surface labelled GLUT4 at the plasma membrane, early endosomes and GSV are respectively, 1, 0 and 0 for the insulin-stimulated state and 0.19, 0.067 and 0.73 after internalisation. 8.9% of total cellular GLUT4 is in the early endosomes in the basal state.

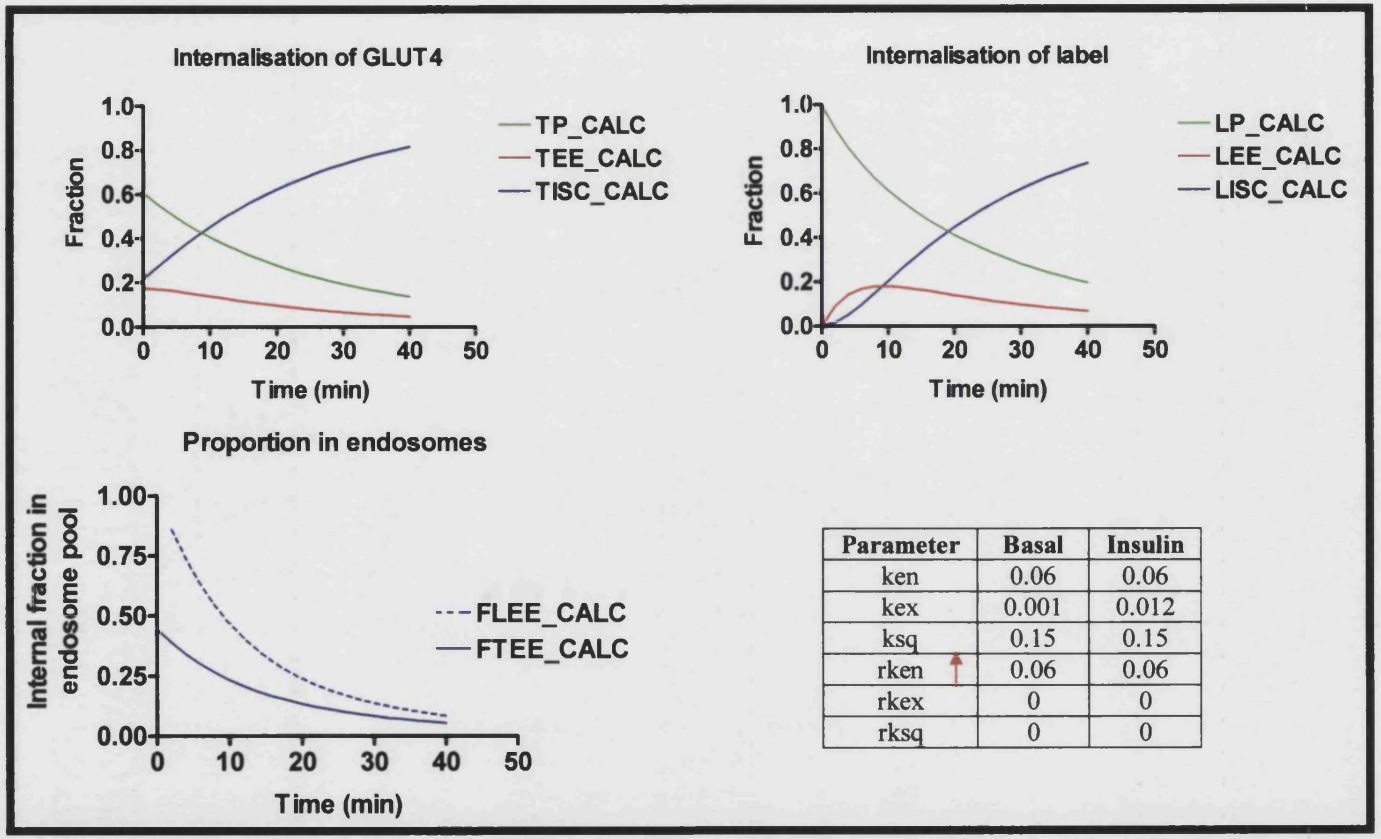

Parameter	Basal	Insulin
ken	0.06	0.06
kex	0.001	0.012
ksq	0.15	0.15
rken	0.06	0.06
rkex	0	0
rksq	0	0

Figure G: Simulation of the glucose transporter subcellular trafficking with rken at 0.06 min^{-1}. The fractional steady state pool sizes of Tp, Tee, and Tisc in the basal (40 mins) and insulin-stimulated states (0 mins) are 0.13, 0.047, and 0.81, and 0.60, 0.17, and 0.21, respectively. The cell surface labelled GLUT4 at the plasma membrane, early endosomes and GSV are respectively, 1, 0 and 0 for the insulin-stimulated state and 0.19, 0.06 and 0.73 after internalisation. The total cellular GLUT4 in the early endosomes in the basal state was 5%, less than that found at the plasma membrane (13%).

6.0 Conclusions

The aims of this study were to establish novel methods for examining GLUT4 trafficking and distribution between different subcellular locations in rat adipocytes.

The first approach was to develop a probe that could be accessible in intact cells. A Bio-LC-G15 photolabel was developed. This compound contained a very long spacer arm between the photolabel and the biotin molecule. It was postulated that the long spacer arm would allow the biotin to interact with avidin at the cell surface and thus provide a means of distinguishing internalised GLUT4. The Bio-LC-G15 tagged GLUT4 efficiently and was used to directly measure GLUT4 exocytosis, (kex: 0.24 min^{-1}). Experiments were conducted to visualise tagged GLUT4 in intact cells with the use of confocal microscopy. Hashimoto was able to detect tagged GLUTs in erythocytes, (Hashimoto *et al.*, 2001a). This was not seen in whole cell rat adipocytes, as background labelling was too high.

A cleavable label, Bio-SS-ATB-BGPA was used in the second approach. It was postulated that the use of a cleavable disulphide bridge would allow the investigator to distinguish cell surface and internal GLUT4 and thereby use the compound as a means to trace GLUT4 movement between these compartments. The Bio-SS-ATB-BGPA did not efficiently tag GLUT4 in white rat adipocytes. In contrast, the Bio-SS-ATB-BGPA labelled GLUT1 in erythocyte membranes. It was unclear why the label detected GLUTs in erythrocyte membranes and not in rat adipocytes. This characteristic of the label may have been attributed to the buffer in which the cells were placed for labelling (PBS or BSA).

GLUT4 is thought to reside in a storage compartment away from the endosomal pool. Some studies have suggested that the carboxyl-terminal of GLUT4 is masked in basal cells. It has been postulated that this epitope masking may act to retain GLUT4 in a specialised compartment. The epitope-masking was re-examined here by using a novel amino-terminal and a carboxyl-terminal GLUT4 antibody in whole cell rat adipocytes. The results suggested that the amount of GLUT4 detected with the carboxyl-terminal GLUT4 antibody was lower in basal cells than in insulin-stimulated cells. The amount of GLUT4 detected with the amino-terminal GLUT4 antibody did not vary between

basal and insulin-stimulated cells. These results are only preliminary findings and need to be quantified, perhaps by using electron microscopy.

The population of GLUT4 in the storage compartment has been shown to differ depending on experimental methods and cell types (Table 5.4). Gradient centrifugation was used as a means to separate different intracellular compartments. It was hoped that this would identify GLUT4 populations in white rat adipocytes. Glycerol gradient centrifugation only revealed one population of GLUT4 vesicles, which were separate from endosome compartments. 14% iodixanol gradients identified two GLUT4 populations: one insulin-sensitive (GSV) and the other of endosomal origin. The GLUT4 population in 3T3-L1 cells also fell into two similar pools (Hashiramoto and James, 2000). However, the 3T3-L1 adipocytes were shown to have a larger population of GLUT4 vesicles associated with the endosome compartment. It was postulated in this thesis that the levels of sequestration of GLUT4 from endosomes into a storage compartment differed in 3T3-L1 and rat adipocytes. The results point towards a dynamic system where GLUT4 vesicles are constantly shuttling between the GSV and an endosome compartment in basal cells. Computer simulations reveal that the reverse rate constant for sequestration is important in 3T3-L1 adipocytes to fit this model.

The studies have shown that to be able to fully understand the underlying mechanism of GLUT4 trafficking, it would be necessary to first understand fully the morphological characteristics of all cell types and their respective compartments. Future studies should examine the extent to which results obtained in cultured cells are representative of the regulation of glucose transport in adipose cells. Electron microscopic studies of the fractions from gradients may also be used to characterise GLUT4 vesicles associated with morphologically distinct membrane structures, such as the Golgi apparatus or tubulovesicluar elements.

References

Ahle,S. and Ungewickell,E. (1989) Identification of a clathrin binding subunit in the HA2 adaptor protein complex. *J. Biol. Chem.* **264**: 20089-20093.

Aledo,J.C.; Lavoie,L.; Volchuk,A.; Keller,S.R.; Klip,A.; and Hundal,H.S. (1997) Identification and characterization of two distinct intracellular GLUT4 pools in rat skeletal muscle: evidence for an endosomal and an insulin- sensitive GLUT4 compartment. *Biochem. J.* **325**: 727-732

Aledo,J.C., Darakhshan,F., and Hundal,H.S. (1995) Rab4, but not the transferrin receptor, is colocalised with GLUT4 in an insulin-sensitive intracellular compartment in rat skeletal muscle. *Biochem. Biophys. Res. Commun.* **215**: 321-8.

Alessi,D.R., James,S.R., downes,C.P., Holmes,A.B., Gaffney,P.R., Reese,C.B. and Cohen,P. (1997) Characterisation of a 3-phosphoinositide-dependent protein kinase which phosphorylates and activates protein kinase ßalpha. *Curr. Biol.* 7:261-269.

Al Hasani,H., Hinck,C.S. and Cushman,S.W. (1998) Endocytosis of the glucose transporter GLUT4 is mediated by the GTPase dynamin. *J. Biol. Chem.* **273**: 17504-17510.

American Diabetes Association (1997) Diabetes facts and figures.
http:www.diabetes.org/wilztest/ada/c20f.asp. **Assessed January 13, 1999**

Apodaca,G., Katz,L.A. and Mostov,K.E. (1994) Receptor-mediated transcytosis of IgA in MDCK cells is via apical recycling endosomes. *J. Cell Biol.* **125**: 67-86.

Araki,S., Yang,J., Hashiramoto,M., Tamori,Y., Kasuga,M., and Holman,G.D. (1996) Subcellular trafficking kinetics of GLU4 mutated at the N- and C-termini. *Biochem. J.* **315**: 153-159.

Arbuckle,M.I., Kane,S., Porter,L.M., Seatter,M.J., and Gould,G.W. (1996) Structure-function analysis of liver-type (GLUT2) and brain- type (GLUT3) glucose transporters: Expression of chimeric transporters in Xenopus oocytes suggests an important role for putative transmembrane helix 7 in determining substrate selectivity. *Biochemistry* **35**: 16519-16527.

Baker,G.F. and Widdas,W.F. (1973) The asymmetry of the facilitated transfer system for hexoses in human red cells and the simple kinetics of a two component model. *J. Physiol.* **231**: 43-165.

Baldwin,S.A. (1993) Mammalian passive glucose transporters: members of an ubiquitous family of active and passive transport proteins. *Biochim. Biophys. Acta* **1154**: 17-49.

Baldwin,S.A., Baldwin,J.M., and Lienhard,G.E. (1982) Monosaccharide transporter of the human erythrocyte. Characterization of an improved preparation. *Biochemistry* **21** 3836-3842.

Baldwin,S.A. and Lienhard,G.E. (1981) Glucose transport across plasma membrane-facilitated diffusion systems. *Trends Biochem. Sci.* **6** 208-211.

Baldwin,S.A. and Lienhard,G.E. (1989) Purification and reconstitution of glucose transporter from human erythrocytes. *Methods Enzymol.* **174**: 39-50.

Bandyopadhyay,G., Standeart,M.L., Kikkawa,U., Ono,Y., Moscat,J. and Farese,R.V. (1999) effects of transiently expressed atypical (ζ,γ) conventional (α,β)and novel (δ,ε) protein kinase C isoforms on insulin-stimulated translocation of epitope-tagged GLUT4 glucose transporters in rat adipocytes: specific interchangeable effects of protein kinases C-ζ and C- γ. *Biochem. J.* **337**: 461-470.

Banerjee,A., Barry,V.A., DasGupta,B.R. and Martin,T.F.J. (1996) N-ethylmaleimide-sensitive factor acts as a perfusion ATP dependent step in Ca^{2}+ activated exocytosis *J. Biol. Chem.* **271**: 20223-20226.

Barnett,J.E., Holman,G.D., and Munday,K.A. (1973) An explanation of the asymmetric binding of sugars to the human erythrocyte sugar-transport systems. *Biochem. J.* **135**: 539-541.

Barr,V.A., Malide,D., Zarnowski,M.J., Taylor,S.I., and Cushman,S.W. (1997) Insulin stimulates both leptin secretion and production of rat white adipose tissue. *Endocrinology* **138**: 4463-4472

Barrett,M.P., Walmsley,A.R., and Gould,G.W. (1999) Structure and function of facilitative sugar transporters. *Curr. Opin. Cell Biol.* **11**: 496-502.

Barthel,A., Nakatani,K., Dandekar,A.A. and Roth,R.A. (1998) Protein kinase C modulates the insulin-stimulated increase in Akt1 and Akt3 activity in 3T3-L1 adipocytes. *Biochem. Biophys. Res. Commun.***243** 509-513.

Batleiger,B., Newhall,W.J., and Jones,R.B. (1982) The use of Tween 20 as a blocking agent in the immunological detection of proteins transferred to nitrocelluose membranes. *J. Immunol. Methods* **55**: 297-307.

Baumann,C.A., Ribon,V., Kanzaki,M., Thurmond,D.C., Mora,S., Shigematsu,S., Bickel,P.E., Pessin,J.E. and Saltiel,A.R. (2000) CAP defines a second signalling pathway required for insulin-stimulated glucose transport. *Nature.* **407**:202-207.

Bayley,H. and Knowles,J.R. (1977) Photoaffinity labeling. *Methods Enzymol.* **46**: 69-114.

Bednarek,S.Y., Ravazzola,M., Hosobuchi,M., Amherdt,M., Perrelet,A., Schekman,R. and Orci,L. (1995) COPI-coated and COPII-coated vesicles bud directly from the endoplasmic reticulum in yeast. *Cell* **83**: 1183-1196.

Beltzer,J.P. and Spiess,M. (1991) *In vitro* binding of the asialoglycoprotein receptor to the β-adaptin in plasma membrane coated vesicles. *EMBO J.* **10**: 3735-3742.

Bennett,M.K., Calakos,N. and Scheller,R.H. (1992) Syntaxin: a synaptic protein implicated in docking of synaptic vesicles at presynaptic active zones. *Science* **257** 255-259.

Bennett,MK and Scheller,RH. (1993) A molecular machinery is conserved from yeast to neurons *Proc. Natl. Acad. Sci. U.S.A* **90**: 2559-2563

Biber,J.W. and Lienhard,G.E. (1986) Isolation of vesicles containing insulin-responsive, intracellular glucose transporters from 3T3-L1 adipocytes. *J. Biol. Chem.* **261**: 16180-16184.

Birnbaum,M.J. (1989) Identification of a novel gene encoding an insulin-responsive glucose transporter protein. *Cell* **57**: 305-315.

Birnbaum,M.J., Haspel,H.C., and Rosen,O.M. (1986) Cloning and characterization of a cDNA encoding the rat brain glucose- transporter protein. *Proc. Natl. Acad. Sci. U.S.A* **83**: 5784-5788.

Bogan,J.S. and Lodish,H.F. (1999) Two compartments for insulin-stimulated exocytosis in 3T3-L1 adipocytes defined by endogenous ACRP30 and GLUT4. *J. Cell Biol.* **146**: 609-620.

Bosshart,H., Humphrey,J., Deignan,E., Davidson,J., Drazba,J., Yuan,L., Oorschot,V., Peter,P.J., and Bonifacio,J.S. (1994) The cytoplasmic domain mediates translocation of furin to the trans-Golgi network en route to the endosomal/lysosomal system. *J. Cell Biol.* **126**: 1157-1172.

Brooks,C.C., Scherer,P.E., Cleveland,K., Whittemore,J.L., Lodish,H.F., and Cheatham,B. (2000) Pantophysin is a phosphoprotein component of adipocyte transport vesicles and associates with GLUT4-containing vesicles. *J. Biol. Chem.* **275**: 2029-2036.

Brose,N., Petrenko,A.G., Sudhof,T.C. and Jahn,R. (1992) Synaptogamin: a calcium sensor on the synaptic vesicle surface. *Science* **256**: 1445-1449.

Brown,S.J., Gould,G.W., Davies,A., Baldwin,S.A., Lienhard,G.E. and Gibbs,E.M. (1988) Characterisation of vesicles containing insulin-reponsive intracellular glucose transporters isolated from 3T3-L1 adipocytes by an improved procedure. *Biochim. Biophys. Acta* 971: 339-350.

Buckley,K.M., Melikian,H.E., Provoda,C.J. and Waring,M.T. (2000) Regulation of neuronal function by protein trafficking: a role for the endosomal pathway. *J. Physiol.* **525**: 11-19.

Cain,C.C., Trimble,W.S., and Lienhard,G.E. (1992) Members of the VAMP family of synaptic vesicle proteins are components of glucose transporter-containing vesicles from rat adipocytes. *J. Biol. Chem.* **267**: 11681-11684.

Calderhead,D.M., Kitagawa,K., Tanner,L.I., Holman,G.D., and Lienhard,G.E. (1990) Insulin regulation of the two glucose transporters in 3T3-L1 adipocytes. *J. Biol. Chem.* **265**: 13801-13808.

Cameron,L.A., Giardini,P.A., Soo,F.S. and Theriot,J.A. (2000) Secrets of actin-based motility revealed by a bacterial pathogen. *Nat. Rev. Mol. Cell Biol.* **1** : 110-119.

Carlier,M.F. (1998) Control of actin dynamics. *Curr. Opin. Cell Biol.* **10**: 45-51

Carter-Su,C., Pessin,J.E., Mora,R., Gitomer,W., and Czech,M.P. (1982) Photoaffinity labelling of the human erythrocyte D-glucose transporter. *J. Biol. Chem.* **257**: 5419-5429.

Charron,M.J., Brosius,F.C., Alper,S.L., and Lodish,H.F. (1989) A glucose-transport protein expressed predominantly in insulin-responsive tissues. *Proc. Natl. Acad. Sci. U.S.A* **86**: 2535-2539.

Chavrier,P. and Goud,B. (1999) The role of ARF and Rab GTPases in membrane transport. *Curr. Opin. Cell Biol.* **11**: 466-475.

Chen,Y.A. and Scheller,R.H. (2001) SNARE-mediated membrane fusion. *Nat. Rev. Mol Cell Biol.* **2**:98-106.

Christoforidis,S., McBride,H.M., Burgoyne,R.D. and Zerial,M. (1999) The Rab5 effector EEA1 is a core component of endosome docking. *Nature* **397**: 621-625.

Clague,M.J. (1998) Molecular aspects of the endocytic pathway. *Biochem. J.* **336**: 271-282.

Clark,A.E. and Holman,G.D. (1990) Exofacial photolabelling of the human erythrocyte glucose transporter with an azitrifluoroethylbenzoyl-substituted bismannose. *Biochem. J.* **269**: 615-622.

Clark,A.E., Holman,G.D., and Kozka,I.J. (1991) Determination of the rates of appearance and loss of glucose transporters at the cell surface of rat adipose cells. *Biochem. J.* **278**: 235-241.

Clark,J.F., Young,P.W., Yonezawa,K., Kasuga,M. and Holman,G.D. (1994) Inhibition of the translocation of GLUT1 and GLUT4 in 3T3-L1 cells by the phosphatidylinositol 3-kinase inhibitor, wortmannin. *Biochem. J.* **300**: 631-635.

Clark,S.F., Martin,S., Carozzi,A.J., Hill,M.M. and James,D.E (1998) Intracellular localization of phosphatidylinositide 3-kinase and insulin receptor substrate-1 in adipocytes: potential involvement of a membrane skeleton. *J.Cell Biol.* **140**: 1211-1225.

Clift-O'Grady,L., Linstedt,A.D., Lowe,A.W., Grote,E., and Kelly,R.B. (1990) Biogenesis of synaptic vesicle-like structures in a pheochromocytoma cell line PC-12. *J. Cell Biol.* **110**: 1693-1703.

Clodi,M., Vollenweider,P., Klarlund,J.K., Nakashima,N., Martin,S., Czech,M.P. and Olefsky, J.M. (1998) Effects of general receptor for phosphoinositides 1 on insulin and insulin-like growth factor 1-induced cytoskeletal arrangement, glucose transporter-4 translocation, and deoxyribonucleic acid synthesis. *Endocrinology* **139**: 4984-4990.

Colombo,M.I.,Beron,W. and Stahl,P.D. (1997) Calmodulin regulates endosome fusion *J. Biol. Chem.* **272**: 7707-7712.

Cong,L.N., Chen,H., Li,Y., Zhoou,L., McGibbon,M.A., Taylor,S.I. and Quon,M.J. (1997) Physiological role of Akt in insulin-stimulated translocation of GLUT4 in transfected rat adipose cells. *Mol Endocrino.* **11**: 1881-1890.

Cope,D.L., Lee,S., Melvin,D.R., and Gould,G.W. (2000) Identification of further important residues within the GLUT4 carboxyl-terminal tail which regulate subcellular trafficking. *FEBS Lett.* **481** 261-265.

Cormont,M., Bortoluzzi,M.N., Gautier,N., Mari,M., van Obberghen,E., and Marchand-Brustel,Y. (1996a) Potential role of Rab4 in the regulation of subcellular localization of Glut4 in adipocytes. *Mol. Cell Biol.* **16**: 6879-6886.

Cormont,M., Tanti,J.F., Zahraoui,A., Van Obberghen,E., Tavitian,A. and Le Marchand-Brustel,Y. (1993) Insulin okadaic acid induce Rab4 redistribution in adipocytes. *J. Biol Chem.* **268**: 19491-19497.

Cormont,M., Van Obberghen,E., Zerial,M. and Le Marchand-Brustel,Y. (1996b) Insulin induces a change in the Rab5 subcellular localisation in adipocytes independently of phosphatidylinositol 3-kinase activation. *Endocrinology* **137**: 3408-3415.

Corvera,S., Chawla,A., Chakrabarti,R., Joly,M., Buxton,J., and Czech,M.P. (1994) A double leucine within the GLUT4 glucose transporter COOH-terminal domain functions as an endocytosis signal. *J. Cell Biol.* **126**: 979-989.

Cosson,P. and Letourner,F. (1994) Coatomer interaction with di-lysine endoplasmic reticulum retention motifs. *Science* **263**: 1629-1631.

Currie,R.A., Walker,K.S., gray,A., Deak,M., Casamayor,A., Downes,C.P., Cohen,P., Alessi,D.R. and Lucocq,J. (1999) Role of phosphatidylinositol 3,4,5-triphosphate in regulating the activity and localisation of 3-phosphoinositide-dependent protein kinase-1. *Biochem. J.* **337**: 575-583.

Cushman,S.W. and Wardzala,L.J. (1980) Potential mechanism of insulin action on glucose transport in the isolated rat adipose cell. *J. Biol. Chem.* **255**: 4758-4762.

Czech,M.P. (1995) Molecular actions of insulin on glucose transport. *Annu. Rev. Nutr.* **15** 441-471.

Czech,M.P., Chawla,A., Woon,C.W., Buxton,J., Armoni,M., Tang,W., Joly,M., and Corvera,S. (1993) Exofacial epitope-tagged glucose transporter chimeras reveal COOH- terminal sequences governing cellular localization. *J. Cell Biol.* **123**: 127-135.

Czech,M.P., Clancy,B.M., Pessino,A., Woon,C.W., and Harrison,S.A. (1992) Complex regulation of simple sugar transport in insulin-responsive cells. *Trends Biochem. Sci.* **17**: 197-201.

Davies,A., Meeran,K., Cairns,M.T., and Baldwin,S.A. (1987a) Antibodies as probes of the human-erythrocyte glucose transporter. *Biochem. Soc. Trans.* **15**: 436-437.

Davies,A., Meeran,K., Cairns,M.T., and Baldwin,S.A. (1987b) Peptide-specific antibodies as probes of the orientation of the glucose transporter in the human erythrocyte membrane. *J. Biol. Chem.* **262**: 9347-9352.

Davis,R.J.; Corvera,S.; Czech,M.P. (1986) Insulin stimulates cellular iron uptake and causes the redistribution of intracellular transferrin receptors to the plasma membrane. *J. Biol. Chem.* **261**: 8708-8711

de Wit,H., Lichtenstein,Y., Geuze,H.J., Kelly,R.B., van der Sluijs,P., Klumperman,J. (1999) Synaptic vesicles form by budding from tubular extensions of sorting endosomes in PC12 cells *Mol Biol Cell.* **10**: 4163-4176.

Defronzo,R.A., Bonadonna,R.C., and Ferrannini,E. (1992) Pathogenesis of NIDDM - a balanced overview. *Diabetes Care* **15**: 318-368.

Dell'Angelica,E.C., Mullins,C. and Bonifacino,J.S. (1999) AP4, a novel protein complex related to clathrin adaptors. *J. Biol. Chem.* **274**:7278-7285.

Dirkx,R.J., Thomas,A., Lernmark,A., Sherwin,R.S., De Camilli,P., and Solimena,M. (1995) Targeting of the 67-kDa isoform of glutamic acid decarboxylase to intracellular organelles is mediated by its interaction with the NH2-terminal region of the 65-kDa isoform of glutamic acid decarboxylase. *J. Biol. Chem.* **270**: 2241-2246.

Doege,H., Bocianski,A., Joost,H.G., and Schurmann,A. (2000) Activity and genomic organization of human glucose transporter 9 (GLUT9), a novel member of the family of sugar-transport facilitators predominantly expressed in brain and leucocytes. *Biochem. J.* **350**: 771-776.

Doornbos,R.P., Theelan,M., van der Hoeven,P.C., van Blitterswijk,W.J., Verkleij,A.J. and van Bergen en Henegouwen,P.M. (1999) Protein kinase czeta is a negative regulator of protein kinase B activity. *J. Biol. Chem.* **274**: 8589-8596.

El Jack,A.K., Kandror,K.V., and Pilch,P.F. (1999) The formation of an insulin-responsive vesicular cargo compartment is an early event in 3T3-L1 adipocyte differentiation . *Mol. Biol. Cell* **10**: 1581-1594.

Elson,E.L., (1988) Cellular mechanics as an indicator of cytoskeletal structure and function. *Annu Rev Biophys Biophys Chem.* **17**: 397-430.

Epps,D.E., Raub,T.J., Caiolfa,V., Chiari,A., and Zamai,M. (1999) Determination of the affinity of drugs toward serum albumin by measurement of the quenching of the intrinsic tryptophan fluorescence of the protein. *J. Pharm. Pharmacol.* **51**: 41-48.

Etgen,G.J., Valasek,K.M., Broderick,C.L. and Millar,A.R. (1999) *In vivo* adenoviral delivery of recombinant human protein kinase Cζ- stimulates glucose transport activity in rat skeletal muscle. *J. Biol. Chem.*. **274**: 22139-22142.

Evans, E. (1993) New physical concepts for cell amoeboid motion. *Biophys. J.* **64**: 1306-22.

Ezaki,O. and Kono,T. (1982) Effects of temperature on basal and insulin-stimulated glucose-transport activities in fat-cells-further support for the translocation hypothesis for insulin action. *J. Biol Chem* **257** : 4306-4310.

Fasshauer,D., Sutton,R.B., Brunger,A.T. and Jahn,R. (1998) Conserved structural features of the synaptic fusion complex: SNARE proteins reclassified as Q- and R- SNAREs. *Proc. Natl. Acad. Sci. U.S.A* **95**: 15781-15786.

Fischer von Mollard,G., Mignery,G.A., Baumert,M., Perin,M.S., Hanson,T.J., Burger,P.M., Jahn,R. and Sudhof,T.C. (1990) Rab3A is a small GTP-binding ptotein exclusively localised to synaptic vesicles. *Proc. Natl. Acad. Sci. U.S.A* **362**: 1988-1992.

Foran,P.G., Fletcher,L.M., Oatey,P.B., Mohammed,N., Dolly,J.O., and Tavare,J.M. (1999) Protein kinase B stimulates the translocation of GLUT4 but not GLUT1 or transferrin receptors in 3T3-L1 adipocytes by a pathway involving SNAP- 23, synaptobrevin-2, and/or cellubrevin. *J. Biol. Chem.* **274**: 28087-28095.

Ford,T., Graham,J., and Rickwood,D. (1994) Iodixanol: a nonionic iso-osmotic centrifugation medium for the formation of self-generated gradients. *Anal. Biochem.* **220**: 360-366.

Friefelder,D. (1973) Zonal centrifugation. *Methods Enzymol.* **27**: 140-150.

Fukumoto,H., Kayano,T., Buse,J.B., Edwards,Y., Pilch,P.F., Bell,G.I., and Seino,S. (1989) Cloning and characterization of the major insulin-responsive glucose transporter expressed in human skeletal muscle and other insulin- responsive tissues. *J. Biol. Chem.* **264**: 7776-7779.

Fukumoto,H., Seino,S., Imura,H., Seino,Y., and Bell,G.I. (1988) Characterization and expression of human HepG2/erythrocyte glucose-transporter gene. *Diabetes* **37**: 657-661.

Gagescu,R., Gruenberg,J. and Smythe,E. (2000) Membrane dynamics in endocytosis: structure-function relationship. *Traffic* **1**: 84-88.

Garippa,R.J., Johnson,A., Park,J., Petrush,R.L., and McGraw,T.E. (1996) The carboxyl terminus of GLUT4 contains a serine-leucine-leucine sequence that functions as a potent internalization motif in Chinese hamster ovary cells. *J. Biol. Chem.* **271**: 20660-20668.

Garvey,W.T., Maianu,L., Zhu,J-H., Brechtel Hook,G., Wallace,P., and Baron,A.D. (1998) Evidence for defects in the trafficking and translocation of GLUT4 glucose transporters in skeletal muscle as a cause of human insulin resistance. *J. Clin. Invest.* **101**: 2377-2386.

Garvey,W.T., Maianu,L., Zhu,J-H., Hancock,J.A., and Golichowski,A.M. (1993). Multiple defects in the adipocyte glucose transport system cause cellular insulin resistance in gestational diabetes. *Diabetes.* **42**: 1773-1785.

Garza,L.A. and Birnbaum,M.J. (2000) Insulin-responsive aminopeptidase trafficking in 3T3-L1 adipocytes. *J. Biol. Chem.* **275**: 2560-2567.

Ghosh,R.N. and Maxfield,F.R. (1995) Evidence for nonvectorial, retrograde transferring trafficking in the early endosomes of Hep2 cells. *J. Cell Biol.* **128**: 549-561.

Gillingham,A.K., Koumanov,F., Pryor,P.R., Reaves,B.J., and Holman,G.D. (1999) Association of AP1 adaptor complexes with GLUT4 vesicles. *J. Cell Sci.* **112**: 4793-4800.

Gliemann,J., Osterlind,K., Vinten,J., and Gammeltoft,S. (1972) A procedure for measurement of distribution spaces in isolated fat cells. *Biochim. Biophys. Acta* 286: 1-9.

Gould,G.W. and Holman,G.D. (1993) The glucose transporter family: structure, function and tissue-specific expression. *Biochem. J.* **295**: 329-341.

Graham,J. (1972) Isolation and characterization of membranes from normal and transformed tissue-culture cells. *Biochem. J.* **130**: 1113-1124.

Graham,J., Ford,T., and Rickwood,D. (1994) The preparation of subcellular organelles from mouse liver in self- generated gradients of iodixanol. *Anal. Biochem.* **220**: 367-373.

Green,N.M. (1975) Avidin. *Advances in Protein Chemisty* **29**: 85

Griffiths,G (1993) Fine structure immunocytochemisty. Ed. Springer-Verlag. Berlin, Heidleberg

Griffiths,G., Hoflack,B., Simons,K., Mellman,I., and Kornfeld,S. (1988) The mannose 6-phosphate receptor and the biogenesis of lysosomes. *Cell* **52**: 329-341.

Gruenberg,J. and Maxfield,F.R. (1995) membrane transport in the endocytic pathway. *Curr. Opin. Cell Biol.* **7**: 552-563.

Gu,F. and Gruenberg,J. (1999) Biogenesis of transport intermediates in the endocytic pathway. *FEBS Lett.* **452**: 61-66.

GuilhermeA., Emoto,M., Buxton,J.M., Bose,S., Sabini,R., Theurkauf,W.E., Leszyk,J., and Czech,M.P. (2000) Perinuclear localization and insulin responsiveness of GLUT4 requires cytoskeletal integrity in 3T3-L1 adipocytes. *J. Biol. Chem.* **275**: 38151-38159.

Haney,P.M., Slot,J.W., Piper,R.C., James,D.E., and Mueckler,M. (1991) Intracellular targeting of the insulin-regulatable glucose transporter (GLUT4) is isoform specific and independent of cell type. *J. Cell Biol.* **114**: 689-699.

Hara,K., Yonezawa,K., Sakaue,H., Ando,A., Kotani,K., Kitamura,T., Kitamura,,Y., Ueda,H., Stephens,L., Jackson,T.R *et al.*, (1994) 1-phosphatidylinositol 3' kinase activity is required for insulin-stimulated glucose transport but not for RAS activation in CHO cells. *Proc. Natl. Acad. Sci. U.S.A* **91**: 7415-7419.

Hartman,G.C, Black,N, Sinclair,R, and Hinton,RH (1974) Methodological developments in biochemistry. Ed. Reid,E. Longman, London. (4); 93-102.

Harwood,R. (1974) Cell separation by gradient centrifugation. *Int. Rev. Cytol* **38** 369-403.

Hashimoto,M., Hatanaka,Y., Yang,J., Dhesi,J., and Holman,G.D. (2001b) Synthesis of biotinylated bis (D-glucose) dervivatives for glucose transport. *Carbohydr. Res.* **331**: 119-127.

Hashimoto,M., Yang,J., and Holman,G.D. (2001a) Cell-surface recognition of biotinylated membrane proteins requires very long spacer arms: An example from glucose transporter probes. *Chem. Bio. Chem.* **2**: 52-59.

Hashiramoto,M. and James,D.E. (2000) Characterization of insulin-responsive GLUT4 storage vesicles isolated from 3T3-L1 adipocytes. *Mol. Cell Biol.* **20**: 416-427.

Hashiramoto,M., Kadowaki,T., Clark,A.E., Muraoka,A., Momomura,K., Sakura,H., Tobe,K., Akanuma,Y., Yazaki,Y., and Holman,G.D. (1992) Site-directed mutagenesis of GLUT1 in helix 7 residue 282 results in perturbation of exofacial ligand binding. *J. Biol. Chem.* **267**: 17502-17507.

Hatanaka,Y., Hashimoto,M., and Kanaoka,Y. (1994) A novel biotinylated heterobifunctional cross-linking reagent bearing an aromatic diazirine. *Biorg. Med. Chem.* **2**: 1367-1373.

Heller-Harrison,R.A., Morin,M., Guilherme,A., and Czech,M.P. (1996) Insulin-mediated targeting of phosphatidylinositol 3-kinase to GLUT4- containing vesicles. *J. Biol. Chem.* **271**: 10200-10204.

Hellwig,B., Brown,F.M., Schurmann,A., Shanahan,M.F., and Joost,H.G. (1992) Localization of the binding domain of the inhibitory ligand forskolin in the glucose transporter GLUT4 by photolabelling, proteolytic clevage and site-specific antiserum. *Biochim. Biophys. Acta* **1111**: 178-184.

Herman,G.A., Bonzelius,F., Cieutat,A.M., and Kelly,R.B. (1994) A distinct class of intracellular storage vesicles, identified by expression of the glucose transporter GLUT4. *Proc. Natl. Acad. Sci. U.S.A* **91**: 12750-12754.

Hill,M.M., Clark,S.F., Tucker,D., Birnbaum,M.J., James,D.E. and MacCauley,S.L. (1999) A role for protein kinase Bb/Akt2 in insulin-stimulated GLUT4 translocation in adiposytes. *Mol. Cell Biol.* **19**: 7771-7781.

Hirst,J. and Robinson,M.S. (1998) Clathrin and adaptors. *Biochim. Biophys. Acta* **1404**: 173-193.

Holman,G.D. and Cushman,S.W. (1994) Subcellular localization and trafficking of the GLUT4 glucose transporter isoform in insulin-responsive cells. *Bioessays* **16**: 753-759.

Holman,G.D. and Cushman,S.W. (1996) Subcellular trafficking of GLUT4 in insulin target cells. *Sem. Cell Dev. Biol.* **7**: 259-268.

Holman,G.D., Karim,A.R., and Karim,B. (1988) Photolabeling of erythrocyte and adipocyte hexose transporters using a benzophenone derivative of bis(D-mannose). *Biochim. Biophys. Acta* **946**: 75-84.

Holman,G.D., Kozka,I.J., Clark,A.E., Flower,C.J., Saltis,J., Habberfield,A.D., Simpson,I.A., and Cushman,S.W. (1990) Cell surface labeling of glucose transporter isoform GLUT4 by bis- mannose photolabel. Correlation with stimulation of glucose transport in rat adipose cells by insulin and phorbol ester. *J. Biol. Chem.* **265**: 18172-18179.

Holman,G.D., Leggio,L.L., and Cushman,S.W. (1994) Insulin-stimulated GLUT4 glucose transporter recycling. A problem in membrane protein subcellular trafficking through multiple pools. *J. Biol. Chem.* **269**: 17516-17524.

Holman,G.D. and Midgley,P.J.W. (1985) Synthesis of novel bis(D-mannose) compounds. *Carbohydr. Res.* **135**: 337-341.

Holman,G.D., Parkar,B.A., and Midgley,P.J. (1986) Exofacial photoaffinity labelling of the human erythrocyte sugar transporter. *Biochim. Biophys. Acta* **855**: 115-126.

Holman,G.D., Pierce,E.J., and Rees,W.D. (1981) Spatial requirements for insulin-sensitive sugar transport in rat adipocytes. *Biochim. Biophys. Acta* **646**: 382-388.

Holman,G.D. and Sandoval,I.V. (2001) Moving the insulin-regulated glucose transporter GLUT4 into and out of storage. *Trends Cell Biol.* **11**:173-179.

Hopkins,C.R., Gibson,A., Shipman,M., Strickland,D.K. and Trowbridge,I.S. (1994) in migrating fibroblasts, recycling receptors are concentrated in narrow tubules in the pericentriolar area, and then routed to the plasma membrane of the leading lamella. *J. Cell Biol.* **125**: 1265-1274.

Horuk,R., Matthei,S., Olefsky,J.M., Baly,D., Cushman,S.W., and Simpson,I.A. (1986) Biochemical and functional heterogeneity of rat adipose glucose transporters. *J. Biol. Chem.* **261**: 1823-1828.

Hresko,R.C., Kruse,M., Strube,M., and Mueckler,M. (1994) Topology of the GLUT1 glucose transporter deduced from glycosylation scanning mutagenesis. *J. Biol. Chem.* **269**: 20482-20488.

Hu,E., Liang,P., and Spiegelman,B.M. (1996) AdipQ is a novel adipose-specific gene dysregulated in obesity. *J. Biol. Chem.* **271**: 10697-10703.

Hudson,A.W., Fingar,D.C., Seidner,G.A., Griffiths,G., Burke,B., and Birnbaum,M.J. (1993) Targeting of the "insulin-responsive" glucose transporter (GLUT4) to the regulated secretory pathway in PC12 cells . *J. Cell Biol.* **122**: 579-588.

Ibberson,M., Uldry,M., and Thorens,B. (2000) GLUTX1, a novel mammalian glucose transporter expressed in the central nervous system and insulin-sensitive tissues. *J. Biol. Chem.* **275**: 4607-4612.

Inukai,K., Asano,T., Katagiri,H., Anai,M., Funaki,M., Ishihara,H., Tsukuda,K., Kikuchi,M., Yazaki,Y., and Oka,Y. (1994) Replacement of both tryptophan residues at 388 and 412 completely abolished cytochalasin-B photolabeling of the GLUT1 glucose transporter. *Biochem. J.* **302**: 355-361.

Jackson,T. (1998) Transport vesicles : coats of many colours. *Current Biology* **8**: R609-612.

James,D.E., Brown,R., Navarro,J., and Pilch,P.F. (1988) Insulin-regulatable tissues express a unique insulin-sensitive glucose transport protein. *Nature* **333**: 183-185.

James,D.E., Hiken,J., Lawrence,J.C.,Jr. (1989b) Isoproterenol stimulates phosphorylation of the insulin-regulatable glucose transporter in rat adipocytes. *Proc. Natl. Acad. Sci. U.S.A* **86**: 8368-8372.

James,D.E., Lederman,L., Pilch,P.F. (1987) Purification of insulin-dependent exocytic vesicles containing the glucose transporter. *J. Biol. Chem.* **262**: 11817-11824.

James,D.E. and Pilch,P.F. (1988) Fractionation of endocytic vesicles and glucose-transporter-containing vesicles in rat adipocytes. *Biochem. J.* **256**: 725-732.

James,D.E., Strube,M., and Mueckler,M. (1989a) Molecular cloning and characterization of an insulin-regulatable glucose transporter. *Nature* **338**: 83-87.

Janmey,P.A. (1998) The cytoskeleton and cell signaling - component localization and mechanical coupling. *Physiol. Rev.* **78**: 763-781.

Jhun,B.H., Rampal,A.L., Liu,H.Z., Lachaal,M., and Jung,C.Y. (1992) Effects of insulin on steady-state kinetics of GLUT4 subcellular distribution in rat adipocytes- evidence of constitutive GLUT4 recycling. *J. Biol. Chem.* **267**: 17710-17715.

Johnson,K.F., Chan,W., and Kornfield,S. (1990) Cation-dependent mannose 6-phosphate receptor contains two internalization signals in its cytoplasmic domain. *Proc. Natl. Acad. Sci. U.S.A* **87**: 10010-10014.

Johnson,K.F. and Kornfield,S. (1992) The cytoplasmic tail of the mannose 6-phosphate/insulin growth factor-II receptor has two signals for lysosomal enzyme sorting in the Golgi. *J. Cell Biochem.* **119**: 249-257.

Joost,H.G. and Steinfelder,H.J. (1987) Forskolin inhibits insulin-stimulated glucose transport in rat adipose cells by a direct interaction with the glucose transporter. *Mol. Pharmacol.* **31**: 279-283.

Kaestner,K.H., Christy,R.J., McLenithan,J.C., Braiterman,L.T., Cornelius,P., Pekala,P.H., and Lane,M.D. (1989) Sequence, tissue distribution, and differential expression of messenger-RNA for a putative insulin-responsive glucose transporter in mouse 3T3-L1 adipocytes. *Proc. Natl. Acad. Sci. U.S.A* **86**: 3150-3154.

Kanaseki,T. and Kadota,K. (1969) The 'vesicle in a basket'. A morphological study of the coated vesicle isolated from the nerve endings of the guinea pig brain, with special reference to the mechanism of membrane movements. *J. Cell Biol.* **42**: 202-220.

Kandror,K.V. (1999) Insulin regulation of protein traffic in rat adipose cells. *J. Biol. Chem.* **274**: 25210-25217.

Kandror,K.V., Coderre,L., Pushkin,A.V., and Pilch,P.F. (1995) Comparison of glucose-transporter-containing vesicles from rat fat and muscle tissues: evidence for a unique endosomal compartment. *Biochem. J.* **307**: 383-390.

Kandror,K.V. and Pilch,P.F. (1994) gp160, a tissue-specific marker for insulin-activated glucose transport. *Proc. Natl. Acad. Sci. U.S.A* **91**: 8017-8021.

Kandror,K.V. and Pilch,P.F. (1996) Compartmentalization of protein traffic in insulin-sensitive cells. *Am. J. Physiol.* **271**: E1-14.

Kandror,K.V. and Pilch,P.F. (1998) Multiple endosomal recycling pathways in rat adipose cells. *Biochem. J.* **331**: 829-835.

Kao, A.W., Ceresa, B.P., Santeler, S.R. and Pessin, J.E. (1998) Expression of a dominant interfering dynamin mutant in 3T3-L1 adipocytes inhibits GLUT4 endocytosis without affecting insulin signalling. *J. Biol. Chem.* **273**: 25450-25457.

Kato,Y., Nakamura,K., and Hashimoto,T. (1983) New ion exchanger for the separation of proteins and nucleic acids. *J. Chromatogr.* **266**: 385-394.

Kayano,T., Burant,C.F., Fukumoto,H., Gould,G.W., Fan,Y.S., Eddy,R.L., Byers,M.G., Shows,T.B., Seino,S., and Bell,G.I. (1990) Human facilitative glucose transporters. Isolation, functional characterization, and gene localization of cDNAs encoding an isoform (GLUT5) expressed in small intestine, kidney, muscle, and adipose tissue and an unusual glucose transporter pseudogene-like sequence (GLUT6). *J. Biol. Chem.* **265**: 13276-13282.

Kessler,A., Tomas,E., Immler,D., Meyer,H.E., Zorzano,A., and Eckel,J. (2000) Rab11 is associated with GLUT4-containing vesicles and redistributes in response to insulin. *Diabetologia* **43**: 1518-1527.

Khayat,ZA, Tong,P., Yaworsky,K., Bloch,R.J. and Klip,A. (2000) Insulin-induced actin filament remodeling colocalizes actin with phosphatidylinositol 3-kinase and GLUT4 in L6 myotubes. *J. Cell Sci.* **113**:279-90

King,H. and Rewers,M. (1991) Diabetes in adults is now a third world problem. *Bulletin World Health Organisation* **69**: 643-648.

Kirchhausen,T. (1999) Adaptors for clathrin-mediated traffic. *Annu. Rev. Cell Dev. Biol.* **15**: 705-732.

Kirchhausen,T., Bonifacino,J.S. and Reizman,H. (1997) Linking cargo to vesicle formation: Receptor tail interactions with coat proteins. *Curr. Opin. Cell Biol.* **9**: 488-495.

Kitagawa,K., Rosen,B.S., Spiegelman,B.M., Lienhard,G.E., and Tanner,L.I. (1989) Insulin stimulates the acute release of adipsin from 3T3-L1 adipocytes. *Biochim. Biophys. Acta* **1014**: 83-89.

Kleinchin VA and Martin TF. (2000) Priming in exocytosis: attaining fusion competence after vesicle docking *Biochimie* **82**: 39-407.

Kono,T., Suzuki,K., Dansey,L.E., Robinson,F.W., and Blevins,T.L. (1981) Energy-dependent and protein synthesis-independent recycling of the insulin sensitive glucose transport mechanism in fat cells. *J. Biol. Chem.* **256**: 6400-6407.

Kotani,K., Carozzi,A.J., Sakaue,H., Hara,K., Robinson,L.J., Clark,S.F., Yonezawa,K. James,D.E. and Kasuga,M. (1995) Requirement for phosphoinositide 3-kinase in insulin-stimultaed GLUT4 translocation in 3T3-L1 adipocytes. *Biochem. Biophys. Res. Commun.* **209**: 343-348.

Kotani,K., Ogawa,w., Matsumoto,M., Kitamura,T., Sakaue,H., Hino,Y., Miyake,K., Sano,w., Akimoto,K., Ohno,S. and Kasuga,M. (1998) Requirement of atypical protein kinase cλ for insulin-stimulation of glucose uptake but not for akt activation in 3T3-L1 adipocytes. *Mol. Cell Biol.* **18**: 6971-6982.

Kotani,K., Yonezawa,K., Hara,K., Ueda,H., Kitamura,Y., Sakaue,H., Ando,A., Chavanieu,A., Calas,B., Grigorescu,F *et al.*, (1994) Involvement of phosphoinositide 3-kinase in insulin or IGF-1-induced membrane ruffling. *EMBO J.* **13**: 2313-2321.

Koumanov,F., Yang,J., Jones,A.E., Hatanaka,Y., and Holman,G.D. (1998) Cell-surface biotinylation of GLUT4 using bis-mannose photolabels. *Biochem. J.* **330**: 1209-1215.

Krook,A., Whitehead,J.P., Dobson,S.P., Griffiths,M.R., Ouwens,M., Baker,C., Hayward,A.C., Sen,S.K., Maasen,J.A., Siddle,K., Tavare,J.M. and O'Rahilly. (1997) Two naturally occurring tyrosine kinase domain mutants provide evidence that phosphoinositide 3-kinase activation alone is not sufficient for the mediation of insulin's metabolic and mitogenic effects. *J. Biol. Chem.* **272**: 30208-30214.

Kuge,O., Dascher,C., Orci,L., Rowe,T., Amherdt,M., Plutner,H., Ravazzola,G., Tanigawa,G., Rothman,J.E. and Balch,W.E. (1994) sar1 promotes vesicle budding from the endoplasmic reticulum but not Golgi compartments. *J. Cell Biol.* 125: 51-65.

Kupriyanova,T.A. and Kandror,K.V. (2000) Cellugyrin is a marker for a distinct population of intracellular GLUT4-containing vesicles. *J. Biol. Chem.* **275**: 36263-36268.

Laemmli,U.K. (1970) Cleavage of structural proteins during the assembly of the head of bacteriphage T4. *Nature* **227**: 680-685.

Laurie,S.M., Cain,C.C., Lienhard,G.E., and Castle,J.D. (1993) The glucose transporter GLUT4 and secretory carrier membrane proteins (SCAMPs) colocalize in rat adipocytes and partially segregate during insulin stimulation. *J. Biol. Chem.* **268**: 19110-19117.

Lavan,B.E., Fantin,V.R., Chang,E.T., Lane,W.S., Keller,S.R. and Lienhard,G.E. (1997b) A novel 160-kDa phosphotyrosine protein in insulin-treated embryonic kidney cells is a new member of the insulin receptor substrate family. *J. Biol. Chem.* **272**: 21403-21407.

Lavan,B.E., Lane,W.S. and Lienhard,G.E. (1997a) The 60-kDa phosphotyrosine protein in insulin-treated adipocytes is a new member of the insulin receptor substrate family. *J. Biol. Chem.* **272**: 11439-11443.

Lawrence,J.C., Jr., Hiken,J.F., and James,D.E. (1990) Stimulation of glucose transport and glucose transporter phosphorylation by okadaic acid in rat adipocytes. *J. Biol. Chem.* **265**: 19768-19776.

Le Borgne,R. and Hoflack,B. (1997) Mannose 6-phosphate receptors regulate the formation of clathrin-coated vesicles in the TGN. *J. Cell Biol.* **137**: 335-345.

Le Borgne,R. and Hoflack,B. (1998) Mechanisms of protein sorting and coat assembly: insights from the clathrin-coated vesicle pathway. *Curr. Opin. Cell Biol* **10**: 499-503.

Lee,W., Ryu,J., Hah,J., Tsujita,T., and Jung,C.Y. (2000) Association of carboxyl esterase with facilitative glucose transporter isoform 4 (GLUT4) intracellular compartments in rat adipocytes and its possible role in insulin-induced GLUT4 recruitment. *J. Biol. Chem.* **275**: 10041-10046.

Lee,W., Ryu,J., Souto,R.P., Pilch,P.F., and Jung,C.Y. (1999) Separation and partial characterization of three distinct intracellular GLUT4 compartments in rat adipocytes. Subcellular fractionation without homogenization. *J. Biol. Chem.* **274**: 37755-37762.

Lin,B.Z., Pilch,P.F., and Kandror,K.V. (1997) Sortilin is a major protein component of GLUT4-containing vesicles. *J. Biol. Chem.* **272**: 24145-24147.

Livingstone,C., James,D.E., Rice,J.E., Hanpeter,D., and Gould,G.W. (1996) Compartment ablation analysis of the insulin-responsive glucose transporter (GLUT4) in 3T3-L1 adipocytes. *Biochem. J.* **315**: 487-495.

Lowe,A.G. and Walmsley,A.R. (1986) The kinetics of glucose transport in human red-blood cells. *Biochim. Biophys. Acta* **857**: 146-154.

Luzio,J.P., Brake,B., Banting,G., Howell,K.E., Braghetta,P., and Stanley,K.K. (1990) Identification, sequencing and expression of an integral membrane protein of the trans-Golgi network (TGN38). *Biochem. J.* **270**: 97-102.

Malide,D., Dwyer,N.K., Blanchette-Mackie,E.J., and Cushman,S.W. (1997a) Immunocytochemical evidence that GLUT4 resides in a specialised translocation post-endosomal VAMP2-positive compartment in rat adipose cells in the absence of insulin. *J. Histochem. Cytochem.* **45**: 1083-1096.

Malide,D., Ramm,G., Cushman,S.W., and Slot,J.W. (2000) Immunoelectron microscopic evidence that GLUT4 translocation explains the stimulation of glucose transport in isolated rat white adipose cells. *J. Cell Sci.* **113**: 4203-4210.

Malide,D., St Denis,J.F., Keller,S.R., and Cushman,S.W. (1997b) Vp165 and GLUT4 share similar vesicle pools along their trafficking pathways in rat adipose cells. *FEBS Lett.* **409**: 461-468.

Malide,D., Tosh,D., Clark,A.E., Cushman,S.W., and Holman,G.D. (1996) Altered GLUT4 subcellular trafficking in primary adipose cell cultures: immunocytochemical evidence. *Mol. Biol. Cell* **7 (suppl.)** A2636

Marsh,B.J., Martin,S., Melvin,D.R., Martin,L.B., Alm,R.A., Gould,G.W., and James,D.E. (1998) Mutational analysis of the carboxy-terminal phosphorylation site of GLUT4 in 3T3-L1 adipocytes. *Am. J. Physiol.* **275**: E412-E422.

Marsh,M. and McMahon,H.T. (1999) The structural era of endocytosis. *Science* **285**: 215-220.

Marshall,B.A., Murata,H., Hresko,R.C., and Mueckler,M. (1993) Domains that confer intracellular sequestration of the GLUT4 glucose transporter in Xenopus oocytes. *J. Biol. Chem.* **268**: 26193-26199.

Martin,S., Haruta,T., Morris,A.J., KlippelA., Williams, L.T. and Olefsky,J.M. (1996b) Activated phosphotidylinositol 3-kinase is sufficient to mediate actin rearrangement and GLUT4 translocation in 3T3-L1 adipocytes. *J. Biol. Chem.* **271**: 17605-17608.

Martin,S., Millar,C.A., Lyttle,C.T., Meerloo,T., Marsh,B.J., Gould,G.W., and James,D.E. (2000) Effects of insulin on intracellular GLUT4 vesicles in adipocytes: evidence for a secretory mode of regulation. *J. Cell Sci.* **113**: 3427-3438.

Martin,S., Reaves,B., Banting,G. and Gould,G.W. (1994) Analysis of the co-localization of the insulin-responsive glucose transporter (GLUT4) and the *trans*-Golgi network marker TGN38 within 3T3-L1 adipocytes. *Biochem. J.* **300**: 743-749.

Martin,S., Rice,J.E., Gould,G.W., Keller,S.R., Slot,J.W., and James,D.E. (1997) The glucose transporter GLUT4 and the aminopeptidase vp165 colocalise in tubulo-vesicular elements in adipocytes and cardiomyocytes. *J. Cell Sci.* **110**: 2281-2291.

Martin,S., Tellam,J., Livingstone,C., Slot,J.W., Gould,G.W., and James,D.E. (1996a) The glucose transporter (GLUT4) and vesicle-associated membrane protein-2 (VAMP-2) are segregated from recycling endosomes in insulin- sensitive cells. *J. Cell Biol.* **134**: 625-635.

Martinez-Acra,S., Lalioti,V.S., and Sandoval,I.V. (2000) Intracellular targeting and retention of the glucose transporter GLUT4 by the perinuclear storage compartment involves distinct carboxyl-tail motifs. *J. Cell Sci.* **113** 1705-1715.

Martinez-Menarguez,J.A., Geuze,H.J. and Ballesta,J. (1996) Identification of two types of beta-COP vesicles in the Golgi complex of rat spermatids. *Eur. J Cell Biol.* **71**:137-43.

Mauxion,F., Le Borgne,R., Munier-Lehmann,H. and Hoflack,B. (1996) A casein kinase II phosphorylation site in the cytoplasmic domain of the cation-dependent mannose-6-phosphate receptor determines the high affinity interaction of the AP1 Golgi assembly proteins with membranes. *J. Biol. Chem.* **271**: 2171-2178.

Mayer,A. and Whickner,W. (1997) Docking of yeast vacuoles is catalysed by the *Ras*-like GTPase Ypt7 after symmetric priming by Sec 18 (NSF). *J. Cell Biol.* **136**: 307-317.

Mayor,S., Presley,J.F. and Maxfield,F.R. (1993) Sorting of membrane components from endosomes and subsequent recycling to the cell surface occurs by a bulk flow process. *J. Cell Biol.* **121**: 1257-1269.

McBride,H.M., Rybin,V., Murphy,C., Giner,A., Teasdale,R. and Zerial,M. (1999) Oligomeric complexes link Rab5 effectors with NSF and drive membrane fusion via interactions between EEA1 and syntaxin 13. *Cell* **98**: 377-386.

McGraw,T.E., Dunn,K.W. and Maxfield,F.R. (1993) Isolation of a temperature-sensitive variant Chinese hamster ovary cell line with a morphologically altered endocytic recycling compartment *J. Cell Physiol.* **155**: 579-594.

McMahon,H.T., Missler,M., Li,C. and Sudhof,T.C. (1985) Complexins: cytosolic proteins that regulate SNAP receptor function. *Cell* **83**: 111-119.

McNew.,J.A., Parlati,,F., Fukuda,R., Johnston,R.J., Paz,K., Paumet,F., Sollner,T.H. and Rothman,J.E. (2000) Compartmental specificity of cellular membrane fusion encoded in SNARE proteins. *Nature* **407**: 153-159.

Mellman,I. (1996) Endocytosis and molecular sorting. *Annu. Rev. Cell Dev. Biol.* **12**: 575-625.

Mellman,I., Fuchs,R. and Helenius,A. (1986) Acidification of the endocytic and exocytic pathways. *Annu. Rev. Biochem.* **55**: 663-700.

Melvin,D.R., Marsh,B.J., Walmsley,A.R., James,D.E., and Gould,G.W. (1999) Analysis of amino and carboxy terminal GLUT4 targeting motifs in 3T3-L1 adipocytes using an endosomal ablation technique. *Biochemistry* **38**: 1456-1462.

Midgley,P.J., Parkar,B.A., and Holman,G.D. (1985a) A new class of sugar analogues for use in the investigation of sugar transport. *Biochim. Biophys. Acta* **812**: 33-41.

Midgley,P.J., Parkar,B.A., Holman,G.D., Thieme,R., and Lehmann,J. (1985b) Transport-properties of photolabile sugar analogs. *Biochim. Biophys. Acta* **812**: 27-32.

Millar,C.A., Campbell,L.C., Cope,D.L., Melvin,D.R., Powell,K.A., and Gould,G.W. (1997) Compartment-ablation studies of GLUT4 distribution in adipocytes: evidence for multiple intracellular pools. *Biochem. Soc. Trans.***25**: 974-977.

Millar,C.A., Meerloo,T., Martin,S., Hickson,G.R.X., Shimwell,N.J., Wakelam,M.J.O., James,D.E., and Gould,G.W. (2000) Adipsin and the glucose transporter GLUT4 traffic to the cell surface via independent pathways in adipocytes. *Traffic* **1**: 141-151.

Millar,C.A., Powell,K.A., Hickson,G.R., Bader,M.F. and Gould,G.W. (1999a) Evidence for a role for ADP-ribosylation factor 6 in insulin-stimulated glucose transporter-4 (GLUT4) trafficking in 3T3-L1 adipocytes. *J. Biol. Chem.* **274**: 17619-17625.

Millar,C.A., Shewan,A., Hickson,G.R., James,D.E., and Gould,G.W. (1999b) Differential regulation of secretory compartments containing the insulin-responsive glucose transporter 4 in 3T3-L1 adipocytes. *Mol. Biol. Cell* **10**: 3675-3688.

Mills,I.G., Jones,A.T. and Clague,M.J. (1998) Involvement of the endosomal autoantigen EEA1 in homotypic fusion of early endosomes. *Curr. Biol.* **8**: 881-884.

Min,J., Okada,S., Kanzaki,M., Elmendorf,J.S., Coker,K.J., Ceresa,B.P., Syu,L.J., Noda,Y., Saltiel,A.R., and Pessin,J.E. (1999) Synip: a novel insulin-regulated syntaxin 4-binding protein mediating GLUT4 translocation in adipocytes. *Mol. Cell* **3**: 751-760.

Mohrmann,K. and van der Sluijs,P. (1999) Regulation of membrane transport through the endocytic pathway by rabGTPases. *Mol. Membr. Biol.* **16**: 81-87.

Molloy,S.S., Thomas,L., VanSlyke,J.K., Stenberg,P.E., and Thomas,G. (1994) Intracellular trafficking and activation of the furin proprotein convertase: localization to the TGN and recycling from the cell surface. *EMBO J.* **13**: 18-33.

Mora,S., Monden,I., Zorzano,A. and Keller,A. (1997) Heterologous expression of rab4 reduces glucose transport and GLUT4 abundance at the cell surface in oocytes. *Biochem J.* **324**:455-9.

Morris,N.J., Ross,S.A., Lane,W.S., Moestrup,S.K., Petersen,C.M., Keller,S.R., and Lienhard,G.E. (1998) Sortilin is the major 110-kDa protein in GLUT4 vesicles from adipocytes. *J. Biol. Chem.* **273**: 3582-3587.

Moyers,J.S., Bilan,P.J., Reynet,C. and Kahn, C.R. (1996) Overexpression of Rad inhibits glucose uptake in cultured muscle and fat cells. *J. Biol. Chem.* **271**: 23111-23116.

Mu,F.T., Callaghan,J.M., Steele-Mortimer,O., Stenmark,H., Parton,R.G., Campbell,P.L., McCluskey,J., Yeo,J.P., Tock,E.P. and Toh,B.H. (1995) EEA1, an early endosome-associated protein. EEA1 is a conserved α-helical peripheral membrane protein flanked by cysteine 'fingers' and contains a calmodulin-binding IQ motif. *J. Biol. Chem.* **270**: 13503-13511.

Mueckler,M., Caruso,C., Baldwin,S.A., Panico,M., Blench,I., Morris,H.R., Allard,W.J., Lienhard,G.E., and Lodish,H.F. (1985) Sequence and structure of a human glucose transporter. *Science* **229**: 941-945.

Mueckler,M. and Makepeace,C. (1997) Identification of an amino acid residue that lies between the exofacial vestibule and exofacial substrate-binding site of the GLUT1 sugar permeation pathway. *J. Biol. Chem.* **272**: 30141-30146.

Muraoka,A., Hashiramoto,M., Clark,A.E., Edwards,L.C., Sakura,H., Kadowaki,M., Holman,G.D., and Kasuga,M. (1995) Analysis of the structural features of the C-terminus of GLUT1 that are required for transport catalytic activity. *Biochem. J.* **311**: 11578-11583.

Newman,L.S., McKeever,M.O., Hirotaka,O.J. and Darnell,R.B. (1995) β-NAP, a cerebellar degeneration antigen, is a neuron-specific vesicle coat protein. *Cell* **82**: 773-783

Novick,P., Ferro,S. and Schekman,R. (1981) Order of events in the yeast secretory pathway. *Cell.* **25**:461-9.

Oatey,P.B., Van Weering,D.H., Dobson,S.P., Gould,G.W. and Tavare,J.M. (1997) GLUT4 vesicle dynamics in living 3T3 L1 adipocytes visualised with green-fluorescent protein. *Biochem. J.* **327**: 637-642.

Oka,Y., Asano,T., Shibasaki,Y., Kasuga,M., Kanazawa,Y., and Takaku,F. (1988) Studies with antipeptide antibody suggest the presence of at least two types of glucose transporter in rat brain and adipocyte. *J. Biol. Chem.* **263**: 13432-13439.

Omata,W., Shibata,H., Li,L., Takata,K., and Kojima,I. (2000) Actin filaments play a critical role in insulin-induced exocytotic recruitment but not in endocytosis of GLUT4 in isolated rat adipocytes. *Biochem. J.* **346**: 321-328.

Omata,W., Shibata,H., Suzuki,Y., Tanaka,S., Suzuki,T., Takata,K. and Kojima, I. (1997) Subcellular distribution of GLUT4 in chinese hamster ovary cells overexpressing mutant dynamin: Evidence that dynamin is a regulatory GTPase in GLUT4 endocytosis. *Biochem. Biophys. Res. Commun.* **241**: 401-406.

Ooi,C.E., Dell'Angelica,E.C. and Bonifacino, J.S. (1998) ADP-ribosylation factor 1 (ARF1) regulates recruitment of the AP-3 adaptor complex to membranes. *J. Cell Biol.* **142**: 391-402.

Oprins,A., Duden,R., Kreis,T.E., Geuze,H.J. and Slot,J.W. (1993) β-COP localises mainly to the cis-Golgi side in exocrine pancreas. *J. Cell Biol.* **121**: 49-59.

Oyler,G.A., Higgins,G.A., Hart,R.A., Battenberg,E., Billingsley,M., Bloom,F.E. and Wilson,M.C. (1989)The identification of a novel synaptosomal-associated protein SNAP-25, differentially expressed by neuronal subpopulations *J. Cell Biol.* **109**: 3039-3052.

Palacios,S., Lalioti,V.V., Martinez-Acra,S., Chattopadhyay,S., and Sandoval,I.V. (2001) Recycling of the insulin-sensitive glucose transporter GLUT4: Access of surface internalised GLUT4 molecules to the perinuclear storage compartment is mediated by the Phe5GlnGlnIle8 motif. *J. Biol. Chem.* **276**: 3371-3383.

Palfreyman,R.W., Clark,A.E., Denton,R.M., Holman,G.D., and Kozka,I.J. (1992) Kinetic resolution of the separate GLUT1 and GLUT4 glucose transport activities in 3T3-L1 cells. *Biochem. J.* **284**: 275-282.

Parkar,B.A., Midgley,P.J.W., and Holman,G.D. (1985) The effect of hydrophobic bis(d-mannose) derivatives on the rat adipocyte sugar-transport system. *Biochem. Soc. Trans.* **13**: 728-729.

Patki,V., Virbasius,J., Lane,W.S., Toh,B.H., Shpetner,H.S., and Corvera,S. (1997) Identification of an early endosomal protein regulated by phosphatidylinositol 3-kinase. *Proc. Natl. Acad. Sci. U.S.A* **94**: 7326-7330.

Pearse,B.M. (1975) Coated vesicles from pig brain: purification and biochemical characterisation. *J. Mol. Biol.* **97**: 93-98.

Pearse,B.M. (1985) Assembly of the mannose-6-phosphate receptor into reconstituted clathrin coats. *EMBO J.* 4:2457-2460.

Pearse,B.M. (1988) Receptors compete for adaptors found in plasma membrane coated pits. *EMBO. J.* **7**: 3331-3336.

Pearse,B.M., Robinson,M.S. (1990) Clathrin, adaptors, and sorting. *Annu. Rev. Cell Biol.* **6**: 151-171.

Pertoft,H., Laurent,T.C., Laas,T., and Kagedal,L. (1978) Density gradients prepared from collodial silica particles coated by polyvinyl pyrrolidone (Percoll). *Anal. Biochem.* **88**: 271-282.

Peters,C. and Mayer,A. (1988) Ca2+/calmodulin signals the completion of docking and triggers a rate step of vacuole fusion. *Nature* **396**: 575-580.

Petersen,C.M., Nielsen,M.S., Nykjaer,A., Jacobsen,L., Tommerup,N., Rasmussen,H.H., Roigaard,H., Gliemann,J., Madsen,P., and Moestrup,S.K. (1997) Molecular identification of a novel candidate sorting receptor purified from human brain by receptor-associated protein affinity chromatography. *J. Biol. Chem.* **272**: 3599-3605.

Pevsner,J., Hsu,S.C. and Schellee,R.H. (1994) n-Sec1: a neuronal-specific syntaxin-binding protein *Proc. Natl. Acad. Sci. U.S.A* **91**: 1445-1449.

Pfeffer,S.R. (1999) Transport-vesicle targeting:tethers before SNAREs. *Nature Cell Biol* **1**: 17-22.

Pierce Chemical Company (1997) Instructions – sulfholink coupling gel [20401, 20402] *http:wwwpiercenet.com* **Printed 10, 2000.**

Piper,R.C., Hess,L.J., and James,D.E. (1991) Differential sorting of two glucose transporters expressed in insulin- sensitive cells. *Am. J. Physiol* **260**: C570-C580.

Piper,R.C., James,D.E., Slot,J.W., Puri,C., and Lawrence,J.C., Jr. (1993) GLUT4 phosphorylation and inhibition of glucose transport by dibutyryl cAMP. *J. Biol. Chem.* **268**: 16557-16563.

Piper,R.C., Tai,C., Slot,J.W., Hahn,C.S., Rice,C.M., Huang,H., and James,D.E. (1992) The efficient intracellular sequestration of the insulin-regulatable glucose transporter (GLUT4) is conferred by the NH2 terminus. *J. Cell Biol.* **117**: 729-743.

Ploug,T., van Deurs,B., Ai,H., Cushman,S.W., and Ralston,E. (1998) Analysis of GLUT4 distribution in whole skeletal muscle fibers: identification of distinct storage compartments that are recruited by insulin and muscle contractions. *J. Cell Biol.* **142**: 1429-1446.

Poirier,M.A., Xiao,W., Macosko,J.C., Chan,C. and Shin,Y.K. (1998) The synaptic SNARE complex is a parallel four-stranded helical bundle. *Nat Struct Biol.* **5**: 765-769.

Powell,K.A., Campbell,L.C., Tavare,J.M., Leader,D.P., Wakefield,J.A., and Gould,G.W. (1999) Trafficking of Glut4-green fluorescent protein chimaeras in 3T3-L1 adipocytes suggests distinct internalization mechanisms regulating cell surface GLUT4 levels. *Biochem. J.* **344**: 535-543.

Presley,J.F., Mayor,S., Dunn,K.W., Johnson,L.S., McGraw,T.E. and Maxfield,F.R. (1993) The End2 mutation in CHO cells slows the exit of transferrin receptors from the recycling compartment but bulk membrane recycling is unaffected. *J. Cell Biol.* **122**: 1231-1241.

Pretlow,T.G., Boone,C.W., Schrager,R.I., and Weiss,G.H. (1969) Rate zonal centrifugation in a ficoll gradient. *Anal. Biochem.* **29**: 230-237.

Pryer,N.K., Wuestehube,L.J. and Schekman,R. (1992) Vesicle-mediated protein sorting. *Annu. Rev. Biochem.* **61**: 471-516.

Ralston,E. and Ploug,T. (1996) GLUT4 in cultured skeletal myotubes is segregated from the transferring receptor and stored in vesicles associated with the TGN. *J. Cell. Sci.* **109**: 2967-2978.

Ramm,G., Slot,J.W., James,D.E., and Stoorvogel,W. (2000) Insulin recruits GLUT4 from specialised VAMP2-carrying vesicles as well as from the dynamic endosomal/trans-Golgi network in rat adipocytes. *Mol. Biol. Cell.* **11**: 4079-4091.

Rapoport,I., Chen,Y.C., Cupers,P., Shoelson,S.E. and Kirchhausen,T. (1998) Dileucine-based sorting signals bind to the β chain of AP-1 at a site distinct and regulated differently from the tyrosine-based motif binding site. *EMBO J.* **17**: 2148-2155.

Rea,S., Martin,L.B., McIntosh,S., Macaulay,S.L., Ramsdale,T., Baldini,G., and James,D.E. (1998) Syndet, an adipocyte target SNARE involved in the insulin-induced translocation of GLUT4 to the cell surface. *J. Biol. Chem.* **273**: 18784-18792.

Reaves,B., Wilde,A., and Banting,G. (1992) Identification, molecular characterisation and immunolocalisation of an isoform of the trans-Golgi netwrok (TGN)-specific integral membrane protein TGN38. *Biochem. J.* **283**: 313-316.

Rees,W.D. and Holman,G.D. (1981) Hydrogen bonding requirements for the insulin-sensitive sugar transport system of rat adipocytes. *Biochim. Biophys. Acta* **646**: 251-260.

Ribon,V., Printen,J.A., Hoffman,N.G., Kay,B.K. and Salteil,A.R. (1998) A novel multifunctional c-Cbl binding protein in insulin receptor signalling in 3T3-L1 adipocytes. *Mol. Cell Biol.* **18**: 872-879.

Rickwood,D (1983) Iodinated density gradient media-A practical approach. 10-21.

Rickwood,D., Hell,A., and Birnie,G.D. (1973) Iospycynic centrifugation of sheared chromatin in metrizamide gradients. *FEBS Lett.* **33**: 221-224.

Robinson,L.J., Pang,S., Harris,D.S., Heuser,J., and James,D.E. (1992) Translocation of the glucose transporter (GLUT4) to the cell surface in permeabilised 3T3-L1 adipocytes: effects of ATP insulin, and GTP gamma S and localization of GLUT4 to clathrin lattices. *J. Cell Biol.* **117**: 1181-1196.

Robinson,M.S. and Bonifacino,J.S. (2001) Adaptor-related proteins. *Curr. Opin. Cell Biol.* **13**: 444-453.

Rodbell,M. (1967) Metabolism of isolated fat cells: preparation of ghosts and their properties; adenyl cyclase and other enzymes. *J. Biol. Chem.* **242**: 5744-5750.

Rodionov,D.G. and Bakke,O. (1998) Medium chains of adaptor complexes recognise leucine-based sorting signals from the invariant chain. *J. Biol. Chem.* **273**: 6005-6008.

Ross,S.A., Keller,S.R., and Lienhard,G.E. (1998) Increased intracellular sequestration of the insulin-regulated aminopeptidase upon differentiation of 3T3-L1 cells. *Biochem. J.* **330**: 1003-1008.

Ross,S.A., Scott,H.M., Morris,N.J., Leung,W.Y., Mao,F., Lienhard,G.E., and Keller,S.R. (1996) Characterization of the insulin-regulated membrane aminopeptidase in 3T3-L1 adipocytes. *J. Biol. Chem.* **271**: 3328-3332.

Roth,M.G. (1999) Snapshots of ARF1: Implications for mechanisms of activation and inactivation. *Cell* **97**:149-152.

Roth,T.F. and Porter,K.R. (1964) Yolk protein uptake in the oocyte of the mosquito *Aedes aegypti. J. Cell Biol.* **20**: 313-332.

Rothman,J.E. (1994) Mechanisms of intracellular protein transport. *Nature* **372**: 55-63.

Rothman, J.E. and Wieland,F.T. (1996) Protein sorting by transport vesicles. *Science* **272**: 227-234.

Rozelle,A.L., Machesky,L.M., Yamamotot,M., Driessens,M.H., Insall,R.H., Roth,M.G., Luby-Phelps,K., Marriott,G., Hall,A. and Yin,H.L. (2000) Phosphatidylinositol 4,5-bisphosphate induces actin-based movement of raft-enriched vesicles through WASP-Arp2/3. *Curr. Biol.* **10** : 311-320.

Saad,M.J.A., Folli,F., Kahn,J.A. and Kahn,C.R. (1993) Modulation of the insulin receptor, insulin receptor substrate-1, and phosphatidylinositol 3-kinase in liver and muscle of dexamethasone-treated rats. *J. Clin. Invest.* **92**: 2065-2072.

Sandoval,I.V., Martinez-Acra,S., Valdueza,J., Palacios,S., and Holman,G.D. (2000) Distinct reading of different structural determinants modulates the dileucine-mediated transport steps of the lysosomal membrane protein LIMPII and the insulin-sensitive glucose transporter GLUT4. *J. Biol. Chem.* **275**: 39874-39875.

Saravolac,EG and Holman,GD (1997) Glucose transport: probing the structure/function relationship in Facilitative Glucose Transporters. Gould, G.W. ed., RG Landes and Company, Georgetown, Texas .(1); 39-61.

Satoh,S., Nishimura,H., Clark,A.E., Kozka,I.J., Vannucci,S.J., Simpson,I.A., Quon,M.J., Cushman,S.W., and Holman,G.D. (1993) Use of bismannose photolabel to elucidate insulin-regulated GLUT4 subcellular trafficking kinetics in rat adipose cells. Evidence that exocytosis is a critical site of hormone action. *J. Biol. Chem.* **268**: 1782-17829.

Scheggenburger,R. and Neher,E. (2000) Intracellular calcium dependence of transmitter release rates at a fast central synapse. *Nature* **406**: 889-893.

Schmid,S.L. (1997) Clathrin-coated vesicle formation and protein sorting: An integrated process. *Annu. Rev. Biochem.* **66**: 511-548.

Schmidt,A., Hannah,M.J. and Huttner,W.B. (1997) Synaptic-like microvessels of neuroendocrine cells originate from a novel compartment that is continuous with the plasma membrane and devoid of transferrin receptor. *J. Cell Biol.* **137**: 445-458.

Schurmann,A., Doege,H., Ohnimus,H., Monser,V., Buchs,A., and Joost,H.G. (1997) Role of conserved arginine and glutamate residues on the cytosolic surface of glucose transporters for transporter function. *Biochemistry* **36**: 12897-12902.

Schurmann,A., Keller,K., Monden,I., Brown,F.M., Wandel,S., Shanahan,M.F., and Joost,H.G. (1993) Glucose transport activity and photolabelling with 3-[125I]ido-4-azidopenethylamido-7-O-succinyldeactyl-forskolin (IAPS)-forskolin of two mutants at tryptophan-388 and -412 of the glucose transporter GLUT1: dissociation of the binding domains of forskolin and glucose. *Biochem. J.* **290**: 497-501.

Seatter,M.J., De la Rue,S.A., Porter,L.M., and Gould,G.W. (1998) QLS motif in transmembrane helix VII of the glucose transporter family interacts with the C-1 position of D-glucose and is involved in substrate selection at the exofacial binding site. *Biochemistry* **37**: 1322-1326.

Seatter,M.J. and Gould,G.W. (1999) The mammalian facilitative glucose transporter (GLUT) family. *Pharm. Biotechnol.* **12**: 21-28.

Shanahan,M.F. (1982) Cytochalasin B. A natural photoaffinity ligand for labelling the human erythrocyte glucose transporter. *J. Biol. Chem.* **257**: 729-7293.

Shapiro,J., Sacky,N., Lee,J., Bosshart,H., Angeletti.R.H., and Bonifacio,J.S. (1997) Localisation of endogenous furin in cultured cell lines. *J. Histochem. Cytochem.* **45**: 3-12.

Sheff,D.R., Daro,E.A., Hull,M., and Mellman,I. (1999) The receptor recycling pathway contains two distinct populations of early endosomes with different sorting functions. *J. Cell Biol.* **145**: 123-129.

Shepherd,P.R., Withers,D.J. and Siddle,K. (1998) Phosphoinositide 3-kinase: the key switch mechanism in insulin signalling. *Biochem. J.* **333**: 471-490.

Shewan,A.M., Marsh,B.J., Melvin,D.R., Martin,S., Gould,G.W., and James,D.E. (2000) The cytosolic C-terminus of the glucose transporter GLUT4 contains an acidic cluster endosomal targeting motif distal to thGe dileucine signal. *Biochem. J.* **350**: 99-107.

Shi,G., Faundez,V., Roos,J., Dell'Angelica,E.C. and Kelly, R.B. (1998) Neuroendocrine synaptic vesicles are formed in vitro by both clathrin-dependent and clathrin-independent pathways. *J. Cell Biol.* **143**: 947-955.

Shibata,H., Omata,W. and Kojima,I. (1997) Insulin stimulates guanine nucleotide exchange on Rab4 via a wortmannin-sensitive signalling pathway in rat adipocytes. *J. Biol. Chem.* **272**: 14542-14546.

Shibata,H., Omata,W., Suzuki,Y., Tanaka,S., and Kojima,I. (1996) A synthetic peptide corresponding to the Rab4 hypervariable carboxyl- terminal domain inhibits insulin action on glucose transport in rat adipocytes. *J. Biol. Chem.* **271**: 9704-9709.

Shibata,H., Suzuki,Y., Omata,W., Tanaka,S. and Kojima,I. (1995) Dissection of GLUT4 recycling pathway into exocytosis and endocytosis in rat adipocytes. Evidence that GTP-binding proteins are involved in both processes. *J. Biol. Chem.* **270**: 11489-11495.

Shpetner,H.S. and Vallee,R.B. (1989) Identification of dynamin a novel mechanochemical enzyme that mediates interactions between microtubules. *Cell* **59**: 421-432.

Simpson,F., Bright,N.A., Newman,L.S., Darnell,R.B. and Robinson,M.S. (1996) A novel adaptor-related protein complex. *J. Cell Biol.* **133**: 749-760.

Simpson,I.A. and Cushman,S.W. (1986) Mechanism of insulins stimulatory action on glucose-transport in the rat adipose cell. *Biochemical Actions of Hormones* **13**: 10-31.

Simpson,I.A., Yver,D.R., and Hissin,P.J. (1983) Insulin-stimulated translocation of glucose transporters in the isolated rat adipose cells. Characterization of subcellular fractions. *Biochim. Biophys. Acta* **763**: 393-407.

Skehel,P.A., Armitage,B.A., Bartsch,D., Hu,Y., Kaang,B.K., Siegelbaum,S.A., Kandel,E.R. and Martin,K.C. (1995) Proteins functioning in synaptic transmission at the sensory to motor synapse of *Aplysia*. *Neuropharmacology.* **34**:1379-85.

Sleeman,M.W., Donegan,N.P., Heller-Harrison,R., Lane,W.S., and Czech,M.P. (1998) Association of acyl-CoA synthetase-1 with GLUT4-containing vesicles. *J. Biol. Chem.* **273**: 3132-3135.

Slot,J.W., Garruti,G., Martin,S., Oorschot,V., Posthuma,G., Kraegen,E.W., Laybutt,R., Thibault,G., and James,D.E. (1997) Glucose transporter (GLUT4) is targeted to secretory granules in rat atrial cardiomyocytes. *J. Cell Biol.* **137**: 1243-1254.

Slot,J.W., Geuze,H.J., Gigengack,S., Lienhard,G.E., and James,D.E. (1991a) Immuno-localization of the insulin regulatable glucose transporter in brown adipose tissue of the rat. *J. Cell Biol.* **113**: 123-135.

Slot,J.W., Geuze,H.J., Gigengack,S., James,D.E., and Lienhard,G.E. (1991b) Translocation of the glucose transporter GLUT4 in cardiac myocytes of the rat. *Proc. Natl. Acad. Sci. U.S.A* **88**: 7815-7819.

Smith,R.M., Charron,M.J., Shah,N., Lodish,H.F., and Jarett,L. (1991) Immunoelectron microscopic demonstration of insulin-stimulated translocation of glucose transporters to the plasma membrane of isolated rat adipocytes and masking of the carboxyl-terminal epitope of intracellular GLUT4. *Proc. Natl. Acad. Sci. U.S.A* **88**: 6893-6897.

Smith,P.K., Krohn,R.I., Hermanson,G.T., Mallia,A.K., Gartner,F.H., Provenzano,M.D., Fujimoto,E.K., Goeke,N.M., Olson,B.J., and Klenk,D.C. (1985) Measurement of protein using bicinchoninic acid *Anal. Biochem.* **150**: 76-85.

Sollner,T., Bennett,M.K., Whiteheart,S.W., Scheller,R.H., and Rothman,J.E. (1993) A protein assembly-disassembly pathway in vitro that may correspond to sequential steps of synaptic vesicle docking, activation, and fusion. *Cell* **75**: 409-418.

Springer,S., Spang,A. and Schekman,R. (1999) A primer on vesicles budding. *Cell* **97**: 145-148.

Stamnes,M.A. and Rothman,J.E. (1993) The binding of AP-1 clathrin adaptor particles to Golgi membranes requires ADP-ribosylation factor, a small GTP-binding protein. *Cell* **73**: 999-1005.

Stenius,K., Janz,R., Sudhof,T.C., and Jahn,R. (1995) Structure of synaptogyrin (p29) defines novel synaptic vesicle protein. *J. Cell Biol.* **131**: 1801-1809.

Stepuro,I.I., Artsukevich,A.N., and Ostrovsky,Y.M. (1981) Changes in serum-albumin conformation under the effect of UV-radiation. *Biofizika* **26**: 777-781.

Stepuro,I.I., Ignatenko,V.A., Artsukevich,A.N., and Kukresh,M.I. (1986) Study of the effect of ultraviolet-radiation and ultrasound on disulfide couplings of human serum albumin. *Zhurnal Fizicheskoi Khimii* **60**: 2535-2539.

Stokoe,D., Stephens,L.R., Copeland,T., Gaffney, P.R., Reese,C.B., Painter,G.F., Holmes, A.B., McCormick,F. and Hawkins, P.T. (1997) Dual role of phosphatidylinositol-3,4,5-triphosphate in the activation of protein kinase C. *Science* **277**: 567-570.

Straub,F.B. (1942) Actin. *Stud. Szeged.* **2**: 3-15.

Sugita,S., Janz,R., and Sudhof,T.C. (1999) Synaptogyrins regulate Ca-2+ dependent exocytosis in PC12 cells. *J. Biol. Chem.* **274**: 18893-18901.

Sun,X.J., Rothenberg,P., Kahn,C.R., Backer,J.M., Araki,E., Wilden,P.A., Cahill,D.A., Goldstein,B.J. and White, M.F. (1991) Structure of the insulin-receptor substrate IRS1 defines a unique signal transduction protein. *Nature* **352**: 73-77.

Sun,X.J., Weng,L., Zhang,Y., Yenush,L., Myers,M.G., Galsheen,E., Lane,W.S., Pierce,J.H. and White,M.F. (1995) Role of IRS-2 in insulin and cytokine signalling. *Nature* **377**: 173-177.

Sutton,R.B., Fasshauer,D., Jahn,R., and Brunger,A.T. (1998) Crystal structure of a SNARE complex involved in synaptic exocytosis at 2.4 A resolution. *Nature* **395**: 347-353.

Suzuki,K. and Kono,T. (1980) Evidence that insulin causes translocation of glucose transport activity to the plasma membrane from an intracellular storage site. *Proc. Natl. Acad. Sci. U.S.A* **77**: 2542-2545.

Tanner,L.I. and Lienhard,G.E. (1987) Insulin elicits a redistribution of transferrin receptors in 3T3-L1 adipocytes through an increase in the rate constant for receptor externalization. *J. Biol. Chem.* **262**: 8975-8980.

Tanner,L.I. and Lienhard,G.E. (1989) Localization of transferrin receptors and insulin-like growth factor II receptors in vesicles from 3T3-L1 adipocytes that contain intracellular glucose transporters. *J. Cell Biol.* 1989 **108**: 1537-45.

Taylor,L.P. and Holman,G.D. (1981) Symmetrical kinetic parameters for 3-O-methyl-D-glucose transport in adipocytes in the presence and in the absence of insulin. *Biochim. Biophys. Acta* **642**: 325-335.

Tellam,J.T., Macaulay,S.L., McIntosh,S., Hewish,D.R., Ward,C.W., and James,D.E. (1997) Characterization of Munc-18c and syntaxin-4 in 3T3-L1 adipocytes. Putative role in insulin-dependent movement of GLUT4. *J. Biol. Chem.* **272**: 6179-6186.

Tellam,J.T., McIntosh,S., and James,D.E. (1995) Molecular identification of two novel Munc-18 isoforms expressed in non- neuronal tissues. *J. Biol.Chem.* **270**: 5857-5863.

Thorens,B. and Roth,J. (1996) Intracellular targeting of GLUT4 in transfected insulinoma cells: evidence for association with constitutively recycling vesicles distinct from synaptophysin and insulin vesicles. *J Cell Sci.* **109**:1311-23.

Timmers,K.I., Clark,A.E., Omatsu-Kanbe,M., Whiteheart,S.W., Bennett,M.K., Holman,G.D., and Cushman,S.W. (1996) Identification of SNAP receptors in rat adipose cell membrane fractions and in SNARE complexes co-immunoprecipitated with epitope-tagged N- ethylmaleimide-sensitive fusion protein. *Biochem. J.* **320**: 429-436.

Tjelle,T.E., Brech,A., Juvet,L.K., Griffiths,G., and Berg,T. (1996) Isolation and characterization of early endosomes, late endosomes and terminal lysosomes: their role in protein degradation. *J. Cell Sci.* **109**: 2905-2914.

Tong,P., Khayat,Z.A., Huang,C., Patel,N., Ueyama,A. and Klip,A. (2001) Insulin-induced cortical actin remodeling promotes GLUT4 insertion at muscle cell membrane ruffles. *J. Clin Invest.* **108**: 371-381.

Tooze,S.A. (1998) biogenesis of secretory granules in the *trans*-Golgi network of neuroendocrine and endocrine cells. *Biochim. Biophys. Acta* **1404**: 231-244.

Tooze,S.A., Martens,G.J.M. and Huttner,W.B. (2001) Secretory granule biogenesis: rafting to the SNARE. *Trends Cell Biol.*11: 116-122.

Tooze,S.A. and Huttner,W.B. (1990) Cell-free protein sorting to the regulated and constitutive secretory pathways. *Cell* **60**: 837-847.

Towbin,H., Theophil,S., and Julian,G. (1979) Electrophoretic transfer of proteins from polyacrylamide gels to nitrocellulose sheets: Procedure and some applications. *Proc. Natl. Acad. Sci. U.S.A* **76**: 4350-4354.

Trimble,W.S., Cowan,D.M. and Scheller,R.H. (1998) VAMP1: a synaptic vesicle-associated integral membrane protein. *Proc. Natl. Acad. Sci. U.S.A* **85:** 4538-4542.

Triscler,M., Stoorvogel,W., and Ullrich,O. (1999) Biochemical analysis of distinct Rab5- and Rab11-positive endosomes along the transferrin pathway. *J. Cell Sci.* **112**: 4773-4783.

Tsakiridis,T., McDowell,H.E., Walker,T., Downes,C.P., Hundal,H.S., Vranic,M. and Klip,A. (1995) Multiple roles of phosphatidylinositol 3-kinase in regulation of glucose transport, amino acid transport, and glucose transporters in L6 skeletal muscle cells. *Endocrinology.* **136** : 4315-4322.

Tsakiridis,T., Vranic,M. and Klip,A. (1994). Disassembly of the actin network inhibits insulin-dependent stimulation of glucose transport and prevents recruitment of glucose transporters to the plasma membrane. *J. Biol. Chem.* **269**: 29934-29942.

Ui,M., Okada,T., Hazeki,K. and Hazeki,O. (1995) Wortmannin as a unique probe for an intracellular signalling protein, phosphoinositide 3-kinase. *Trends Biochem. Sci.* **20**: 303-307

Ullrich,O., Reinsch,S., Urbé,S., Zerial,M. and Parton,R.G. (1996) Rab11 regulates recycling through the pericentriolar recycling endosome. *J. Cell Biol.* **135**: 913-924.

Urrutia,R., Henley,J.R., Cook,T. and McNiven, M.A. (1997). The dynamins: redundant or distinct functions for an expanding family of related GTPases. *Proc. Natl. Acad. Sci. U.S.A* **94**: 377-384.

Verhey,K.J. and Birnbaum,M.J. (1994) A Leu-Leu sequence is essential for COOH-terminal targeting signal of GLUT4 glucose transporter in fibroblasts. *J. Biol.Chem.* **269**: 2353-2356.

Verhey,K.J., Hausdorff,S.F., and Birnbaum,M.J. (1993) Identification of the carboxy terminus as important for the isoform- specific subcellular targeting of glucose transporter proteins. *J. Cell Biol.* **123**: 137-147.

Verhey,K.J., Yeh,J.I., and Birnbaum,M.J. (1995) Distinct signals in the GLUT4 glucose transporter for internalization and for targeting to an insulin-responsive compartment. *J. Cell Biol.* **130**: 1071-1079.

Vlahos,C.J., Matter,W.F., Hui,K.Y. and Brown,R.F. (1994) A specific inhibitor of phosphatidylinositol 3-kinase, 2-(4-Morpholinyl-)8-phenyl-4H-1-benzopyran-4-one (LY294002). *J. Biol. Chem.* **269**: 5241-5248.

Volchuk,A., Narine,S., Foster,L.J., Grabs,D., De Camilli,P and Klip, A. (1998). Perturbation of dynamin II with an amphiphysin SH3 domain increases GLUT4 glucose transporters at the plasma membrane in 3T3-L1 adipocytes. Dynamin II participates in GLUT4 endocytosis. *J. Biol. Chem.* **273**: 8169-8176.

Volchuk,A., Sargeant,R., Sumitani,S., Liu,Z., He,L., and Klip,A. (1995) Cellubrevin is a resident protein of insulin-sensitive GLUT4 glucose transporter vesicles in 3T3-L1 adipocytes. *J. Biol. Chem.* **270**: 8233-8240.

Volchuk,A., Wang,Q., Ewart,H.S., Liu,Z., He,L., Bennett,M.K., and Klip,A. (1996) Syntaxin 4 in 3T3-L1 adipocytes: regulation by insulin and participation in insulin-dependent glucose transport. *Mol. Biol. Cell* **7**: 1075-1082.

Vollenweider,P., Clodi,M., Martin,S.S., Imamura,T., Kavanaugh,W.M. and Olefsky,J.M. (1999) An SH2 domain containing 5' inositolphosphatase inhibits insulin-induced GLUT4 translocation and growth factor induced actin filament rearrangement. *Mol. Cell Biol.* **19**: 1081-1091.

Vollenweider,P, Martin,S.S., Haruta,T., Morris,A.J., Nelson,J.G., Cormont,M., Marchand-Brustel,Y., Rose,D.W. and Olefsky, J.M. (1997) The small guanosine triphosphate-binding protein Rab4 is involved in insulin-induced GLUT4 translocation and actin filament rearrangement in 3T3-L1 cells. *Endocrinology* **138**: 41-4949.

Wadzinski,B.E., Shanahan,M.F., Clark,R.B., and Ruoho,A.E. (1987) Derivitization of the human erythrocyte glucose transporter using a novel forskolin photoaffinity label. *J. Biol. Chem.* **262**: 17683-17689.

Wallach,DFH (1967) The specificity of cell surfaces. Davies,B.D; Warren,L. ed., Prentice Hall, Englewood Cliff, New Jersey. p129

Walmsley,A.R. (1988) The dynamics of the glucose transporter. *Trends Biochem. Sci.* **13**: 226-231.

Wang,Q., Bilan,P.J., Tsakiridis,T., Hinek,A.. and Klip,A. (1998) Actin filaments participate in the relocalisation of phosphatidylinositol 3-kinase to glucose transporter-containing compartments and in the stimulation of glucose uptake in 3T3-L1 adipocytes. *Biochem. J.* **331**: 917-928.

Wang,Q., Somwar,R., Bilan,P.J., Liu,Z., Jin,J., Woodgett,J.R. and Kip,A. (1999) Protein kinase B/Akt participates in GLUT4 translocation by insulin in L6 myoblasts. *Mol. Cell Biol.* **19**: 4008-4018.

Wang,W., Hansen,P.A., Marshall,B.A., Holloszy,J.O., and Mueckler,M. (1996) Insulin unmasks a COOH-terminal GLUT4 epitope and increases glucose transport across T-tubules in skeletal muscle. *J. Cell Biol.* **135**: 415-430.

Warnock,D.E. and Schmid,S.L. (1996) Dynamin GTPase, a force-generating molecular switch. *Bioessays* **18**: 885-893.

Watson,R.T. and Pessin,J.E. (2001) Subcellular compartmentalization and trafficking of the insulin-responsive glucose transporter, GLUT4. *Exper. Cell Res.* **271**: 75-83.

Weber,TM, Joost,HG, Simpson,IA, and Cushman,SW (1988) Methods of assessment of glucose transport activity and the number of gluocse transporters in isolated rat adipose cells and membrane fractions in Insulin Receptors, Part B: Clinical Assessment, Biological Responses and Comparison to IGF-1 Receptor Alan R. Liss, Inc.ed. 171-187.

Wei,M.L., Bonzelius,F., Scully,R.M., Kelly,R.B., and Herman,G.A. (1998) GLUT4 and transferrin receptor are differentially sorted along the endocytic pathway in CHO cells. *J. Cell Biol.* **140**: 565-575.

Weidman,P.J., Melancon,P., Block,M.R. and Rothman,J.E. (1989) Binding of an N-ethylmaleimide-sensitive fusion protein to Golgi membranes requires both a soluble protein(s) and an integral membrane receptor. *J. Cell Biol.***108**: 1589-1596.

Wennstrom.S., Hawkins,P., Cooke,F., Hara,K., Yonezawa,K., Kasuga,M., Jackson,T., Claesson-Welsh,L. and Stephens,L. (1994a) Activation of phosphoinositide 3-kinase is required for PDGF-stimulated membrane ruffling. *Curr. Biol.* **4**: 385-393.

Wennstrom.S., Siegbahn,A., Yokote,K., Arvidsson,A.K., Heldin,C.H., Mori,S. and Claesson-Welsh,L. (1994b) membrane ruffling and chemotaxis transduced by the PDGF beta-receptor require the binding site for phosphatidylinositol 3'kinase. *Oncogene* **9**: 651-660.

White,M.F. (1998) The IRS-signalling system: a network of docking proteins that mediate insulin action. *Mol. Cell Biochem.* **182**: 3-11.

Whitesell,R.R. and Gliemann,J. (1979) Kinetic parameters of transport of 3-O-methylglucose and gluocse in adipocytes. *J. Biol.Chem.* 254: 5276-5283.

Whitney,J.A., Gomez,M., Sheff,D., Kreis,T.E. and Mellman,I. (1995) Cytoplasmic coat proteins involved in endosome function. *Cell* **83**: 703-713.

Wiedenmann,B. and Franke,W.W. (1985) Identification and localistaion of synaptophysin, an integral membrane glycoprotein of Mr 38,000 characteristic of presynaptic vesicles. *Cell* **41**: 1017-1028.

Williams,S.A. and Birnbaum,M.J. (1988) The rat facilitated glucose transporter gene. Transformation and serum-stimulated transcription initiate from identical sites. *J. Biol. Chem.* **263**: 19513-19518.

Wilson,J.M. and Colton,T.L. (1997) Targeting of an intestinal apical endosomal protein to endosomes in nonpolarized cells. *J. Cell Biol.* **136**: 319-330.

Wolf,AV and Brown,MG (1967) Handbook of Chemistry and Physics. **48th** D144-D183.

World Health Organisation (1998) World Health Report 1998 Geneva. *World Health report*

Yamashiro,D.J., Tycko,B., Fluss,S.R. and Maxfield,F.R. (1984) Segregation of transferrin to a mildly acidic (pH 6.5) para-Golgi compartment in the recycling pathway. *Cell* **37**: 789-800.

Yang,J., Clark,A.E., Harrison,R., Kozka,I.J., and Holman,G.D. (1992b) Trafficking of glucose transporters in 3T3-L1 cells. Inhibition of trafficking by phenylarsine oxide implicates a slow dissociation of transporters from trafficking proteins. *Biochem. J.* **281**: 809-817.

Yang,J., Clark,A.E., Kozka,I.J., Cushman,S.W., and Holman,G.D. (1992a) Development of an intracellular pool of glucose transporters in 3T3-L1 cells. *J. Biol. Chem.* **267**: 10393-10399.

Yang,J. and Holman,G.D. (1993) Comparison of GLUT4 and GLUT1 subcellular trafficking in basal and insulin-stimulated 3T3-L1 cells. *J. Biol. Chem.* **268**: 4600-4603.

Yang,C., Watson,R.T, Elemendorf,J.S., Sacks,D.B. and Pessin,J.E. (2000) Calmodulin antagonists inhibit insulin-stimulated GLUT4 (glucose transporter 4) translocation by preventing the formation of phosphatidylinositol 3,4,5-trisphosphate in 3T3-L1 adipocytes. *Mol. Endocrinol.* **14**: 317-326.

Yeh,J.I., Verhey,K.J., and Birnbaum,M.J. (1995) Kinetic analysis of glucose transporter trafficking in fibroblasts and adipocytes. *Biochemistry* **34**: 15523-15531.

Zaremba,S., Keen,J.H. (1983). Assembly polypeptides from coated vesicles mediate reassembly of unique clathrin coats. *J. Cell Biol.* **97**: 1339-1347.

Zerial,M. and McBride,H. (2001) Rab proteins as membrane organisers. *Nat. Rev. Mol. Cell Biol.* **2**: 107-117.

Zorzano,A., Wilkinson,W., Kotliar,N., Thoidis,G., Wadzinski,B.E., Ruoho,A.E., and Pilch,P.F. (1989) Insulin-regulated glucose uptake in rat adipocytes is mediated by two transporter isoforms present in at least two vesicle populations. *J. Biol. Chem.* **264**: 12358-12363.

Appendices

Appendix I

Mathematical Equations for Computer Simulations

```
// 3 pool recycling model

IndVars: t
DepVars: tp,tee,tisc,lp,lee,lisc,ftee,flee
Params: ken,rken,kex,rkex,ksq,rksq,ken1,rken1,kex1,rkex1,ksq1,rksq1

tp' = rken*tee+kex*(1.0-tp-tee)-tp*(ken+rkex)
tee' = tp*ken+rksq*(1.0-tp-tee)-tee*(rken+ksq)
lp' = rken*lee+kex*(1.0-lp-lee)-lp*(ken+rkex)
lee' = lp*ken+rksq*(1.0-lp-lee)-lee*(rken+ksq)

tisc=1.0-tp-tee
lisc=1.0-lp-lee
ftee=tee/(tisc+tee)
flee=lee/(lisc+lee)

// parameters:
ken=0.06
kex=0.001
ksq=0.15
rken=0.0
rkex=0.0
rksq=0.0

ken1=0.06
kex1=0.12
ksq1=0.15
rken1=0.0
rkex1=0.0
rksq1=0.0

// initial conditions:

tot=kex1*(rken1+ksq1)+rksq1*rken1+ken1*(kex1+rksq1)+rkex1*rksq1+ksq1*(ken1+rkex1)+rken
1*rkex1
tp=(kex1*(rken1+ksq1)+rksq1*rken1)/tot
tee=(ken1*(kex1+rksq1)+rkex1*rksq1)/tot
ttv=(ksq1*(ken1+rkex1)+rken1*rkex1)/tot

lp=1.0
lee=0.0
t=0.0

***
```

Appendix II

Hashimoto,M., Hatanaka,Y., Yang,J., Dhesi,J., and Holman,G.D. (2001) Synthesis of Biotinylated Bis (D-Glucose) Derivatives for Glucose Transport. ***Carbohydr. Res.*** **331 119-127.**

ELSEVIER

www.elsevier.nl/locate/carres

Carbohydrate Research 331 (2001) 119–127

CARBOHYDRATE RESEARCH

Synthesis of biotinylated bis(D-glucose) derivatives for glucose transporter photoaffinity labelling

Makoto Hashimoto,[a] Yasumaru Hatanaka,[b] Jing Yang,[a] Jaswant Dhesi,[a] Geoffrey D. Holman[a,*]

[a]*Department of Biology and Biochemistry, University of Bath, Claverton Down, Bath BA2 7AY, UK*
[b]*Research Institute for Wakan-Yaka, Toyama Medical and Pharmaceutical University, Sugitani 2630, Toyama 930-0194, Japan*

Received 20 September 2000; accepted 18 January 2001

Abstract

New diazirine based bis-glucose derivatives for tagging glucose transporters have been synthesised. These included two biotinylated compounds linked either by an aminocaproate or by a cleavable dithiol link. These compounds have been derivatised via a key skeleton compound that can be easily used for introduction of additional tags. Studies on the erythrocyte glucose transporter (GLUT1) and the insulin-stimulated adipose cell transporter (GLUT4) have revealed the biotinylated photoreactive bis-glucose compounds are effective labelling reagents.

Keywords: Bis-glucose; Biotin; Photolabels; Glucose transporters

1. Introduction

There are five major glucose transporters in mammalian tissues (GLUTs 1–5)[1] but new isoforms are being discovered.[2] These proteins catalyse one of the most important cell membrane transport events since glucose plays a central role in cellular homeostasis and metabolism.

The GLUT transporters have broad specificities for hexoses and, in addition to glucose, other monosaccarides such as galactose and mannose are transported. Previous studies have established that bulky groups are tolerated around the 4-OH position when the hexose occupies the exofacial binding sites of the transporters.[3] We have previously found that a bis-hexose structure has advantages for photolabelling of the exofacial surface of the transporters. The bis-structure allows a hydrophobic moiety to be inserted in the bridge in a form that produces a molecule, that overall, still has a hydrophilic character and is water-soluble. In addition, the bis-hexoses are bulky and consequently act as powerful inhibitors of glucose transport but are not themselves transported because of steric constraints imposed by the bulky substituents. Consequently as these probes are too hydrophilic to enter cells through the membrane lipid, they act specifically at the exofacial binding site. This bis-structure has previously been reported for bis-mannose[4] linked by a 2-propylamine bridge and bis-glucose derivatives linked by a secondary amine bridge.[5] The bis-mannose

* Corresponding author. Tel.: +44-1225-826874; fax: +44-1225-826779.

ing a biotinylated derivative[6] have been particularly useful in tagging the glucose transporters and therefore we have examined here a bis-glucose compound with the versatile 2-propylamine bridge. The choice of photoreactive substituent for studying glucose transporters was also considered to be important. Bis-mannose derivatives in which aryl azide or benzophenone groups have been introduced have been previously described.[7,8] The disadvantages of the aryl azides is that nucleophilic side reactions reduce the specificity of the labelling reaction while the disadvantage of the benzophenone groups is that long irradiation times are needed to produce a high yield of cross-linked adduct. By contrast, diazirine groups have been found to generate highly reactive carbenes smoothly and specifically with short irradiation times. Furthermore, we have found that a carbene-introduced linkage is more stable than those introduced by the other two species.[9] We have consequently concluded that diazirine is the most useful photophor[10,11] and have synthesised new bis-glucose compounds that contain this photoreactive group. We have chosen to introduce biotin groups attached by either amino-hexanoate or cleavable dithiol links. The advantage of the latter is that it allows release, under mild reducing conditions at moderate temperatures, of the photolabelled protein from the avidin or streptavidin matrix used to isolate and purify the protein. We have found that the release of photolabelled transporters, tagged with the previously described biotin-amino-hexanoate linked bis-mannose photolabel Bio-LC-ATB-BMPA, from streptavidin agarose requires that the adduct be heated at 100 °C for 30 min in the presence of denaturing SDS.

In our consideration of the route to produce new bis-glucose photolabels we thought it useful to prepare a key intermediate that could subsequently be used to introduce new tags as required. In this paper we describe the synthesis of novel amino BOC protected diazirine-based photoreactive bis-glucose derivative as this key intermediate. Removal of a BOC protecting group leaves an amine group that can then be easily coupled to any probe moiety containing a carboxylate group via amide bond formation. To determine the utility of the approach we studied the interaction of the biotinylated bis-glucose photoaffinity probes with the human erythrocyte transporter, GLUT1 and the with the adipose cell transporter, GLUT4.

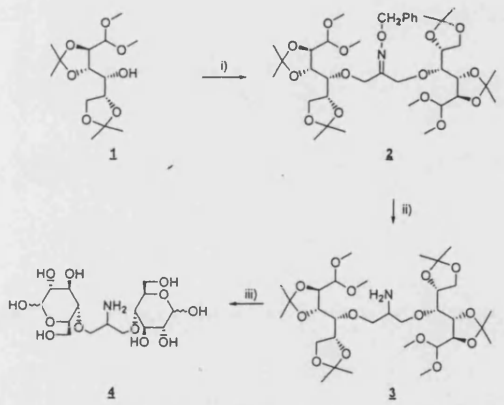

Fig. 1. (i) (a) NaH, DMF, room temperature; (b) 1,3-dichloro-2-propane benzyloxime, room temperature, 74%. (ii) H_2, Raney nickel, ethanol, H_2O, NH_4OH, room temperature, 94%. (iii) 1 M HCl, 100 °C, quant.

2. Results and discussion

Synthesis of bis-glucose photoreactive probes.—The route for synthesis of the bis-glucose compounds is shown in Fig. 1. 2,3,5,6-Di-*O*-isopropylidene-D-glucose dimethyl acetal (**1**)[12] was converted to the 4-O-linked dimer **2** with 1,3-dichloro-2-propanone *O*-benzyloxime. This crosslinking reagent has been previously used to synthesise bis-D-mannose-2-propylamine.[13] The reaction proceeds rapidly to a monochloro intermediate (which could be isolated and characterised) and then more slowly to the bis- compound. These conversions can be followed by thin layer chromatography (TLC). Following purification, **2** was hydrogenated using Raney nickel as catalyst to give the amine **3** in good yield. The protecting acetal groups were then removed by acid hydrolysis to generate the 1,3-bis(glucos-4-yloxy) 2-propylamine compound (**4**).

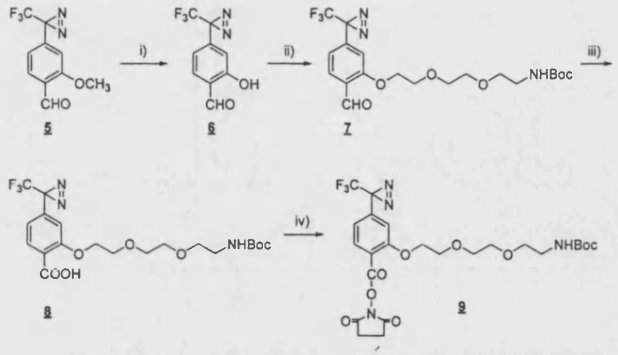

Fig. 2. (i) BBr_3, CH_2Cl_2, room temperature, 64%. (ii) 2-[2-(2-*tert*-Butoxycalbonylaminoethoxy)ethoxy]ethyl bromide, K_2CO_3, *n*-Bu_4NI, DMF, 60 °C, 91%. (iii) *n*-Bu_4NMnO_4, pyridine, room temperature, 90%. (iv) *N*-Hydroxysuccinimide, dicyclohexylcarbodiimide, CH_2Cl_2, CH_3CN, room temperature, 99%.

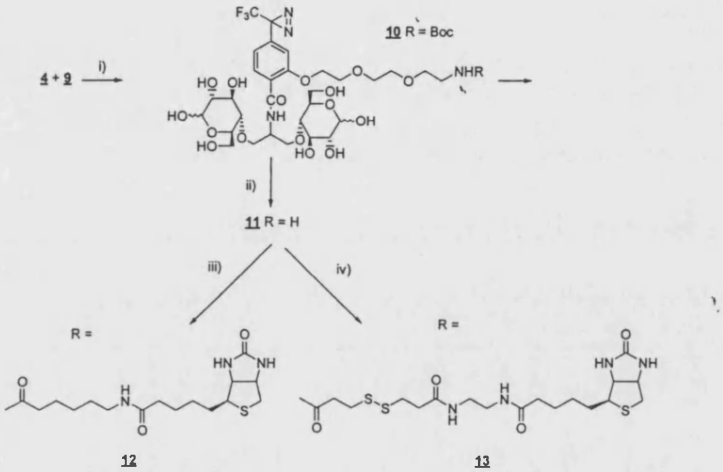

Fig. 3. (i) 0.1 M $NaHCO_3$, DMF, room temperature, 88%. (ii) 50% Trifluoroacetic acid, CH_2Cl_2, 0 °C, 86%. (iii) *N*-Biotinylamino caproic acid *N*-hydroxysuccinimide ester, 0.1 M $NaHCO_3$–DMF, room temperature, 37%. (iv) ([2-(Biotinyl)ethylamido]-3,3′-dithiodipropionic acid *N*-hydroxysuccinimide ester, 0.1 M $NaHCO_3$–DMF, room temperature, 40%.

We have previously reported the synthesis of a diazirinyl aryl carboxylate with a polyether spacer linked to biotin[14] that can be used to biotin tag proteins directly. However, we considered it more useful in the present study to synthesise from **4**, a photoreactive skeleton compound first and then subsequently couple this to biotin via ether aminocaproate or dithiol linkers (Figs. 2 and 3). Many more applications of the intermediate **11** are then possible as it can be further substituted with any additional tags as required for additional applications. For synthesis of the key skeleton compound **11**, we required the novel compound **9**, the production of which, itself required modifications of previously described syntheses (Fig. 2). We were able to achieve ether cleavage of **5**[15] with BBr_3 without protection of the aldehyde group of this diazirine compound. Phenol alkylation with the BOC protected ethylene glycol spacer[14] then afforded **7** in good yield. The aldehyde group of **7** was then oxidised to the carboxylic acid in **8** which was then converted to its *N*-hydroxy-succinimide ester derivative **9** (Fig. 2).

The condensation of compound **4** and **9** in nonaqueous conditions (triethylamine or morpholine in DMF) was slow and only produced low yields of **10** (less than 20%), possibly due to low solubility of the bis-glucose-2-propylamine compound in DMF We therefore used a water–DMF mixture for coupling. The bis-glucose-2-propylamine compound and the diazirine were dissolved in 0.1 M $NaHCO_3$ and DMF, respectively. The reaction proceeded smoothly with a moderate yield of the desired product.

The BOC protected skeleton was stable on storage and could be conveniently deprotected by TFA treatment for immediate coupling to an appropriate biotin-NHS ester as required. The biotinylated compounds studied here included compounds with aminocaproate and dithiol spacers, compounds **12** and **13**, respectively (Fig. 3).

Photoaffinity labelling of human GLUT1.—Erythrocytes provide a rich source of GLUT1, which is present as 3–5% of the membrane protein. GLUT1 was purified as previously described.[16] Purified GLUT1 was then mixed with stoichiometric amount of compound **12** or **13**, and the samples were then irradiated and the protein was resolved by SDS-PAGE and transferred to nitrocellulose as described in Section 3. Extravidin peroxidase conjugation revealed strong biotinylated bands at approximately 50 kDa for both compounds **12** and **13** and these signals were competitively reduced in the incubations with D-glucose (Fig. 4). Under the labelling conditions employed, the signal was therefore specific for the binding site of GLUT1. One of our aims was to test the feasibility of using compound **13** in experiments in which the biotin moiety is removed by a reducing agent that breaks the dithiol spacer arm. We therefore incubated the GLUT1 samples (phototagged with **13**) either in the absence or presence of dithiothreitol and resolved the labelled proteins under non-reducing conditions (Fig. 4). The biotin group was found to be cleaved under quite mild conditions and therefore, this compound is likely to be useful in future studies in which release of biotin-tagged protein or binding-site peptides under mild conditions is required.

Photolabelling of insulin-stimulated GLUT4 in adipocytes.—To determine the affinity of the interaction between the ligands **12** and **13** and GLUT4, each of the compounds was tested as a competitive inhibitor of 2-deoxy-D-glucose uptake into insulin-stimulated rat adipocytes (Fig. 5). K_i values or half-maximal inhibition constants for **12** and **13** were 195 and 142 μM, respectively. The K_i value for **12** was similar to, but slightly better than that of the equivalent bis-mannose compound Bio-

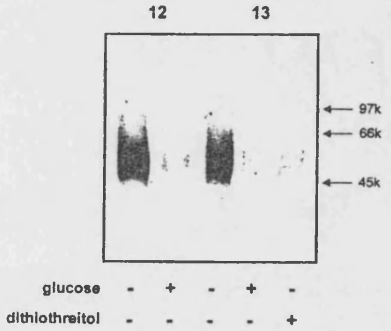

Fig. 4. Chemiluminescence detection of photoaffinity labelled human GLUT1. Compounds **12** and **13** were used to photolabel GLUT1 purified from human erythrocytes. Glucose (0.17 M) was added as a competitor for the binding site during the photolabelling reaction (lanes 2 and 4). The susceptibility of the dithiol bridge in GLUT1 photolabelled with compound **13** to reducing agent was examined by adding 0.5 M dithiothreitol at room temperature for 15 min after the photolabelling reaction. Photolabelled samples were resolved by SDS-PAGE on 10% gels run under reducing conditions (compound **12**) and non-reducing conditions (compound **13**) and then transferred to nitrocellulose for analysis of the biotin signal by using avidin-HRP and ECL detection.

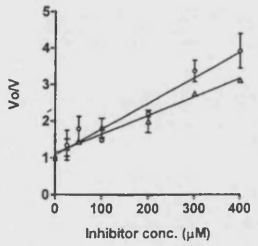

Fig. 5. Determination of half maximal inhibition constants for bis D-glucose ligands. The uptake of tracer 2-deoxy-[^{14}C]-D-glucose in insulin-stimulated rat adipose cells was determined at the indicated concentrations of compounds **12** (△) and **13** (○). The rate constants (mean and S.E.M. are shown) for uptake in the presence (V) and absence (V_0) of inhibitor (I) which were then used to calculate the K_i according to the equation $V_0/V = 1 + I/K_i$. Results shown are from three experiments

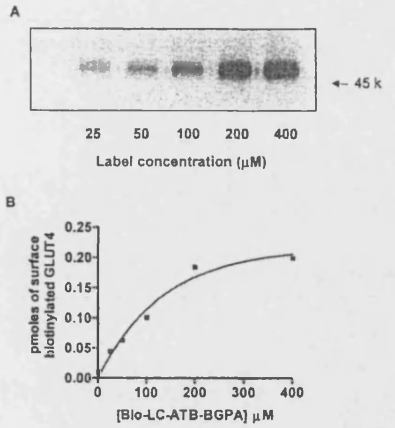

Fig. 6. Quantification of GLUT4 labelling. Rat adipose cells were UV irradiated in the presence of compound **12** at the indicated concentrations. Cell membrane protein was then isolated and solubilised. Streptavidin beads was then used to precipitate the biotin-tagged GLUT4, which was resolved by SDS-PAGE and detected using an anti-GLUT4 antibody, peroxidase coupled secondary antibody and ECL (A). The ECL signal was quantified by comparison with a GLUT4 standard and the extent to which the labelling became saturated with increasing ligand concentrations was determined (B).

LC-ATB-BMPA (K_i of 273 μM Ref. 6). We have also determined the most appropriate concentration of **12** to use in GLUT4-tagging experiments (Fig. 6). To do this we have photolabelled, washed and solubilised the adipose cell protein as described in Section 3 and then precipitated the biotin-tagged protein with streptavidin-agarose. A wash step then allowed removal of the non-biotinylated GLUT4. The precipitated material was next resolved by SDS-PAGE and an antibody to the C-terminal section of GLUT4 was used to detect the tagged protein (Fig. 6(A)). Only a single labelled band was obtained and the amount of GLUT4 was quantified by reference with a standard containing a known amount of this protein.[17] This quantification (Fig. 6(B)) revealed that maximal tagging with biotin occurred when 200–400 μM ligand was used, a value that is consistent with the affinity constant revealed in the transport inhibition experiments.

3. Experimental

General methods.—Silica Gel for column chromatography was Kieselgel 60 (E. Merck, 230–400 mesh). Structural characterisations of synthetic products were performed with a JEOL JNM GX-400 spectrometer (^{1}H NMR) and a Micromass Autospec (MS). Elemental analysis was carried out by the microanalysis service (Bath University). The purity of those compounds that were not available in sufficient quantity for elemental analysis were determined by a combination of diazirine UV detection, biotin detection and hexose detection techniques applied to the compounds on TLC plates. Furthermore, no extraneous lines were detected in the NMR spectra and UV spectra and extinction coefficients at 350 nM were consistent with those previously established compounds containing the diazirine moiety. (Extravidin-peroxidase conjugate was obtained from Sigma. Chemiluminescence detection reagent and Hyper-film ECL were obtained from Amersham. Nitrocellulose membrane (BioTrace NT) was obtained from GelmanScience.)

*1,3-Bis(2,3, 5, 6-di-*O*-isopropylidene-*D*-glucose dimethylacetal-4-yloxy)-2-propane-*O*-benzyloxime* (**2**).—2,3,5,6-Di-*O*-isopropylidene glucopyranosyl dimethyl acetal (**1**)[12] (2.36 g, 7.7 mmol) was dissolved in DMF (15 mL). Sodium hydride (60%, 0.34 g, 8.5 mmol) was added to this solution at rt. After bubbling had ceased, 1,3-dichloro-2-propanone *O*-benzyloxime[13] (0.89 g, 3.9 mmol) was added. The reaction mixture was stirred at rt for 2 h. Additional NaH (0.09 g, 2.2 mmol) was then added. The reaction mixture was stirred for a further 1 h, quenched by AcOH (0.3 mL) and partitioned between CH_2Cl_2 and water. The aqueous phase was further extracted into CH_2Cl_2 twice. The combined organic layer was washed with 1 M HCl, saturated $NaHCO_3$ and satd NaCl, and then dried over Na_2SO_4. After filtration, the product was concentrated. The residue was purified with silica column chromatography (4:1 *n*-hexane–EtOAc) to afford a colourless oil (2.21 g, 74%). ^{1}H NMR ($CDCl_3$): δ 7.28–7.38 (5 H, m, Ph), 5.07 (2 H, s, $NOCH_2Ph$), 4.58 (4 H, s, $OCH_2C{=}NO$), 4.35 (2 H, d, $J = 6.0$ Hz, H-1),

4.30 (2 H, ddd, $J = 5.0$, 6.0, 6.0 Hz, H-5), 4.17 (2 H, dd, $J = 6.0$, 7.6 Hz, H-2), 4.00–3.95 (6 H, m, H-3 and 6), 3.62 (2 H, dd, $J = 2.6$, 5.0 Hz, H-4), 3.40 (12 H, s, OCH_3), 1.37 (24 H, s, $C(CH_3)_2$); FABMS: *m/z* 772 ($[M+H]^+$); HR-FABMS: Calcd for $C_{38}H_{62}NO_{15}$ ($[M+H]^+$) 772.4119; Found 772.4110. Anal. Calcd for $C_{38}H_{61}NO_{15}$ C, 59.13; H, 7.97; N, 1.81. Found: C, 59.2; H, 7.82; N, 1.88.

*1,3-Bis(2,3,5, 6-di-*O*-isopropylidene-*D*-glucose dimethylacetal-4-yloxy)-2-propylamine* (**3**).—Compound **2** (2.02 g, 2.6 mmol) and Raney nickel (59%, 8 mL) were suspended in 16:8:1 water–EtOH–NH_3 (20 mL). The reaction mixture was vigorously stirred at rt under a hydrogen atmosphere for 19 h. The mixture was filtered through Celite and was then concentrated. The residue was partitioned between EtOAc and water. The organic phase was washed with saturated NaCl, dried over Na_2SO_4, filtered and then concentrated to afford a colourless oil (1.63 g, 94%). ^{1}H NMR ($CDCl_3$): δ 4.36 (2 H, d, $J = 6.2$ Hz, H-1), 4.23 (2 H, ddd, $J = 5.0$, 6.0, 6.0 Hz, H-5), 4.14 (2 H, dd, $J = 6.2$, 7.4 Hz, H-2), 4.03–3.98 (6 H, m, H-3 and 6), 3.67 (1 H, t, $J = 5.9$ Hz, $CHNH_2$), 3.61 (2 H, dd, $J = 2.4$, 5.0 Hz, H-4), 3.48 (4 H, d, $J = 5.9$ Hz, OCH_2), 3.40 (12 H, s), 1.37 (24 H, s), 4.36 (4 H, d, $J = 6.3$ Hz), 4.3–3.5 (14 H, m), 4.00 (4 H, d, $J = 6.3$ Hz), 3.45 (12 H, s, OCH_3), 3.20 (1 H, m), 1.76 (1 H, br), 1.42, 1.40, 1.34 (total 24 H, each s, $C(CH_3)_2$). FABMS: *m/z* 668 ($[M+H]^+$); HR-FABMS: Calcd for $C_{31}H_{58}N0_{14}$ ($[M+H]^+$) 668.3857; Found 668.3848. Anal. Calcd For $C_{31}H_{57}NO_{14}\cdot 0.5\ H_2O$: C, 55.02; H, 8.64; N, 2.07. Found: C, 55.2; H, 8.52; N, 2.09.

*1,3-Bis(*D*-glucopyranos-4-yloxy)-2-propylamine* (**4**).—Compound **3** (0.56 g, 0.83 mmol) was suspended in 1 M HCl (2 mL) and heated at 100 °C for 3 h. The reaction mixture was neutralised with Amberlite IRA-93 (OH form) and the resin was removed by filtration. The filtrate was concentrated to afford light brown oil (0.39 g, quant.). ^{1}H NMR (CD_3OD): δ 5.05 (1 H, d, $J = 3.6$ Hz, 1-α, 4.40 (1 H, d, $J = 7.6$ Hz, 1-β), 3.4–4.0 (17 H, m). FABMS *m/z* 416 ($[M+H]^+$). HRFABMS Calcd for $C_{15}H_{30}NO_{12}$ ($[M+H]^+$): 416.1768. Found: 416.1745.

2-Hydroxy-4-[3-(trifluoromethyl)-3H-diazirin-3-yl] benzaldehyde (**6**).—2-Methoxy-4-[3-(trifluoromethyl)-3H-diazirin-3-yl] benzaldehyde (**5**)[15] (3.396 g, 13.9 mmol) was dissolved in CH_2Cl_2 at −20 °C. BBr_3 (1.4 mL, 14.8 mmol) was added in portions. The reaction mixture was stirred at 0 °C for 1 h and water was added to quench the reaction. The organic layer was washed with saturated NaCl, dried over $MgSO_4$, filtered and then concentrated. The residue was purified with silica column chromatography (5:1 *n*-hexane–CH_2Cl_2) to afford a pale yellow oil (2.048 g, 64%). ^{1}H NMR ($CDCl_3$): δ 9.90 (1 H, s, CHO), 7.59 (1 H, d, $J = 7.9$ Hz, Ph), 6.07 (1 H, d, $J = 7.9$ Hz, Ph), 6.75 (1 H, s, Ph). EIMS: *m/z* 230 ($[M]^+$). HRMS Calcd for $C_9H_5F_3N_2O_2$ ($[M]^+$): 230.0303; Found: 230.0291.

*2-[2-[2-[2-(2-*tert*-Butoxycarbonylaminoethoxy)ethoxy]ethoxy]-4-[3-(trifluoromethyl)-3H-diazirin-3-yl] benzaldehyde* (**7**).—Compound **6** (2.001 g, 8.69 mmol), 2-[2-(2-*tert*-butoxycalbonylaminoethoxy)ethoxy]ethyl bromide,[14] K_2CO_3 (1.999 g, 14.4 mmol) and nBu$_4$NI (0.403 g, 1.08 mmol) were suspended in DMF (109 mL). The suspension was heated at 60 °C for 12 h, concentrated and partitioned between EtOAc and water. The organic layer was washed with 1 M HCl, satd $NaHCO_3$ and satd NaCl, and then dried over $MgSO_4$. After filtration, the product was concentrated and subjected to silica column chromatography (1:1 *n*-hexane–EtOAc) to afford a pale yellow oil (3.658 g, 91%). ^{1}H NMR ($CDCl_3$): δ 10.48 (1 H, s, CHO), 7.85 (1 H, d, $J = 8.2$ Hz, Ph), 6.86 (1 H, d, $J = 8.2$ Hz, Ph), 6.74 (1 H, s, Ph), 4.27 (2 H, t, $J = 4.7$ Hz), 3.92 (2 H, t, $J = 4.7$ Hz), 3.71 (2 H, m), 3.64 (2 H, m), 3.54 (2 H, m), 3.32 (2 H, m), 1.43 (9 H, s, $C(CH_3)_3$). FABMS *m/z* 462 ($[M+H]^+$). HRFABMS Calcd for $C_{20}H_{27}F_3N_3O_6$ ($[M+H]^+$): 462.1582; Found: 462.1844.

*2-[2-[2-[2-(2-*tert*-Butoxycarbonylaminoethoxy)ethoxy]ethoxy]-4-[3-(trifluoromethyl)-3H-diazirin-3yl] benzoic acid* (**8**).—Compound **7** (2.135 g, 4.63 mmol) and tetrabutylammonium permanganate (2.485 g, 6.87 mmol) were dissolved in Py (45 mL) at rt and stirred for 2 h. The reaction mixture was diluted with toluene and washed with 1 M Na_2SO_4, 1 M HCl and satd NaCl.

The organic layer was dried over $MgSO_4$, filtered and concentrated to afford a yellow oil (1.988 g, 90%). ^1H NMR ($CDCl_3$): δ 8.16 (1 H, d, $J = 8.2$ Hz, Ph), 6.94 (1 H, d, $J = 8.2$ Hz, Ph), 6.78 (1 H, s, Ph), 4.37 (2 H, m), 3.92 (2 H, m), 3.72 (2 H, m), 3.65 (2 H, m), 3.55 (2 H, m), 3.32 (2 H, m), 1.42 (9 H, s, s, $C(CH_3)_3$). FABMS: *m/z* 478 ($[M+H]^+$). HRFABMS Calcd for $C_{20}H_{27}F_3N_3O_7$ ($[M+H]^+$): 478.1801; Found: 478.1799.

*2-[2-[2-[2-(2-*tert*-Butoxycarbonylamino-ethoxy)ethoxy]ethoxy]-4-[3-(trifluoromethyl)-3H-diazirin-3-yl] benzoic acid N-hydroxysuccinimide ester* (**9**).—*N*-hydroxysuccinimide (0.490 g, 4.26 mmol) and compound **8** (1.837 g, 3.85 mmol) were dissolved in 5:1 CH_2Cl_2–CH_3CN (12 mL) at rt. Dicyclohexylcarbodiimide (0.877 g, 4.25 mmol) in CH_2Cl_2 was added. The reaction mixture was stirred at rt for 3 h, filtered, and then concentrated. The residue was partitioned between EtOAc and water. The organic layer was washed with saturated NaCl, dried over $MgSO_4$, filtered and concentrated to afford a yellow oil (2.186 g, 99%). ^1H NMR ($CDCl_3$): δ 8.03 (1 H, d, $J = 8.2$ Hz, Ph), 6.87 (1 H, d, $J = 8.2$ Hz, Ph), 6.76 (1 H, s, Ph), 4.24 (2 H, m), 3.91 (2 H, m), 3.72 (2 H, m), 3.61 (2 H, m), 3.53 (2 H, m), 3.31 (2 H, m), 2.90 (s, 4 H, CH_2CH_2), 1.43 (9 H, s, $C(CH_3)_3$). FABMS: *m/z* 575 ($[M+H]^+$); HRFABMS Calcd for $C_{24}H_{30}F_3N_4O_9$ ($[M+H]^+$): 575.1965; Found: 575.1973. Anal. Calcd For $C_{24}H_{29}F_3N_4O_9 \cdot 0.5\ H_2O$: C, 49.40; H, 5.18; N, 9.60. Found: C, 49.55; H, 5.35; N, 9.35.

N-*[2-[2-[2-(2-*tert*-Butoxycarbonylamino-ethoxy)ethoxy] ethoxy]-4-[3-(trifluoromethyl)-3H-diazirin-3-yl]benzoyl]-1,3-bis(*D*-glucopyranose-4-yloxy)-2-propylamine* (**10**).—Compound **9** (0.162 g, 0.28 mmol) was dissolved in DMF (2.5 mL) and compound **4** (0.162 g, 0.17 mmol) was added in 3 mL of 0.1 M $NaHCO_3$. The reaction mixture was stirred at rt for 12 h. The product was then applied to a column of Amberlite IRN-150L (2 mL, neutral form) and was washed through the column with water. The eluate was concentrated and the product was purified with silica column chromatography (13:5:1 $CHCl_3$–CH_3OH–water) to afford a colourless oil (0.131 g, 88%). ^1H NMR (D_2O): δ 7.88 (1 H, d, $J = 8.2$ Hz, Ph), 7.05 (1 H, d, $J = 8.2$ Hz, Ph), 6.89 (1 H, s, Ph), 5.23 (1 H, d, $J = 3.6$ Hz, 1-α), 4.44 (1 H, d, $J = 7.6$ Hz, 1-β), 4.40–3.20 (29 H, m), 1.37 (9 H, s, $C(CH_3)_3$). FABMS: *m/z* 875 ($[M+H]^+$). HRFABMS Calcd for $C_{35}H_{54}F_3N_4O_{18}$ ($[M+H]^+$): 875.3385; Found 875.3370.

N-*[2-[2-[2-(2-aminoethoxy)ethoxy]ethoxy]-4-[3-(trifluoromethyl)-3H-diazirin-3-yl]-benzoyl]1,3-bis(*D*-glucopyranos-4-yloxy)-2-propylamine* (**11**).—Trifluoroacetic acid (1 mL) was added to compound **10** (0.181 g, 0.21 mmol) in CH_2Cl_2 (1 mL) at 0 °C and the mixture was stirred for 0.5 h. The reaction mixture was concentrated and then redissolved in water (2 mL). The solution was passed through a 3 mL column of Amberlite IRA-93 (OH form) and the product was washed through with distilled water. The eluate was concentrated to afford colourless oil (0.138 g, 86%). FABMS *m/z* 775 ($[M+H]^+$).

N-*[2-[2-[2-(2-(*N*-biotinylcaproylamino)-ethoxy)ethoxy]ethoxy]-4-[3-(trifluoromethyl)-3H-diazirin-3-yl]benzoyl]1,2-bis(glucopyranosyl-4-yloxy)-2-propylamine* (**12**).—*N*-biotinyl caproic acid succinimide ester (0.301 g, 0.66 mmol) was dissolved in DMF (2 mL). To this solution compound **11** (0.464 g, 0.60 mmol) in 0.1 M $NaHCO_3$ (2 mL) was added at rt and the reaction mixture was stirred for 12 h. The reaction mixture was then concentrated. The residue was dissolved in water and applied to a column of Amberlite IRN-150L (2 mL, neutral form) and the product was washed through the column with distilled water. The eluate was then concentrated to afford pale-yellow oil. The eluate was concentrated and the product was purified with silica column chromatography (13:5:1 $CHCl_3$–CH_3OH–water) to afford a colourless oil (0.271 g, yield 37%). ^1H NMR (CD_3OD): δ 7.95 (1 H, d, $J = 8.2$ Hz, Ph), 7.02 (1 H, d, $J = 8.2$ Hz, Ph), 6.85 (1 H, s, Ph), 5.10 (1 H, d, $J = 3.6$ Hz, 1-α), 4.58 (1 H, d, $J = 7.6$ Hz, 1-β), 4.40–2.80 (37 H, m), 1.80–1.20 (10 H, m). FABMS: *m/z* 1114 ($[M+H]^+$). HRFABMS *m/z* ($[M+H]^+$) Calcd for $C_{46}H_{71}F_3N_7O_{19}S$: 1114.4478; Found 1114.4530.

N-*[2-[2-[2-(2-(2-Biotinyl)ethylamido]-3,3'-dithiodipropionylamino)ethoxy)ethoxy]-ethoxy]-4-[3-(trifluoromethyl)-3H-diazirin-*

*3-yl]benzoyl]1,3-bis(*D*-glucopyranos-4-yloxy)-2 - propylamine* (**13**).—[2 - (Biotinyl)ethylamido]-3,3′-dithiodipropionic acid *N*-hydroxysuccinimide ester (0.105 g, 0.18 mmol) was dissolved in DMF (1 mL). To this solution, compound **11** (0.163 g, 0.21 mmol) in 0.1 M $NaHCO_3$ (0.5 mL) was added at rt and the reaction mixture was stirred for 12 h. The reaction mixture was then concentrated. The residue was dissolved in water and applied to a column of Amberlite IRN-150L (2 mL, neutral form) and the product was washed through the column with distilled water. The eluate was then concentrated to afford pale yellow oil. The eluate was concentrated and the product was purified with silica column chromatography (50:25:1 $CHCl_3$–CH_3OH–water) to afford a colourless oil (0.089 g, yield 40%). ^1H NMR (CD_3OD): δ 7.42 (1 H, d, $J = 8.2$ Hz, Ph), 7.10 (1 H, d, $J = 8.2$ Hz, Ph), 6.90 (1 H, s, Ph), 5.23 (1 H, d, $J = 3.6$ Hz, 1-α), 4.60 (1 H, d, $J = 7.6$ Hz, 1-β), 4.50–4.20 (4 H, m), 4.00–3.20 (28 H, m), 3.0–2.50 (14 H, m), 2.25 (2 H, m), 1.80–1.40 (6 H, m). FABMS: *m/z* 1235 ($[M + H]^+$). HRFABMS *m/z* ($[M + H]^+$) Calcd for $C_{48}H_{74}F_3N_8O_{20}S_3$: 1235.4117; Found 1235.4134.

Photoaffinity labelling of GLUT1.—Human GLUT1 was prepared as described by Baldwin and Lienhard.[16] GLUT1 (10 μg) and compound **12** or **13** (0.25 nmol) were suspended in 0.1 M NaCl, 1 mM EDTA, 50 mM sodium phosphate buffer pH 7.4 (23 μL) at rt for 10 mm. Where indicated in the figure legends, D-glucose was included for competitive inhibition. The mixture was irradiated three times for 30 s with 30 s intervals between successive irradiations at 0 °C in a Rayonet photochemical reactor using 300 nm lamps. The solution was then centrifuged at 400,000*g* at 4 °C for 30 mm. The pellet was resuspended in (20 μL) of 1 mM EDTA, 50 mM Tris pH 7.4. A sample (0.5 μg) was then subjected to electrophoresis on a 10% acrylamide gel and transferred to nitrocellulose. The nitrocellulose was blocked for 1 h in 10% skimmed milk suspended with 0.1% Tween 20, Tris-buffered saline pH 7.4 (T-TBS), washed twice with T-TBS for 5 min and immersed in Extravidin peroxidase (a 1:4000 dilution of the manufacturers solution) with 1% skimmed milk in T-TBS for 40 mm. After washing 6 times with T-TBS for 5 min, the membrane was immersed in chemiluminescence reagents for 1 min and exposed to film for 0.5 min.

Photoaffinity labelling of GLUT4.—Rat adipocytes isolation, K_i measurements, and UV irradiation for labelling experiments were carried out as previously described. After labelling, cell samples were homogenised in HES buffer (255 mM sucrose, 1 mM EDTA, 20 mM HEPES, 1 μg/mL antipain, aprotinin, pepstatin, leupeptin and 100 μM 4-(2-aminoethyl) benzenesulfonyl fluoride hydrochloride (AEBSF), pH 7.2). Homogenates were washed once with HES buffer and subjected to centrifugation (554,000*g* for 30 min at 4 °C) to obtain a total membrane fraction. This pellet was solubilised in PBS pH 7.2, with 2% of Thesit ($C_{12}E_9$) and protease inhibitors (antipain, aprotinin, pepstatin, and leupeptin each at a concentration of 1 μg/mL and 100 μM AEBSF). The samples were solubilised for 50 min at 4 °C with rotation and were then subjected to centrifugation (20,000*g* for 20 min at 4 °C). Biotinylated proteins in the supernatants were either immuno-precipitated using a GLUT4 antiserum as previously described[6] or were precipitated with streptavidin beads (Pierce, Rockford, IL). Following GLUT4 immuno-precipitation complexes were released into electophoresis sample buffer (62.5 mM Tris, pH 6.8, 2% SDS, 10% glycerol) at rt. The steptavidin precipitates were washed four times with PBS buffer con taining 1% Thesit with protease inhibitors, four times with PBS containing 0.1% Thesit plus protease inhibitors and once in PBS. Electrophoresis sample buffer was added to each pellet. The sample was then heated to 95 °C for 30 min. The samples were subjected to centrifugation (2,300*g* for 1 min) and the supernatants were removed. The pellets were washed with additional electrophoresis sample buffer, heated to 95 °C for 30 min and resubjected to centrifugation. Mercaptoethanol was added (10% final concentration) to the above samples in the electrophoresis sample buffer and these were then subjected to SDS-PAGE (10% gel). Proteins were transferred to nitrocellulose membranes. Membranes were blocked with 5% non-fat milk in TBS-0.1%

Tween (TBS-T) and washed six times with TBS-T. Membranes were then incubated with affinity purified anti-GLUT4 C-terminal antibody[18] in TBS-T containing 1% BSA (2 h at rt), followed by washing (6 times in TBST) and detection using secondary antibody linked to horseradish peroxidase. GLUT4 protein was visualised with enhanced chemiluminescence (ECL). Pmoles of labelled GLUT4 were determined by comparison with a GLUT4 standard protein as described.[17]

Acknowledgements

This work was supported by the Medical Research Council (UK), the Wellcome Trust and Diabetes (UK).

References

1. Gould, G. W.; Holman, G. D. *Biochem. J.* **1993**, *295*, 329–341.
2. Ibberson, M.; Uldry, M.; Thorens, B. *J. Biol. Chem.* **2000**, *275*, 4607–4612.
3. Barnett, J. E. G.; Holman, G. D.; Munday, K. A. *Biochem. J.* **1973**, *135*, 539–541.
4. Holman, G. D.; Midgley, P. J. W. *Carbohydr. Res.* **1985**, *135*, 337–341.
5. Abbadi, M.; Holman, G. D.; Morin, C.; Rees, W. D.; Yang, J. *Tetrahedron Lett.* **1999**, *40*, 5861–5864.
6. Koumanov, F.; Yang, J.; Jones, A. E.; Hatanaka, Y.; Holman, G. D. *Biochem. J.* **1998**, *330*, 1209–1215.
7. Holman, G. D.; Parkar, B. A.; Midgley, P. J. W. *Biochim. Biophys. Acta* **1986**, *855*, 115–126.
8. Holman, G. D.; Karim, A. R.; Karim, B. *Biochim. Biophys. Acta* **1988**, *946*, 75–84.
9. Yoshida, E.; Nakayama, H.; Hatanaka, Y.; Kanaoka, Y. *Chem. Pharm. Bull.* **1990**, *38*, 982–987.
10. Clark, A. E.; Holman, G. D. *Biochem. J.* **1990**, *269*, 615–622.
11. Gillingham, A. K.; Koumanov, F.; Hashimoto, M.; Holman, G. D. In *Membrane Transport. A Practical Approach*; Baldwin, S. A., Ed.; Oxford University Press: London, 2000; pp. 193–207.
12. Stevens, J. D. *Carbohydr. Res.* **1975**, *45*, 143–150.
13. Sher, P. M.; Kronenthal, D. R. *J. Label. Compd. Radiopharm.* **1997**, *39*, 21–27.
14. Hatanaka, Y.; Hashimoto, M.; Kanaoka, Y. *Bioorg. Med. Chem.* **1994**, *2*, 1367–1373.
15. Hashimoto, M.; Kanaoka, Y.; Hatanaka, Y. *Heterocycles* **1997**, *46*, 119–122.
16. Baldwin, S. A.; Lienhard, G. E. *Methods Enzymol.* **1989**, *174*, 39–50.
17. Ryder, J. W.; Yang, J.; Galuska, D.; Rincón, J.; Björnholm, M.; Krook, A.; Lund, S.; Pedersen, O.; Wallberg-Henriksson, H.; Zierath, J. R.; Holman, G. D. *Diabetes* **2000**, *49*, 647–654.
18. Holman, G. D.; Kozka, I. J.; Clark, A. E.; Flower, C. J.; Saltis, J.; Habberfield, A. D.; Simpson, I. A.; Cushman, S. W. *J. Biol. Chem.* **1990**, *265*, 18172–18179.